Fisheries New Zealand

Tini a Tangaroa

An updated stock assessment for Foveaux Strait dredge oysters (*Ostrea chilensis*) for the 2017 fishing year

New Zealand Fisheries Assessment Report 2021/23

K. Large,
I. Doonan,
K. Michael,
S. Datta

ISSN 1179-5352 (online)
ISBN 978-1-99-100375-1 (online)

April 2021

New Zealand Government

Requests for further copies should be directed to:

Publications Logistics Officer
Ministry for Primary Industries
PO Box 2526
WELLINGTON 6140

Email: brand@mpi.govt.nz
Telephone: 0800 00 83 33
Facsimile: 04-894 0300

This publication is also available on the Ministry for Primary Industries websites at:
http://www.mpi.govt.nz/news-and-resources/publications
http://fs.fish.govt.nz go to Document library/Research reports

TABLE OF CONTENTS

EXECUTIVE SUMMARY

Large, K.; Doonan, I.; Michael, K.; Datta, S. (2021). An updated stock assessment for Foveaux Strait dredge oysters (*Ostrea chilensis*) for the 2017 fishing year.

***New Zealand Fisheries Assessment Report 2021/23*. 112 p.**

This report summarises an update of the stock assessment for Foveaux Strait dredge oysters (OYU 5) with the inclusion of fishery data from the 2013 to 2016 years and abundance indices up to the February 2017 survey. The report describes the available data, model structure, and model estimates, including current and projected stock status. This report fulfils Objective 5 of Project BOM17302, to update the basic model and the revised model from the 2012 assessment (Fu 2013) with new data but with no change to the model structure of Dunn (2005a).

The data available since the last assessment include the revised catch history (numbers of oyster landed in the commercial catch) and unstandardised CPUE (catch and effort data converted to sacks per hour) up to the 2016 fishing year, commercial catch sampling for the size structure of landed oysters in 2013, 2014, 2015, and 2016, and abundance indices (estimates of population sizes for recruit, pre-recruit and small oysters) from the February 2014, 2015, 2016 and 2017 surveys. Commercial catches were 13.2 million oysters in 2013 and 2014, and 10.0 million for 2015 and 2016. Catch rates (sacks per hour) decreased from 6.4 in 2000 to 1.8 in 2005, increased to 5.5 in 2013 and then decreased to 3.8 in 2016. The recruit-sized (legal-sized) population in the stock assessment area increased from 408 million oysters in 2005 to 918 million in 2012, which then decreased to 527 million in 2017.

The Foveaux Strait oyster stock assessment model is a length-based model (instead of the more common age based models) because oysters cannot be aged reliably. In 2017, sensitivity runs were included to test the effect of changes to the CPUE models to account for recent changes in fishing practices such as high-grading. These population models partition Foveaux Strait oysters into length classes 2 mm to 100 mm in groups of 2 mm, with the last group defined as oysters equal to or greater than 100 mm. The oyster population is assumed to reside in a single, homogeneous stock area. The assessment does not take into account the spatial distribution of oyster density within the stock area. The partition accounted for numbers of oysters by length class within an annual cycle where movement between length classes was determined by growth parameters. The values for these growth parameters were fixed in the basic model and estimated in a revised model with the inclusion of mark-recapture data. The revised model incorporated a more complex structure than the basic model, as investigated by Dunn (2007), including: (i) estimation of growth by the inclusion of the growth increment estimates from tag recapture data , (ii) a penalty function on the disease which encourages annual estimates of the rate of disease mortality to be smooth, (iii) decoupling of the maturity and disease selectivity ogive, (iv) removal of the 1976 survey data, and (v) estimation of the relative catchability for the abundance surveys (the base model uses a catchability of 1).

The fishing year (October to September) is divided into two time-steps (Summer and Winter) or ‘periods’, containing different processes accounting for the addition and removal of oysters from each of the length classes. Sexual maturation, growth, half of all natural mortality, and *B. exitiosa* mortality occur in time step 1 (October-February); and recruitment, the rest of natural mortality and fishing (winter) mortality occur in time step 2 (March-September). Natural mortality is assumed to be a constant value of 0.1 y^{-1}, implying a maximum age (at which 1% survive) of 46 years. The models assume disease mortality to be zero in the years when there were no reports of unusual mortality, and otherwise estimated by the model as the numbers of oysters not accounted for by natural mortality and fishing. In the basic model we assume that the proportions of oysters in each length class available to be removed by the disease rate was the same as the proportions of mature oysters. The revised model uses estimates of *B. exitiosa* summer mortality from February surveys.

The updated model estimates of the state of the Foveaux Strait oyster stock show that the stock has declined since 2012 suggesting a trend in stock status reflecting the heightened levels of *B. exitiosa* mortality between 2012 and 2015 (peaking at approximately 20% of recruit sized oysters in 2014) along with recruitment also remaining low during this period. However, along with the indication of a slight increase in recruitment in 2016 there is evidence of a slowing down and levelling in the stock decline in the most recent years (2016 and 2017). Model estimates of spawning stock population in 2017 were about 19% (17–21%) B_0, and recruit size stock abundance was about 16% (14–20%) of the initial state.

These models predict that the rebuilding of the oyster population is expected to be initially slow, but increasing much more quickly in 2019 and 2020 under long-term average *Bonamia* mortality (about 10%) and long-term average recruitment, and with catches below 30 million oysters per year (the highest projected catch tested by the model). Model projections indicate that annual catch levels between 7.5 and 20 million oysters are unlikely to have any detectable impact on future stock status. Depending on the level of assumed disease mortality, projected status in 2020 ranged from about 41% more than current levels (assuming no disease mortality) to a level about 30% less than the current level (assuming disease mortality of 0.2 y^{-1}). Projections were also run out to 2022, with a range in stock status from about 93% more than current levels (assuming no disease mortality) to a level about 32% less than the current level (assuming disease mortality of 0.2 y^{-1}). The levels of uncertainty associated with the 5-year projections was about double that of the three-year projections, and so were not reported in this assessment.

Projections show that recruit-sized stock abundance in future years is primarily dependent on levels of disease mortality (i.e. that catch at recent levels of 10 million oysters per year has little influence on future stock size). Estimates of future stock size, under assumptions of high or nil future disease mortality, ranged (respectively) between 70% and 150% of current levels. The assessment does not account for the numbers of high-density patches important to catch rates and to the transmission of *Bonamia* infection. The two cycles of recovery and decline in stock abundance since the *B. exitiosa* epizootic in the mid-1980s suggest that the latest period of recovery was at a slightly lower level in 2013 compared to 1999, but that the latest level of decline has been at a slower rate and not to as low a level than the previous decline in the late 1980s.

Model developments that incorporate recruitment data and that account for spatially explicit population processes were considered. A method was developed to incorporate a recruitment index (based on spat monitoring data) into the model to better enable useful projections beyond three years. However, this assessment identified the need to better understand the model structure and its influence on levels of uncertainty associated with model estimates of stock status; this work is required before new types of data or any model restructuring are considered. In particular, the parameterisation of additional model processes is not advised for a model more complex than the current one which may already be over-parameterised, particularly in relation to disease processes.

1. INTRODUCTION

Foveaux Strait dredge oysters have been commercially exploited for almost 140 years (Sorensen 1968, Cranfield et al. 1999), with historical records suggesting that commercial landings have totalled about 5000 million oysters since 1907.

Before 2004 the Foveaux Strait oyster fishery was managed by current annual yield (CAY, Method 1, see Ministry of Fisheries Science Group (2006)) based on survey estimates of the population in designated commercial fishery areas. Since 2004, the TACC has been based on estimates of recruit size stock abundance from the Foveaux Strait oyster stock assessment model (Dunn 2005a, 2005b, 2007, Fu & Dunn 2009, Fu 2013) and projections of future recruit size stock abundance under different assumptions of catch limits and heightened mortality from *B. exitiosa* . A co-developed spatially explicit epidemiological model of *B. exitiosa* (Gilbert & Michael 2006) and fish stock model may be used in the future to provide stock assessment of subareas of the fishery.

There were four models used in this assessment. The first two were those used in the previous assessment and the 'basic' model developed by Dunn (2005a, 2005b) using data up to the 2004–05 fishing year, and updated in 2007 (Dunn 2007) with inclusion of catch data up to the end of the 2006–07 fishing year and the February 2007 abundance survey. A more complex variant, where growth data was included and growth parameters estimated within the model (the 'revised' model) was also investigated in that assessment, with other similar data input. Both models were updated in 2009 (Fu & Dunn 2009); in 2010 (D. Fu, unpublished); and in 2013 (Fu 2013). In this report, we update both the basic model and the revised model with the inclusion of data available since the last assessment including the commercial catches and catch sampling, and unstandardized CPUE for the 2013–2016 fishing years, and abundance indices from surveys in 2014–2017 (Table 1).

Table 1: Summary of the data used in the latest three stock assessments (2010, 2012 and 2017). Note, each successive assessment used the data from the previous assessment plus that listed in 'New data available'.

	New data available		
	2010 Assessment	2012 Assessment	2017 Assessment
Commercial catch data:			
Summer season catches	1993–2000		
Winter season catches	1907–2010	2011, 2012	2013–2016
Winter season CPUE	1948–2010	2011, 2012	2013–2016
Commercial length frequency data:			
Winter season catches	1907–2010	2011, 2012	2013–2016
Survey abundance data:			
March dredge survey	1992, 1995, 2005, 2007, 2009, 2010	2012	2014–2017
October dredge survey	1962, 1990, 1993, 1995, 1997, 1999, 2001, 2002		
July dredge survey	1990		
Mark-recapture survey	1974, 1975		
1976 dredge survey	1976		
Survey length frequency data:			
October dredge survey	1999, 2001		
October dive survey	1990		

In addition, the two variants of the above models were investigated to account for changes in fishing practices since 2010 (i.e., a different fishing selectivity after 2010), to try to obtain a better fit of the models to the later CPUE data.

The introduction of five-yearly stock assessments in 2012 placed a greater onus on the annual *Bonamia* surveys to monitor changes in the oyster population in commercial fishery areas as well as the status of *Bonamia* and these changes constitute a new time series of surveys with emphasis on both the status of the oyster population and *Bonamia* mortality (Michael et al. 2016). The first of the new time series of *Bonamia* surveys was undertaken in February 2014 (Michael et al. 2015a), and incorporated a fully randomised, two-phase sampling design and a standard *Bonamia* survey area to make these surveys comparable from year to year (Michael et al. 2016). This stock assessment is the second of the five-yearly assessments, and the first assessment to incorporate the annual survey data from 2014 (Table 1).

The stock assessment was implemented using Bayesian estimation with the general-purpose stock assessment program CASAL v2.20 (Bull et al. 2008). The report describes the available data, model structure and model output. Model estimates, including current and projected stock status, are also presented.

This report fulfils Objective 5 of Project BOM17302, to update the basic model and the revised model from the 2013 assessment (Fu 2013) with new data but with no change to the model structure (Dunn 2005a). Results from this assessment indicate that the basic and revised model structure requires re-evaluation, due to difficulties in fitting the model to the most recent data. Therefore, the inclusion of spat monitoring data and formulating multi-area assessments (Objectives 6 and 7) were not carried out and are being considered as part of project OYS2020-02 for development of the new stock assessment model'.

OBJECTIVES

5. To undertake the OYU5 stock assessment.
6. To evaluate the utility of the spat monitoring data as an early recruitment index in the model.
7. To run assessments in subareas of the fishery to determine their value, and the data required to develop spatially explicit assessments.

2. DESCRIPTION OF THE FISHERY

Oysters have been commercially harvested from around Stewart Island by hand gathering since the 1860s and from Foveaux Strait by dredging since the 1870s. Since then, fishing methods, vessels, and dredges have changed considerably. In the 1870s small sailing cutters, that each towed one small hand-hauled dredge, were used. Oil-powered engines were introduced in 1890 to haul the dredges. By 1913, sailing cutters were replaced with steam-powered vessels that towed two 3.35-m wide dredges weighing about 150 kg. With time, oyster vessels became more powerful and dredges heavier.

Currently oyster vessels tow two steel double-bit dredges, each 3.3–3.35-m wide and weighing 450–530 kg, on steel warps. The dredges are towed simultaneously on the vessel's port side, with each dredge towed off its own derrick. The dredges are usually towed along an elliptical track. Once the dredges are shot the vessel drifts down tide under minimal power turning into the tide to haul. The dredge contents are emptied on to culching benches and the oysters sorted and sized by hand.

Legal sized oysters (those that cannot pass through a 58 mm internal diameter ring) are sorted from the catch and small oysters and bycatch returned to the sea through chutes. Legal sized oysters are packed live into sacks and are landed daily. Oysters are trucked from the docks to opening facilities, mainly in Bluff and Invercargill, on the day of landing. Oysters are shucked by hand the following day and marketed fresh chilled in New Zealand.

Oysters are harvested during a six-month season, defined by regulation (Southland Commercial Fisheries Regulations) as 1 March to 31 August, but oyster fishers determine the season start date between March and early June to avoid disturbing oysters after spawning, meet market demands and, more recently, to avoid increased risk of exacerbating *B. exitiosa*. The quota is usually fully caught some time before the end of August.

Boundaries of statistical areas for recording catch and effort were first established in 1960 (and have been revised periodically since) with the outer boundary of the licensed oyster fishery promulgated in 1979. The western fishery boundary in Foveaux Strait is a line from Oraka Point to Centre Island to Black Rock Point (Codfish Island) to North Head (Stewart Island). The eastern boundary is from Slope Point, south to East Cape (Stewart Island). Foveaux Strait and the current statistical reporting areas are shown in Figure 1.

From the late 1880s to 1962, the fishery was managed by limiting the number of vessels licensed to fish (typically between 5 and 12). The fishery was de-licensed in 1962 and boat numbers had increased to 30 by 1969. Catch limits were introduced between 1963 and 1969. From 1970 vessel numbers were regulated at 23, restricting vessel numbers as well as restricting catch. In 1979 the oyster fishery was declared a licensed fishery for the 23 vessels, closing a loophole that allowed vessels to fish outside the designated fishery area. The number of vessels in the fishery then dropped from 23 in 1996 to 15 in 1997 and 12 in 2002. Since 2004, a total of 11 vessels fished annually.

In 1993 the fishery was closed after a *B. exitiosa* epizootic caused catastrophic mortality of oysters from 1986 to 1992. The fishery was reopened in 1996 with a reduced catch limit. In 1998, individual quotas were granted (Fisheries (Foveaux Strait Dredge Oyster Fishery) Amendment Act 1998) and quota holders permitted to fish their entire quota on one vessel. A second *B. exitiosa* epidemic in 2000 reduced oyster catch rates and resulted in a reduction in catch from about 15 million oysters in 2002 to about 7.5 million oysters since 2003.

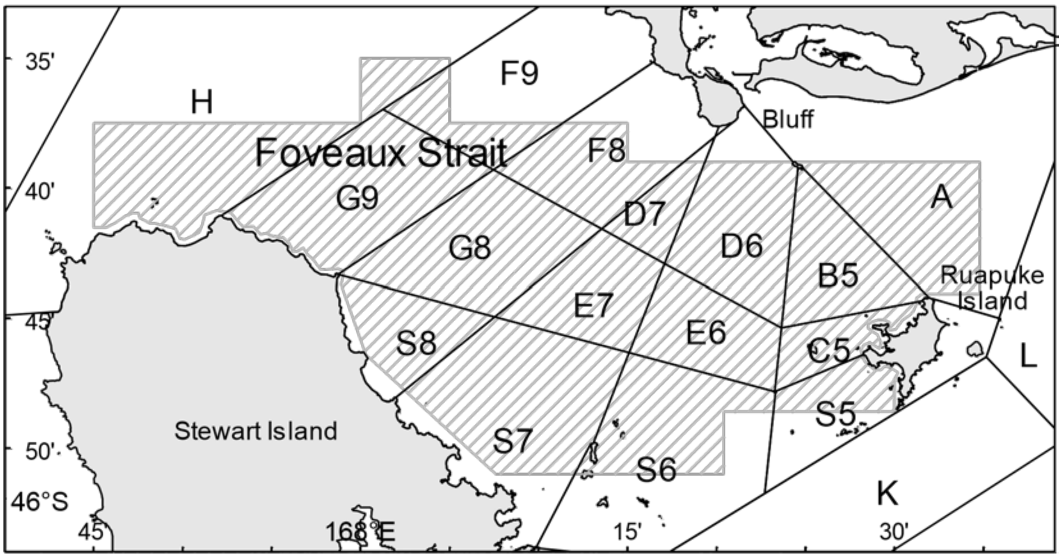

Figure 1: Foveaux Strait (OYU 5) statistical areas, with the shaded region showing the outer boundary of the October 2002 dredge survey and the region of Foveaux Strait considered by the population model.

3. MODEL STRUCTURE, INPUT, AND ESTIMATION

3.1 Model structure

The population models partitioned Foveaux Strait oysters into a single sex population, with length (i.e., the anterior-posterior axis) classes 2 mm to 100 mm, in groups of 2 mm (i.e., from 2 to 4 mm, 4 mm to 6 mm, etc.), with the last group defined as oysters 100 mm or longer. The stock was assumed to reside in a single, homogeneous area. The model accounted for numbers of oyster in each length class within an annual cycle, where movement between length classes was determined by the growth parameters. Oysters entered the partition following recruitment and were removed by natural mortality, disease mortality and fishing mortality.

The model's annual cycle was based on the fishing year, divided into two time-steps, representing summer and winter (Table 2). Note that model references to 'year' within this paper refer to the fishing year, and are labelled as the most recent calendar year, i.e., the fishing year 1998–99 is referred to as '1999' throughout. Any references to calendar years are denoted specifically.

The models were run for the years 1907–2016 (see Section 3.2). Catch data were available for 1907–2016. Catches occurred in both time steps — with special permit and some customary catch assigned to the first time-step (summer fishing mortality), and commercial, recreational, the remaining customary, and illegal catch assigned to the second time step (winter fishing mortality).

Oysters were assumed to recruit at age 1+ (see Section 3.3.1), with a Beverton-Holt stock recruitment relationship (with an assumed steepness of 0.9) and length at recruitment defined by a normal distribution with mean 15.5 mm and CV 0.4. Recruitment was assumed to take place at the beginning of the second time-step (i.e., the time step immediately following summer spawning, but one year on).

Relative year class strengths were assumed known and equal to initial recruitment until 1984 — nine years before the first available length and abundance data on small (oysters less than 50 mm minimum diameter) and pre-recruits (oysters between 50 and 58 mm minimum diameter) were available; otherwise relative year class strengths were deterministic.

Growth and natural mortality were assumed known, except in the revised models where growth was estimated from tag-recapture data. Disease mortality is assumed to be zero in the years when there were no reports of unusual mortality, and otherwise estimated (see Section 3.3.5)

The models used six types of selectivity ogives: the commercial fishing selectivity (assumed constant in each year group and both time steps of the fishery, with year groups based on changes in the definition of legal size, and for the two new models introduced here, by the change in fishing pattern in 2010); a survey selectivity, which was then partitioned into three selectivities (one for each of the size-groups) — small (less than 50 mm minimum diameter), pre-recruit (greater than or equal to 50 mm and less than 58 mm minimum diameter), and recruit (greater than or equal to 58 mm minimum diameter); maturity ogive; and disease selectivity — assumed to follow a logistic curve equal to the maturity ogive (see Section 3.3.5 for detail).

The selectivity ogives for fishing selectivity, maturity, and disease mortality were all assumed to be logistic, where the parameterisation for each length class x was

$$f(x) = 1/\left[1 + 19^{(a_{50}-x)/a_{to95}}\right]$$

where x is the centre of the length class and estimable parameters are a_{50} and a_{to95}.

The overall survey selectivity ogive was assumed to be logistic with an additional parameter a_{min}, that describes the minimum possible value of the logistic curve. The overall survey selectivity ogive was then split into three size categories using a compound selectivity (see Figure 2 for a graphical example of the compound logistic ogive parameterisation). Here, the selectivity of recruit sized oysters was assumed to be the product of the overall selectivity and a standard logistic ogive; the selectivity of pre-recruit sized oysters was assumed to be the product of the overall selectivity and a double logistic ogive; and the selectivity of small sized oysters was assumed to be the product of the overall selectivity and an inverse logistic ogive. Further, values for parameters of the respective selectivities for recruits, pre-recruits, and small oysters were constrained so that they shared common values, i.e.,

$$f_{Overall}(x) = (1 - a_{min})/\left[1 + 19^{(a_{50}-x)/a_{to95}}\right] + a_{min}$$

$$f_{small}(x) = f_{Overall}(x) \times \left(1 - 1/\left[1 + 19^{(b_{50}-x)/b_{to95}}\right]\right)$$

$$f_{Pre-recruit}(x) = f_{Overall}(x) \times 1/\left[1 + 19^{(b_{50}-x)/b_{to95}}\right] \times \left(1 - 1/\left[1 + 19^{(b_{50}+b_{to50}-x)/b_{to95}}\right]\right)$$

$$f_{Recruit}(x) = f_{Overall}(x) \times 1/\left[1 + 19^{(b_{50}+b_{to50}-x)/b_{to95}}\right]$$

where a_{50} is the value of the 50% selectivity of the overall logistic curve, a_{to95} describes its slope, and a_{min} is the minimum value of the curve; b_{50} is the 50% selectivity of the left (inverse) logistic curve and b_{to95} describes its slope; $b_{50} + b_{to50}$ is the 50% selectivity of the right logistic curve and b_{to95} describes its slope; and the middle double logistic is the product of the inverse of the left and right logistics.

Selectivity functions were fitted to length data from the survey proportions-at-length (survey selectivities), and to the commercial catch proportions-at-length (fishing selectivity). The data are described in Section 3.7.

The maximum exploitation rate (i.e., the ratio of the maximum catch to vulnerable numbers of oysters in any year) was assumed to be a relatively medium value and was set at 0.5. No data are available on the maximum exploitation rate, but this value can determine the minimum possible virgin stock size (B_0) allowed by the model.

Table 2: Annual cycle of the population model, showing the processes taking place at each time step, their sequence within each time step, and the available observations. Fishing and natural mortality that occur together within a time step occur after all other processes, with 50% of the natural mortality for that time step occurring before and 50% after the fishing mortality.

Step	Period	Process	Proportion in time step
1	Oct–Feb	Maturation	1.0
		Growth	1.0
		Natural mortality	0.5
		Fishing (summer) mortality	1.0
		B. exitiosa mortality	1.0
2	Mar–Sep	Recruitment	1.0
		Natural mortality	0.5
		Fishing (winter) mortality	1.0

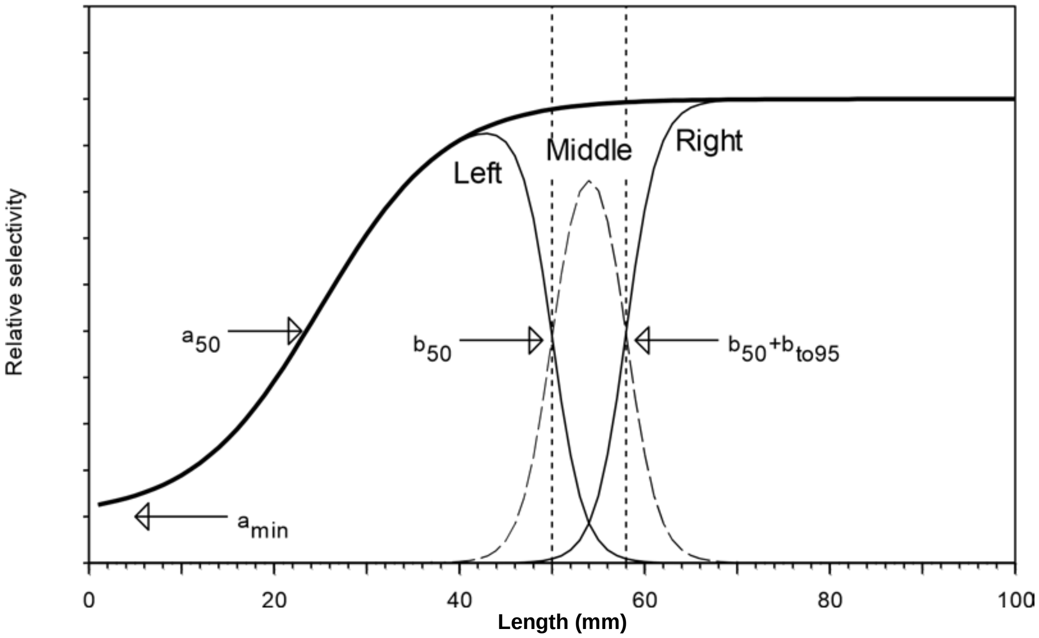

Figure 2: An example of the compound survey selectivity showing the overall selectivity (bold line, where a_{50}=25, a_{to95}=20, and a_{min}=0.1) and compound selectivity (where b_{50}=50, b_{to50}=8, b_{to95}=5) for (Left) small (solid line), (Middle) pre-recruit (dashed line), and (Right) recruit sized (solid line) oysters. Vertical dotted lines show the nominal lengths of pre-recruit (≥ 50 mm and <58 mm) and recruit (≥ 58 mm) size groups.

3.2 2017 model runs

The 2017 basic model is an update of the 2012 basic model from the 2012 assessment (Fu 2013). The 2012 basic model ran for the years 1907–2012 with the inclusion of data up to the end of the 2012 fishing year. This model was updated in this project, with the addition of observations of CPUE, commercial catch proportions-at-length, and catch for the fishing years 2013–2016, and similarly the summer surveys for 2014–2017 were included as a part of the March survey series (i.e., as a pre-fishing season survey, occurring after all summer natural mortality, growth, and *B. exitiosa* disease mortality has occurred). Hence, the model ran from 1907 to 2017, with the commercial catch in 2017 assumed to be 10 million oysters, and the recreational, customary, and illegal catch in 2017 assumed equal to 2016 levels.

Dunn (2007) investigated a more complex model structure in the 2007 assessment (‘revised model’), which included (i) estimation of growth by the inclusion of the growth increment estimates from the tag-recapture data (Section 3.3.2), (ii) a penalty function on the disease to encourage annual estimates of the rate of disease mortality to be smooth, (iii) decoupling of the maturity and disease selectivity ogive, (iv) removal of the 1976 survey data, and (v) estimation of the relative catchability for the abundance surveys (the base model uses a catchability of 1). We also update the revised model with the new data available to 2017, the ‘revised 2017 model’.

The revised model assumed, as with the 2017 basic model, that growth occurred in a single episode at the start of the first time-step, but we estimate the growth parameters with the inclusion of the mark recapture data. Growth data were included in the model as a separate ‘stock’ of fixed size and with growth equal to that of the main population, but with no recruitment and mortality (natural mortality, disease, and fishing mortality). Disease selectivity was decoupled from the maturity ogive and fitted to the disease proportions-at-length, i.e., a 3+ level *B. exitiosa* infection (Diggles et al. 2003).

As a sensitivity test, the basic and revised models were rerun with the CPUE series ‘C’ (1985–2016) split such that C series included years 1985–2009, and an additional fourth series ‘D’ included years 2010–

2016. The rationale for the split was based on the introduction of dredge modifications increasing fishing efficiency and the establishment of fiscal high grading to target oysters greater than 72 mm. These models were labelled ‘2017 basic 4cpue’ and 2017 revised 4cpue’.

3.3 Biological inputs, priors, and assumptions

3.3.1 Recruitment

Spat monitoring data and the numbers of 0+ oysters landed on commercial sized oysters provide indices of early recruitment. These two indices are highly correlated over time with a Pearson’s correlation coefficient of 0.96 ($p < 0.001$) (Keith Michael, NIWA, unpublished data).

Relative year class strengths were assumed to average 1.0 over all years of the model and, further, relative year class strengths in the period before 1985 were assumed constant and defined to be equal to the initial recruitment. Lognormal priors on relative year class strengths were assumed, with mean 1.0 and CV 0.2.

Spawning stock size is not a reliable predictor of recruitment to the population or the fishery. Low recruitment can persist during periods of high spawning stock size and spawner densities (Michael & Shima 2018) and can be high at times of low spawning stock size and spawner densities (Michael et al. 2019a).

Typically, recruitment for sessile organisms is highly variable and often environmentally driven (see Jamieson & Campbell 1998). A strong recruitment pulse was observed in the fishery between 1993 and 2000, suggesting that high levels of recruitment are plausible during periods of low abundance. More recently, even at low stock levels, the numbers of small oysters found in population surveys have remained relatively high. Here, we assumed a Beverton-Holt stock-recruit relationship, with steepness of 0.9 to reflect that recruitment is not strongly dependent on spawning stock size.

Oysters entered the partition at age 1+, prior to growth as 2 year-olds. The distribution was assumed to be normally distributed with mean 15.5 mm and CV 0.4, truncated at 2 mm (Figure 3). These values were based on experiments that collected spat settlement and growth data (H.J. Cranfield, NIWA, pers. comm.).

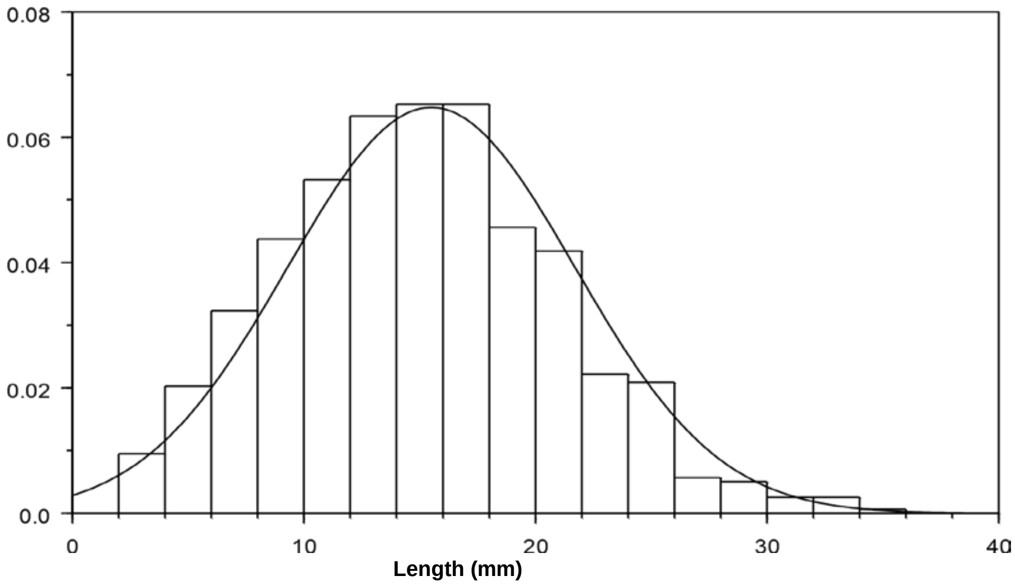

Figure 3: Size at recruitment for 1+ spat (H.J. Cranfield, NIWA, pers. comm.), overlaid with the assumed distribution for recruiting oysters — normal with mean 15.5 mm and CV 0.4.

3.3.2 Growth tag data and growth estimates

Growth increment data (Dunn et al. 1998b) were available for two samples of oysters marked and retained in cages anchored to the sea floor in Foveaux Strait in 1979 and 1981 (n = 259 and 395 respectively with lengths at release 10–84 mm). The samples were subsequently re-measured in 1980–1982 and 1982 respectively.

Dunn et al. (1998b) estimated growth rates from this experiment using a modified, length-increment von Bertalanffy growth model based on maximum likelihood mixed effects models. However, growth estimates from Dunn et al. (1998b) were seasonal, and allowed for areal, yearly, and breakage effects. The complexity of these processes cannot easily be reproduced within the population model and hence the data were re-fitted using the maximum likelihood von Bertalanffy growth model, based on the parameterisation of Francis (1988), i.e.,

$$\Delta L = \left(\frac{\beta g_\alpha - \alpha g_\beta}{g_\alpha - g_\beta} - L_1\right)\left(1 - \left[1 + \frac{g_\alpha - g_\beta}{\alpha - \beta}\right]^{\Delta t}\right)$$

where ΔL is the expected increment for an oyster of initial size L_1; g_α and g_β are the mean annual growth increments for oysters with arbitrary lengths α and β. Variation in growth was normally distributed with $\sigma = \max(c\mu_i, \sigma_{min})$ (where c is the coefficient of variation, σ_{min} is the minimum standard deviation, and μ_i is the expected growth at length L) truncated at zero.

The likelihood was then defined as (M.H. Smith, NIWA, pers. comm.);

$$L_i(\mu_i, \sigma_i, \sigma_E) = \frac{1}{\sigma_E}\phi\left(\frac{y_i}{\sigma_E}\right)\Phi\left(-\frac{\mu_i}{\sigma_i}\right) + \frac{1}{\sqrt{\sigma_i^2 + \sigma_E^2}}\phi\left(\frac{y_i - \mu_i}{\sqrt{\sigma_i^2 + \sigma_E^2}}\right)\Phi\left(\frac{\sigma_i^2 y_i + \sigma_E^2 \mu_i}{\sqrt{\sigma_i^2 \sigma_E^2(\sigma_i^2 + \sigma_E^2)}}\right)$$

where y_i is the measured growth increment for the ith oyster; μ_i and σ_i are the expected growth (truncated at zero to exclude the possibility of negative growth) and standard deviation respectively; σ_E is the standard deviation of measurement error (assumed to be normally distributed with mean zero); and ϕ and Φ are the standard normal probability density function and cumulative density function respectively.

Winter length measurements were ignored, and hence annual growth increment measurements only were considered. The growth parameters at $\alpha = 30$ and $\beta = 55$ were estimated outside the population model, as $g_\alpha = 11.91$ mm and $g_\beta = 3.61$ mm; variation in growth had an estimated CV of c = 0.31 and $\sigma_{min} = 4.45$ mm; and estimated measurement error σ_E was 2.12 mm. The (annualised) growth data are shown in Figure 4, overlaid with the growth model (and 95% confidence intervals) used in the population model.

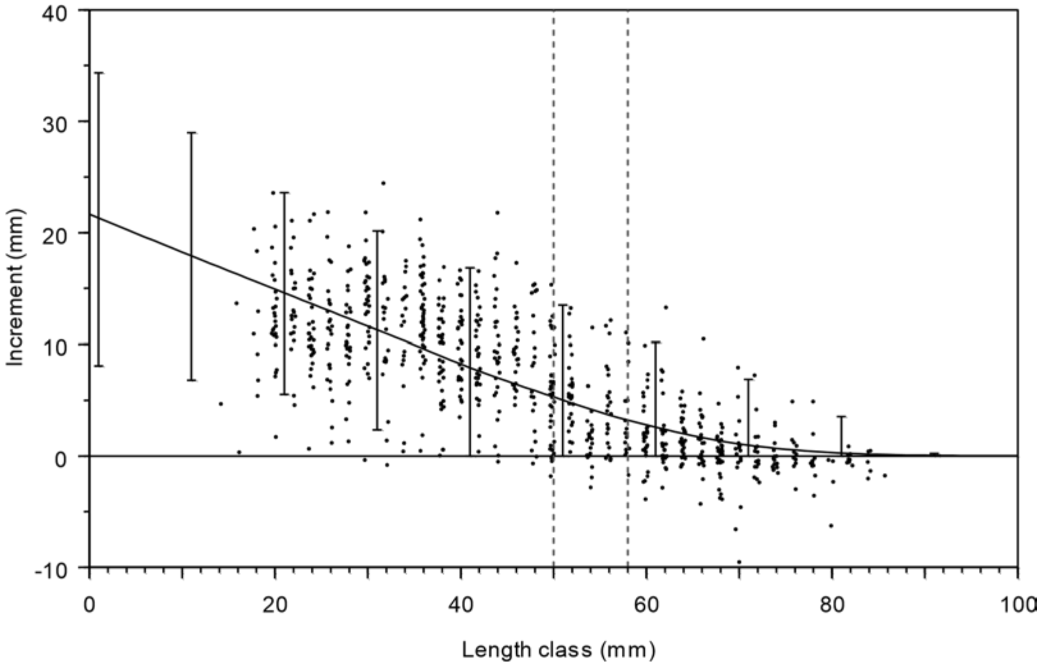

Figure 4: Initial size and mean annual increment data from Dunn et al. (1998b). Lines (and 95% confidence intervals) indicate the growth model assumed in the population model, and dashed lines separate the small (<50 mm), pre-recruit (≥ 50 mm and <58 mm), and recruit (≥ 58 mm) size groups.

In the revised 2007 model, Dunn (2007) estimated growth using the tag-recapture data. Observations of the length of the recaptured caged oysters, given their release length and time at liberty, were fitted with a multinomial likelihood, and were based on the observed proportions-at-length given the expected proportions-at-length from the marked population with the sample size equal to the number of individuals observed, i.e.,

$$-\log(L_t) = -\log(N_t!) + \sum_t [\log((N_t O_{ti})!) - N_t O_{ti} \log E_{ti}]$$

where N_t = the number of observed oysters at time *t*, O_{ti} = proportion of oysters at length *i* that were observed at time *t*, and E_{ti} = expected proportion of oysters at length *i* in the population at time *t*.

Stead (1971a) also carried out tagged growth measurements between 1960 and 1964. The raw data for that study are not available and therefore were not used in this analysis.

3.3.3 Maturity

Foveaux Strait dredge oysters are protandrous hermaphrodites that breed during the late spring and summer. Most (70–90%) develop male gonads and only a small proportion (10–12%) breed as females (Jeffs & Creese 1996). Jeffs & Hickman (2000) estimated measures of maturity from the re-analysis of sectioned oyster gonads. The data for the proportion of oysters with female ova during October– March were used to determine the maturity ogive within the model. Figure 5 shows the estimated proportions mature (i.e., proportions of oysters with presence of female ova) by length class, along with exact 95% confidence intervals.

Maturity was not considered to be a part of the model partition, and proportions mature were fitted within the population model with a logistic ogive (see earlier) using a binomial likelihood (Bull et al. 2008).

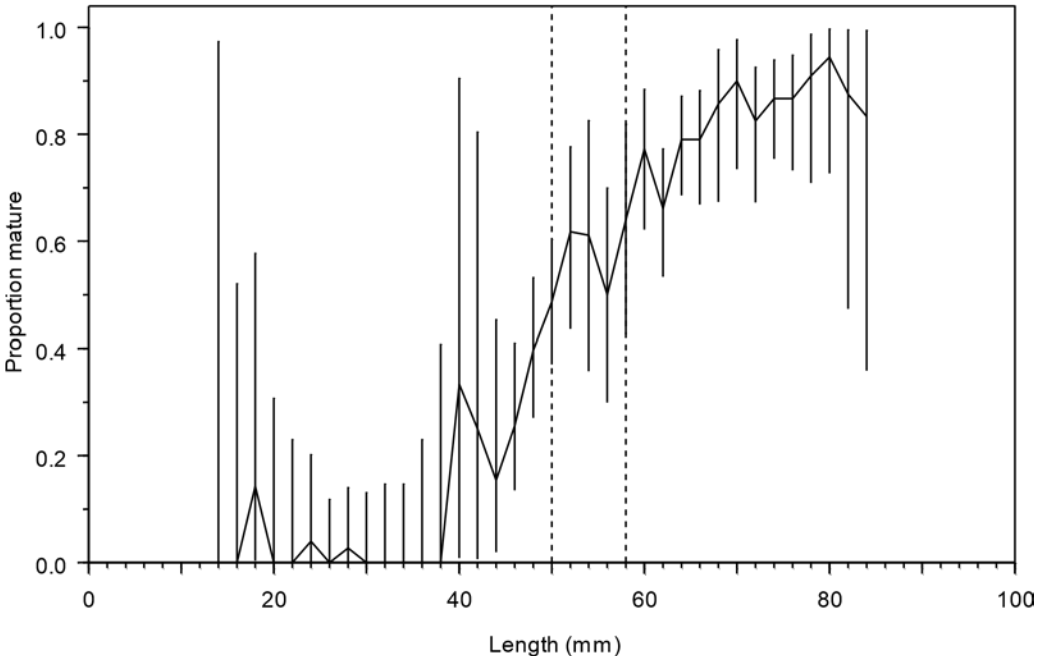

Figure 5: Proportions of mature oysters (defined as the proportion of oysters with female ova) by length (Jeffs & Hickman 2000). Vertical bars give exact 95% confidence intervals, and dashed lines separate the small (<50 mm), pre-recruit (≥ 50 mm and <58 mm), and recruit (≥ 58 mm) size groups.

3.3.4 Natural mortality

Dunn et al. (1998a) estimated natural mortality *M* for the years 1974 to 1986 by re-analysing data from Cranfield & Allen (1979). Estimated natural mortality was found to increase from 0.017 y^{-1} to 0.188 y^{-1} from 1974 to 1986 for oysters released in 1974, and from 0.009 y^{-1} to 0.199 y^{-1} for oysters released in 1973. Dunn et al. (1998a) concluded that they were unable to determine how good these estimates of natural mortality were, and they suggested that the observed increase in rates of *M* with time may be related to senescence.

A constant value for natural mortality of 0.1 y^{-1} was assumed, implying a maximum age (at which 1% survive) of 46 years. However, there were few data available, other than Dunn et al. (1998b), on which to base this assumption — except that two oysters tagged at recruit size (one from 1973 and one from 1976 or 1977 — see Cranfield & Allen (1979)) were recaptured (live) in early 2003 (K.P. Michael, NIWA, pers. comm.), suggesting that the value of *M* plus *F* was not high, as at least two oysters lived to recruit size and survived a further 26–29 years.

3.3.5 Disease mortality

Data on disease mortality events in the early years are limited. Anecdotal reports exist of a mortality event during the late 1940s (H.J. Cranfield, pers. comm.). Stead (1971b) noted that "during a parasite outbreak in 1960–63 many oysters died; this caused a sharp decline in dredging catch rates". In addition, Stead (1971b) reported the height frequencies of 11 576 live oysters and 8 612 clocks (i.e., articulated shells of recently dead oysters with the ligament attaching the two valves intact) from Foveaux Strait, suggesting that clocks made up about 43% of the catch — a rate similar to that found in abundance surveys during the *B. exitiosa* epidemics in the early 1990s and early 2000s. Hine (1996) later noted that the most likely cause of the mortality during the 1960s was *B. exitiosa*.

No other reports exist of unusual mortality events in the Foveaux Strait fishery until the late 1980s. The *B. exitiosa* outbreak in the late 1980s was thought to have started in 1985–86, with evidence of continued *B. exitiosa* mortality up until March 1995. No further evidence of unusual mortality was found in the fishery until the summer of 2000. Disease mortality is set to zero for 1907–48 (the period before any abundance estimates); 1952–59 (to allow for disease mortality in the late 1940s); 1967–84 (to allow for disease mortality in the early 1960s); and 1996–99 (to allow for the epizootic in the late 1980s and the subsequent epizootic in 2000). Where disease mortality was estimated, a normal prior with mean -0.2, standard deviation 0.2, and bounds [0.0, 0.8] was used (see Figure 6). The derivation of this prior is undocumented and it appears to be a subjective proposal by Dunn (2005a,b) to enable the assessment to proceed.

At the time of the model by Dunn (2005a), there were no studies that quantified the relationship between disease mortality, oyster length, or oyster maturity. Dunn (2005a) assumed that it was the same as the maturity ogive. He based this on the relationship inferred from the proportion-by-length of oysters infected with *B. exitiosa* (stage 1 or greater) from the October 2001, January 2002, March 2002, October 2002, and February 2003 surveys (Figure 7), and data published by Stead (1971b) on relative catches of live oysters and clocks in the 1960–64 survey (Figure 8). We assume that the disease ogive was equal to the maturity ogive in the 2017 basic model.

B.K. Diggles (NIWA, unpublished data) analysed 500 oysters from a survey in January 2004 for *B. exitiosa* infection, sex, and maturity with lengths between 24 and 81 mm. These data provide information on the disease selectivity of oysters and can be used to determine a length-based selectivity of *B. exitiosa* (Figure 9). These data are included within the revised 2017 model to estimate the disease selectivity ogive.

The disease selectivity ogive was therefore assumed to be the same as the maturity ogive, i.e. that disease causes oyster mortality, for each length class, at a rate equal to the maturity selectivity multiplied by the estimated yearly rate. However, other relationships may have considerable effect on model estimates.

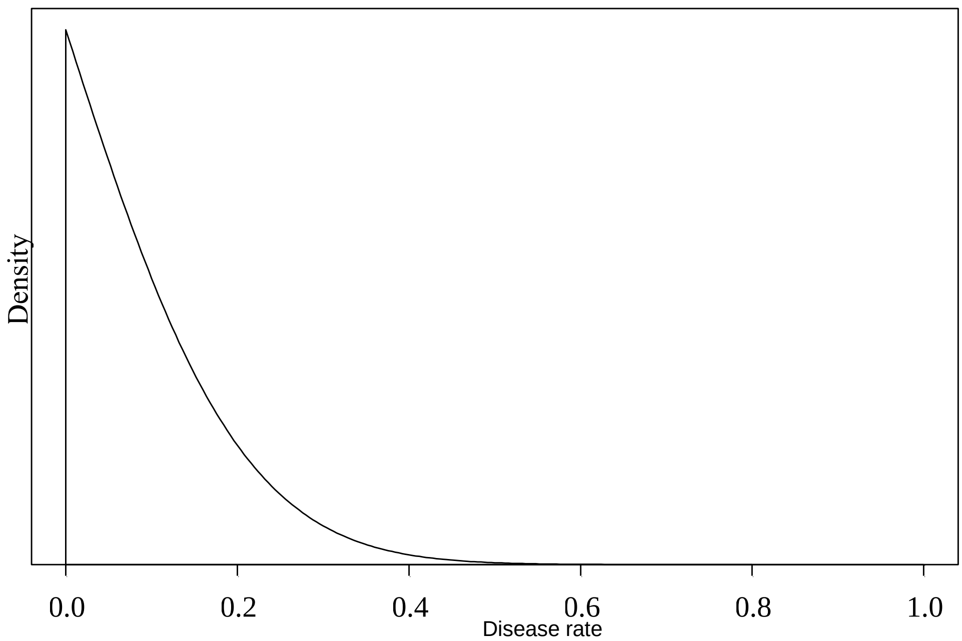

Figure 6: Prior assumed for the rate of disease mortality (normal with mean –0.2, standard deviation 0.2, and bounds [0.0–0.8]).

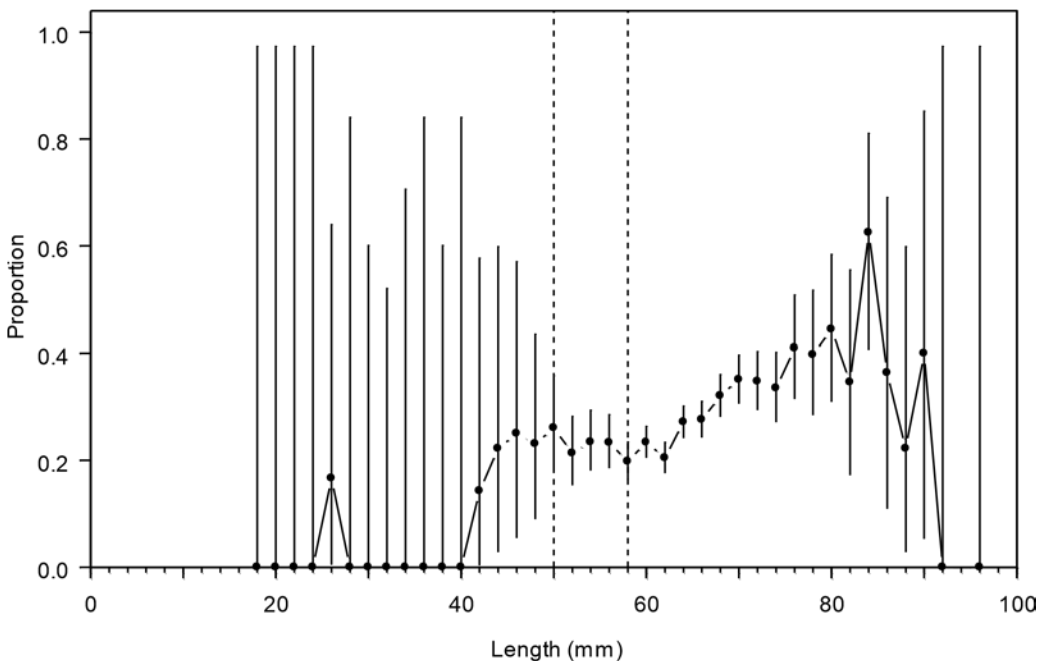

Figure 7: Proportions of oysters (and 95% confidence intervals) with a *B. exitiosa* infection of level 1+ from *B. exitiosa* sampling in the October 2001, January 2002, March 2002, and October 2002 surveys by length. Dashed lines separate the small (<50 mm), pre-recruit (≥ 50 mm and <58 mm), and recruit (≥ 58 mm) size groups.

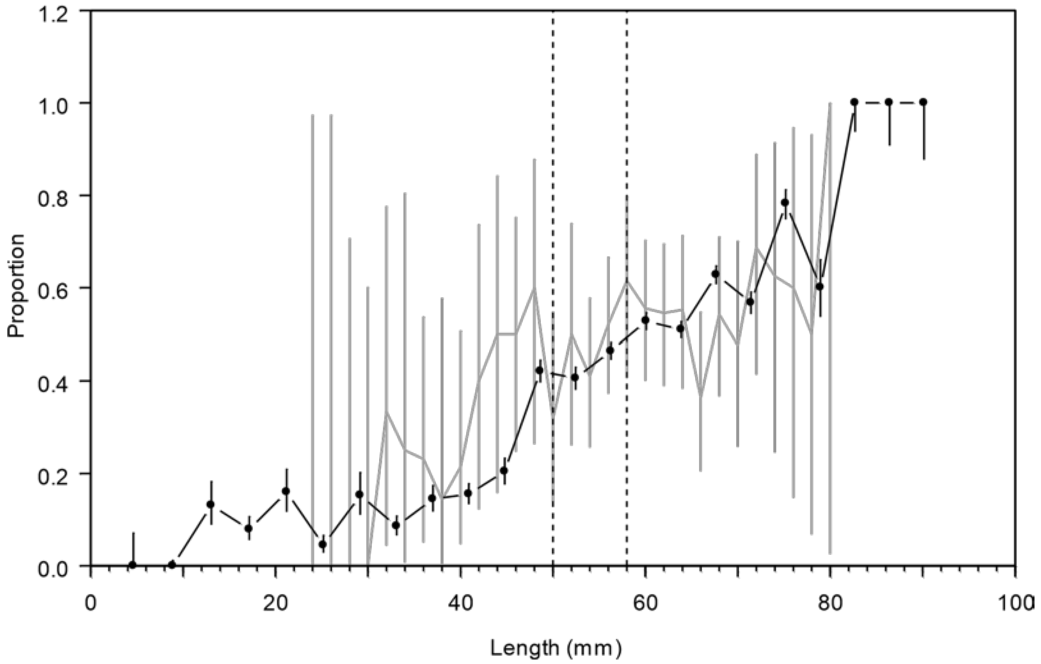

Figure 8: Proportions of clocks (and 95% confidence intervals) in the catch from the 1960–64 survey by length (solid circles and lines, data reproduced from a figure in Stead 1971b), overlaid with the proportion of mature oysters (and 95% confidence intervals) by length derived from Jeffs & Hickman (2000). Dashed lines separate the small (<50 mm), pre-recruit (≥ 50 mm and <58 mm), and recruit (≥ 58 mm) size groups.

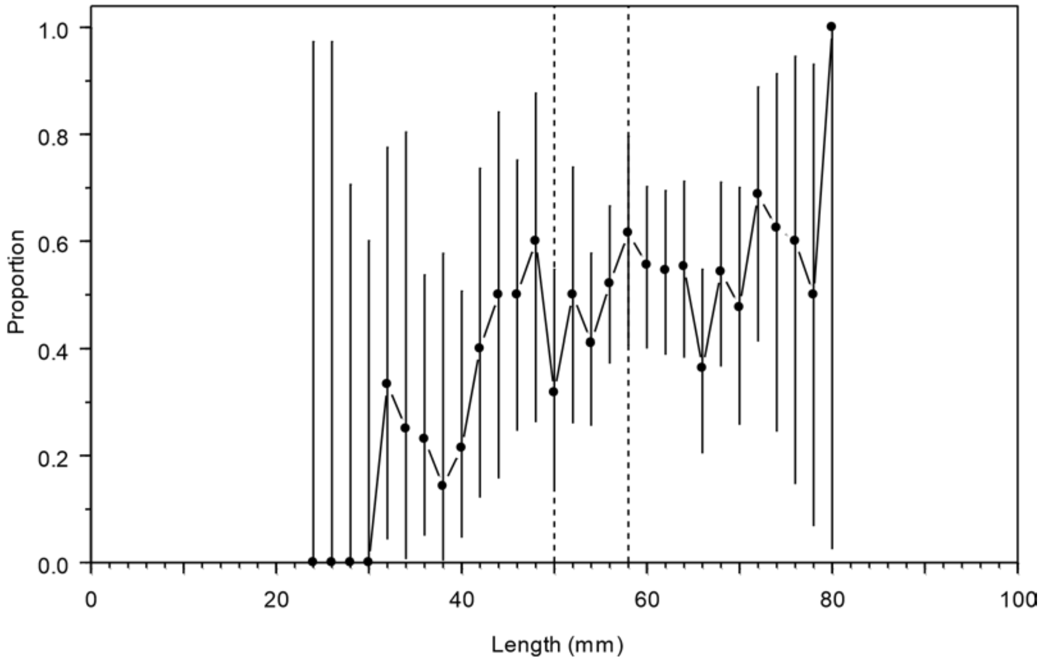

Figure 9: Proportions of oysters (and 95% confidence intervals) with a *B. exitiosa* infection of level 1+ from *B. exitiosa* histological sampling from the January 2004 surveys by length (B.K. Diggles, NIWA, unpublished data). Dashed lines separate the small (<50 mm), pre-recruit (≥ 50 mm and <58 mm), and recruit (≥ 58 mm) size groups.

3.4 Commercial catch data

3.4.1 Winter season commercial catch

The total commercial catch of oysters in Foveaux Strait has been recorded since at least 1907, initially in annual reports of the Marine Department, and later by MAF (Fisheries), the Ministry of Fisheries, and the Ministry for Primary Industries. The recorded catch was in “sacks” of oysters up to 1997, and total numbers of oysters since. The catch history (converted to millions of oysters) is given in Table 3 and Figure 10.

The conversion rate of 774 oysters per sack was reported by Cranfield et al. (1999). Data from early Marine Department annual reports (where measures of dozens of oysters and sacks of oysters were occasionally referred to together) suggest that this figure is broadly correct. The Annual Report of the Marine Department (1910) suggested a figure of 1103 oysters per sack, while the Report of the Sea Fisheries Investigation Committee (1937–38) suggested a figure of 720 oysters per sack. The Marine Department Report on Fisheries (1944) reported that the mean number of oysters in a sack in 1943 “had increased from 62–65 dozen (744–780) to 70–80 dozen (840–960)” as a result of the declining quality (size) of oysters at that time.

Before 1929 the minimum takeable size limit was defined as 44.45 mm (1.75 inches) minimum diameter, increased to 50.8 mm (2.0 inches) in 1929, then increased again to 53.975 mm (2.125 inches) in 1941. In 1969, a takeable size limit of 57.15 mm (2.25 inches) minimum diameter was introduced, where it has remained since. The shape of the fishing selectivity ogive was assumed to have remained constant and was defined by the size selectivity determined by model fits to the commercial catch sampling in 2002–08. But the changes in the legal size were allowed for by shifting the selectivity curve to the left by 12.700 mm (0.5 inches) for years before 1929, 6.350 mm (0.25 inches) for 1929 to 1940, and 3.175 mm (0.125 inches) for 1941 to 1968.

Table 3: Total fishing season (winter) landings of Foveaux Strait oysters 1901–2012 (millions of oysters; sacks converted using numbers assuming a conversion rate of 774 oysters per sack for 1909–92). (Data from 1901–71 from Marine Department Annual Reports, 1972–94 MAF (Fisheries), 1996–2008 QMS.), '–' denotes not available. The catch given for the 2017 fishing season is assumed.

Year	Catch	Year	Catch	Year	Catch	Year	Catch	Year	Catch
1901	–	1926	21.54	1951	70.15	1976	89.06	2001	14.79
1902	–	1927	16.26	1952	72.51	1977	92.14	2002	14.45
1903	–	1928	30.03	1953	55.44	1978	96.4	2003	7.46
1904	–	1929	30.44	1954	51.29	1979	88.36	2004	7.48
1905	–	1930	33.11	1955	60.84	1980	88.41	2005	7.48
1906	–	1931	28.28	1956	58.63	1981	89.04	2006	7.47
1907	18.83	1932	29.01	1957	60.14	1982	87.98	2007	7.37
1908	17.34	1933	32.64	1958	64.44	1983	89.06	2008	7.49
1909	19.19	1934	40.44	1959	77	1984	89.01	2009	8.22
1910	18.2	1935	38.48	1960	96.85	1985	81.79	2010	9.68
1911	18.9	1936	49.08	1961	84.3	1986	60.22	2011	10.48
1912	19	1937	51.38	1962	53.42	1987	47.64	2012	12.06
1913	26.26	1938	52.05	1963	57.86	1988	67.81	2013	13.5
1914	19.15	1939	58.16	1964	73.51	1989	65.81	2014	13.49
1915	25.42	1940	51.08	1965	95.3	1990	35.69	2015	10.07
1916	22.61	1941	57.86	1966	124.14	1991	41.8	2016	10.29
1917	17.2	1942	56.87	1967	127.2	1992	4.51	2017	10
1918	19.36	1943	56.59	1968	113.93	1993	0		
1919	16.56	1944	49.5	1969	51.3	1994	0		
1920	20.67	1945	58.85	1970	87.92	1995	0		
1921	19.01	1946	69.16	1971	89.08	1996	13.41		
1922	21.11	1947	63.09	1972	77.43	1997	14.82		
1923	22.28	1948	73.1	1973	97.45	1998	14.85		
1924	18.42	1949	75.34	1974	92.47	1999	14.94		
1925	20.01	1950	58.09	1975	88.78	2000	14.96		

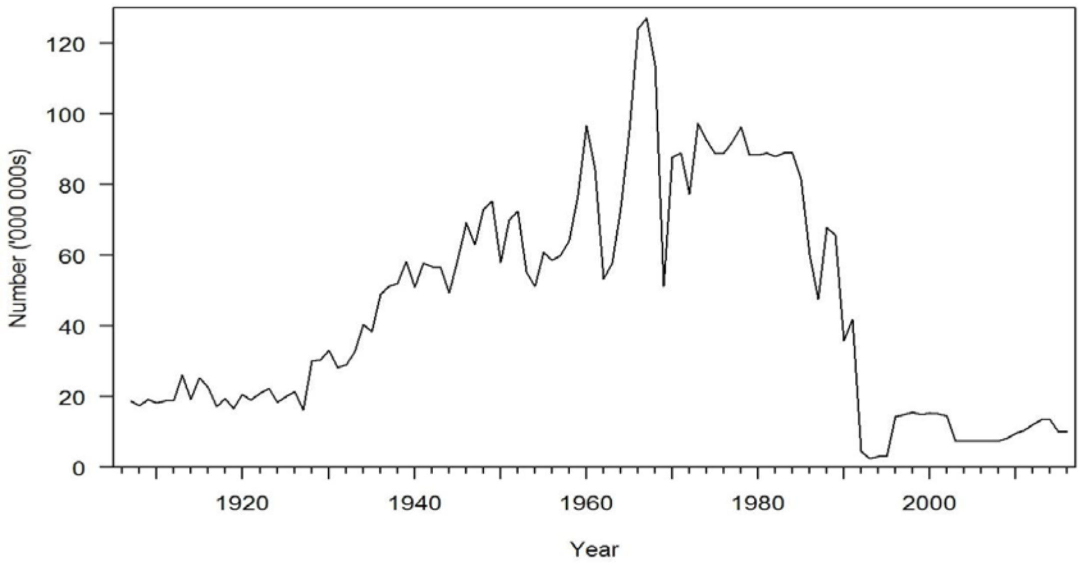

Figure 10: Total commercial catch (winter and summer) by year (millions of oysters), 1907–2016.

3.4.2 Summer season catches made under special permits

Between 1992 and 2000, the Bluff Oyster Management Company Ltd. was granted a special permit to catch oysters during the breeding season as part of their study of the viability of enhancing the oyster population using spat settled on oyster shell. These were issued for the summer period (November–February), and were in addition to the usual commercial catch (Table 4).

Table 4: Reported oyster catch of vessels fishing under special permits for Bluff Oyster Management Company Ltd. 1992–93 to the 1999–2000 fishing years. Fishing took place over the summer season (November– February). No special permit was issued for the 1998–99 fishing year.

Year	Number (millions)	Year	Number (millions)	Year	Number (millions)
1993	2.43	1996	0.93	1999	0.00
1994	3.09	1997	0.20	2000	1.00
1995	3.03	1998	0.72		

3.4.3 Length frequency of the winter season commercial catch

Length samples from the commercial catch were taken during each fishing season from 2002 to 2016 (except for 2014). The number of oysters measured each season and the associated catch sampling report are listed in Table 5. Estimates of the catch-at-length frequencies (with associated CVs) of the commercial catch were derived using catch-at-age software (Bull & Dunn 2002), using 2 mm length classes, and CVs were calculated by bootstrapping. The software scaled the length frequency from each stratum up to the total catch to yield length frequency distributions by stratum and overall (Figure 11). Strata were defined from the sampling regime, where each vessel's catch was sampled at approximately two-week intervals.

Proportions at length were included in the model with a multinomial likelihood. The effective sample sizes for the length frequency data with a multinomial likelihood were estimated by calculating a sample size that represented the best least squares fit of $\log(cv_i) \sim \log(P_i)$, where cv_i was the bootstrap CV for the ith proportion, P_i. Estimated and actual sample sizes are given in Table 5, and a plot of the $\log(cv_i) \sim \log(P_i)$ relationship in Figure 12.

Table 5: Actual sample sizes and effective sample sizes determined for the multinomial likelihood for the commercial catch proportions at length data.

Year	Total	Effective	Catch sampling report
2002	15 580	11 795	Michael et al. 2004a
2003	18 940	12 740	Dunn & Michael 2006
2004	–	–	–
2005	6 509	5 072	Dunn & Michael 2006
2006	6 801	4 818	Dunn & Michael 2007
2007	6 829	5 383	Dunn & Michael 2008
2008	6 831	5 177	Dunn & Michael 2009
2009	7 010	5 698	Fu et al. 2009
2010	6 798	6 199	Fu et al. 2010
2011	7 034	5 653	Fu et al. 2011
2012	7 029	5 737	Fu et al. 2012
2013	6 807	5 443	Fu et al. 2014
2014	21 336	16 599	Fu et al. 2015
2015	15 202	12 076	Marsh et al. 2016
2016	17 603	13 163	Large et al. 2018

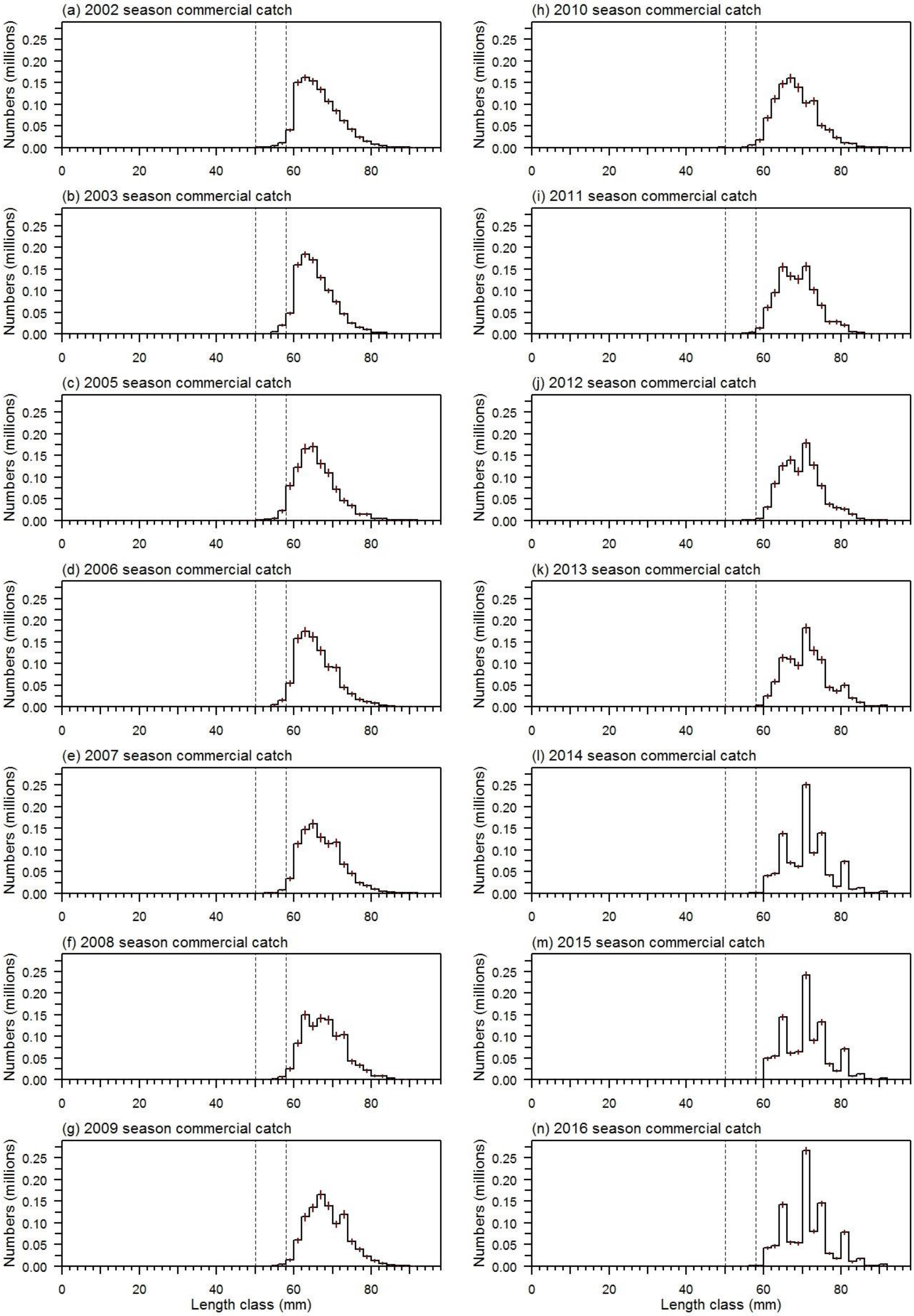

Figure 11: Estimated commercial length frequency distributions for the years 2002–2009 (a-g) and 2010-2016 (h-n), vertical lines on bars indicating the approximate 95% bootstrapped confidence intervals. Dashed lines indicate length breaks for small (<50 mm), pre-recruit (≥ 50 mm and <58 mm) and recruited (≥ 58 mm) size groups.

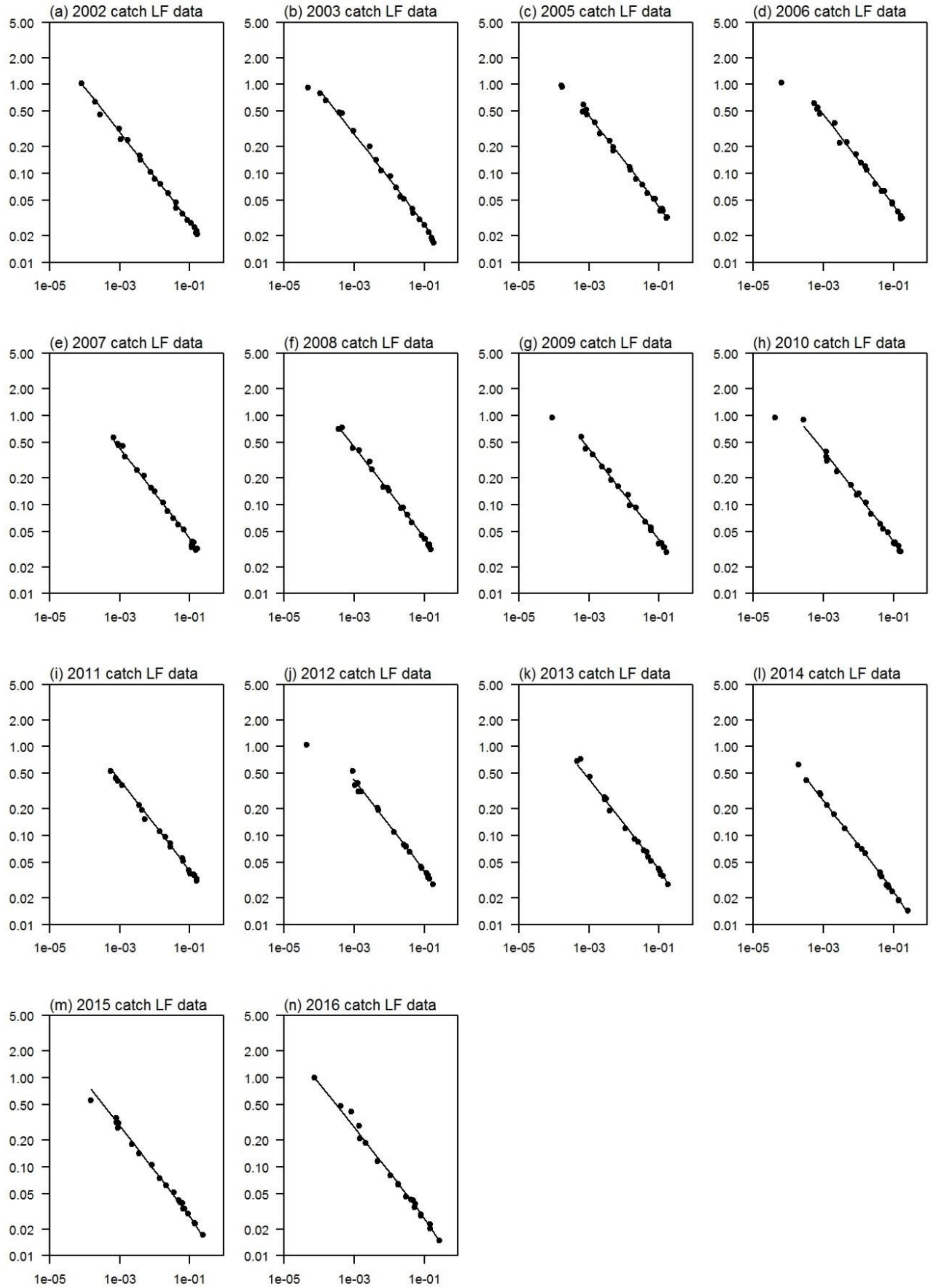

Figure 12: Estimated proportions (x-axis) versus CVs (y-axis) for the commercial catch length frequencies for the 2002, 2003, and 2005–2016 fishing years. Lines indicate best least squares fit for the effective sample size of the multinomial distribution.

3.5 Non-commercial catch

The non-commercial catch is made up of recreational, customary, and illegal catch (described below). Non-commercial catch is poorly estimated but may be as high as 8% of the commercial catch in recent years (Figure 13).

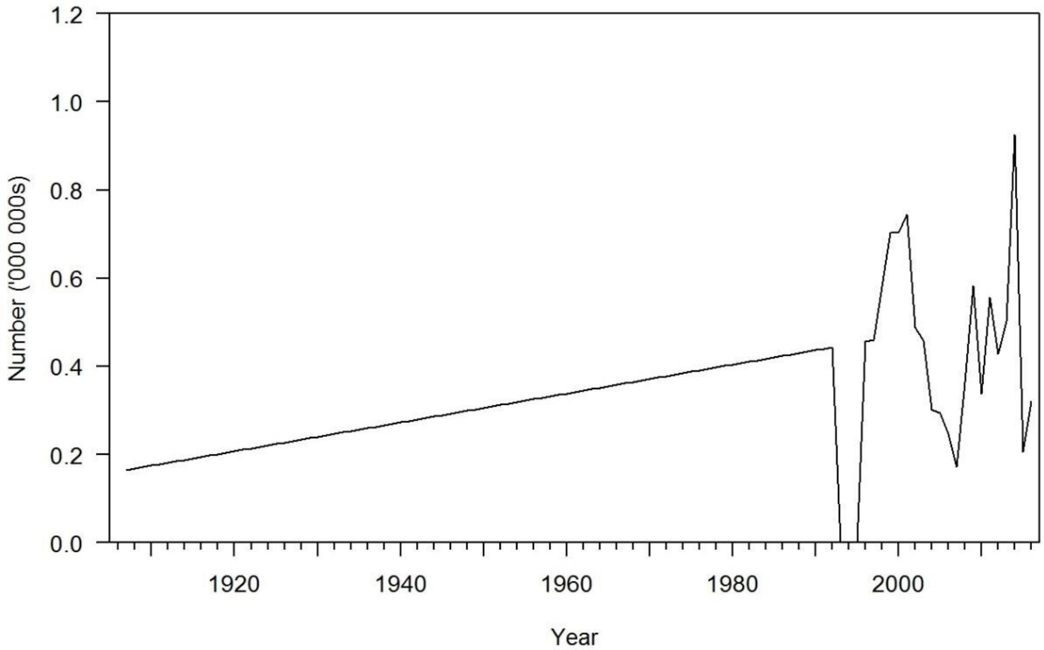

Figure 13: Total non-commercial catch (winter and summer) by year (millions of oysters), 1907–2016.

3.5.1 Recreational catch

The Ministry of Fisheries commissioned two surveys of recreational fishing, the South region 1991–92 survey (Teirney et al. 1997) and the 1996 national survey (Bradford 1998). However, the catch of oysters cannot be reliably estimated from these surveys because of the small number of local respondents who reported catches of oysters in their diaries. The Southland Recreational Marine Fishers Association estimated the annual recreational catch of oysters in Foveaux Strait in 1995 to be about 390 sacks (equivalent to 387 000 oysters) (Ministry of Fisheries Science Group 2006). Ministry of Fisheries officials believe the catch has increased significantly since (Ministry of Fisheries Science Group 2006). The recreational catch reported by commercial fishers between 2002 and 2016 is summarised in Table 6.

The Ministry of Fisheries estimated that commercial oyster fishers land an additional 140 000 oysters as amateur catch during the fishing season (as commercial fishers are entitled to a recreational catch of 50 oysters per fisher per day). Hence, the best estimate of the total recreational catch is about 430 000 (500 sacks) (Ministry of Fisheries Science Group 2006). The reliability of these estimates of recreational catch is not known.

The recreational catch in each year was assumed to have increased linearly from 150 000 in 1907 to 430 000 in 2003, and linearly since — except that the recreational catch in 1993–95 (when the fishery was closed) was assumed to be zero. Further, the recreational harvest was assumed to take place over the winter season with a selectivity equal to the commercial fishing selectivity.

Table 6: Reported recreational catch by commercial fishers (numbers) from 2002 to 2016 (source: Ministry for Primary Industries data extract 11118).

Year	Number	Year	Number
2002	236 103	2010	194 306
2003	282 645	2011	179 587
2004	146 567	2012	219 068
2005	190 345	2013	231 816
2006	139 252	2014	678 987
2007	90 544	2015	187 489
2008	141 587	2016	188 951
2009	182 331		

3.5.2 Customary catch

Reporting of Māori customary harvest is specified in the Fisheries (South Island Customary Fisheries) Regulations 1999. Ngāi Tahu reports customary catch of Foveaux Strait oysters to the Ministry for Primary Industries quarterly (Table 7). The customary catch in each year was assumed to be equal to the reported catch, but with all catch allocated to the winter season (i.e., the dominant season for customary harvest, see Table 6). Further this is assumed to take place with a selectivity equal to the commercial fishing selectivity.

Table 7: Reported customary catch (numbers) between 1 July 1998 to 31 December 2016 by year and quarter from Kaitiaki data collected by Ngāi Tahu. '–' denotes not available (source: Ministry for Primary Industries data extract 11118).

Year	1 Jan–31 Mar	1 Apr–30 Jun	1 Jul–30 Sep	1 Oct–31 Dec	Total
1998	–	–	106380	37560	143 940
1999	0	107520	69 840	–	177 360
2000	63 582	113634	34 356	11 760	223 332
2001	25 514	136 973	72 996	23 760	259 243
2002	–	117 219	67 116	–	184 335
2003	1 560	85 920	45 840	–	133 320
2004	26 546	9 820	91 342	–	127 708
2005	43 320	25 920	7 224	9 360	85 824
2006	306	30 492	45 100	20 520	75 898
2007	–	44 880	–	64380	109 260
2008	42 528	59 700	22 964	77 760	202 952
2009	72 562	182 584	14 484	24 780	294 410
2010	35 868	22 310	29 480	170 760	258 418
2011	79 286	46 440	30 040	166 732	322 498
2012	840	3 180	–	98 970	102 990
2013	4 980	70 210	49 560	–	124 750
2014	17 080	88 728	57 180	–	162 988
2015	102 450	73 434	46 068	–	221 952
2016	7 020	–	–	–	7 020

3.5.3 Illegal catch

The Ministry of Fisheries estimated the illegal catch of oysters for the 1998 and 1999 fishing years to be about 10% of the total non-commercial catch — 66 436 oysters. However, this estimate cannot be verified (Ministry of Fisheries Science Group 2006).

The illegal catch in each year was assumed to be equal to exactly 10% of the sum of the recreational and customary catch in each year. Further, this is assumed to take place over the winter season with a selectivity equal to the commercial fishing selectivity.

3.5.4 Incidental mortality

Cranfield et al. (1997) investigated the incidental mortality of oysters from a single encounter with a dredge in March 1997. They found that a light dredge (320 kg) caused less damage and resulting mortality than a heavy dredge (550 kg). Mortality resulting from both types of dredge was inversely proportional to the size of the oysters. They concluded that recruited oysters appeared robust to dredge encounters (1–2% mortality from the heavy dredge), but pre-recruits were less so (6–8% mortality). Spat were very fragile and many were killed. The mortality of spat less than 10 mm in height ranged from 19 to 36%.

As these mortality estimates are low, and the estimated level of fishing mortality (see Results) was also low, the effects of incidental dredge damage or mortality are ignored in this model.

3.6 Resource surveys and other abundance information

3.6.1 Absolute abundance estimates

Resource surveys of Foveaux Strait dredge oysters have been conducted since 1906 (Hunter 1906). However, different survey designs, areas of coverage, and dredge designs confound the interpretation of the time series. Re-analysed estimates of abundance were made for surveys since 1990 and were based on an estimate of the population size within the 2002 survey area using the dredge calibration from the 1990 dredge/dive survey. These estimates were generated to provide a consistent time series over a constant region (Table 8). This process is described in more detail below.

In general, resource surveys counted the number of "takeable" oysters. Early surveys often used uncalibrated dredges, and/or failed to document the survey methodology. Later surveys also estimated the number of pre-recruit sized oysters (50 mm to 58 mm) and small oysters (less than 50 mm), as well as estimating the number of clocks and levels of *B. exitiosa* infection.

Clocks are the articulated shells of recently dead oysters with the ligament attaching the two valves intact. New clocks are defined as those shells that have clean inner valves that have retained their lustre without fouling. The shells of oysters that are fouled or in which the inner valves have lost their lustre are termed old clocks and can be covered in fouling organisms on both external and internal surfaces. The ligaments of oysters break down over a three-year period, and hence, old clocks represent oysters that died between 6 months and 3 years previously (Cranfield et al. 1991). New clocks are usually assumed to be the shells of those oysters that died since the settlement of fouling organisms in the previous summer — although this may depend on the timing of the survey — and may give an indication of levels of recent mortality.

Typically, the catch from each survey tow was sorted into live oysters, gapers, and new and old clocks. The numbers of each were counted within three size groups (recruit, pre-recruit, and small), where size was determined by the ability of the oyster to pass through a 58 mm or 50 mm diameter reference ring.

More recently, surveys have also counted the number of gapers. Gapers are live moribund oysters in which the two shells are parted, which when tapped, do not fully close as the adductor muscle has lost its ability to fully contract. These have been counted as "new clocks", as they are considered very close to death.

3.6.2 Dredge efficiency

Two estimates of dredge efficiency have been made. Allen & Cranfield (1979) estimated the dredge efficiency of the 1.25 m-wide survey dredge (for recruit-sized oysters) from the 1975–76 surveys, as 0.16 (95% confidence intervals 0.04–0.42). Doonan & Cranfield (1992) estimated dredge efficiency for a 3.35 m width dredge from a dive and dredge survey (for recruit-sized oysters) in 1990 as 0.17 (95% confidence intervals 0.11–0.24).

The Doonan & Cranfield (1992) value was used to determine absolute abundance measures of recruit sized oysters from resource surveys between 1990 and 2002. However, uncertainty in dredge efficiency was incorporated into the uncertainty of the abundance estimates (i.e., in the estimated CVs). Estimates of abundance for pre-recruit and small oysters were generated using the same estimate of dredge efficiency.

3.6.3 Pre-1960 surveys

No abundance data from the early surveys of Foveaux Strait (i.e., 1906, 1926, 1927, and 1945) are available and no abundance estimates from these surveys were reported. However, individual length data were collected on the 1926–27 surveys by M.W. Young and reported by Sorensen (1968) (see Section 3.7).

3.6.4 1960–64 survey

Stead (1971b) surveyed Foveaux Strait extensively between 1960 and 1964 using a light 0.9 m-wide survey dredge towed for 5 minutes in a straight line. Although the tow length and methods were similar to those used in later surveys, there was no calibrated estimate of the efficiency of the much lighter dredge.

However, Stead (1971b) also conducted some experiments in which data were collected that could be used to determine the overall dredge efficiency. Fifteen samples were taken where divers estimated the number of takeable oysters (defined as greater than or equal to 53.975 mm in size, reflecting the legal size of takeable oysters at that time) in a single quadrat (1 m^2) and where the survey dredge was towed using the standard methodology (Figure 14). These data were used to estimate the dredge efficiency of the 1960–64 sampling and calculate an absolute abundance. Estimates of CVs were also made by bootstrapping. Survey stations outside the 1999–2002 survey boundary were ignored, and the remainder used to calculate a calibrated survey absolute abundance (for recruit sized oysters) estimate that is consistent with later surveys. The estimated dredge efficiency was 0.11 (95% confidence intervals 0.08–0.16) resulting in an estimated mean (takeable) population from the 1960– 64 survey from stations within the 2001 survey boundary of 3059 million oysters (CV 0.21). The estimated dredge efficiency compares reasonably well to the estimates of efficiency from Doonan & Cranfield (1992), 0.17, for the larger (3.35 m width) and heaver commercial dredge.

Although the survey was conducted over a number of years, the year of the abundance estimate from the survey was assumed to be 1962. The shape of the selectivity of the gear was assumed to be the same as for later surveys (1993–2002) using the larger, commercial dredge. The 1962 estimate thus became a part of the October survey series of recruit-sized oysters. However, to account for the change in definition of legal size (i.e., 2.125 inches in the 1960s compared with 2.25 inches from 1969), the selectivity curve was shifted to the left by 3.175 mm (0.125 inches) for the 1962 survey. Some individual height data were reported by Stead (1971b) (see Section 3.7).

3.6.5 2014–2016 surveys

The introduction of five-yearly stock assessments in 2012 has placed greater onus on the annual *Bonamia* surveys to monitor changes in the oyster population in commercial fishery areas as well as the status of *Bonamia*. These surveys estimate the densities and population sizes of recruit-sized, pre-recruit, and small live oysters, and recruit-sized and pre-recruit new and old clocks (see Michael et al. 2016 for definitions). These surveys incorporate a fully randomised, two-phase sampling design aimed at better estimating oyster densities and population sizes of oysters and new clocks. A standard *Bonamia* survey area was established in 2014 to ensure that surveys are comparable from year to year. This area was determined from fishery independent survey data and fishers' logbook data and represents the core commercial fishery that has been consistent through the fluctuations in relative oyster abundance driven by *Bonamia* mortality. *Bonamia* survey strata make up 14 of the 26 stock assessment survey strata. The remaining twelve strata are combined into a single background stratum. The *Bonamia* survey area is 46% of the stock assessment survey area and represented 75% and 69% of the recruit-sized oyster population in 2012 and 2017 respectively. Some limited sampling in the background stratum is also undertaken to ensure that these surveys are comparable from year to year and can be incorporated into stock assessments. Estimates of population size for the background stratum are taken from a sample of only five random stations in an area of 578 km^2 and should be used with caution.

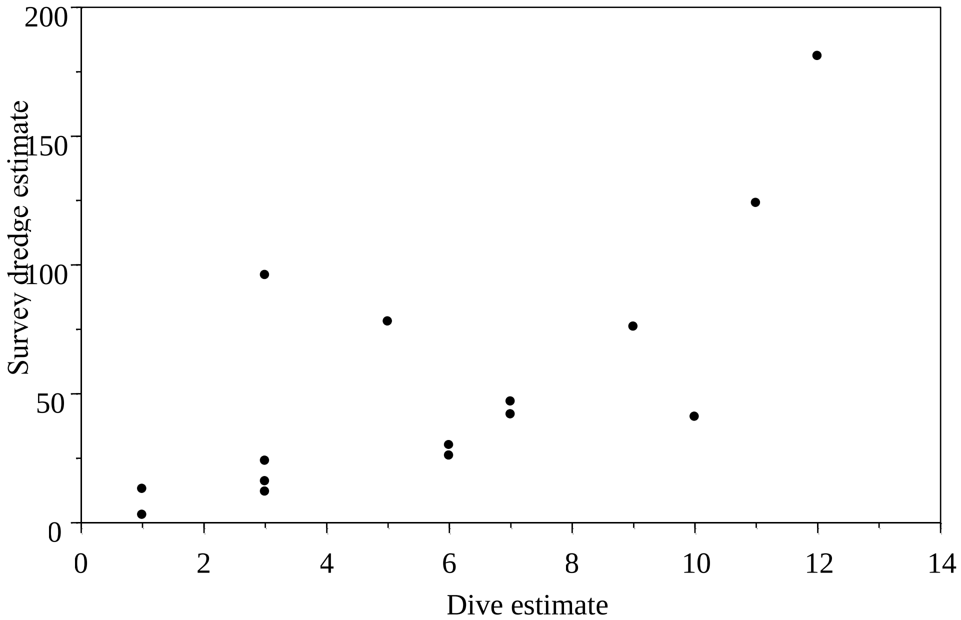

Figure 14: Data used to calibrate the 1960–64 dredge survey. Estimated number of "takeable" oysters sampled by divers on 1 m^2 quadrats (x-axis) and from 5-minute survey tows using the 0.9 m-wide survey dredge (y-axis) (reproduced from data in Stead 1971b).

Table 8: Summary of Foveaux Strait dredge oyster survey data 1906–2016 (numbers of live, new clocks, and old clocks in millions). '–' indicates unknown. (Continued over next three pages)

Date	Design[1]	Area (km²)	Stations	Type[2]	Category	Live	CV	New clocks	Old clocks	*B. exitiosa*.	Lengths	Reference
Jan 1906	Unknown	*ca.* 1 200		A								(Hunter 1906)
			–			–	–	–	–	–	–	
Mar–Aug 1926[3]	CD	*ca.* 400	–	B		–	–	–	–	–	19 272	(Sorensen 1968)
Jan 1927[3]	Unknown	–	–	B		–	–	–	–	–	4 135	(Sorensen 1968)
1945[4]	CD	*ca.* 400		B		–	–	–	–	–	–	(Sorensen 1968)
1960–64	Grid	*ca.* 1 800	542	E	Recruit	~1 000	–	–	–	–	11 576[5]	(Stead 1971b)
		1 055	310	E*	Recruit	3 059	0.21	–	–	–	–	Re-analysed estimate
1962	Specific	–	36	Dive	Recruit	–	–	–	–	–	–	(Stead 1971b)
1965–1971	Specific	374	6	C	–	–	–	–	–	–	–	(Street & Crowther 1973)
1973	Grid	–	150	F	Recruit	–	–	–	–	–	–	(Allen & Cranfield 1979)
Apr–Aug 1974	MR	374	–	C	Recruit	~1 800	0.20	–	–	–	–	(Cranfield & Allen 1979)
Apr–Aug 1975	MR	374	–	C	Recruit	~1 500	0.11	–	–	–	–	(Cranfield & Allen 1979)
1975–76	Grid	374	929	F	Recruit	1 140	0.15	–	–	–	–	(Allen & Cranfield 1979)
Sep 1986	Specific	–	27	F	Recruit	–	–	–	–	–	–	(Dinamani et al. 1987)
Jan 1987	Specific	–	67	F	Recruit	–	–	–	–	–	–	(Dinamani et al. 1987)
Jul 1990	Grid	1 116	293	D*	Recruit	771	0.14*	–	–	Yes	–	(Cranfield et al. 1991)
		1 055	293	D*	Recruit	707	0.11	41	574	–	–	Re-analysed estimate
Oct 1990	SR	646	83	Dive	Recruit	–	–	–	–	–	412[5]	(Cranfield et al. 1991)
		646	83	Dive	Pre-recruit	–	–	–	–	–	420[5]	(Cranfield et al. 1991)
		646	83	Dive	Small	–	–	–	–	–	1 280[5]	(Cranfield et al. 1991)
Oct 1990	SR	646	116	F	Recruit	607	0.11	–	–	Yes	–	(Cranfield et al. 1991)
		1 055	116	F*	Recruit	623	0.12	35	–	–	–	Re-analysed estimate
Mar 1992	Grid	1 229	370	D*	Recruit	319	0.18	–	–	Yes	–	(Doonan & Cranfield 1992)
		1 055	293	D*	Recruit	285	0.12	2	285	–	–	Re-analysed estimate
Oct 1993	Grid	875	177	D*	Recruit	372	0.21	–	–	–	–	(Cranfield et al. 1993)
		1 055	177	D*	Recruit	397	0.10	1	292	–	–	Re-analysed estimate
		1 055	177	D*	Pre-recruit	383	0.11	2	173	–	–	Re-analysed estimate
		1 055	177	D*	Small	1 004	0.10	–	–	–	–	Re-analysed estimate
Mar 1995	SR	680	50	D*	Recruit	543	0.30	–	–	Yes	–	(Cranfield et al. 1995)
		680	50	D*	Pre-recruit	–	–	–	–	Yes	–	(Cranfield et al. 1995)
		1 055	49	D*	Recruit	576	0.25	6	48	–	–	Re-analysed estimate
		1 055	49	D*	Pre-recruit	401	0.28	15	40	–	–	Re-analysed estimate
		1 055	49	D*	Small	402	0.25	–	–	–	–	Re-analysed estimate
Oct 1995	SR	680	154	D*	Recruit	639	0.19	–	–	–	–	(Cranfield et al. 1996)
		1 055	154	D*	Recruit	782	0.11	1	44	–	–	Re-analysed estimate
		1 055	154	D*	Pre-recruit	380	0.10	~0	22	–	–	Re-analysed estimate
		1 055	154	D*	Small	718	0.21	–	–	–	–	Re-analysed estimate

Date	Design[1]	Area (km²)	Stations	Type[2]	Category	Live	CV	New clocks	Old clocks	*B. exitiosa*.	Lengths	Reference
Oct 1997	SR	693	107	D*	Recruit	630	0.21	–	–	–	–	(Cranfield et al. 1998)
		1 055	107	D*	Recruit	660	0.14	~0	74	–	–	Re-analysed estimate
		1 055	107	D*	Pre-recruit	727	0.14	~0	111	–	–	Re-analysed estimate
		1 055	107	D*	Small	918	0.14	–	–	–	–	Re-analysed estimate
Jan 1998	Specific	–	–	D*	Recruit	–	–	–	–	Yes	–	(Cranfield 1998)
		–	–	D*	Pre-recruit	–	–	–	–	–	–	(Cranfield 1998)
Oct 1999	SR	1 055	199	D*	Recruit	1 461	0.16	–	–	–	–	(Michael et al. 2001)
		1 055	199	D*	Recruit	1 453	0.16	~0	176	–	16 054	Re-analysed estimate
		1 055	199	D*	Pre-recruit	896	0.12	0	97	–	8 424	Re-analysed estimate
		1 055	199	D*	Small	1 364	0.11	–	–	–	16 085	Re-analysed estimate
Mar 2000	Specific	–	35	D*	Recruit	–	–	–	–	Yes	–	(Dunn et al. 2000)
Oct 2001	SR	1 055	192	G*	Recruit	995	0.11	10	466	Yes	4 227	(Michael et al. 2004b)
		1 055	192	G*	Pre-recruit	872	0.12	3	111	Yes	3 460	(Michael et al. 2004b)
		1 055	192	G*	Small	1 410	0.12	–	–	Yes	7 475	(Michael et al. 2004b)
Jan 2002	Specific	–	35	G*	Recruit	–	–	–	–	Yes	–	(Dunn et al. 2002b)
Mar 2002	Specific	–	35	G*	Recruit	–	–	–	–	Yes	–	(Dunn et al. 2002a)
Oct 2002	SR	1 055	155	G*	Recruit	502	0.14	68	587	Yes	–	(Michael et al. 2004a)
		1 055	155	G*	Pre-recruit	520	0.11	11	94	Yes	–	(Michael et al. 2004a)
		1 055	155	G*	Small	1 243	0.10	–	–	–	–	(Michael et al. 2004a)
Feb 2003	Specific	–	16	G*	Recruit	–	–	–	–	Yes	–	(Dunn et al. 2003)
Jan 2004	Specific	–	40	G*	Recruit	–	–	–	–	Yes	–	(Michael et al. 2005)
Jan 2005	SR	1 055	80	G*	Recruit	408	0.13	3	287	Yes	–	(Michael et al. 2006)
		1 055	80	G*	Pre-recruit	415	0.15	4	152	Yes	–	(Michael et al. 2006)
		1 055	80	G*	Small	1 345	0.12	–	–	Yes	–	(Michael et al. 2006)
Feb 2006	Specific	407	44	G*	Recruit	242	0.14	13	148	Yes	–	(Michael et al. 2008a)
		407	44	G*	Pre-recruit	257	0.17	9	72	Yes	–	(Michael et al. 2008a)
		407	44	G*	Small	622	0.13	–	–	Yes	–	(Michael et al. 2008a)
Feb 2007[6]	SR	1 070	103	G*	Recruit	624	0.10	11	222	Yes	–	(Michael et al. 2008b)
		1 070	103	G*	Pre-recruit	464	0.11	4	72	Yes	–	(Michael et al. 2008b)
		1 070	103	G*	Small	848	0.09	–	–	Yes	–	(Michael et al. 2008b)
		1 055	101	G*	Recruit[7]	622	0.10	11	222	Yes	–	Re-analysed estimate
		1 055	101	G*	Pre-recruit[7]	463	0.11	4	72	Yes	–	Re-analysed estimate
		1 055	101	G*	Small[7]	842	0.09	–	–	Yes	–	Re-analysed estimate
Feb 2008	Specific	671	40	G*	Recruit	694	0.11	18	136	Yes	–	(Michael et al. 2009a)
		671	40	G*	Pre-recruit	269	0.10	5	42	Yes	–	(Michael et al. 2009a)
		671	40	G*	Small	702	0.13	–	–	Yes	–	(Michael et al. 2009a)

Date	Design[1]	Area (km^2)	Stations	Type[2]	Category	Live	CV	New clocks	Old clocks	B. exitiosa.	Lengths	Reference
Feb 2009[8]	SR	1 070	105	G*	Recruit	725	0.08	17	170	Yes	–	(Michael et al. 2009b)
		1 070	105	G*	Pre-recruit	358	0.10	4	68	Yes	–	(Michael et al. 2009b)
		1 070	105	G*	Small	910	0.10	–	–	Yes	–	(Michael et al. 2009b)
		1 055	101	G*	Recruit[7]	720	0.08	16	166	Yes	–	Re-analysed estimate
		1 055	101	G*	Pre-recruit[7]	354	0.10	4	67	Yes	–	Re-analysed estimate
		1 055	101	G*	Small[7]	889	0.10	–	–	Yes	–	Re-analysed estimate
Feb 2010	Specific			G*	Recruit	809	0.12	602	–	Yes	–	(Michael et al. 2011)
				G*	Pre-recruit	367	0.10	–	–	Yes	–	(Michael et al. 2011)
				G*	Small	939	0.09	–	–	Yes	–	(Michael et al. 2011)
Feb 2011	Specific			G*	Recruit	596	0.11	23	–	Yes	–	(Michael et al. 2012)
				G*	Pre-recruit	278	0.11	–	–	Yes	–	(Michael et al. 2012)
				G*	Small	516	0.12	–	–	Yes	–	(Michael et al. 2012)
Feb 2012[8]	SR	1 070	146	G*	Recruit	918	0.08	30	–	Yes	–	(K.P. Michael, unpublished)
		1 070	146	G*	Pre-recruit	414	0.10	12	–	Yes	–	(K.P. Michael, unpublished)
		1 070	146	G*	Small	612	0.14	–	–	Yes	–	(K.P. Michael, unpublished)
		1 055	143	G*	Recruit[7]	913	0.08	29	–	Yes	–	Re-analysed estimate
		1 055	143	G*	Pre-recruit[7]	410	0.10	12	–	Yes	–	Re-analysed estimate
		1 055	143	G*	Small[7]	607	0.14	–	–	Yes	–	Re-analysed estimate
Feb 2014[9]	SR	1 070	60	G*	Recruit	1021	0.12	84.1	–	Yes	–	(Michael et al. 2016)
		1 070	60	G*	Pre-recruit	226	0.14	5.3	–	Yes	–	(Michael et al. 2016)
		1 070	60	G*	Small	303	0.11	–	–	Yes	–	(Michael et al. 2016)
Feb 2015[9]	SR	1 070	60	G*	Recruit	510	0.09	23.7	–	Yes	–	(Michael et al. 2016)
		1 070	60	G*	Pre-recruit	122	0.11	4.5	–	Yes	–	(Michael et al. 2016)
		1 070	60	G*	Small	249	0.20	–	–	Yes	–	(Michael et al. 2016)
Feb 2016[9]	SR	1 070	60	G*	Recruit	561	0.13	3.6	–	Yes	–	(Michael et al. 2016)
		1 070	60	G*	Pre-recruit	191	0.17	0.8	–	Yes	–	(Michael et al. 2016)
		1 070	60	G*	Small	364	0.15	–	–	Yes	–	(Michael et al. 2016)
Feb 2017[9]	SR	1 070	60	G*	Recruit	527	0.09	7.8	–	Yes	–	(Michael et al. 2019b)
		1 070	60	G*	Pre-recruit	168	0.10	1.3	–	Yes	–	(Michael et al. 2019b)
		1 070	60	G*	Small	361	0.09	–	–	Yes	–	(Michael et al. 2019b)

1. Survey designs either circumscribed the known oyster beds (CD), sampled specific stations non-randomly (specific), followed a grid pattern (grid), were stratified random (SR), or were mark-recapture surveys (MR).
2. * indicates a calibrated estimate. A–F indicate the type of dredge, while 'Dive' indicates a dive survey. The dredges are: (A) Light, hand-hauled commercial dredge about 1 m wide, used up to 1913; (B) Commercial dredge, about 3.35 m wide with single-bit and single ring bag, weighing about 150 kg and used up to 1968; (C) Commercial dredge, about 3.35 m wide, introduced in 1968 with double-bit and double ring bag and weighing about 400 kg; (D) The 1968 commercial

dredge, about 3.35 m wide, modified in 1984 increasing weight to about 530 kg; (E) 0.91 m wide, light survey dredge with a rigid mesh catch bag; (F) 1.25 m wide survey dredge, designed to be a smaller version of 1968 commercial dredge with double-bit and double flexible ring bag; (G) 3.32 m wide commercial dredge similar to the 3.35 m wide dredge introduced in 1968 with double-bit and double ring bag, and weighing 400 kg.

3. The 1945 survey data are suspected of being destroyed in a fire in the 1950s.
4. The original reports detailing the Mar–Aug 1926 and Jan 1927 surveys have been lost; these summaries are reproduced from Sorensen (1968).
5. Data recorded as height, not length. In the October 1990 dive survey, height frequencies were grouped by size class according to the height measurement, and not their ability to pass through a 50 mm or 58 mm diameter ring.
6. The February 2007 included an additional stratum in north Foveaux Strait. Re-analysed estimates ignore this stratum, and hence are estimates of abundance over an area comparable to earlier surveys.
7. Two errors in the length of tows resulted in a revised estimate of the number of recruits and small oysters for the February 2007 survey. Model runs presented below used values of 661 recruits and 877 small oysters for the February 2007 abundance indices, instead of the corrected values of 663 and 879 respectively.
8. The February 2007 included an additional stratum in north Foveaux Strait. Re-analysed estimates ignore this stratum, and hence are estimates of abundance over an area comparable to earlier surveys.
9. Population estimates from *Bonamia* surveys, 12 of the 26 stock assessment survey strata combined into a single stratum and sampling intensity is low (n=5).

3.6.6 1974–75 mark-recapture surveys

Cranfield & Allen (1979) reported the results of a mark-recapture experiment, based on the recapture of tagged, recruit-sized oysters released in 1974 and 1975. Tagged oysters were released over a number of beds within the main commercial fishery (about 374 km^2, and roughly corresponding to the region surveyed in the 1975–76 dredge survey). The number of tagged oysters returned by fishers was used to estimate the size of the standing crop for 1974 and 1975 respectively.

In the model, the estimates of abundance were assumed to be relative estimates, with selectivity set equal to the dredge survey selectivity for recruit-sized oysters and the survey catchability coefficient q is the ratio of abundance inside the 1974–75 survey region to that inside the 2001 survey region.

3.6.7 1975–76 survey

The 1975–76 survey was carried out over two seasons (actually as three separate surveys in February 1975, June 1975, and May 1976 on adjacent areas), using a light, 1.25 m-wide survey dredge. The survey region encompassed the extent of the commercial fishery region at that time (374 km^2). Survey abundance estimates were calibrated from both diving observations and the recapture rate of tagged oysters from the mark-recapture experiment in 1974 and 1975. The estimate used here is a reanalysed estimate based on data from Cranfield et al. (1991).

The estimate of abundance is assumed to be a relative estimate, with a selectivity set equal to the dredge survey selectivity for recruit-sized oysters. However, as this is used as a single survey estimate in the model with associated catchability, the data have almost no impact on resulting model estimates (other than as a direct result of the influence of the prior on the catchability constant, q). Hence, the resulting estimates of q can be considered to be a measure of the ratio of abundance inside the 1975–76 survey region compared with that for the 2001 survey region.

3.6.8 1990 to 1997 surveys

The design of some of the abundance surveys (in particular, the 1960–64 survey and surveys between 1990 and 1997 inclusive) allow an estimate to be made that is comparable to those conducted between 1999 and 2002. Where possible, revised estimates using a consistent estimate of dredge efficiency were made (see Table 8).

Survey data from the October series between 1990 and 1997 were re-analysed to (a) scale up (or down) the estimates to account for the part of the population outside the original survey region but within the region bounded by the 1999–2002 surveys, and (b) to account for revised estimates of dredge efficiency that have been made since the original survey estimates were published. The 1960– 64 survey (Stead 1971b) covered an area larger than any survey since. These data allow an estimate of the ratio of recruit-sized oysters that occurred inside and outside the survey regions defined in the 1990–2002 abundance surveys (1055 km^2). These data were post-stratified to estimate that about 5% of oysters were outside the region surveyed in the October 1990–97 and inside the 1999–2002 survey region. The re-analysed estimates of the 1990 to 1997 October surveys were therefore multiplied by 1.05 to account for oysters outside the survey boundaries. This makes the strong assumption that the ratio of densities of oysters within each of these regions does not change over time.

Estimates for the July 1990 and March 1992 surveys were re-stratified using the external boundary of the surveys from 1999 to 2005, and re-analysed with the revised dredge efficiency estimates (Table 8, Figure 15, Figure 16).

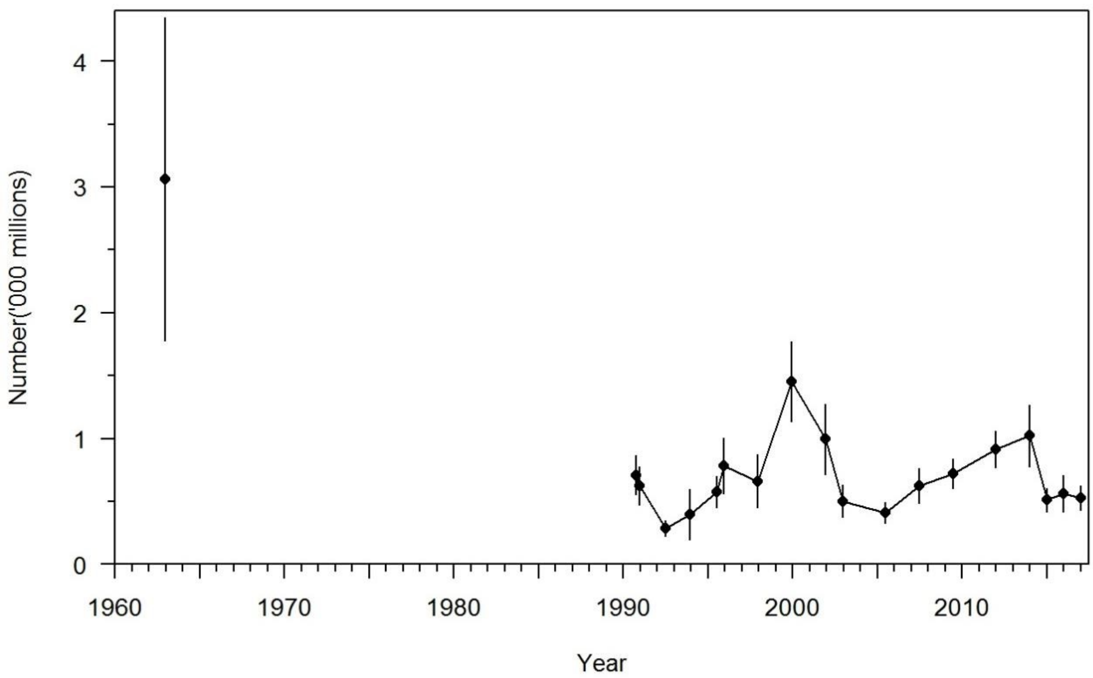

Figure 15: Estimates of the recruit-sized absolute abundance from surveys between 1962 and 2017. Vertical lines show approximate 95% confidence intervals.

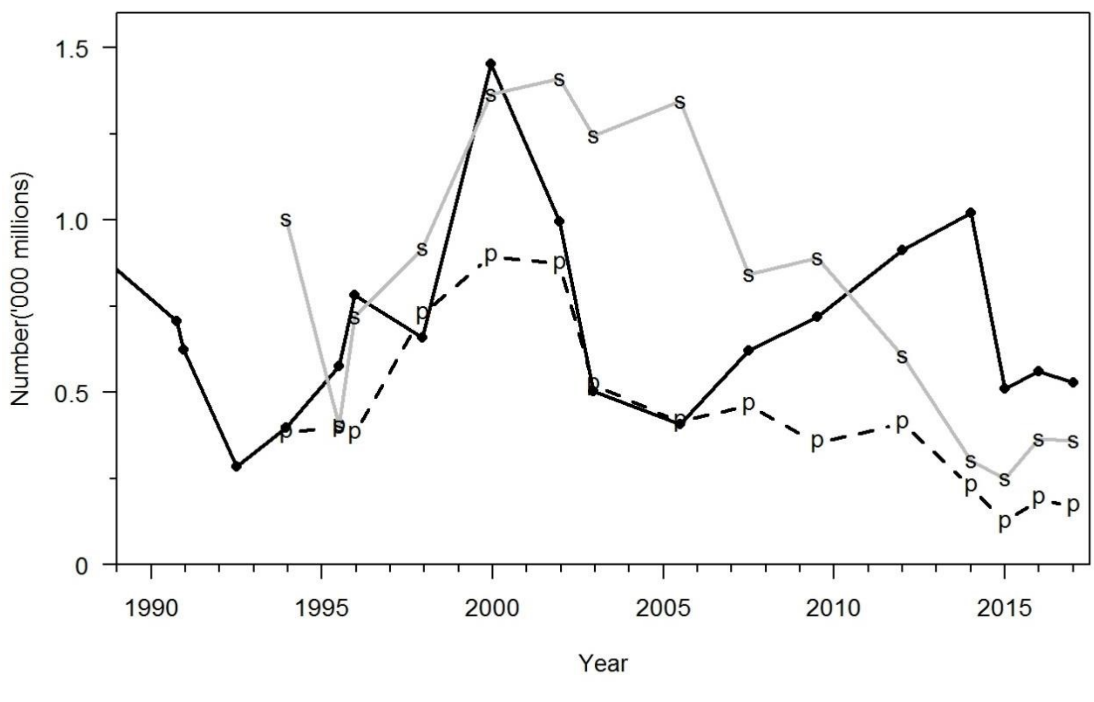

Figure 16: Estimated numbers of recruit (dots), pre-recruit (p), and small (s) oysters found in the biomass surveys between 1990 and 2017.

3.6.9 1999–2002 surveys

The abundance surveys between 1999 and 2002 used the current survey boundary and current estimates of dredge efficiency (see Figure 1). However, the 1999 survey also included an additional stratum of a recreational area closed to commercial fishing on the eastern side of Stewart Island. The estimates reported here exclude that stratum.

3.6.10 2005, 2007, 2009, 2012, and 2014–2017 surveys

The 2005 abundance survey was conducted in January, and surveys in 2007, 2009, 2012, and 2014–2017 were all conducted on February. Previous surveys had occurred at different times of year (typically these have been in either March or October). In this model we assume that these surveys are a measure of the beginning of fishing season biomass, and hence include it within the population model as a biomass index at the end of the first time-step, in March 2005, 2007, 2009, 2012, and 2014–2017 respectively.

In addition, the February surveys (in 2007, 2009, 2012 and 2014–2017) covered a slightly larger region than that used to standardise previous surveys (i.e., 1070 km^2 versus 1055 km^2 – see Table 8), by the inclusion of one additional stratum. We ignore the strata that were outside the 2002 region, and hence use the estimates of abundance for the equivalent 2002 region (Table 8).

3.6.11 Catch-effort data

Raw (unstandardised) catch and effort data have been collected in the Foveaux Strait dredge oyster fishery since about 1948. The total number of sacks landed from Foveaux Strait and the total number of hours fished from 1948 to 1971 were tabulated in Marine Department annual reports from 1972 to 1994 by MAF (Fisheries), and since then by the Ministry of Fisheries and Ministry for Primary Industries.

The definition of minimum legal size (i.e., the legal takeable size) of oysters and regulations governing dredge design and size have changed over time. Hence, the CPUE indices may not be comparable over the full time series. In previous assessments, the data were split into three series, namely (i) Series A, from 1948 to 1968 when the legal size was defined as 2.125 inches and the typical commercial dredge was about 3.35-m wide with single-bit and single ring bag and weighing 150 kg; (ii) Series B, from 1969 to 1984 when the legal size was 2.25 inches, and the typical commercial dredge was about 3.35 m wide with double-bit and double ring bag and weighing 400 kg; and (iii) Series C, years after 1984 when the typical commercial dredge was modified by increasing its weight to about 530 kg (Table 9 and Figure 17).

Dunn (2005a) presented an analysis of the raw catch-rate and a standardised CPUE analysis for the years using CELR data and logbook data. He found that the standardised and unstandardised indices showed very similar trends, with only slight differences discernible with different data sets or methods of analysis. Hence, unstandardised indices were used as an index of fishable abundance in the stock model, with a lognormal likelihood and assumed CVs of 0.25. The 2012 stock assessment was updated with CPUE data for 2011 and 2012. We use the same CPUE data (i.e., series A, B, and C) updated to include data for 2013–2016. These index series were used in the basic and revised models.

In this assessment, we also used an alternative CPUE series (4-cpue) by splitting the C-series into a reduced-C (1985 to 2009) and D (2010-) series (Table 9). Preliminary runs showed that the old C series were mis-fitting in opposite directions before and after 2010. Fishers state that fishing practice changed around 2010 to target larger oysters which implicitly moves the fishing selectivity curve to larger oysters after 2010. With all C-data included, the estimated selectivity curve is a weighted average of that before 2010 and after 2010 and so it does not fit either set.

Table 9: Reported catch rate estimates and revised estimates from source records for series A, B, and C (unbroken at 2010), for Foveaux Strait oysters 1901–2016 (sacks per hour). (Data from 1948–1971 Marine Department annual reports, 1972 MAF (Fisheries) Annual Report). Rep is reported, Rev is revised.

Year	Series	Rep	Rev	Year	Series	Rep	Rev	Year	Series	Rep	Rev
1948	A	14.7	14.7	1969	B	6.5		1985	C	12.1	13.8
1949	A	14.6	14.6	1970	B	7.3	9.3	1986	C[3]	10.5	12.1
1950	A	14.2	14.2	1971	B	6.9	7.7	1987	C	10.9	10.5
1951	A	12.6	12.6	1972	B[1]	6.7	6.6	1988	C	10.0	9.1
1952	A	13.7	13.7	1973	B[1]	10.0	6.7	1989	C	10.7	10.0
1953	A	12.6	12.6	1974	B	11.5	10.0	1990	C	6.4	9.7
1954	A	11.0	11.0	1975	B	11.9	10.8	1991	C[4]	5.8	5.8
1955	A	12.2	12.2	1976	B	13.4	11.9	1992	C[5]	3.4	3.2
1956	A	10.0	10.0	1977	B[2]	15.9	13.3	1993	C[6]	-	-
1957	A	9.0	9.0	1978	B[2]	17.1	15.4	1994	C[6]	-	-
1958	A	9.5	9.5	1979	B	16.6	15.6	1995	C[6]	-	-
1959	A	10.7	10.7	1980	B	15.2	14.5	1996	C	5.9	5.4
1960	A	10.5	10.5	1981	B	13.4	15.2	1997	C	7.0	6.4
1961	A	10.5	10.5	1982	B	13.2	13.4	1998	C	8.3	6.3
1962	A	8.0	8.0	1983	B	12.3	13.2	1999	C	7.5	6.3
1963	A	6.0	6.0	1984	B	13.8	12.3	2000	C	7.2	6.6
1964	A	6.8	6.8					2001	C	7.0	6.5
1965	A	7.9	7.9					2002	C	3.2	3.2
1966	A	10.6	10.6					2003	C	2.3	2.4
1967	A	9.3						2004	C	2.2	2.2
1968	A	7.7						2005	C	1.7	1.8
								2006	C	1.9	1.9
								2007	C[7]	-	2.4
								2008	C[7]	-	3.3
								2009	C[7]	-	3.1
								2010	C[7]	-	4.2
								2011	C[7]	-	4.1
								2012	C[7]	-	4.1
								2013	C[7]	-	5.5
								2014	C[7]	-	4.4
								2015	C[7]	-	3.4
								2016	C[7]	-	3.8

1. Landings include catch given as incentive to explore “un-fished” areas.
2. Landings include catch given as an incentive to fish Area A.
3. Season closed early after diagnosis of *B. exitiosa.*
4. Landings include catch given as an incentive to fish a 'firebreak' to stop the spread of *B. exitiosa.*
5. Fishing permitted only in outer areas of fishery.
6. Between 1993 and 1995, the fishery was closed and therefore no catch rate data are available
7. An alternative CPUE series used in model sensitivities, splitting the C-series into a reduced-C (1985 to 2009) and D (2010-) series.

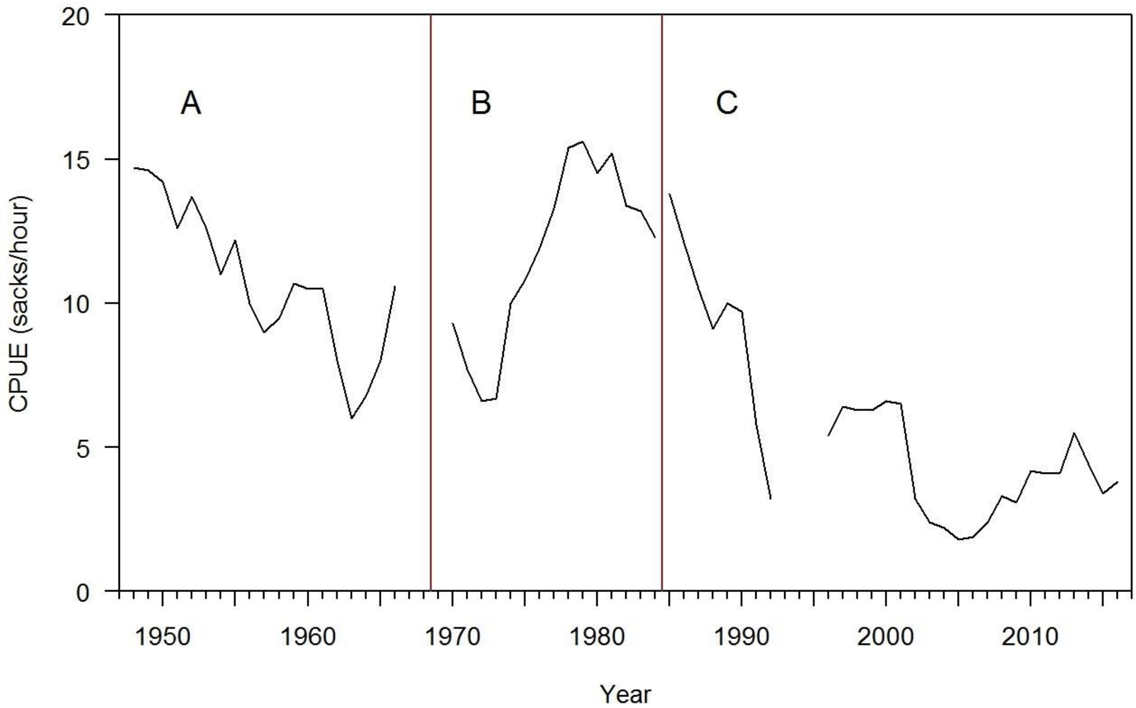

Figure 17: Revised estimates (dark lines) from source records for series A, B, and unbroken C, for Foveaux Strait oysters 1948–2016 (sacks per hour). (Data from Table 9.)

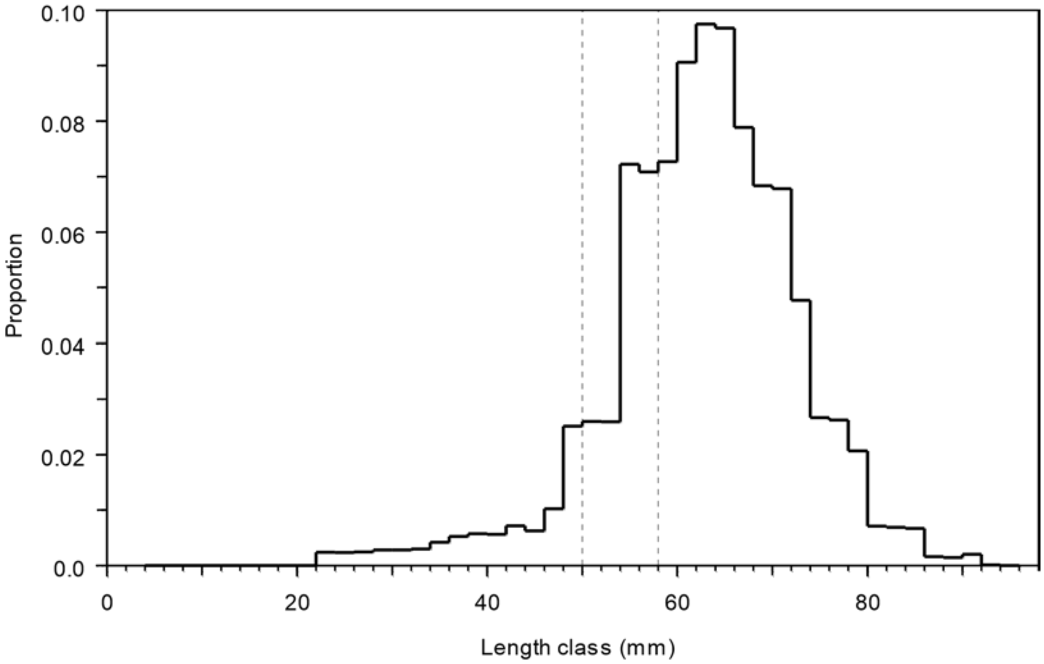

Figure 18: Proportions of oysters by length class from the 1926–27 survey, reproduced from data given in table 3 from Sorensen (1968). Dashed lines separate the small (<50 mm), pre-recruit (≥ 50 mm and <58 mm), and recruit (≥ 58 mm) size groups.

3.7 Population length frequency estimates

Height data were collected on the October 1990 dive survey and the 1960–64 dredge survey. Length data were collected from the 1926–27, 1999, and 2001 surveys. The length and height samples collected from the 1926–27 and the 1960–64 dredge surveys have not been included within the model but are described here for completeness.

3.7.1 1926 Survey

Individual length data were collected on the 1926–27 surveys by M.W. Young and reported in table 3 of Sorensen (1968). However, the method of sampling, dredge selectivity, and dredge calibration are unknown for that survey, and hence these data are not able to be included within the population model. The data in Sorensen (1968) are reproduced in Figure 18, after converting the length measurements from inches to millimetres.

3.7.2 1960–64 survey

Individual height data were collected on the 1960–64 survey and reported in a graph by Stead (1971b). Raw height frequency data from that survey are unavailable but can be inferred from the published graph. Height measurements of oysters are about 25% larger than length measurements, and using an appropriate conversion factor (based on the length and height of oysters collected in 2001–03), the height frequencies can be converted to length frequencies, i.e.,

$$\log(length) = a \log(height) + \varepsilon$$

where $\varepsilon \sim N(0, \sigma^2)$, and hence we estimated the conversion factor (in log space) as $a = 0.949$. The data in Stead (1971b) are reproduced in Figure 19 below, after converting the height measurements to length.

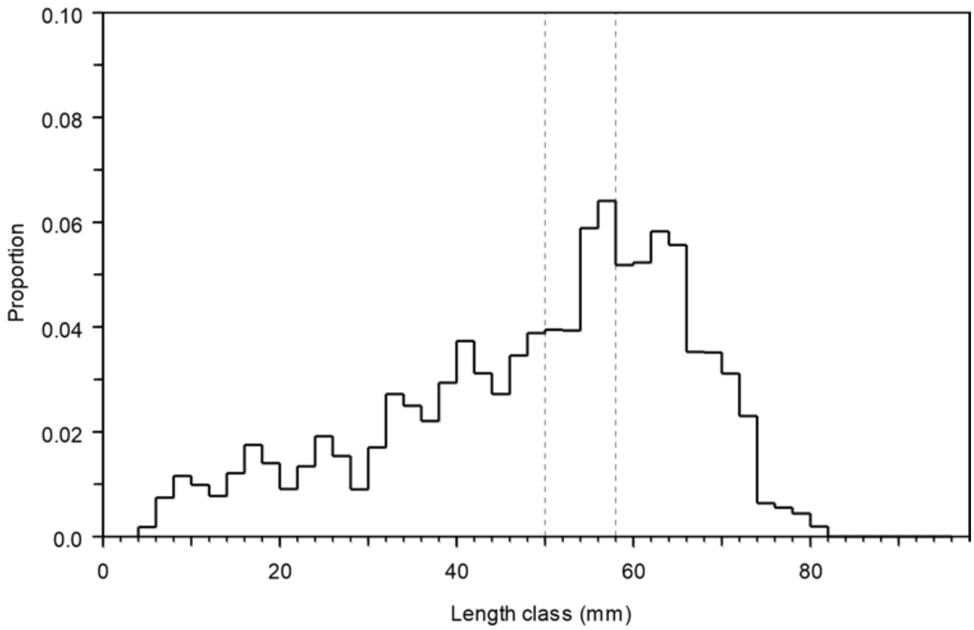

Figure 19: Proportions of oysters by length class from the 1960–64 survey, reproduced from data given in figure 1 in Stead (1971b). Dashed lines separate the small (<50 mm), pre-recruit (≥ 50 mm and <58 mm), and recruit (≥ 58 mm) size groups.

3.7.3 October 1990 dive survey

During the dive survey in October 1990, height measurements were collected from the oysters sampled. These were converted to lengths using the conversion factor described above. The dive survey length frequency distribution was assumed to be equal to the population length frequency distribution at the time of the survey (Figure 20, after converting the height measurements to length, truncated at 10 mm). Proportions at length were included into the model with multinomial likelihood. The effective sample sizes for the length frequency data were estimated by calculating a sample size that represented the best least squares fit of $\log(cv_i)\sim\log(P_i)$, where cv_i was the bootstrap CV for the ith proportion, P_i.

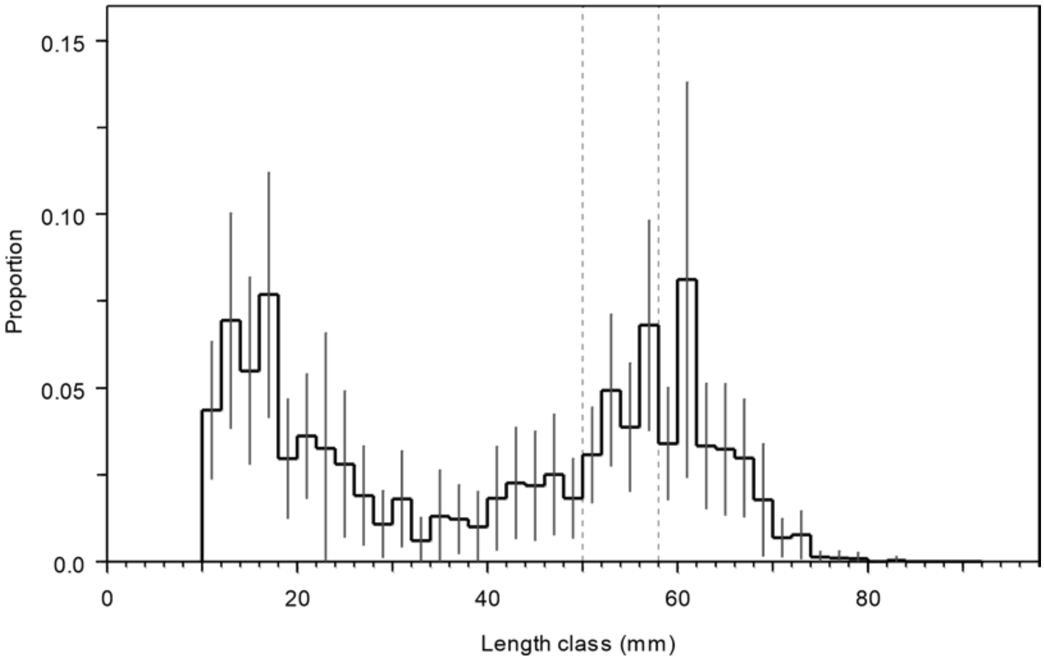

Figure 20: Proportions of oysters by length class from the 1990 dive survey. Dashed lines separate the small (<50 mm), pre-recruit (≥ 50 mm and <58 mm), and recruit (≥ 58 mm) size groups.

3.7.4 1999 and 2001 survey

Length samples from the 1999 and 2001 October resource surveys were collected for oysters classified as ‘smalls’, ‘pre-recruits’, and ‘recruits’. Catch-at-length estimates were produced using the catch-at-age software (Bull & Dunn 2002). This software scales the length frequency of fish from each tow up to the total tow catch, sums over tows in each stratum, and scales up to the total stratum catch, to yield length frequencies by stratum and overall. The CVs are calculated by bootstrapping; individual oyster length measurements are resampled within each tow and tows are resampled within each stratum (Figures 21−26).

Proportions at length were included into the model with a multinomial likelihood. The effective sample sizes were estimated by calculating a sample size that represented the best least squares fit of $\log(cv_i)\sim\log(P_i)$, where cv_i was the bootstrap CV for the ith proportion, P_i .

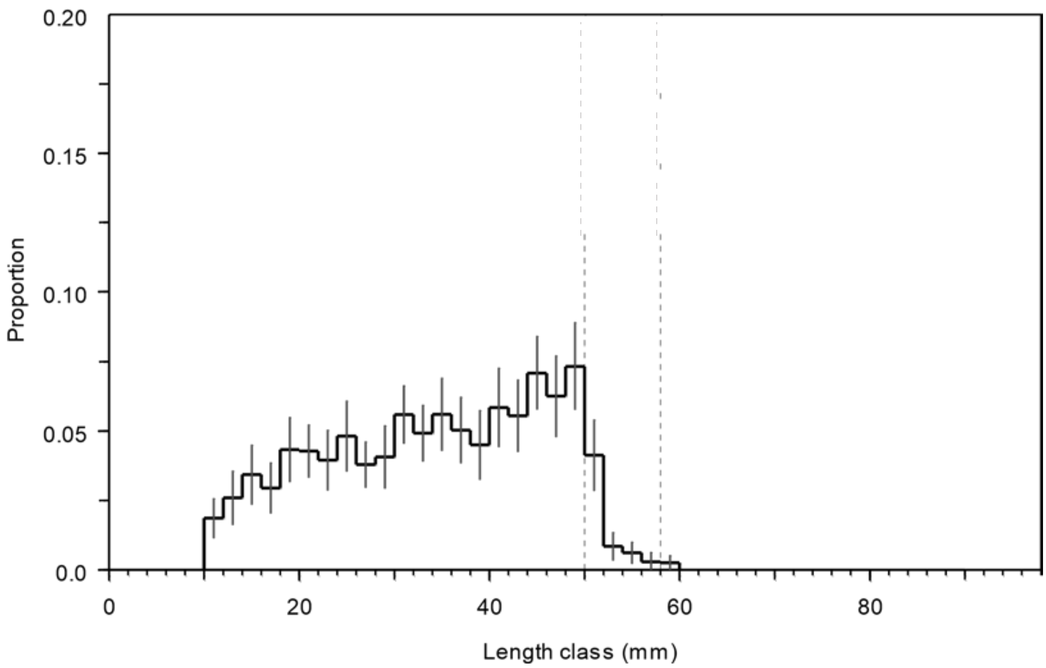

Figure 21: Proportions of oysters classified as “smalls” by length class from the 1999 October resource survey. Vertical bars give approximate 95% confidence intervals. Dashed lines separate the small (<50 mm), pre-recruit (≥ 50 mm and <58 mm), and recruit (≥ 58 mm) size groups.

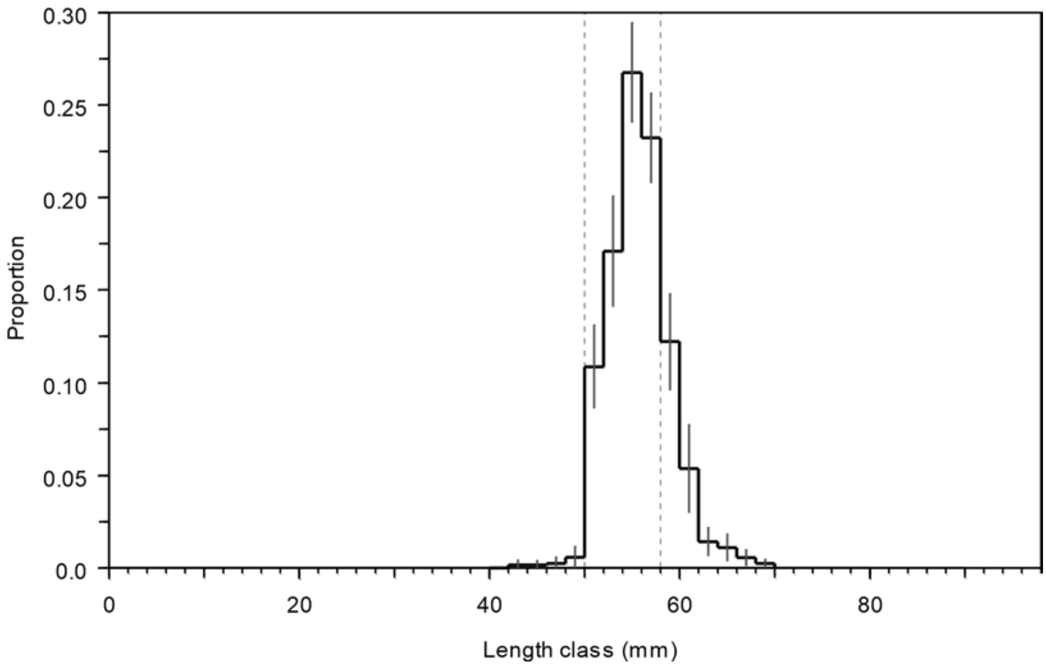

Figure 22: Proportions of oysters classified as “pre-recruits” by length class from the 1999 October resource survey. Vertical bars give approximate 95% confidence intervals. Dashed lines separate the small (<50 mm), pre-recruit (≥ 50 mm and <58 mm), and recruit (≥ 58 mm) size groups.

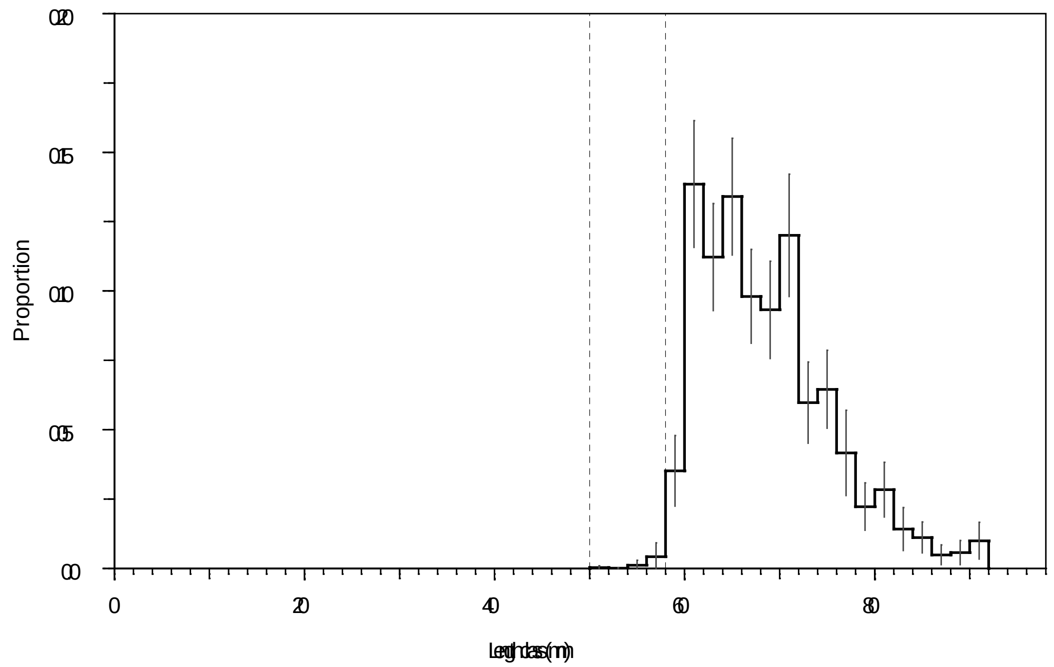

Figure 23: Proportions of oysters classified as "recruits" by length class from the 1999 October resource survey. Vertical bars give approximate 95% confidence intervals. Dashed lines separate the small (<50 mm), pre-recruit (≥ 50 mm and <58 mm), and recruit (≥ 58 mm) size groups.

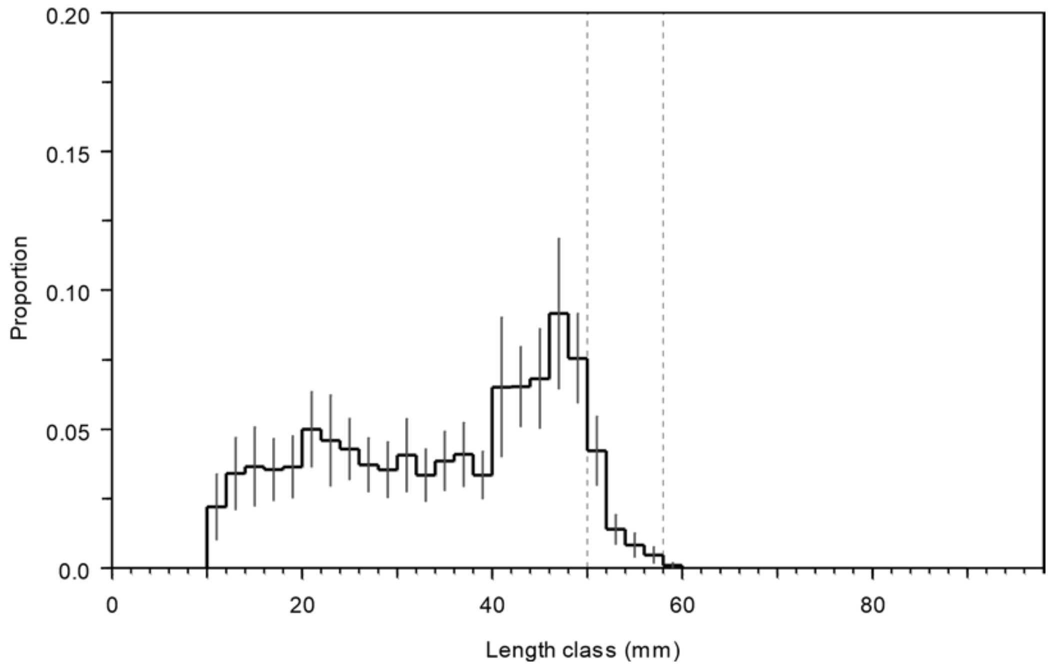

Figure 24: Proportions of oysters classified as "smalls" by length class from the 2001 October resource survey. Vertical bars give approximate 95% confidence intervals. Dashed lines separate the small (<50 mm), pre-recruit (≥ 50 mm and <58 mm), and recruit (≥ 58 mm) size groups.

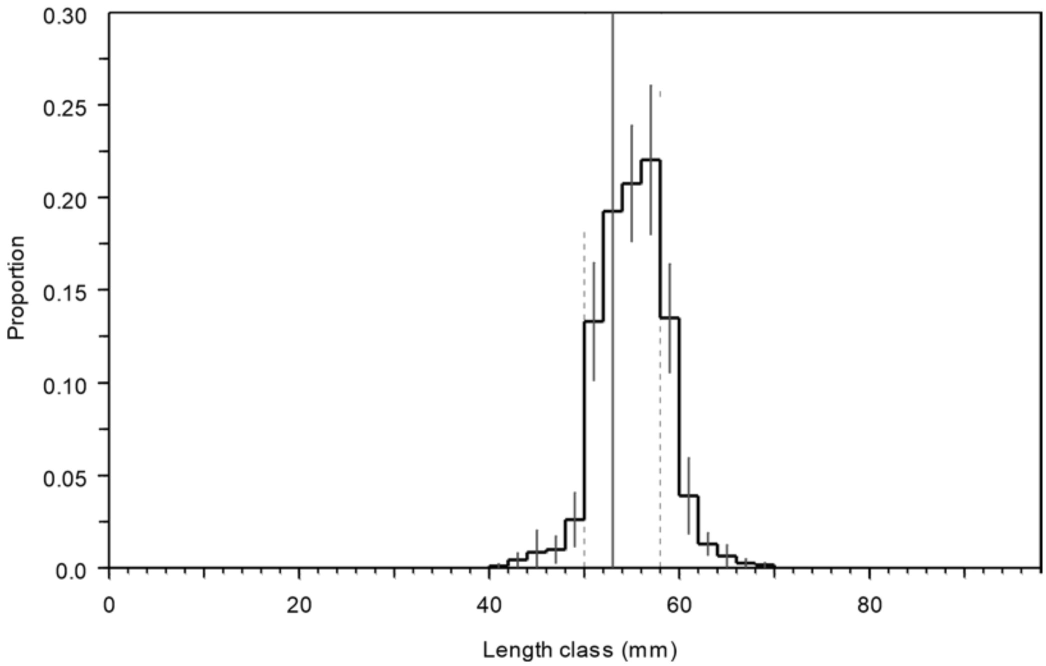

Figure 25: Proportions of oysters classified as “pre-recruits” by length class from the 2001 October resource survey. Vertical bars give approximate 95% confidence intervals. Dashed lines separate the small (<50 mm), pre-recruit (≥ 50 mm and <58 mm), and recruit (≥ 58 mm) size groups.

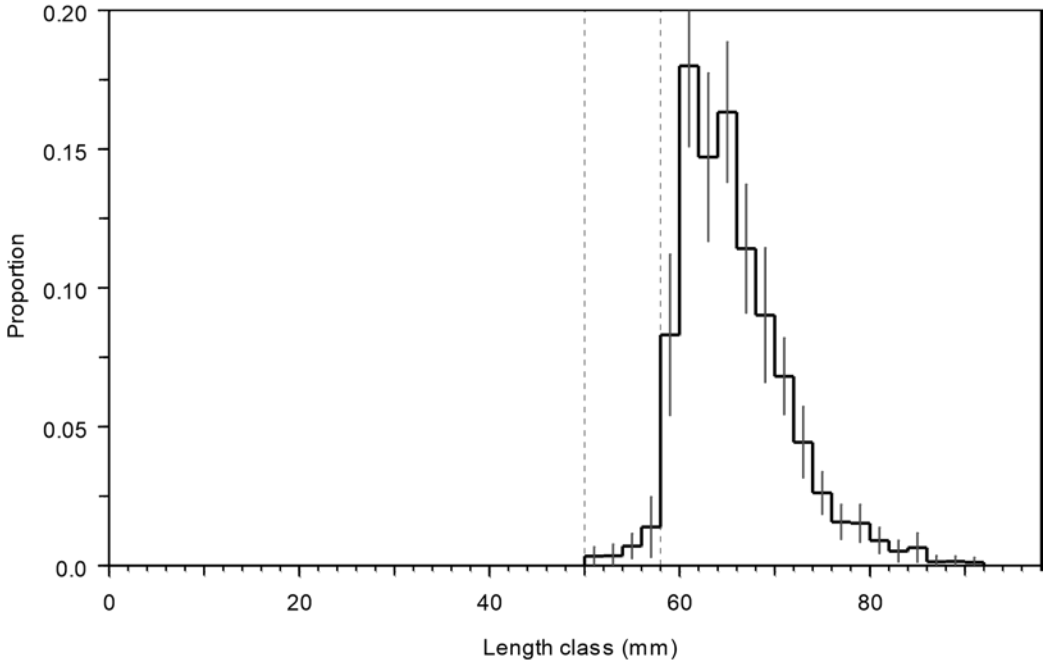

Figure 26: Proportions of oysters classified as “recruits” by length class from the 2001 October resource survey. Vertical bars give approximate 95% confidence intervals. Dashed lines separate the small (<50 mm), pre-recruit (≥ 50 mm and <58 mm), and recruit (≥ 58 mm) size groups.

3.8 Process error

The effective sample sizes (in the case of observations fitted with multinomial likelihoods) or CVs (for observations fitted with lognormal likelihoods) were assumed to have allowed for sampling error only. Additional variance (here called process error), assumed to arise from differences between model simplifications and real world variation, was added to the sampling variance for each observation.

Estimates of the process error and hence the model sample size for the proportions-at-length observations were made via a two-step process; (a) first, the sample sizes were derived by assuming the relationship between the observed proportions, E_i, and estimated CVs, c_i, followed that for a multinomial distribution with unknown sample size N_j as described earlier (see Sections 3.4.3, 3.7.3, and 3.7.4), and (b) by estimating an effective sample size, N_j', by adding additional process error, N_{PE}, to the sample size calculated in (a) above, where,

$$N'_j = 1/\left({}^{1}/_{N_j} + {}^{1}/_{N_{PE}}\right)$$

i.e., from an initial MPD model fit, an estimate of the additional process error was made by solving the following equation for N_{PE},

$$n = \sum_{ij} \frac{(O_{ij} - E_{ij})^2}{E_{ij}(1 - E_{ij})\left({}^{1}/_{N_j} + {}^{1}/_{N_{PE}}\right)}$$

where n was the number of multinomial cells, O_{ij} was the observed proportions for length class i in year j, E_{ij} was the expected proportions, N_j was the effective sample size estimated in (a) above, and N_{PE} was the associated process error for that class of observations.

Estimates of the effective CV for biomass observations were made by fitting the process error within each model run, where the effective CV c_i was determined from the process error c_{PE} and the observed CVs c_i by,

$$c_i' = \sqrt{c_i^2 + c_{PE}^2}$$

4. MODEL ESTIMATES AND RESULTS

Model estimates of numbers of oysters were made using the biological parameters and model input parameters described in Section 3.3. The 2017 basic model and 2017 revised model were defined as having the same structure as the 2012 models, but with catch and CPUE data for the 2013, 2014, 2015 and 2016 fishing years, and the inclusion of the biomass survey indices from 2014, 2015, 2016 and 2017 in the second time step (March to September). A catch of 10 million oysters was assumed for the 2017 fishing year. In addition, sensitivity to the basic and revised models was tested with four CPUE series rather than three; the 2017 basic-4cpue model and the 2017 revised-4cpue model.

The priors assumed for most parameters are summarised in Table 10. In general, ogive priors were chosen to be non-informative and were uniform across wide bounds. The prior for disease mortality was defined so that estimates of disease mortality were encouraged to be low. The basic model assumed fixed values of growth parameters (estimated outside the model with mean growth g_{30} = 11.9 mm and g_{55} = 3.61 mm, and an estimated CV of 0.31). The revised model estimated growth within the model (with the CV fixed at 0.31) incorporating the tag-recapture observations.

Table 10: The priors assumed for key parameters. For each parameter the third and fourth columns show respectively the value for the mean and CV for lognormal distributions (in natural space), and the mean and s.d. for normal distributions.

Parameter	Distribution	Parameters		Bounds	
CPUE *q*	Uniform-log	–	–	1×10^{-8}	0.1
1976 survey *q*	Lognormal	0.6	0.3	0.15	0.95
Mark-recapture survey *q*	Lognormal	0.6	0.3	0.10	0.90
YCS	Lognormal	1.0	0.2	0.01	100.0
Disease mortality	Normal	-0.2	0.2	0.00	0.80

4.1 MPD Results

Mode of the posterior distribution (MPD) trajectories for the basic and revised models for stock abundance are shown in Figure 27. Summaries of the objective function values (negative loglikelihood) are shown in Table 11, with distributions of the likelihood profiles of B_0 for the basic and revised models shown in Figure 28. Additional summary plots of the 2017 model MPD fits are given as Appendix A.

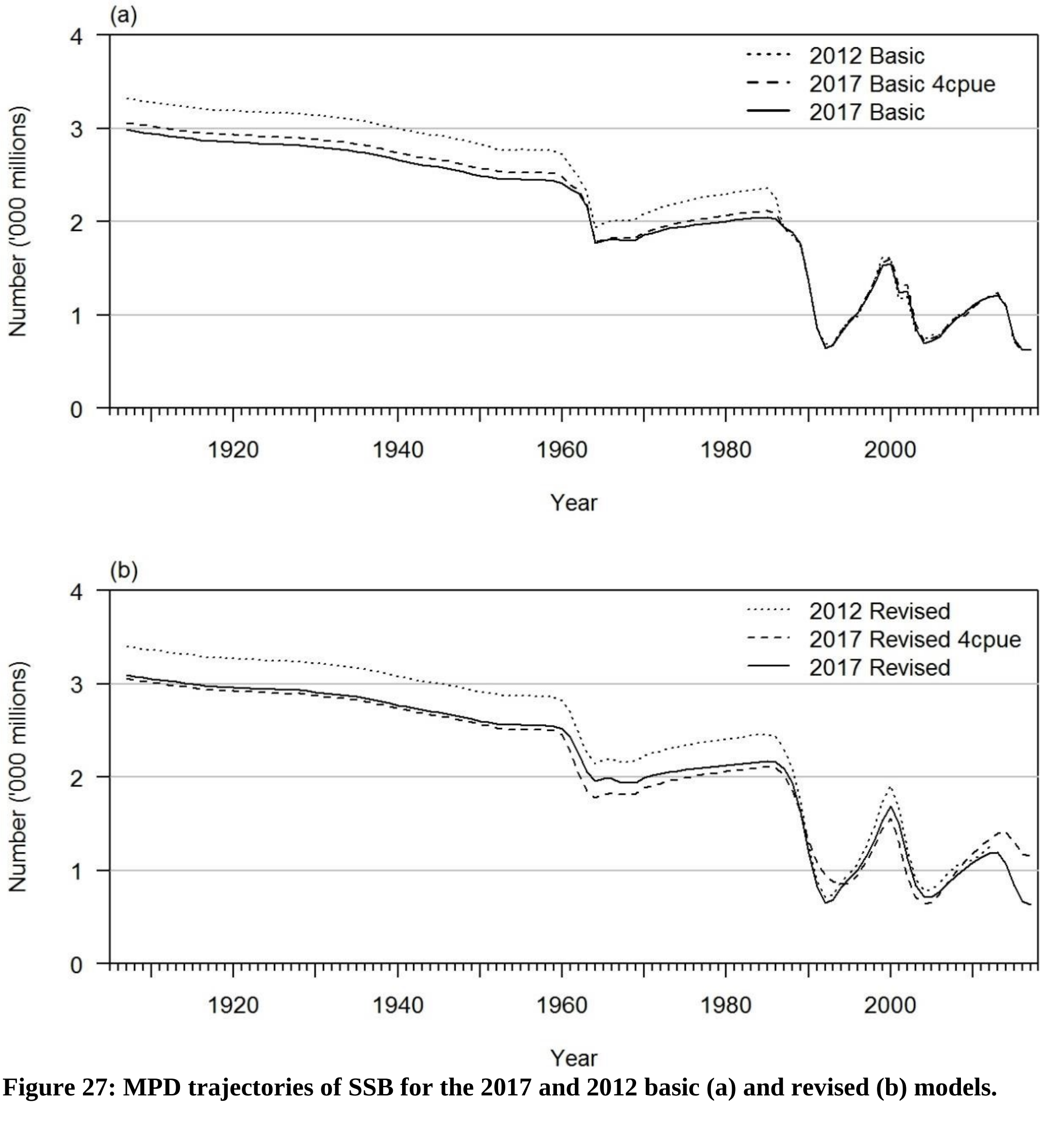

Figure 27: MPD trajectories of SSB for the 2017 and 2012 basic (a) and revised (b) models.

The MPD estimates of spawning stock abundance for recent years were similar to those from the last assessment for both the basic and revised models (Figure 27), and with the stock trajectories very close between the updated basic and revised models. For the new models using the 4-CPUE series, the results from the basic 4-cpue model were similar to the basic model (especially so for recent years), whereas results from the revised 4-cpue model were different, particularly from 2010 onwards when the stock is shown to decline at less of a rate than the other models, and to a level in 2017 that is nearly twice that from the revised and basic models.

MPD model fits to abundance indices for the basic model (see Appendix A Figures 51–52) and revised model (see Appendix A Figures 63–65) are similar to the previous assessment, as are those for the basic 4-cpue model (see Appendix A Figures 77–79), and show no strong evidence of poor fit to the data. In contrast, the revised 4-cpue model does not have a good fit to the abundance data (see Appendix A Figures 80–88), with expected values from 2010 estimated higher for the March survey index and lower for the October survey index. For the revised models, the fits to the tag-recapture length frequency distributions were reasonable (see Appendix A Figures 73 and 100). Estimates of growth parameters for the revised model (g30 = 11.86 mm and g55 = 3.89 mm) are similar to those obtained externally, and slightly lower for the revised 4-cpue model (g30 = 11.40 mm and g55 = 3.55 mm)

The CPUE increased from 2006 to 2010 as the stock rebuilt from the last outbreak of *B. exitiosa*, but it is still below the catch rate levels in the late-1990s and early-2000s. CPUE stayed around this 2010 level through to 2016. The revised 4-cpue model provides a better fit to the CPUE data from 2010 (series D), and changes the fit to the shortened series C, estimating higher rates in the 1990s and late-2000s than the other models. The revised 4-cpue model also has a better fit to the commercial catch data from 2010 compared to the other models, with a slight shift in the distribution of expected values to larger lengths. To enable a better fit to the CPUE data and commercial catch length data since 2010 (and in comparison to the other models) the revised 4-cpue model has to increase the values expected from the March survey series (reducing the fit to these data), reduce the estimated disease mortality rate (see Appendix A Figure 101) and increase relative year class strengths (i.e. higher recruitment) (see Appendix A Figure 102).

As noted in previous assessments (Fu & Dunn, 2009) it has been suggested that oyster CPUE can remain high in years of rapidly declining abundance, as fishers can easily target any remaining high-density patches. This, coupled with increased gear efficiency in recent years and the introduction of high-grading since 2010 (targeting oysters larger than 72 mm), could introduce a bias in CPUE estimates that is difficult to determine. Therefore, while the stock is now rebuilding after a period of high disease mortality and successive years of low recruitment, it would be prudent to be cautious about interpreting the recent increases in CPUE during this same period as a signal of an increase in abundance.

It is difficult to determine the combinations of data and priors that are likely to be driving the estimation of B_0 and other model outputs. For the basic and revised models, likelihood profiles were run for B_0, evaluating the minimum objective function while fixing B_0 and allowing all other parameters to vary. Values for each of the likelihood components (datasets and priors), along with the total objective function are plotted for each model in Figure 28. While the estimate of B_0 is similar for both models at around 3 million oysters, the upper limit of B_0 is not as well defined as the lower limit, with the likelihood surface in the region of the global minimum being particularly “flat” in the basic model (as was the case for both the 4-cpue models (Figure 30).

Using all catch sampling data, the model estimates B_0 to be 3 million oysters (Figure 28). If the commercial catch sampling data is truncated at 65 mm in the basic model (effectively removing observations of recruit sized oysters), the likelihood surface becomes flatter, and the model estimate (total negLL) of B_0 is 9+ million oysters (Figure 29). These profiles (along with the results from the 4-cpue models) highlight the need to better understand how the datasets (along with data weightings), and the priors are behaving within the model.

Without further investigation it is difficult to interpret the difference in model outputs, particularly the variance around model estimates and the extent to which the different models can make projected estimates beyond the current assessment year. The basic and revised models were used to construct MCMC estimates of current and projected stock status.

Table 11: Objective function values (negative log-likelihood) for MPD fits to data, penalties and priors, and the total objective function value, for the basic and revised models, and the 4-cpue sensitivity cases.

Component	Basic	Basic 4cpue	Revised	Revised 4cpue
1976 survey	-1.8	-1.8	–	–
1979 recapture data	–	–	165.6	165.2
1981 recapture data	–	–	83.0	84.0
Bonamia selectivity data	–	–	64.3	57.2
CPUE-A	-24.1	-24.3	-24.6	-25.2
CPUE-B	-13.3	-13.5	-12.9	-13.7
CPUE-C	-17.5	-12.4	-19.0	-15.3
CPUE-D	–	-7.7	–	-9.2
Commercial catch sampling	701.7	645.1	764.7	634.5
Jeffs Hickman maturity data	64.4	63.8	63.6	63.6
July survey (recruits)	-2.2	-2.2	-2.1	-0.9
Mark recapture Survey (recruits)	-2.4	-2.5	-2.7	-2.7
March survey (recruits)	-10.3	-12.9	-7.9	-4.3
March survey (pre-recruits)	-7.0	-6.5	-8.9	-1.9
March survey (smalls)	13.0	8.9	11.9	0.9
October survey (recruits)	-4.8	-6.9	2.6	-2.4
October survey (pre-recruits)	1.8	2.8	-0.8	-0.3
October survey (smalls)	-6.2	-5.4	-5.4	-2.5
October dive survey	46.1	40.9	71.4	59.0
October survey length frequency (recruits)	66.8	60.7	98.5	79.0
October survey length frequency (pre-recruits)	39.4	35.5	58.7	47.9
October survey length frequency (smalls)	81.4	75.1	109.2	94.5
Subtotal (data)	924.9	836.8	1409.2	1207.4
Catch limit penalties	0.0	0.0	0.0	0.0
Disease smoothing penalties	–	–	4.9	2.7
Subtotal (penalties)	0.0	0.0	4.9	2.7
Priors	172.0	154.0	137.6	74.8
Total	1097.0	990.9	1551.7	1285.0

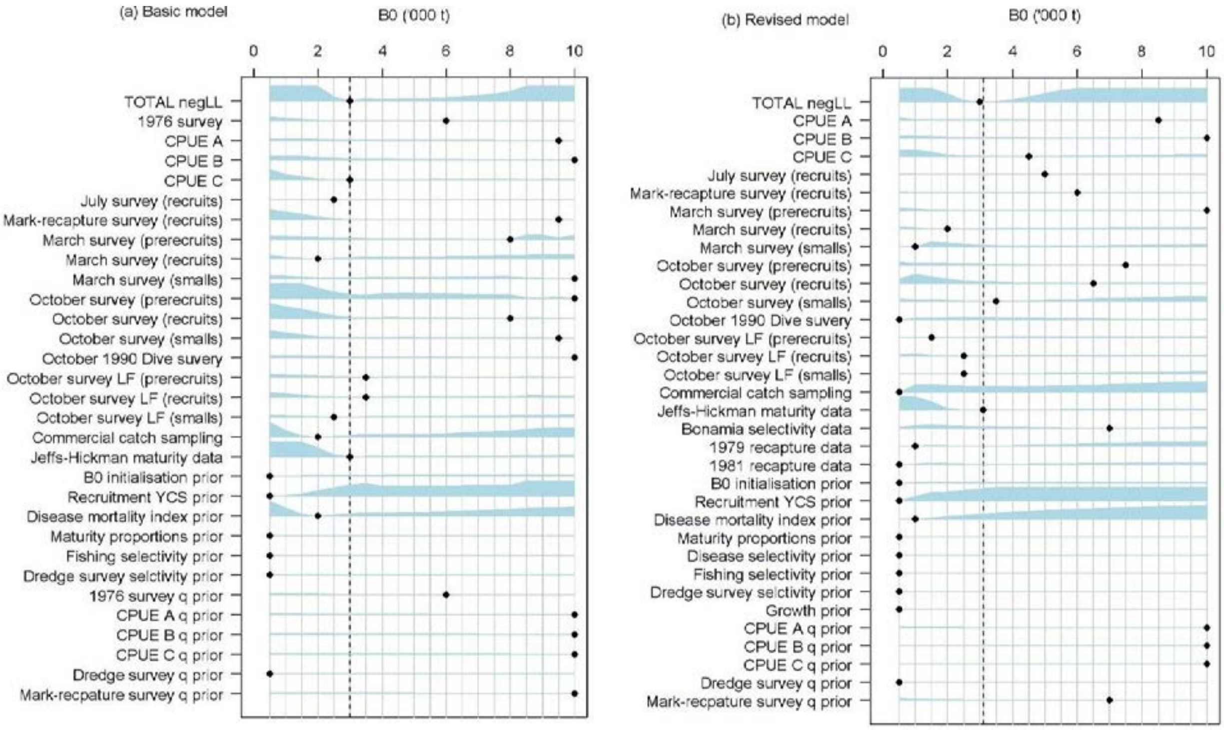

Figure 28: Likelihood profiles of B_0 for the 2017 basic model (a) and revised model (b). Negative log-likelihood values rescaled to have minimum 0 for each dataset, the dashed line indicates the MPD value of B_0 in all cases. B_0 is on the x-axis and datasets on the y-axis, with the profile shaded (negLL at values of B_0 between 0.5 and 10 million) in blue and best MPD value for that dataset as a black dot.

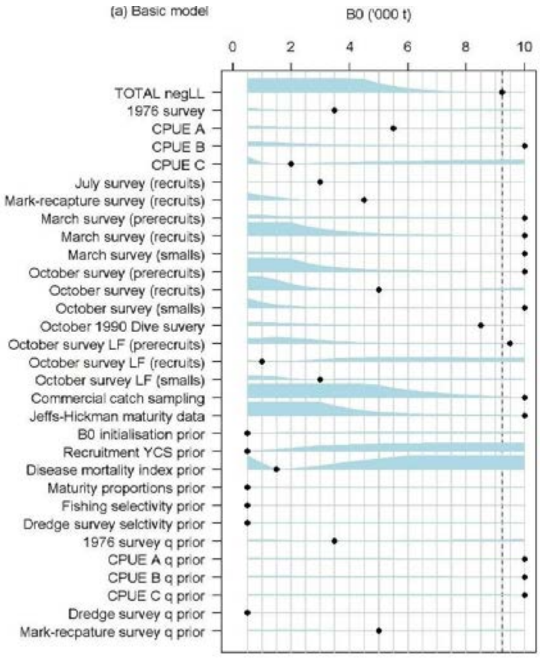

Figure 29: Likelihood profiles of B_0 for the 2017 basic model (truncated commercial catch sampling data). Negative log-likelihood values rescaled to have minimum 0 for each dataset, the dashed line indicates the MPD value of B_0 in all cases. B_0 is on the x-axis and datasets on the y-axis, with the profile shaded (negLL at values of B_0 between 0.5 and 10 million) in blue and best MPD value for that dataset as a black dot.

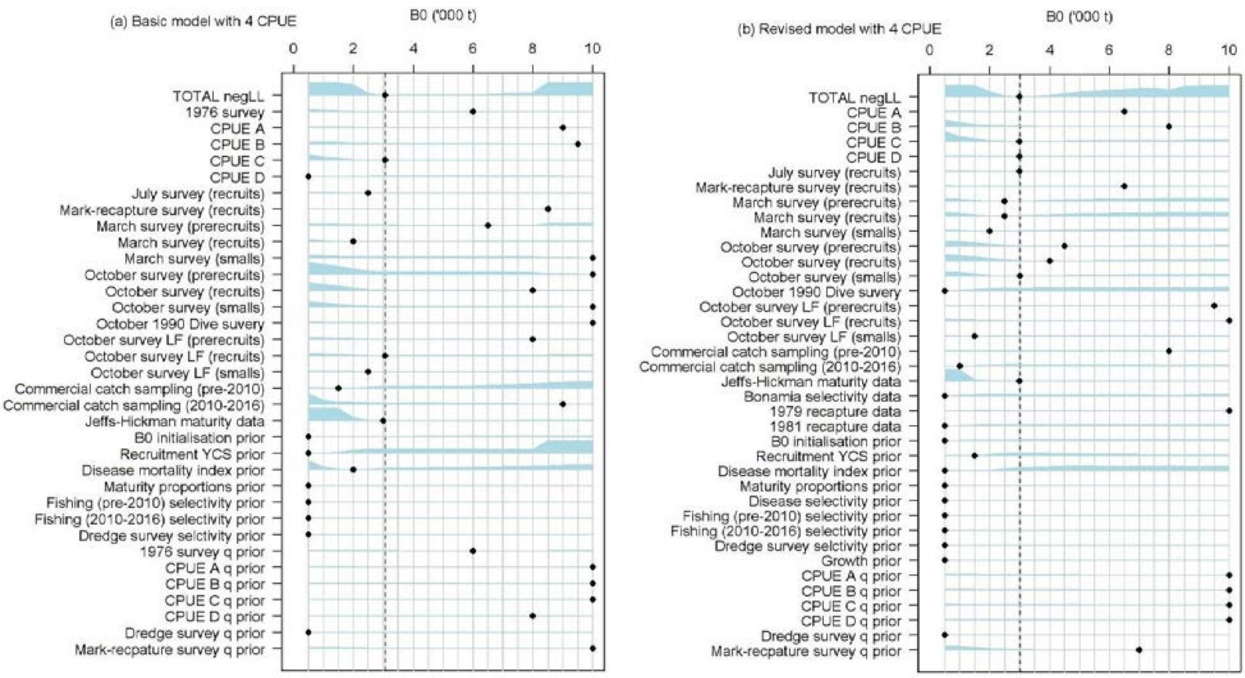

Figure 30: Likelihood profiles of B_0 for the 2017 basic 4-cpue model (a) and revised 4-cpue model (b). Negative log-likelihood values rescaled to have minimum 0 for each dataset, the dashed line indicates the MPD value of B_0 in all cases. B_0 is on the x-axis and datasets on the y-axis, with the profile shaded in blue (negLL at values of B_0 between 0.5 and 10 million) and best MPD value for that dataset as a black dot.

4.2 MCMC Results

Initially, a single Markov chain Monte-Carlo (MCMC) was run for each model, with length 3×10^6 iterations including a burn-in of 0.5×10^6 and systematic subsampling ("thinning") of the chain, excluding the burn-in, to 2500 samples for the 2017 basic model. Evidence of non-convergence for this chain was apparent. The initial chain for the revised model was run for a greater number of iterations than that for the basic model in response to the problems encountered with the MCMC of the basic model. For the 2017 revised model, an MCMC was run with length 8×10^6 iterations, including a burn-in of 3×10^6 iterations and thinning of the chain (excluding burn-in) to 5000 samples.

Although a reasonable looking trace plot was achieved from the initial chain run for the revised model (Figure 31) with no indication of non-convergence, this was not the case for the initial chain of the basic model (Figures 32, 33). Trace plots from running a longer chain of 10×10^6 iterations (with a burn in of 2×10^6) for the basic model indicated that convergence was still problematic (Figure 34). To improve mixing, a chain was run of length 6×10^6, where the correlation matrix was re-estimated after 2×10^6 and 4×10^6 iterations, based on the previous iterations thinned to 1500 after a burn-in of 0.5×10^6. The trace plot of the final 1500 samples from the posterior distribution of B_0 indicated improved mixing (Figure 34). Three chains were run for each model, with model estimation made from the final samples from the three chains combined. For comparison to previous stock assessment models, the MCMC trace plots for the 2007 and 2009 assessments are shown in Figure 35. The posterior distributions for B_0 from the models of 2007, 2009, 2012, and 2017 are compared in Figure 36.

The differences in the MCMC posterior samples generated from each model are consistent with the differences in the likelihood surface near the minimum ('best') value from the MPD of each model described in the previous section. The likelihood surface is poorly defined at the upper limits for the basic model compared to the revised model. And, though MCMC diagnostics for the two models do not indicate non-convergence (Appendix A), it is difficult to determine how well defined the parameter spaces are; whether or not the chain for each model is performing an optimal exploration of the parameter space, and what bias (if any) may be associated with any non-optimal exploration. That is, is the narrower posterior distribution due to the MCMC chain becoming "stuck" in a local minimum? And, are the wider posterior distributions providing parameter estimates that are biased "high" due to the upper limit being poorly defined? Structural issues within the model may be responsible for these patterns in the MPD profiles and MCMC trace plots, and further investigation is required to determine if this is the case. We note that a comparable situation was evident in the 2007 and 2009 stock assessments, but in those cases, it was the revised models with the wider MCMC posterior distributions (Figure 36).

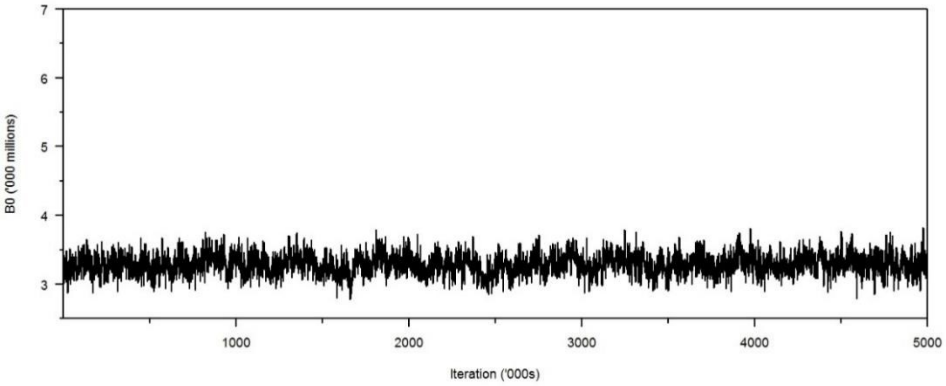

Figure 31: MCMC trace plot of B_0 for the 2017 Revised model.

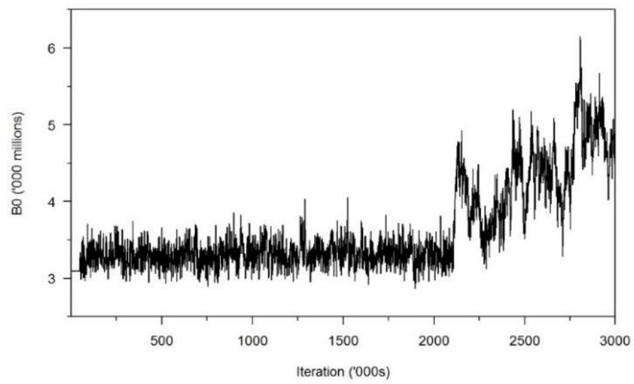

Figure 32: Trace plot (including the burn in) of B_0 for the 2017 Basic model initial MCMC run (short chain, without any recalculation of the covariance matrix).

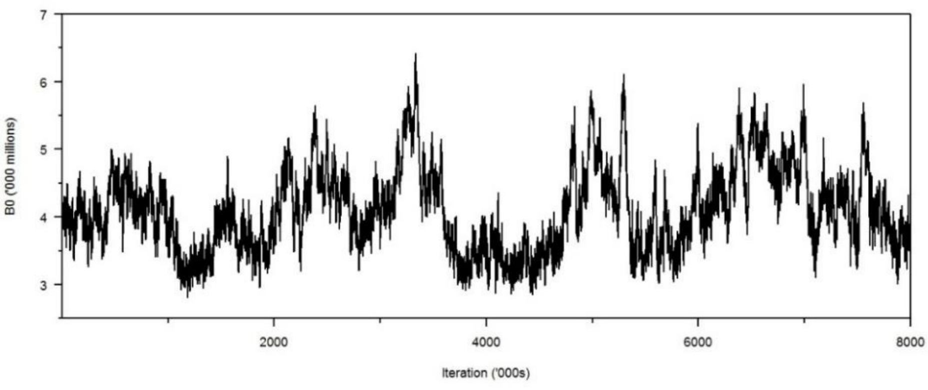

Figure 33: Trace plot of B_0 for the 2017 Basic model initial MCMC run (long chain, without any recalculation of the covariance matrix).

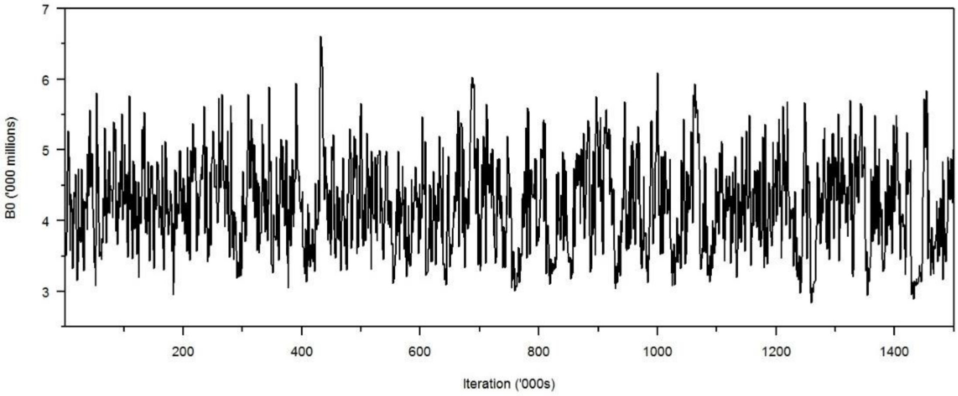

Figure 34: MCMC trace plot of B_0 for the 2017 Basic model (long chain, with re-estimation of the correlation matrix after 2×10^6 and 4×10^6 iterations and thinned to 1500 samples).

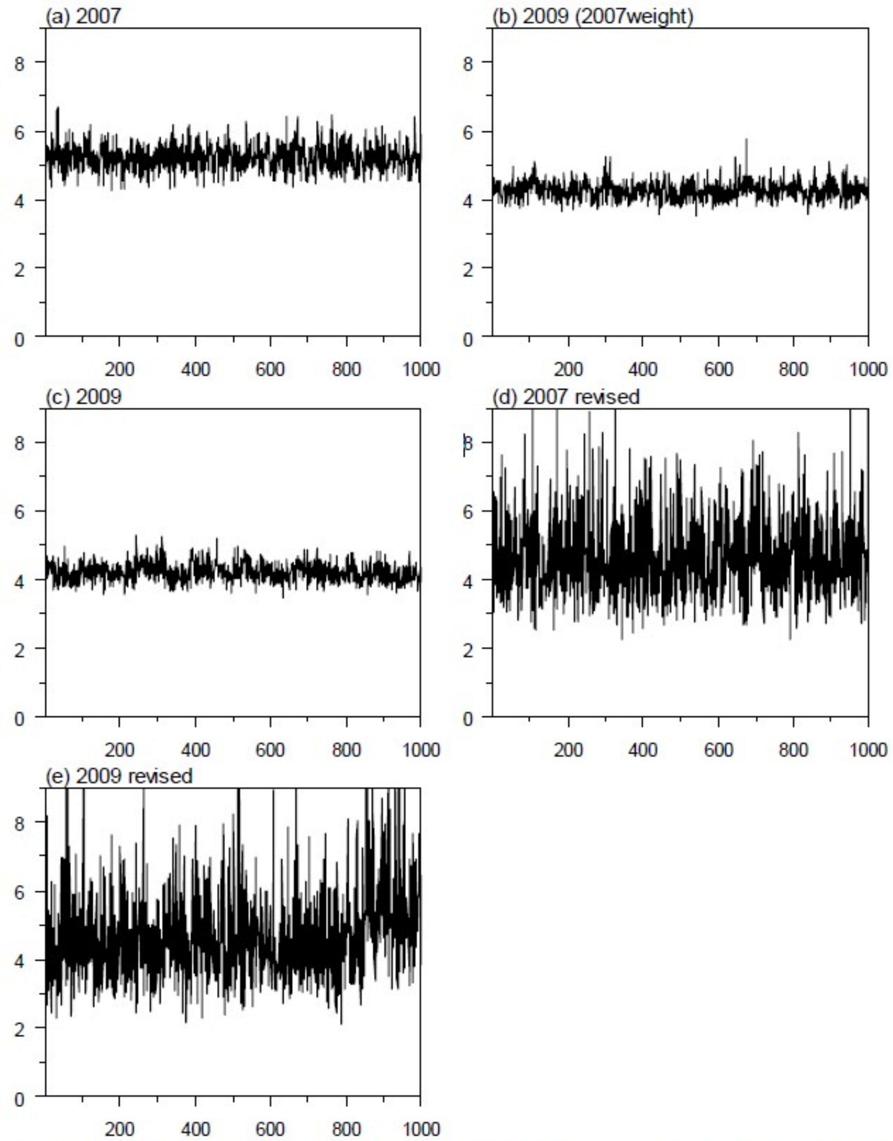

Figure 27: MCMC trace diagnostic plot for the (a) 2007 basic model, (b) 2009 model (2007 weight), (c) 2009 model, (d) revised 2007 model, and (e) revised 2009 model.

Figure 35: Trace plots of B_0 from the 2007 and 2009 stock assessment models, figure and caption reproduced from Fu & Dunn (2009).

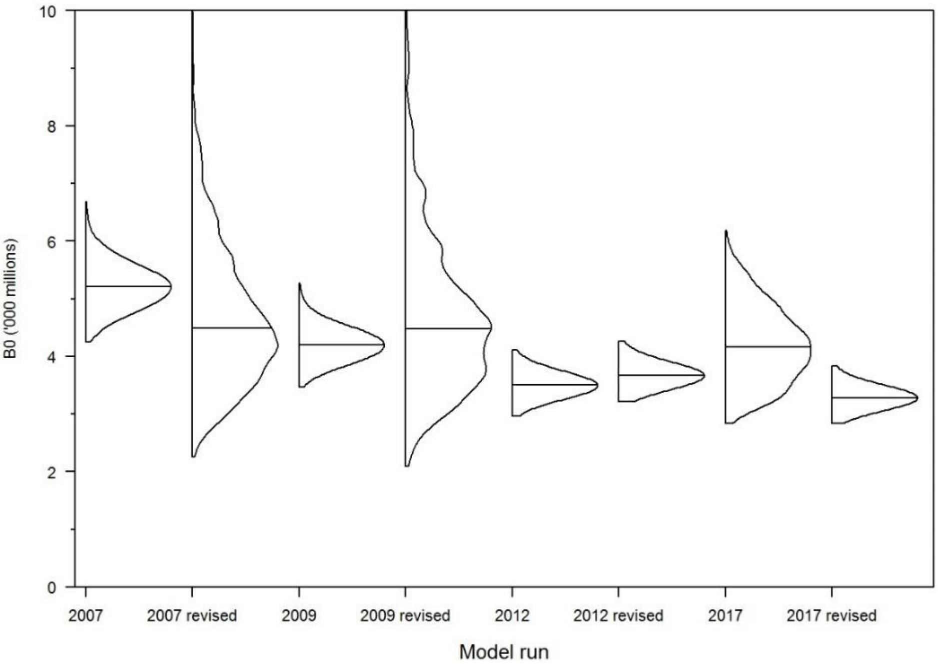

Figure 36: Posterior distribution of B_0 for the basic and revised models from the 2007, 2009, 2012, and 2017 stock assessments.

4.2.1 Current status

The 2017 basic model estimated the virgin equilibrium spawning stock population size to be about 4191 (3053–5503) million oysters and current spawning stock size to be 800 (590–1041) million oysters (Table 12 and Figure 37). The current stock status of the recruit-sized population was estimated as 703 (511–923) million oysters (Table 13), which was about 16.8% (14.3–19.6%) of the initial state (Figure 38). Stock size estimates from the revised model were lower than those from the basic model. The revised 2017 model estimated the equilibrium spawning stock population size to be about 3581 (3008–3593) million oysters and current spawning stock size to be 631 (567–704) million oysters (Figure 39). The relative estimates of B_0 from these model runs suggest much greater variability in the estimates of the initial population size. The estimated current stock size (B_{2017}) also varies between the models, and while the estimate from the revised model falls within the 95% credible interval of the basic model's estimate, the estimate from the basic model is above the upper limit of the interval estimated for the revised model. However, the estimates of current status of the stock from the revised model of 17.1% (14.5–20.0%) (Figure 40) is very similar to that from the basic model. The posterior distributions of both the basic and revised 2017 models for model parameters other than B_0 are shown in Figures 41 and 42.

Estimates of the disease mortality rate ranged from 0.0 up to a maximum of 0.8 y^{-1} (the upper bound) with high rates of disease mortality in the late 1980s and early 2000s, accounting for the dramatic declines in abundance of oysters during periods of epidemic (Figure 43 and Figure 44). Disease mortality rates were estimated as relatively low (less than 0.1 y^{-1}) from 2005 through to 2012, with rates increasing to above 0.2 y^{-1} in 2014 and 2015 then sitting at a lower rate in the last two years. Applying a smoothing penalty to the estimated annual disease mortality rates gave more favourable annual estimates of disease mortality but this may have had little effect on the model estimates of current stock status.

Estimates of relative year class strength were uncertain and variable but suggest that there may have been a pulse of strong recruitment during the mid to late 1990s (Figure 45 and Figure 46). Recruitment since then was estimated to be lower than average, However, without other, better, data on historical levels of recruitment, these estimates cannot be validated. Both models also suggest that the decline in recruitment levels has slowed in the most recent years, with an increase in the last year.

Table 12: Bayesian median and 95% credible intervals of B_0 (millions), and SSBs (millions) for 2017 and 2012 basic and revised models.

Model	B_0	B_{2017}	B_{2012}
2012 Basic	3 510 (3 200–3 870)	-	1 170 (1 060–1 290)
2012 Revised	3 670 (3 350–4 050)	-	1 200 (1 090–1 330)
2017 Basic	4 191 (3 053–5 503)	800 (590–1 041)	1 507 (1 091–1 952)
2017 Revised	3 581 (3 008–3 593)	631 (567–704)	1 130 (1 023–1 238)

Table 13: Bayesian median and 95% credible intervals of B_0 (millions), recruit-sized biomass and recruit-sized biomass as % B_0 for 2017 and 2012 basic and revised models.

Model	B_0	rB_{2017}	rB_{2017} (%B_0)	rB_{2012}	rB_{2012} (%B_0)
2012 Basic	3 510 (3 200–3 870)	-	-	1 070 (960–1 180)	30.6 (26.5–34.3)
2012 Revised	3 670 (3 350–4 050)	-	-	1 050 (950–1 160)	28.8 (25.4–33.0)
2017 Basic	4 191 (3 053–5 503)	703 (511–923)	16.8 (14.3–19.6)	1 485 (1 088–1 926)	35.4 (31.7–39.1)
2017 Revised	3 581 (3 008–3 593)	564 (496–639)	17.1 (14.5–20.0)	1 097 (991–1 196)	33.4 (29.5–37.2)

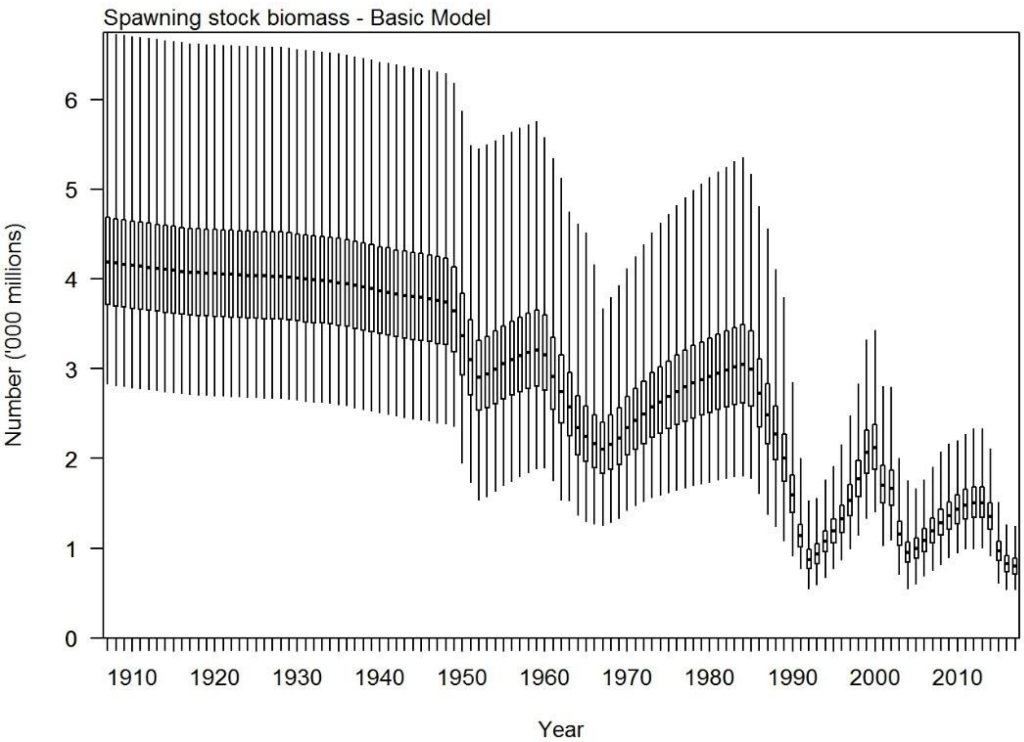

Figure 37: 2017 basic model estimated posterior distribution of *SSB*. Individual distributions show the marginal posterior distribution, with horizontal lines indicating the median.

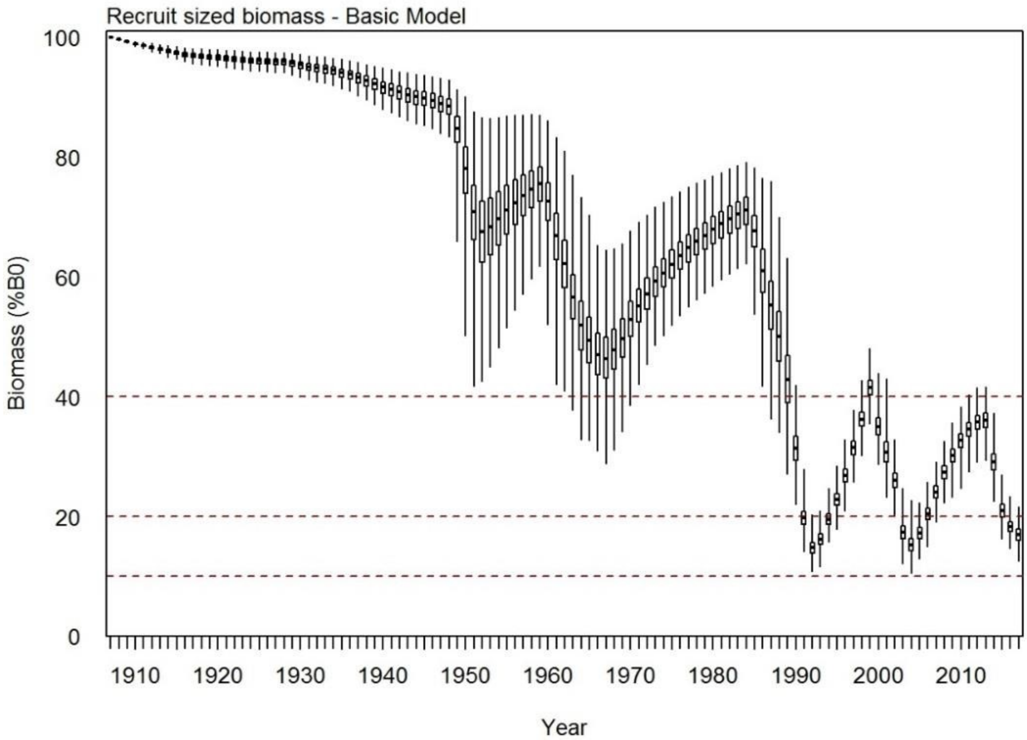

Figure 38: 2017 basic model estimated posterior distribution of recruit-size stock abundance as a percentage of B_0. Individual distributions show the marginal posterior distribution, with horizontal lines indicating the median of each distribution. Dashed horizontal lines indicate the level equal to 10%, 20% and 40% of the 1907 stock abundance.

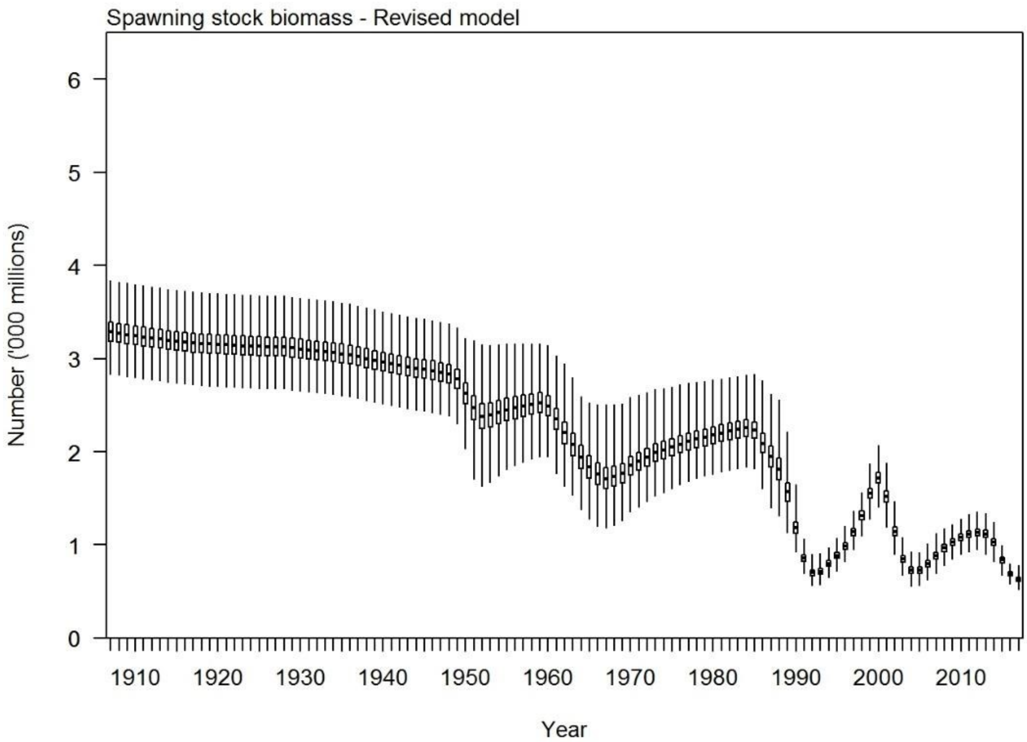

Figure 39: 2017 revised model estimated posterior distribution of *SSB*. Individual distributions show the marginal posterior distribution, with horizontal lines indicating the median.

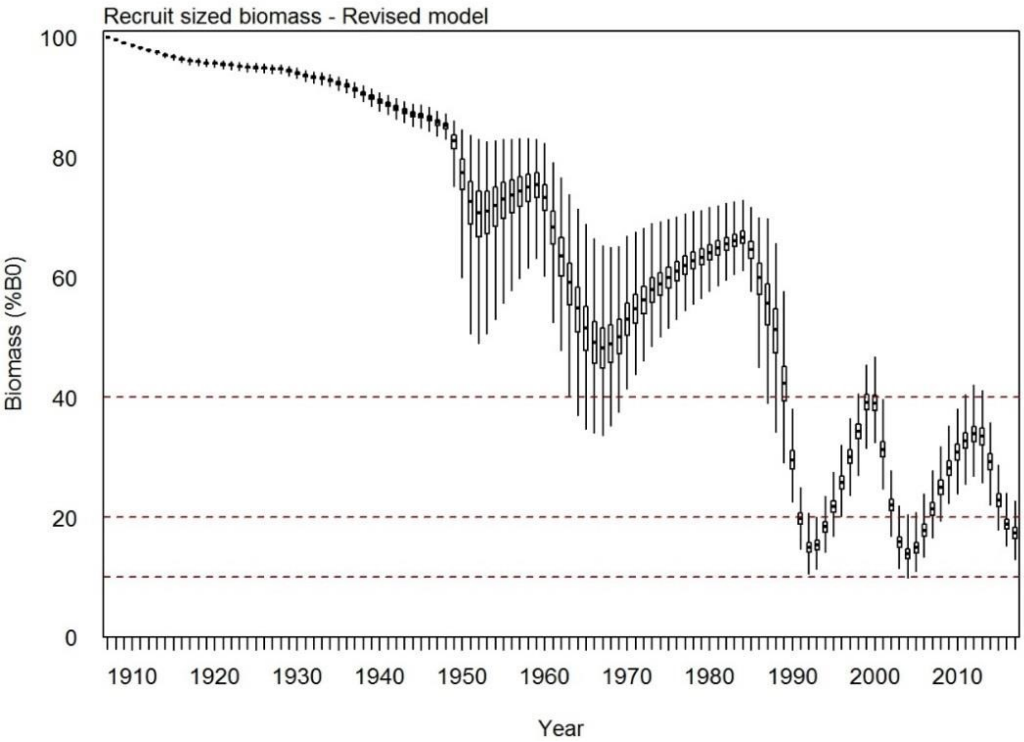

Figure 40: 2017 revised model estimated posterior distribution of recruit-size stock abundance as a percentage of B_0. Individual distributions show the marginal posterior distribution, with horizontal lines indicating the median of each distribution. Dashed horizontal lines indicate the level equal to 10%, 20%, and 40% of the 1907 stock abundance.

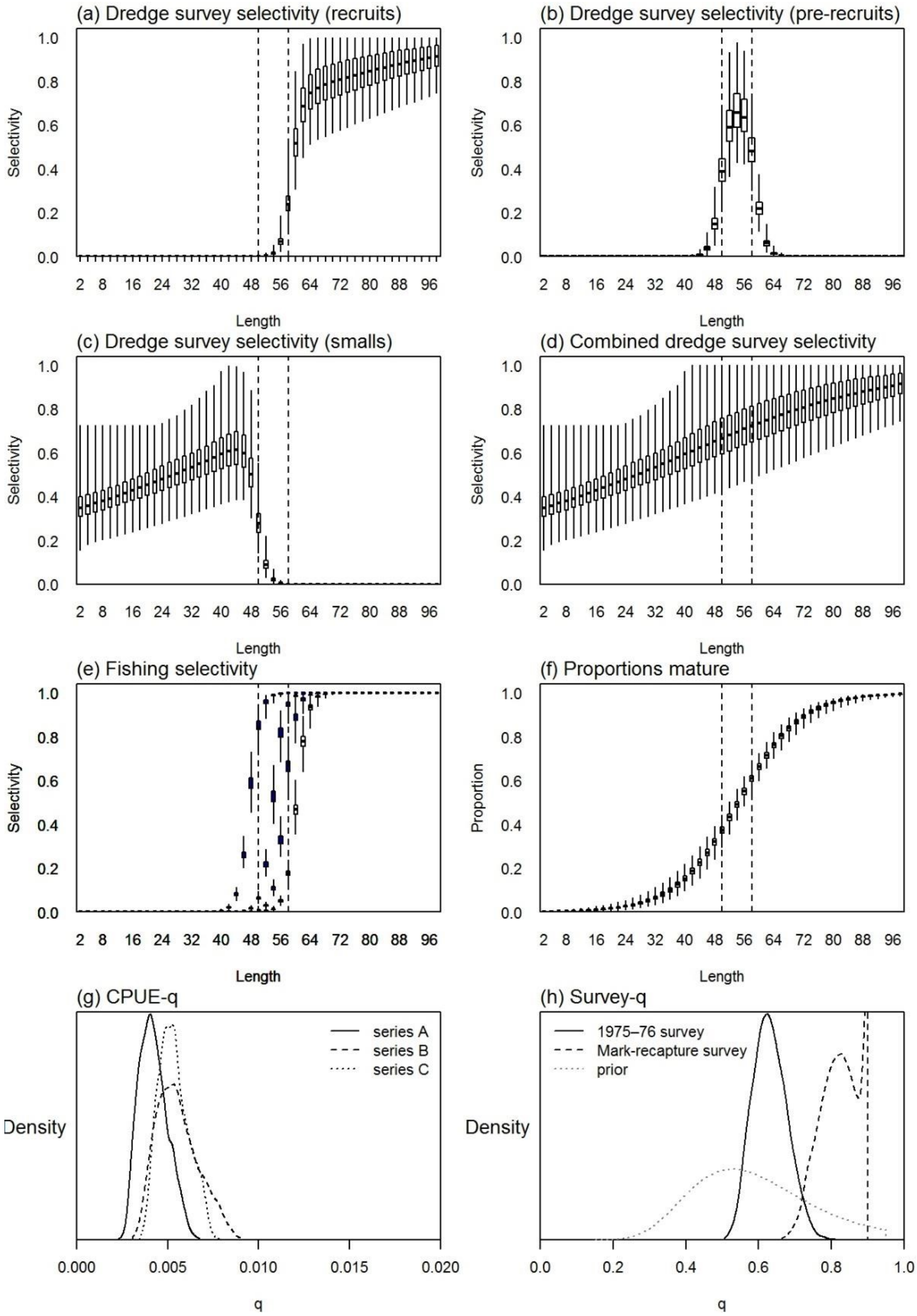

Figure 41: 2017 basic model estimated posterior distributions of selectivity by length for (a) dredge survey recruits; (b) dredge survey pre-recruits; (c) dredge survey smalls; (d) total recruit, pre-recruit, and small dredge survey selectivities combined; (e) fishing selectivities; and (f) proportions mature (equivalent to disease selectivity). Individual distributions show the marginal posterior distribution, with horizontal lines indicating the median. Dashed lines separate the small (<50 mm), pre-recruit (≥ 50 mm and <58 mm), and recruit (≥ 58 mm) size groups.

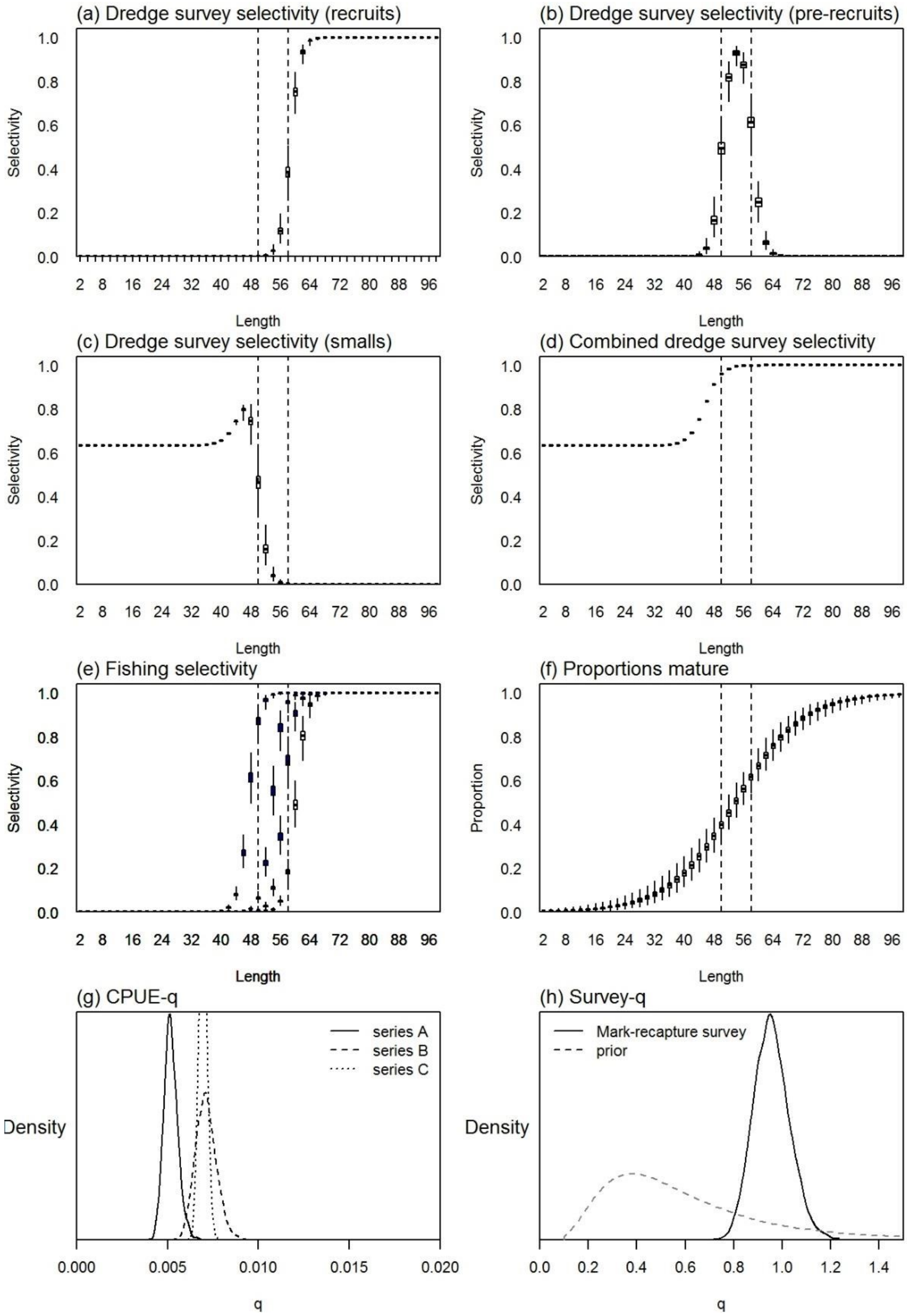

Figure 42: 2017 revised model estimated posterior distributions of selectivity by length for (a) dredge survey recruits; (b) dredge survey pre-recruits; (c) dredge survey smalls; (d) total recruit, pre-recruit, and small dredge survey selectivities combined; (e) fishing selectivities; and (f) proportions mature (equivalent to disease selectivity). Individual distributions show the marginal posterior distribution, with horizontal lines indicating the median. Dashed lines separate the small (<50 mm), pre-recruit (≥ 50 mm and <58 mm), and recruit (≥ 58 mm) size groups.

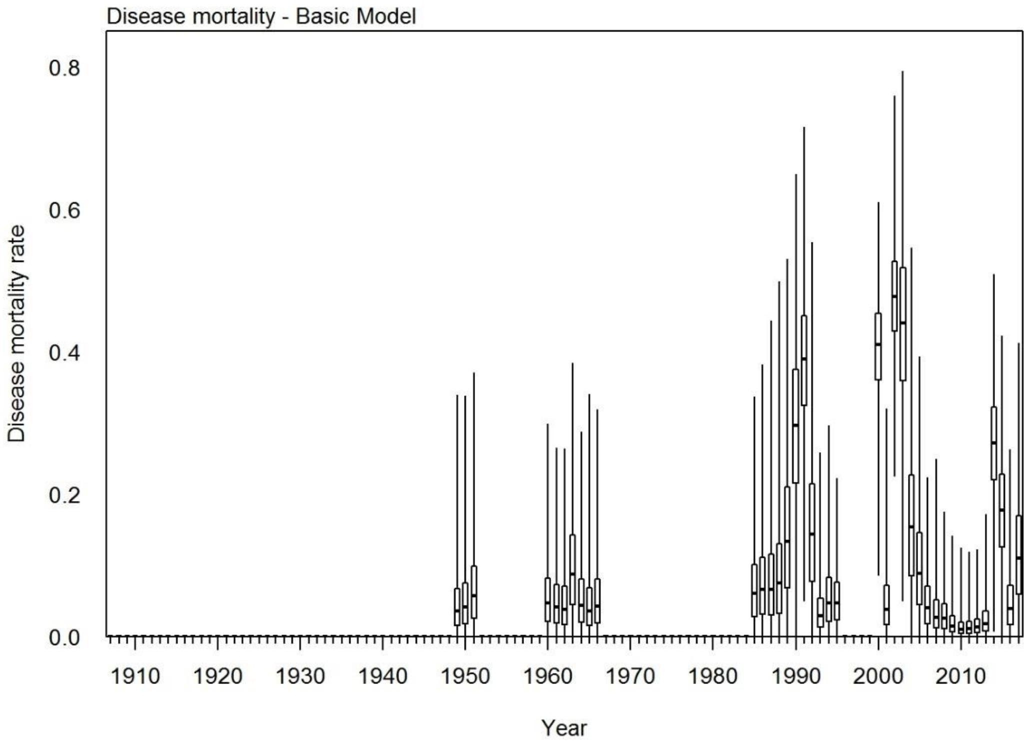

Figure 43: 2017 basic model estimated posterior distributions of disease mortality. Individual distributions show the marginal posterior distribution, with horizontal lines indicating the median of each distribution.

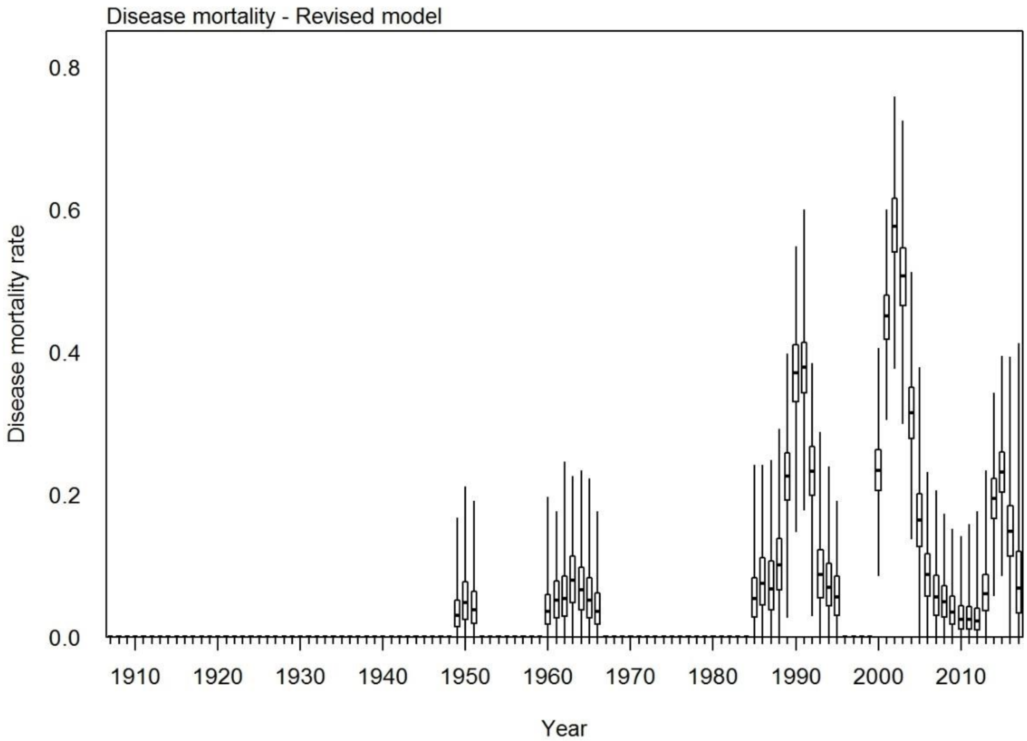

Figure 44: 2017 revised model estimated posterior distributions of disease mortality. Individual distributions show the marginal posterior distribution, with horizontal lines indicating the median of each distribution.

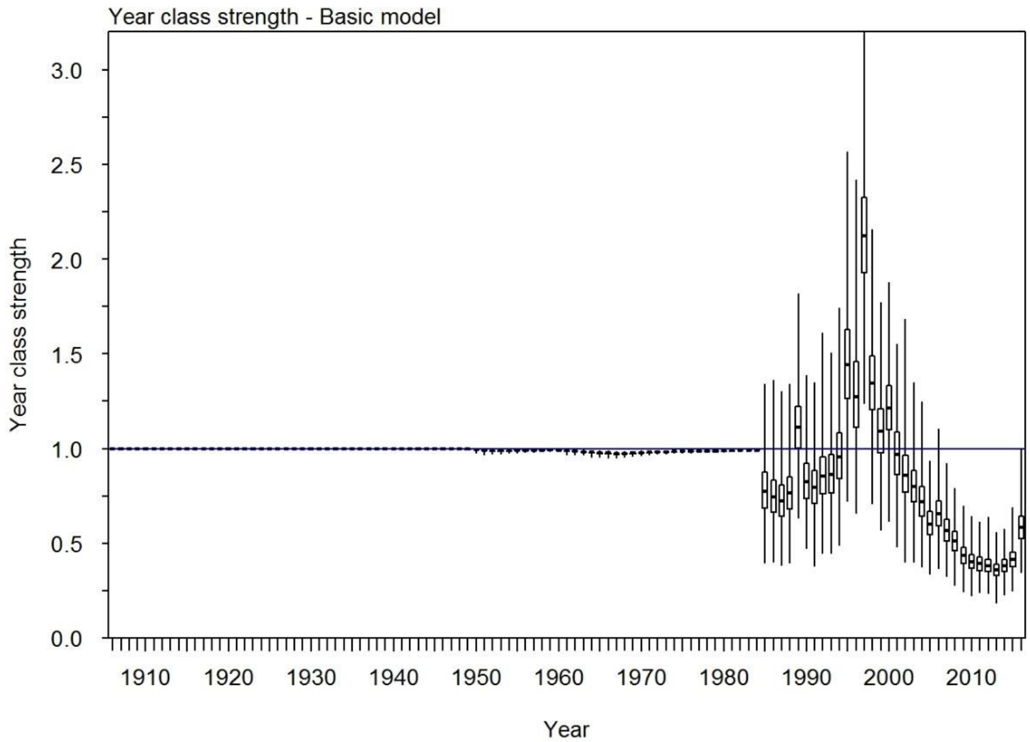

Figure 45: 2017 basic model estimated posterior distributions of year class strength. Individual distributions show the marginal posterior distribution, with horizontal lines indicating the median of each distribution.

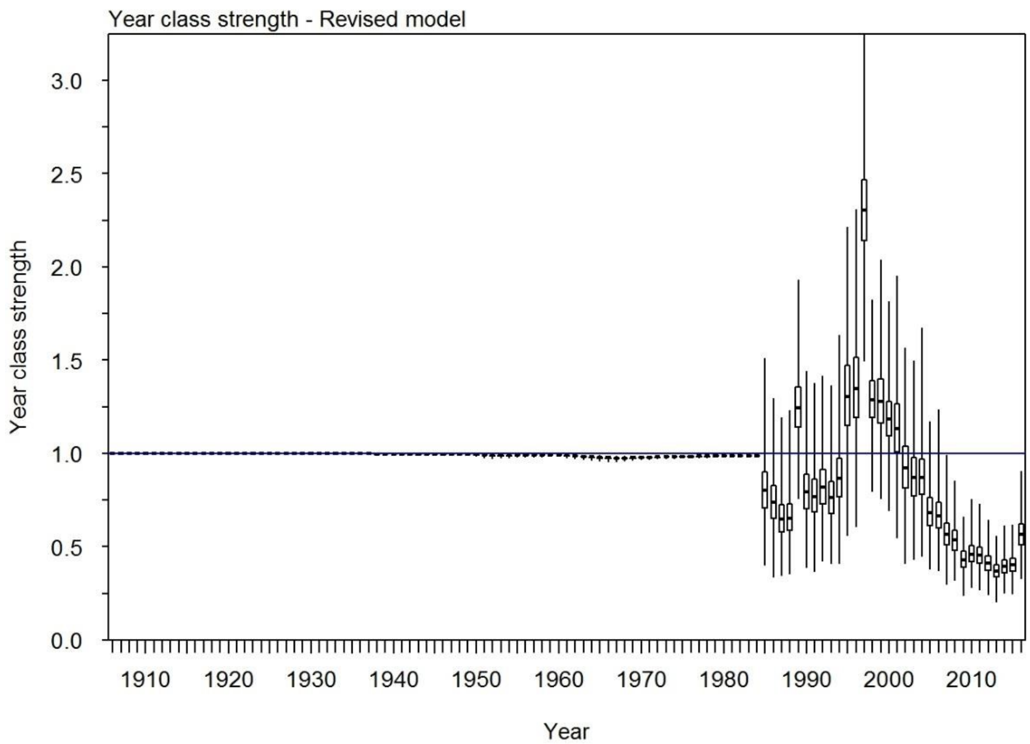

Figure 46: 2017 revised model estimated posterior distributions of year class strength. Individual distributions show the marginal posterior distribution, with horizontal lines indicating the median of each distribution.

4.2.2 Projected status

Projected stock estimates were made assuming that future recruitment will be lognormally distributed with a mean of 1.0 and standard deviation equal to the standard deviation of the log of recruitment between 1985 and 2015. Projections were made assuming no future disease mortality and with future disease mortality assumed to be 0.10 y^{-1} and 0.20 y^{-1}. Four future annual commercial catches were considered of either 7.5, 15, 20 or 30 million oysters. Future customary, recreational, and illegal catch were assumed equal to levels assumed for 2017. Projected output quantities are summarised in Tables 14–17. The plots of the median expected recruit-sized population for each model are given in Figure 47 for the basic model and Figure 48 for the revised model.

Under the assumptions of future disease mortality for the basic model, projections of commercial catch at either 7.5, 15, 20, or 30 million showed relatively little difference in expected population size. For example, the projected population size in 2020 with a commercial catch of 7.5 million was less than 1% higher than that with a commercial catch of 20 million oysters (Tables 14 and 16). Depending on the level of assumed disease mortality, projected status in 2020 ranged from about 41% more than current levels (assuming no disease mortality) to a level about 30% less than the current levels (assuming disease mortality of 0.2 y^{-1}) for the 2017 basic model (Table 15), and from about 54% more than current levels (assuming no disease mortality) to a level about 24% less than the current levels (assuming disease mortality of 0.2 y^{-1}) for the 2017 revised model (Table 17).

Table 14: 2017 basic model median and 95% credible intervals of current spawning stock biomass 2017 (B_{2017}), and projected spawning stock abundance for 2018–20 (B_{2018}–B_{2020}) as a percentage of B_0, with an assumption of a future catch of 7.5, 15, 20, or 30 million oysters in 2018–22, and disease mortality of 0.0, 0.1, or 0.2 y^{-1}.

Disease mortality	Catch (millions)	B_{2017} (% B_0)	B_{2018} (% B_0)	B_{2019} (% B_0)	B_{2020} (% B_0)
0	7.5	23.6 (20.5–28.0)	24.5 (19.1–31.9)	28.7 (22.0–38.6)	33.1 (25.1–45.9)
	15	23.6 (20.5–28.0)	24.5 (19.1–31.9)	28.6 (21.8–38.5)	32.8 (24.9–45.7)
	20	23.6 (20.5–28.0)	24.5 (19.1–31.9)	28.5 (21.7–38.4)	32.6 (24.7–45.5)
	30	23.6 (20.5–28.0)	24.5 (19.1–31.9)	28.3 (21.6–38.2)	32.3 (24.3–45.2)
0.1	7.5	23.6 (20.5–28.0)	23.8 (18.5–31.0)	25.0 (18.9–33.9)	26.3 (19.7–37.2)
	15	23.6 (20.5–28.0)	23.8 (18.5–31.0)	24.9 (18.7–33.8)	26.0 (19.5–37.0)
	20	23.6 (20.5–28.0)	23.8 (18.5–31.0)	24.8 (18.7–33.7)	25.9 (19.3–36.8)
	30	23.6 (20.5–28.0)	23.8 (18.5–31.0)	24.6 (18.5–33.5)	25.6 (18.9–36.6)
0.2	7.5	23.6 (20.5–28.0)	23.1 (17.9–30.1)	21.9 (16.5–30.1)	21.3 (15.7–30.8)
	15	23.6 (20.5–28.0)	23.1 (17.9–30.1)	21.8 (16.4–30.0)	21.1 (15.5–30.5)
	20	23.6 (20.5–28.0)	23.1 (17.9–30.1)	21.7 (16.3–29.9)	21.0 (15.4–30.4)
	30	23.6 (20.5–28.0)	23.1 (17.9–30.1)	21.6 (16.1–29.8)	20.7 (15.1–30.1)

Table 15: 2017 basic model median and 95% credible intervals of expected recruit-size stock abundance for 2017–20 with an assumption of a future catch of 7.5, 15, 20, or 30 million oysters in 2017–20, and disease mortality rates of 0.0, 0.1, or 0.2 y^{-1}.

Disease mortality	Catch (millions)	rB_{2017} /r B_{2017}	rB_{2018} /r B_{2017}	rB_{2018} /r B_{2017}	rB_{2020} /r B_{2017}
0	7.5	1.0 (1.0–1.0)	1.01 (0.88–1.13)	1.18 (1.00–1.46)	1.41 (1.14–1.91)
	15	1.0 (1.0–1.0)	1.01 (0.88–1.13)	1.07 (0.99–1.45)	1.39 (1.13–1.89)
	20	1.0 (1.0–1.0)	1.01 (1.88–1.13)	1.16 (0.99–1.45)	1.38 (1.12–1.88)
	30	1.0 (1.0–1.0)	1.01 (1.88–1.13)	1.15 (0.97–1.44)	1.36 (1.10–1.86)
0.1	7.5	1.0 (1.0–1.0)	0.94 (0.82–1.04)	0.94 (0.80–1.18)	1.01 (0.80–1.38)
	15	1.0 (1.0–1.0)	0.94 (0.82–1.04)	0.94 (0.79–1.17)	0.99 (0.79–1.36)
	20	1.0 (1.0–1.0)	0.94 (0.82–1.04)	0.93 (0.79–1.17)	0.99 (0.78–1.36)
	30	1.0 (1.0–1.0)	0.94 (0.82–1.04)	0.92 (0.78–1.16)	0.97 (0.76–1.34)
0.2	7.5	1.0 (1.0–1.0)	0.86 (0.75–0.96)	0.76 (0.64–0.96)	0.73 (0.57–1.01)
	15	1.0 (1.0–1.0)	0.86 (0.75–0.96)	0.75 (0.63–0.95)	0.72 (0.55–1.00)
	20	1.0 (1.0–1.0)	0.86 (0.75–0.96)	0.75 (0.63–0.95)	0.71 (0.55–1.00)
	30	1.0 (1.0–1.0)	0.86 (0.75–0.96)	0.74 (0.62–0.94)	0.70 (0.53–0.99)

Table 16: 2017 revised model median and 95% credible intervals of current spawning stock biomass 2017 (B_{2017}), and projected spawning stock abundance for 2018–20 (B_{2018}–B_{2020}) as a percentage of B_0, with an assumption of a future catch of 7.5, 15, 20, or 30 million oysters in 2018–22, and disease mortality of 0.0, 0.1, or 0.2 y^{-1}.

Disease mortality	Catch (millions)	B_{2017} (% B_0)	B_{2018} (% B_0)	B_{2019} (% B_0)	B_{2020} (% B_0)
0	7.5	21.4 (18.3–25.7)	23.7 (18.7–30.2)	28.0 (22.1–36.5)	32.4 (25.6–42.8)
	15	21.4 (18.3–25.7)	23.7 (18.7–30.2)	27.8 (21.9–36.3)	32.1 (25.2–42.5)
	20	21.4 (18.3–25.7)	23.7 (18.7–30.2)	27.7 (21.8–36.2)	31.8 (25.0–42.2)
	30	21.4 (18.3–25.7)	23.7 (18.7–30.2)	27.7 (21.8–36.2)	31.8 (25.0–42.2)
0.1	7.5	21.4 (18.3–25.7)	23.1 (18.2–29.5)	23.1 (18.2–29.5)	23.1 (18.2–29.5)
	15	21.4 (18.3–25.7)	23.1 (18.2–29.5)	24.9 (19.5–32.8)	26.7 (20.8–35.8)
	20	21.4 (18.3–25.7)	23.1 (18.2–29.5)	24.7 (19.4–32.6)	26.5 (20.6–35.6)
	30	21.4 (18.3–25.7)	23.1 (18.2–29.5)	24.5 (19.2–32.4)	26.1 (20.2–35.2)
0.2	7.5	21.4 (18.3–25.7)	23.1 (18.2–29.5)	24.5 (19.2–32.4)	26.1 (20.2–35.2)
	15	21.4 (18.3–25.7)	22.5 (17.8–28.8)	22.3 (17.4–29.6)	22.4 (17.5–30.5)
	20	21.4 (18.3–25.7)	22.5 (17.8–28.8)	22.2 (17.3–29.5)	22.3 (17.3–30.4)
	30	21.4 (18.3–25.7)	22.5 (17.8–28.8)	22.0 (17.1–29.3)	21.9 (16.9–30.0)

Table 17: 2017 revised model median and 95% credible intervals of expected recruit-size stock abundance for 2017–20 with an assumption of a future catch of 7.5, 15, 20, or 30 million oysters in 2017–20, and disease mortality rates of 0.0, 0.1, or 0.2 y^{-1}.

Disease mortality	Catch (millions)	rB_{2017} /r B_{2017}	rB_{2018} /r B_{2017}	rB_{2019} /r B_{2017}	rB_{2020} /r B_{2017}
0	7.5	1.00 (1.00–1.00)	1.07 (0.95–1.16)	1.27 (1.10–1.53)	1.54 (1.27–2.02)
	15	1.00 (1.00–1.00)	1.07 (0.95–1.16)	1.26 (1.08–1.52)	1.52 (1.24–1.99)
	20	1.00 (1.00–1.00)	1.07 (0.95–1.16)	1.25 (1.07–1.51)	1.50 (1.23–1.97)
	30	1.00 (1.00–1.00)	1.07 (0.95–1.16)	1.23 (1.06–1.50)	1.47 (1.20–1.94)
0.1	7.5	1.00 (1.00–1.00)	1.00 (0.89–1.09)	1.06 (0.91–1.30)	1.18 (0.95–1.57)
	15	1.00 (1.00–1.00)	1.00 (0.89–1.09)	1.06 (0.91–1.30)	1.18 (0.95–1.57)
	20	1.00 (1.00–1.00)	1.00 (0.89–1.09)	1.18 (0.95–1.57)	1.14 (0.92–1.53)
	30	1.00 (1.00–1.00)	1.00 (0.89–1.09)	1.03 (0.88–1.26)	1.12 (0.90–1.51)
0.2	7.5	1.00 (1.00–1.00)	0.94 (0.83–1.02)	0.89 (0.76–1.10)	0.91 (0.72–1.22)
	15	1.00 (1.00–1.00)	0.94 (0.83–1.02)	0.88 (0.75–1.09)	0.89 (0.71–1.20)
	20	1.00 (1.00–1.00)	0.94 (0.83–1.02)	0.87 (0.75–1.08)	0.88 (0.70–1.19)
	30	1.00 (1.00–1.00)	0.94 (0.83–1.02)	0.86 (0.73–1.07)	0.86 (0.68–1.17)

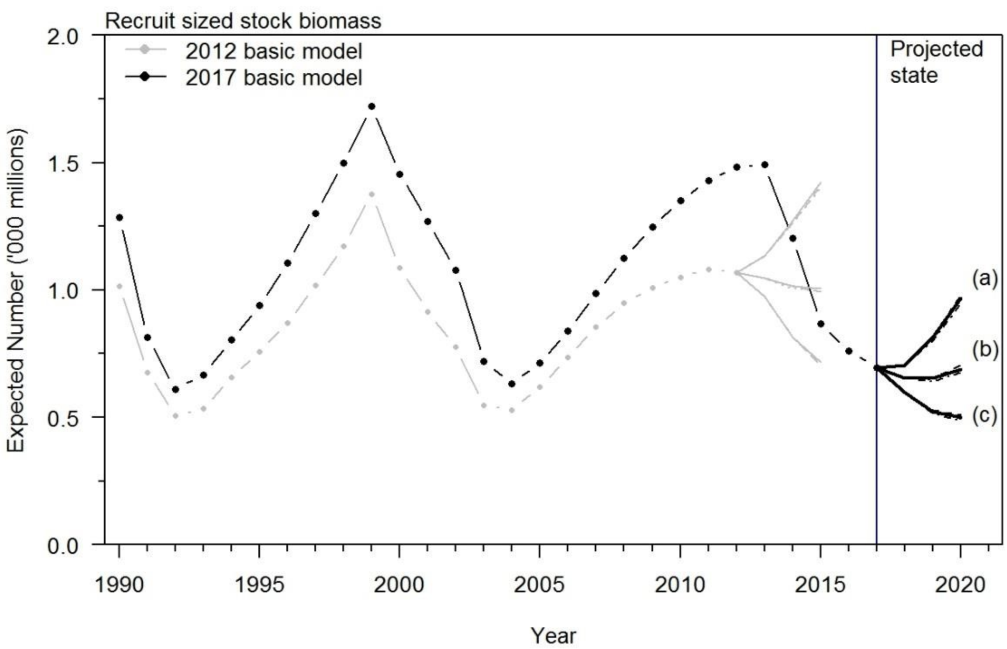

Figure 47: Model estimates of recent recruit-sized stock abundance and projected recruit-sized stock abundance with catch of 7.5 (solid line), 15 (dash dot), and 20 million oysters (dash line) under assumptions of (a) no disease mortality, (b) disease mortality of 0.10 y^{-1}, and (c) disease mortality of 0.20 y^{-1}, for the 2012 and 2017 basic models.

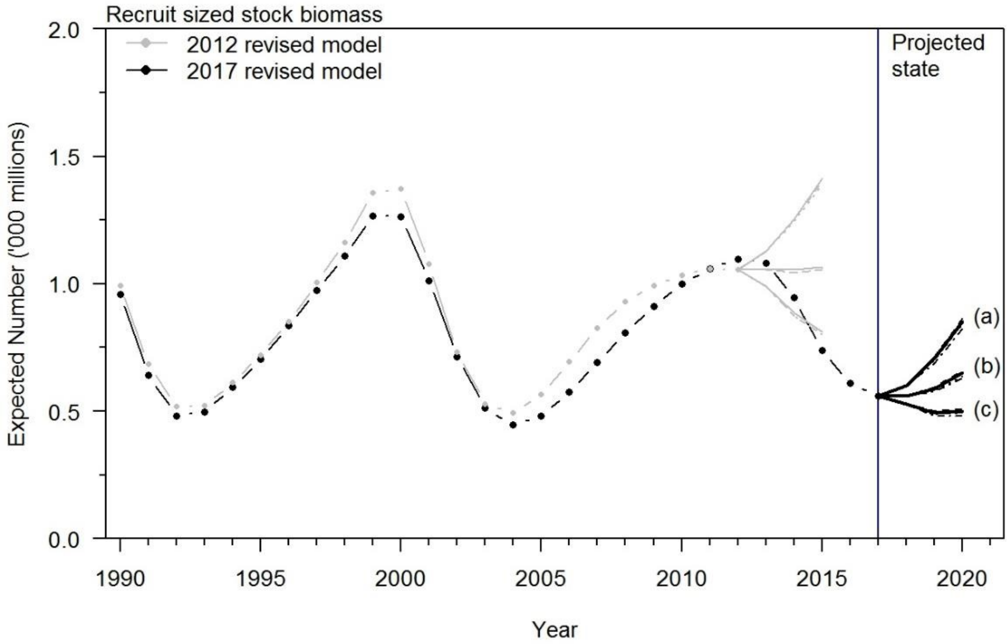

Figure 48: Model estimates of recent recruit-sized stock abundance and projected recruit-sized stock abundance with catch of 7.5 (solid line), 15 (dash dot), and 20 million oysters (dash line) under assumptions of (a) no disease mortality, (b) disease mortality of 0.10 y^{-1}, and (c) disease mortality of 0.20 y^{-1}, for the 2012 and 2017 revised models.

5. DISCUSSION

Dunn (2005b) concluded that there had been a dramatic reduction in the vulnerable abundance of oysters since the outbreak of the 1999–2000 *B. exitiosa* epizootic, but that fishing exploitation rates had been low. The 2007 assessment suggested reduced levels of *B. exitiosa* mortality in recent years and that the current spawning stock size was 20% (18–23%) B_0 and recruit-sized stock abundance was about 14% (12–17%) of the initial state. That assessment also noted that there was considerable uncertainty about the possible level of future recruitment and *B. exitiosa* related mortality, with the future stock status depending primarily on the level of future disease mortality.

Subsequent assessments in 2009 and 2012 suggest a similar state, with *B. exitiosa* mortality remaining low but with the stock appearing to rebuild in recent years. Model estimates of spawning stock population in 2009 were about 25% (23–28%) B_0, and recruit size stock abundance was about 20% (18–23%) of initial state. Model estimates of spawning stock population in 2012 were about 35% (31–41%) B_0, and recruit size stock abundance was about 30% (26–34%) of initial state.

The updated model estimates presented here suggest a trend in stock status that reflects the heightened levels of *B. exitiosa* mortality from 2012 to 2015 (peaking at approximately 20% of recruit sized oysters in 2014) with recruitment also remaining low during this period, although with some indication of a slight increase of recruitment in 2016. Model estimates of spawning stock population in 2017 were about 19% (17–21%) B_0, and recruit size stock abundance was about 16% (14–20%) of initial state. The trajectory of the predicted state of the population from the 2012 models, assuming a disease mortality rate of 0.2 y^{-1}, is similar to the estimated stock abundance from the 2017 updated models.

These models suggest that the rebuilding of the oyster population is expected to be initially slow but increasing much more quickly in 2019 and 2020 under long-term average *Bonamia* mortality and recruitment. Projections show that the stock abundance of recruit-sized oysters in future years is primarily dependent on levels of disease mortality (i.e. that catch at recent levels has little influence on future stock size). Estimates of future stock size, under assumptions of high or nil future disease mortality, ranged between 70% and 150% of current levels. The two cycles of recovery and decline in stock abundance since the *B. exitiosa* epizootic in the mid-1980s suggest that the latest period of recovery was at a slightly lower level in 2013 compared with 1999, but that the latest level of decline has been at a slower rate and not to as low a level as the previous decline in late 1980s.

Splitting the C series CPUE into a reduced C and a separate D series did improve the fits to both the CPUE and the commercial length frequency distributions. These involved three extra parameters (catchability, and two parameters for selectivity), but the decrease in the log-likelihood was large (i.e., better fits), about 100 for the basic and over 200 for the revised model (3 units of decrease is significant for one extra parameter). The main improvements were to the fits to the length frequency data; commercial and the October surveys. The shift in the fishing selectivity was about 2 mm at the 50% selection point. The fits to the CPUE after 2010 were also slightly better.

The improvements can be seen by eye in the left-hand side (LHS) of the commercial length frequency distributions, an important point since length frequencies dominate the total log-likelihood and improvements to fits to the length frequencies have been known to out-weigh fits to other datasets with no discernible improvement in the fits to the length frequencies themselves (I. Doonan, pers. comm.). The improved fit to the commercial length frequency distribution is expected since the new selectivity directly affects their fits. The improved fit to the October survey length frequency distributions is harder to explain but demonstrates the inter-connectedness of data fits in a non-linear model. When the selectivity for commercial data after 2010 was introduced, these YCS no longer had to be tweaked and both data sets could fit better.

Using a 4-CPUE made little difference to the MPD recruited biomass of the basic model, but for the revised model, the 4-CPUE gave a similar biomass trajectory up to the last four years but gave a much more optimistic trajectory thereafter. However, this model does not fit the recruit-sized population size from the biomass survey series and it ignores the decline in this index at the end of its sequence. We did not have time to investigates this, but there is clearly a structural problem in the model as it stands.

Model estimates of recent recruitment and short-term projections may be unreliable in predicting absolute outcomes due to the lack of data available to the model to estimate historical recruitment. Current work is being undertaken to construct a recruitment index and a method of incorporating this index into the model has been developed. However, it is recommended that the model performance issues described in this assessment be investigated further prior to/or along with any redesign of the model or the incorporation of new types of datasets. Future work should include an investigation of how best to parameterise disease mortality in the model and the impact this may have on model performance.

6. ACKNOWLEDGMENTS

We thank the many NIWA and industry staff who were involved in the collection of oyster data. The project was funded by the Bluff Oyster Management Company under project code BOM17302. We thank NIWA colleagues Jim Roberts and Matt Dunn for their helpful comments, Sophie Mormede for code from which Figures 28 and 29 were developed, and Adele Dutilloy for reviewing a previous version of this report.

7. REFERENCES

Allen, R.L.; Cranfield, H.J. (1979). A dredge survey of the oyster population in Foveaux Strait. *Rapports et Procès-verbaux des Réunions Conseil Permanent International pour l'Exploration de la Mer 175*: 50–62.

Bradford, E. (1998). Harvest estimates from the 1996 national marine recreational fisheries surveys. New Zealand Fisheries Assessment Research Document 98/16. 27 p. (Unpublished report held by the NIWA library, Wellington.)

Bull, B.; Dunn, A. (2002). Catch-at-age: User manual v1.06.2002/09/12. NIWA Internal Report 114. 23 p. (Unpublished report held in NIWA library, Wellington.)

Bull, B.; Francis, R.I.C.C.; Dunn, A.; McKenzie, A.; Gilbert, D.J.; Smith, M.H.; Bian, R. (2008). CASAL (C++ algorithmic stock assessment laboratory): CASAL User Manual v2.20-2008/02/14. *NIWA Technical Report 130.* 275 p.

Cranfield, H.J. (1998). 1997 Foveaux Strait Bonamia survey. Final Research Report to the Ministry of Fisheries. Project OYS9701. 11 p. (Unpublished report held by Fisheries New Zealand, Wellington.)

Cranfield, H.J.; Allen, R.L. (1979). Mark-recapture surveys of the Foveaux Strait dredge oyster (*Ostrea lutaria*) population. *Rapports et Procès-verbaux des Réunions Conseil Permanent International pour l'Exploration de la Mer 175*: 63–69.

Cranfield, H.J.; Doonan, I.J.; Michael, K.P. (1991). Assessment of the effects of mortality due to Bonamia sp. on the oyster population of Foveaux Strait in 1990 and the outlook for management in 1991. New Zealand Fisheries Assessment Research Document 91/18. 36 p. (Unpublished report held in NIWA library, Wellington.)

Cranfield, H.J.; Doonan, I.J.; Michael, K.P. (1993). Foveaux Strait oyster (*Tiostrea chilensis*) assessment, 1993. New Zealand Fisheries Assessment Research Document 93/21. 14 p. (Unpublished report held by the NIWA library, Wellington.)

Cranfield, H.J.; Doonan, I.J.; Michael, K.P. (1997). Incidental mortality of Foveaux Strait Dredge oysters during dredging. Final Research Report to the Ministry of Fisheries for Project SOOY002. 17 p. (Unpublished report held by Fisheries New Zealand, Wellington.)

Cranfield, H.J.; Michael, K.P.; Doonan, I.J. (1996). Foveaux Strait oyster (*Tiostrea chilensis*) assessment, 1995. New Zealand Fisheries Assessment Research Document 96/19. 25 p. (Unpublished report held by the NIWA library, Wellington.)

Cranfield, H.J.; Michael, K.P.; Doonan, I.J. (1998). Dredge survey of Foveaux Strait oysters, 1997. *NIWA Technical Report 45*. 18 p.

Cranfield, H.J.; Michael, K.P.; Doonan, I.J. (1999). Foveaux Strait oyster (*Tiostrea chilensis*) assessment, 1997. New Zealand Fisheries Assessment Research Document 99/11. 31 p. (Unpublished report held by the NIWA library, Wellington.)

Cranfield, H.J.; Michael, K.P.; Wesney, B.; Doonan, I.J. (1995). Distribution of Foveaux Strait oysters (*Tiostrea chilensis*) and prevalence of infection by Bonamia sp. in March 1995. New Zealand Fisheries Assessment Research Document 95/25. 18 p. (Unpublished report held by the NIWA library, Wellington.)

Diggles, B.K.; Cochennec-Laureau, N.; Hine, P.M. (2003). Comparison of diagnostic techniques for *Bonamia exitiosus* from flat oysters *Ostrea chilensis* in New Zealand. *Aquaculture 220(1–4)*: 145–156.

Dinamani, P.; Hickman, R.W.; Hine, P.M.; Jones, J.B.; Cranfield, H.J. (1987). Report on investigations into the disease outbreak in Foveaux Strait oysters, *Tiostrea lutaria*, 1986–87. 30 p. (Unpublished report held by the NIWA library, Wellington.)

Doonan, I.J.; Cranfield, H.J. (1992). Foveaux Strait oyster (*Tiostrea chilensis*) assessment, 1992. New Zealand Fisheries Assessment Research Document 92/11. 29 p. (Unpublished report held by the NIWA library, Wellington.)

Dunn, A. (2005a). Stock assessment of Foveaux Strait dredge oysters (*Ostrea chilensis*) for the 2003 04 fishing year. *New Zealand Fisheries Assessment Report 2005/25*. 63 p.

Dunn, A. (2005b). Stock assessment of Foveaux Strait dredge oysters (*Ostrea chilensis*) for the 2003–04 fishing year, updated for 2004–05. Final Research Report to the Ministry of Fisheries for Project OYS2004/01. 67 p. (Unpublished report held by Fisheries New Zealand.)

Dunn, A. (2007). Stock assessment of Foveaux Strait dredge oysters (*Ostrea chilensis*) for the 2005–06 fishing year. Final Research Report to the Ministry of Fisheries for Project OYS2007/01. 63 p. (Unpublished report held by Fisheries New Zealand.)

Dunn, A.; Cranfield, H.J.; Michael, K.P. (1998a). Estimates of natural mortality of the Foveaux Strait oyster (*Tiostrea chilensis*) between 1974 and 1986. Final Research Report to the Ministry of Fisheries for Project OYS9801. 12 p. (Unpublished report held by Fisheries New Zealand, Wellington.)

Dunn, A.; Doonan, I.J.; Cranfield, H.J.; Michael, K.P.; Stotter, D.R. (1998b). Modelling growth of the Foveaux Strait oyster (*Tiostrea chilensis*). Final Research Report to the Ministry of Fisheries for Project OYS9801. 16 p. (Unpublished report held by Fisheries New Zealand, Wellington.)

Dunn, A.; Michael, K.P. (2006). Estimates of the length frequency from the commercial catch sampling for Foveaux Strait dredge oysters (*Ostrea Chilensis*) in 2005. Final Research Report to the Ministry of Fisheries for Project OYS2004/01. 11 p. (Unpublished report held by Fisheries New Zealand, Wellington.)

Dunn, A.; Michael, K.P. (2007). Estimates of the length frequency from the commercial catch sampling for Foveaux Strait dredge oysters (*Ostrea Chilensis*) in 2006. Final Research Report to the Ministry of Fisheries for Project OYS2005/01. 14 p. (Unpublished report held by Fisheries New Zealand, Wellington.)

Dunn, A.; Michael, K.P. (2008). Estimates of the length frequency from the commercial catch sampling for Foveaux Strait dredge oysters (*Ostrea chilensis*) in 2007. Final Research Report to the Ministry of Fisheries for Project OYS2006/01. 14 p. (Unpublished report held by Fisheries New Zealand, Wellington.)

Dunn, A.; Michael, K.P. (2009). Estimates of the length frequency from the commercial catch sampling for Foveaux Strait dredge oysters (*Ostrea chilensis*) in 2008. Final Research Report to the Ministry of Fisheries for Project OYS2008/01. 16 p. (Unpublished report held by Fisheries New Zealand, Wellington.)

Dunn, A.; Michael, K.P.; Diggles, B.K. (2002a). Updated estimates of the commercial population size, yields, and estimates of intensity and prevalence of infection by *Bonamia exitiosus* in Foveaux Strait oysters for selected sites in Foveaux Strait in March 2002. Final Research Report to the Ministry of Fisheries for Project MOF2001/03L. 20 p. (Unpublished report held by Fisheries New Zealand, Wellington.)

Dunn, A.; Michael, K.P.; Forman, J.S.; Diggles, B.K. (2003). Estimates of intensity and prevalence of infection by *Bonamia exitiosus* in oysters for selected sites in Foveaux Strait in February 2003. NIWA Client Report WLG2003/10. 25 p.

Dunn, A.; Michael, K.P.; Hine, P.M.; Andrew, N.L.; Diggles, B.K.; Cranfield, H.J. (2000). Analysis of a survey of the prevalence and intensity of Bonamia sp. in Foveaux Strait oysters. *New Zealand Fisheries Assessment Report 2000/32*. 28 p.

Dunn, A.; Michael, K.P.; Parsons, M.; Diggles, B.K. (2002b). Updated estimates of the commercial population size, yields, and estimates of intensity and prevalence of infection by *Bonamia exitiosus* in Foveaux Strait oysters for selected sites in Foveaux Strait in January 2002. Final Research Report to the Ministry of Fisheries for Project MOF2001/03I. 15 p. (Unpublished report held by Fisheries New Zealand, Wellington.)

Fernandez-i-Marin, X. (2016). gmcmc: Analysis of MCMC Samples and Bayesian Inference. *Journal of Statistical Software 70(9)*: 305 311, doi: 10.18637/jss.v070.i09.

Francis, R.I.C.C. (1988). Maximum likelihood estimation of growth and growth variability from tagging data. *New Zealand Journal of Marine and Freshwater Research 22(1)*: 43–51.

Fu, D. (2013). An updated stock assessment for Foveaux Strait dredge oysters (*Ostrea chilensis*) for the 2012 fishing year. *New Zealand Fisheries Assessment Report 2013/51*. 57 p.

Fu, D.; Dunn, A. (2009). An updated stock assessment for Foveaux Strait dredge oysters (*Ostrea chilensis*) for the 2008–09 fishing year. *New Zealand Fisheries Assessment Report 2009/53*. 71 p.

Fu, D.; Dunn, A.; Michael, K.P. (2008). Estimates of the length frequency from the commercial catch sampling for Foveaux Strait dredge oysters (*Ostrea Chilensis*) in 2008. Final Research Report to the Ministry of Fisheries for Project OYS2007/01. 16 p. (Unpublished report held by Fisheries New Zealand, Wellington.)

Fu, D.; Michael, K.P.; Dunn, A. (2009). Estimates of the length frequency from the commercial catch sampling for Foveaux Strait dredge oysters (*Ostrea Chilensis*) in 2009. Final Research Report to the Ministry of Fisheries for Project OYS2008/01. 17 p. (Unpublished report held by Fisheries New Zealand, Wellington.)

Fu, D.; Michael, K.P.; Dunn, A. (2010). Estimates of the length frequency from the commercial catch sampling for Foveaux Strait dredge oysters (*Ostrea Chilensis*) in 2010. Final Research Report to the Ministry of Fisheries for Project OYS2009/01. 18 p. (Unpublished report held by Fisheries New Zealand, Wellington.)

Fu, D.; Michael, K.P.; Dunn, A.; Wright, G. (2011). Estimates of the length frequency from the commercial catch sampling for Foveaux Strait dredge oysters (*Ostrea Chilensis*) in 2011. Final Research Report to the Ministry of Fisheries for Project OYS2009/01B. 21 p. (Unpublished report held by Fisheries New Zealand, Wellington.)

Fu, D.; Michael, K.P.; Dunn, A.; Wright, G. (2012). Estimates of the length frequency from the commercial catch sampling for Foveaux Strait dredge oysters (*Ostrea Chilensis*) in 2012. Final Research Report to the Ministry of Fisheries for Project OYS2009/01C. 23 p. (Unpublished report held by Fisheries New Zealand, Wellington.)

Fu, D.; Michael, K.P.; Dunn, A. (2014). Estimates of the length frequency from commercial catch sampling of Foveaux Strait dredge oysters (*Ostrea chilensis*) in 2013. Final Research Report to the Ministry of Fisheries for project OYS2012/01. 24 p. (Unpublished report held by Fisheries New Zealand, Wellington.)

Fu, D.; Michael, K.P.; Wright, G.; Dunn, A. (2015). Estimates of the length frequency distribution of Foveaux Strait dredge oysters (*Ostrea chilensis*) from commercial catch sampling in 2014. Final Research Report to the Ministry of Fisheries for Project OYS2013/01. 25 p. (Unpublished report held by Fisheries New Zealand, Wellington.)

Gilbert, D.J.; Michael, K.P. (2006). Preliminary epidemiological model fit for Foveaux Strait oyster population. Final Research Report to the Ministry of Fisheries for Project OYS2005/01. 26 p. (Unpublished Report held by Fisheries New Zealand.)

Hine, P.M. (1996). The ecology of Bonamia and decline of bivalve molluscs. *New Zealand Journal of Ecology* 20: 109–116.

Hunter, R.C. (1906). Report on oyster beds in Foveaux Strait. *Report on New Zealand Fisheries 1905*: 16-17.

Jamieson, G.S.; Campbell, A. (eds.) (1998). Proceedings of the North Pacific Symposium on invertebrate stock assessment and management. *Canadian Special Publication of Fisheries and Aquatic Sciences*. 462 p. National Research Council of Canada, Nanaimo, Canada.

Jeffs, A.G.; Creese, R.G. (1996). Overview and bibliography of research on the Chilean oyster *Tiostrea chilensis* (Philippi, 1845) from New Zealand waters. *Journal of Shellfish Research 15(2)*: 305–311.

Jeffs, A.G.; Hickman, R.W. (2000). Reproductive activity in a pre-epizootic wild population of the Chilean oyster, *Ostrea chilensis*, from southern New Zealand. *Aquaculture 183(3–4)*: 241–253.

Large, K.; Michael, K.P.; Wright, G. (2018). OYU 5 Catch Sampling 2016. Estimates of the length frequency distribution of Foveaux Strait dredge oysters (*Ostrea chilensis*) from catch sampling in 2016. Prepared for Bluff Oyster Management Company Ltd (BOMC). NIWA Client Report: 2018197WN (Project BOM17302). 41 p.

Marsh, C.; Michael, K.P.; Wright, G.; Fu., D. (2016). Estimates of the length frequency distribution of Foveaux Strait dredge oysters (*Ostrea chilensis*) from commercial catch sampling in 2015. Final Research Report to the Ministry of Fisheries for project OYS2013/01. 22 p. (Unpublished report held by Fisheries New Zealand, Wellington).

Michael, K.P.; Bilewitch, J.; Forman, J.; Hulston, D.; Sutherland, J.; Moss, G.; Large, K. (2019a). A survey of the Foveaux Strait oyster (*Ostrea chilensis*) population (OYU 5) in commercial fishery areas and the status of bonamia (*Bonamia exitiosa*) in February 2018. *New Zealand Fisheries Assessment Report 2019/02*. 57 p.

Michael, K.P.; Dunn, A.; Andrew, N.L.; Breen, P.A. (2001). Foveaux Strait dredge oyster (*Tiostrea chilensis*) stock assessment, 1999. *New Zealand Fisheries Assessment Report 2001/38*. 42 p.

Michael, K.P.; Dunn, A.; Diggles, B.K. (2004a). Foveaux Strait dredge oyster (*Ostrea chilensis*) population and Bonamia surveys, October 2002. *New Zealand Fisheries Assessment Report 2004/14*. 22 p.

Michael, K.P.; Dunn, A.; Diggles, B.K. (2004b). Foveaux Strait dredge oyster (*Ostrea chilensis*) stock assessment: population and Bonamia surveys October 2001, January and March 2002, and yields for the 2002 oyster season. *New Zealand Fisheries Assessment Report 2004/13*. 18 p.

Michael, K.P.; Dunn, A.; Forman, J. (2005). A survey of *Bonamia exitiosa* infection in Foveaux Strait dredge oysters (*Ostrea chilensis*), oyster density, and recruitment, January 2004. Final Research Report for project OYS2003/01 objective 1. 31 p. (Unpublished report held by Fisheries New Zealand, Wellington.)

Michael, K.P.; Dunn, A.; Forman, J. (2006). A survey of *Bonamia exitiosa* infection, and oyster density and recruitment in Foveaux Strait dredge oysters (*Ostrea chilensis*), January 2005. *New Zealand Fisheries Assessment Report 2006/40*. 31 p.

Michael, K.P.; Dunn, A.; Forman, J. (2008a). A survey of *Bonamia exitiosa* and oyster density and recruitment in Foveaux Strait oysters (*Ostrea chilensis*), February 2006. *New Zealand Fisheries Assessment Report 2008/47*. 35 p.

Michael, K.P.; Dunn, A.; Forman, J. (2009a). The status of infection by *Bonamia exitiosa* in Foveaux Strait oysters (*Ostrea chilensis*), changes in the distributions and densities of recruit, pre-recruit, and small oysters, and projections of disease mortality in February 2008. *New Zealand Fisheries Assessment Report 2009/32*. 50 p.

Michael, K.P.; Dunn, A.; Forman, J.; Arlidge, A. (2008b). A survey of the distribution and absolute abundance of pre-recruit and recruited dredge oysters (*Ostrea chilensis*) in both non-commercial and designated commercial areas of Foveaux Strait, and estimates of the prevalence and intensity of infection by *Bonamia exitiosa*, February 2007. *New Zealand Fisheries Assessment Report 2008/61*. 49 p.

Michael, K.P.; Forman, J.; Hulston D.; Bilevitch, J.; Moss, G. (2019b). Foveaux Strait oyster and Bonamia surveys, February 2017. *New Zealand Fisheries Assessment Report 2019/46*. 83 p.

Michael, K.P.; Forman, J.; Hulston, D.; Fu, D. (2011). The status of infection by Bonamia (*Bonamia exitiosa*) in Foveaux Strait oysters (*Ostrea chilensis*), changes in the distributions and densities of recruit, pre-recruit, and small oysters in February 2010, and projections of disease mortality. *New Zealand Fisheries Assessment Report 2011/5*. 51 p.

Michael, K.P.; Forman, J.; Hulston D.; Fu, D. (2012). The status of infection by Bonamia (*Bonamia exitiosa*) in Foveaux Strait oysters (*Ostrea chilensis*) in February 2011, estimates of pre-survey and projections of post-survey disease mortality, and implications for the projections of future stock status made in the 2009 stock assessment for OYU 5. *New Zealand Fisheries Assessment Report 2012/37*. 55 p.

Michael, K.P.; Forman, J.; Hulston D.; Sutherland, J. (2016). A survey of the Foveaux Strait oyster (Ostrea chilensis) population (OYU 5) in commercial fishery areas and the status of bonamia (*Bonamia exitiosa*) in February 2016. *New Zealand Fisheries Assessment Report 2016/67*. 91 p.

Michael, K.P.; Fu, D.; Forman, J. (2009b). Foveaux Strait oyster (*Ostrea chilensis*) 2009 stock assessment: estimates of oyster population size, the distribution of oyster densities, the status of Bonamia infection in oysters, and status of the fishery. *New Zealand Fisheries Assessment Report 2009/45*. 54 p.

Michael, K.P.; Shima, J.S. (2018). Four-year decline in *Ostrea chilensis* recruits per spawner in Foveaux Strait, New Zealand suggests a diminishing stock-recruitment relationship. *Marine Ecology Progress Series 600*. 10.3354/meps12641.

Ministry of Fisheries Science Group (2006). Report from the Fishery Assessment Plenary, May 2006: stock assessments and yield estimates. 875 p. (Unpublished report held by the NIWA library, Wellington.)

Sorensen, J.H. (1968). Dredge oyster surveys Foveaux Strait pre-1960. Compiled mainly from Marine Department records. *Fisheries Technical Report 28*. 27 p.

Stead, D.H. (1971a). Observations on the biology and ecology of the Foveaux Strait dredge oyster (*Ostrea lutaria*, Hutton). *Fisheries Technical Report 68*. 49 p.

Stead, D.H. (1971b). Survey of Foveaux Strait oyster beds 1960–1964. *Fisheries Technical Report 59*. 64 p.

Street, R.J.; Crowther, G.S. (1973). Foveaux Strait oyster surveys 1965–1971. *Fisheries Technical Report 118*. 37 p.

Teirney, L.D.; Kilner, A.R.; Millar, R.B.; Bradford, E.; Bell, J.D. (1997). Estimation of recreational harvests from 1991–92 to 1993–94. New Zealand Fisheries Assessment Research Document 97/15. 43 p. (Unpublished report held by the NIWA library, Wellington.)

8. APPENDIX A: SUMMARY MPD MODEL FITS

8.1 2017 Basic model

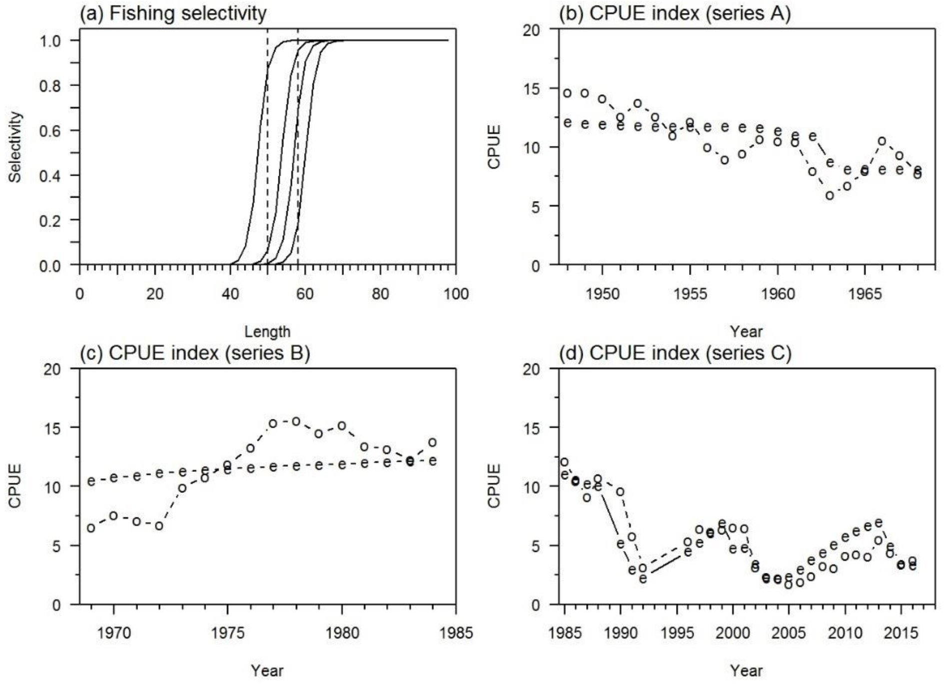

Figure 49: 2017 basic model MPD estimates of (a) fishing selectivity and model fits to (b) series A, (c) series B, and (d) series C CPUE indices ("e"=expected and "o"=observed). Dashed lines separate the small (<50 mm), pre-recruit (≥ 50 mm and <58 mm), and recruit (≥ 58 mm) size groups.

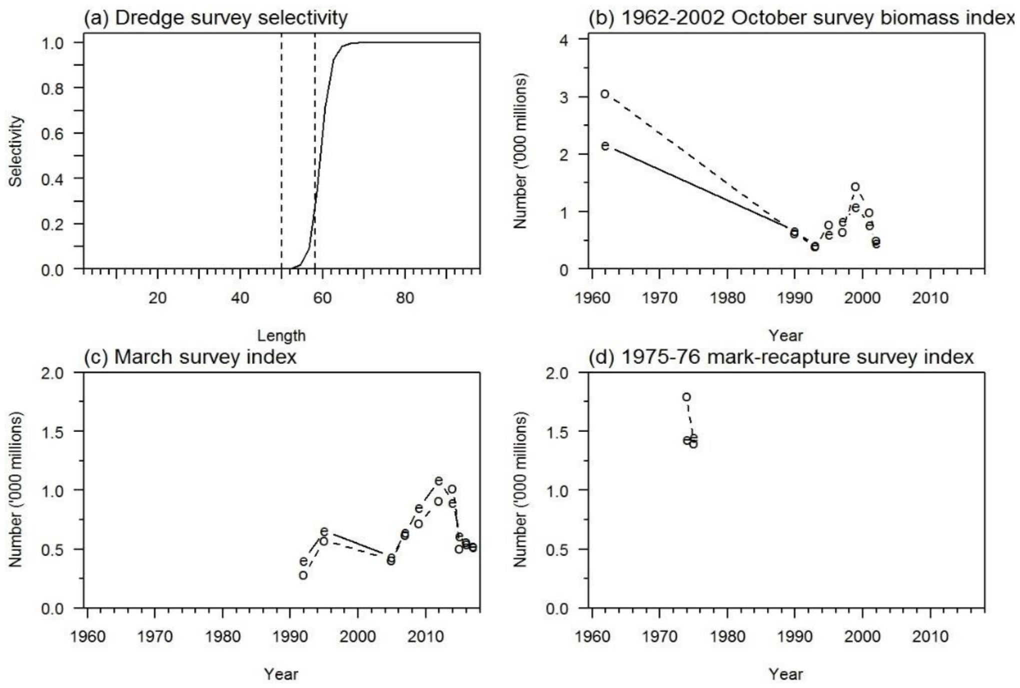

Figure 50: 2017 basic model MPD estimates of (a) recruit-sized dredge survey selectivity and model fits to recruit-sized oyster abundance indices for the (b) October surveys 1964–2002, (c) March surveys 1992–2017, and (d) 1975–76 mark-recapture survey ("e"=expected and "o"=observed). Dashed lines separate the small (<50 mm), pre-recruit (≥ 50 mm and <58 mm), and recruit (≥ 58 mm) size groups.

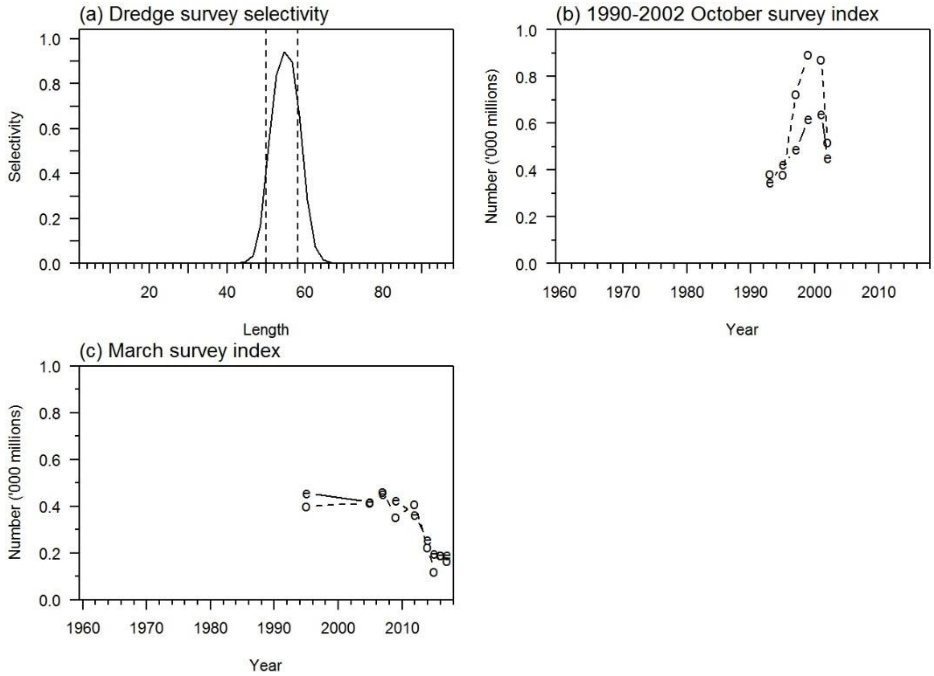

Figure 51: 2017 basic model MPD estimates of the (a) pre-recruit-sized dredge survey selectivity and model fits to pre-recruit-sized oyster abundance indices for the (b) October surveys 1990–2002, and (c) March surveys 1995– 2017 ("e"=expected and "o"=observed). Dashed lines separate the small (<50 mm), pre-recruit (≥ 50 mm and <58 mm), and recruit (≥ 58 mm) size groups.

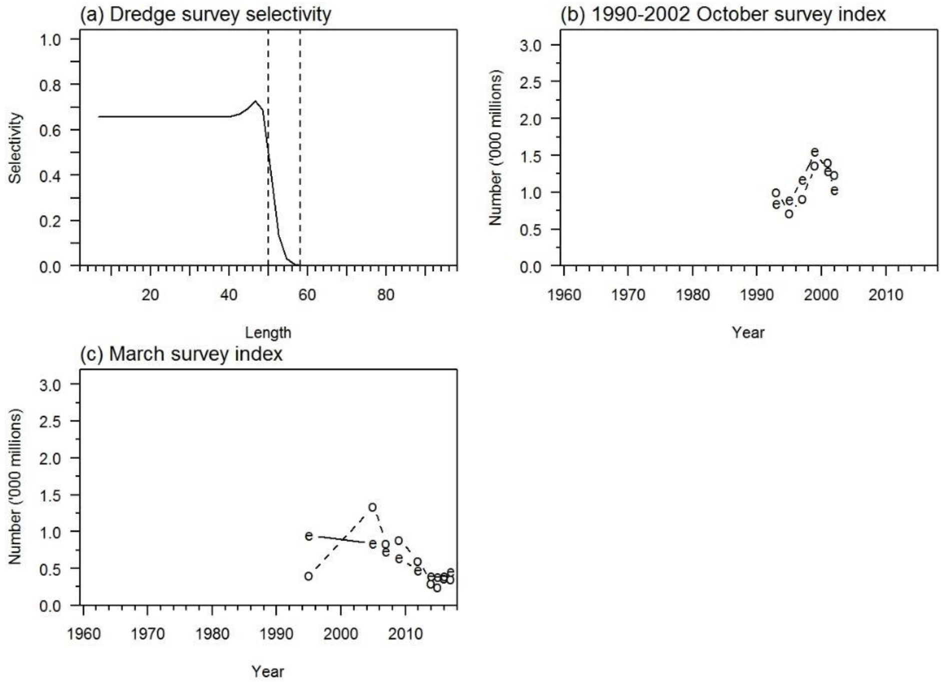

Figure 52: 2017 basic model MPD estimates of (a) small-sized oyster dredge survey selectivity and model fits to small-sized oyster abundance indices for the (b) October surveys 1990–2002, and (c) March surveys 1995–2017 ("e"=expected and "o"=observed). Dashed lines separate the small (<50 mm), pre-recruit (≥ 50 mm and <58 mm), and recruit (≥ 58 mm) size groups.

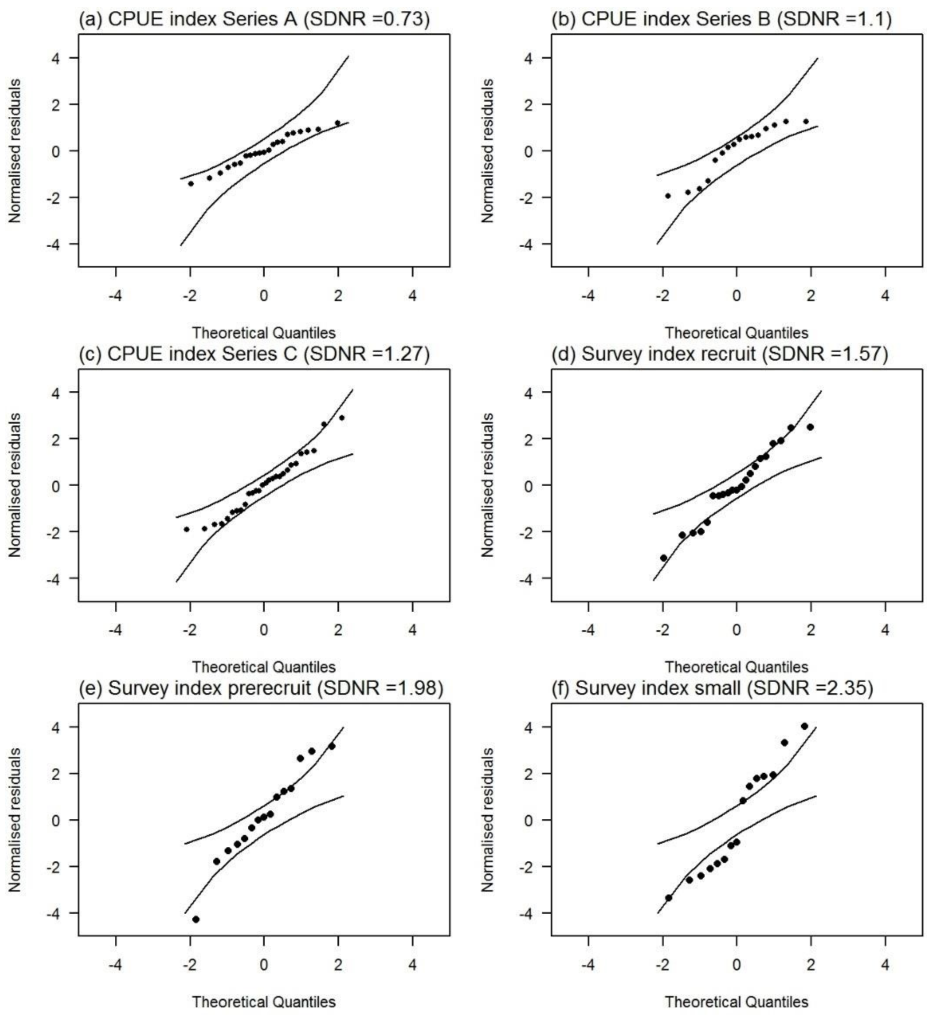

Figure 53: 2017 basic model MPD estimates of fits (normal quantile-quantile plots) to the (a) series A, (b) series B, (c) series C CPUE indices, and 1964–2017 survey indices combined for (d) recruits (≥ 58 mm), (e) pre-recruit (≥ 50 mm and <58 mm), (f) small (<50 mm) size groups.

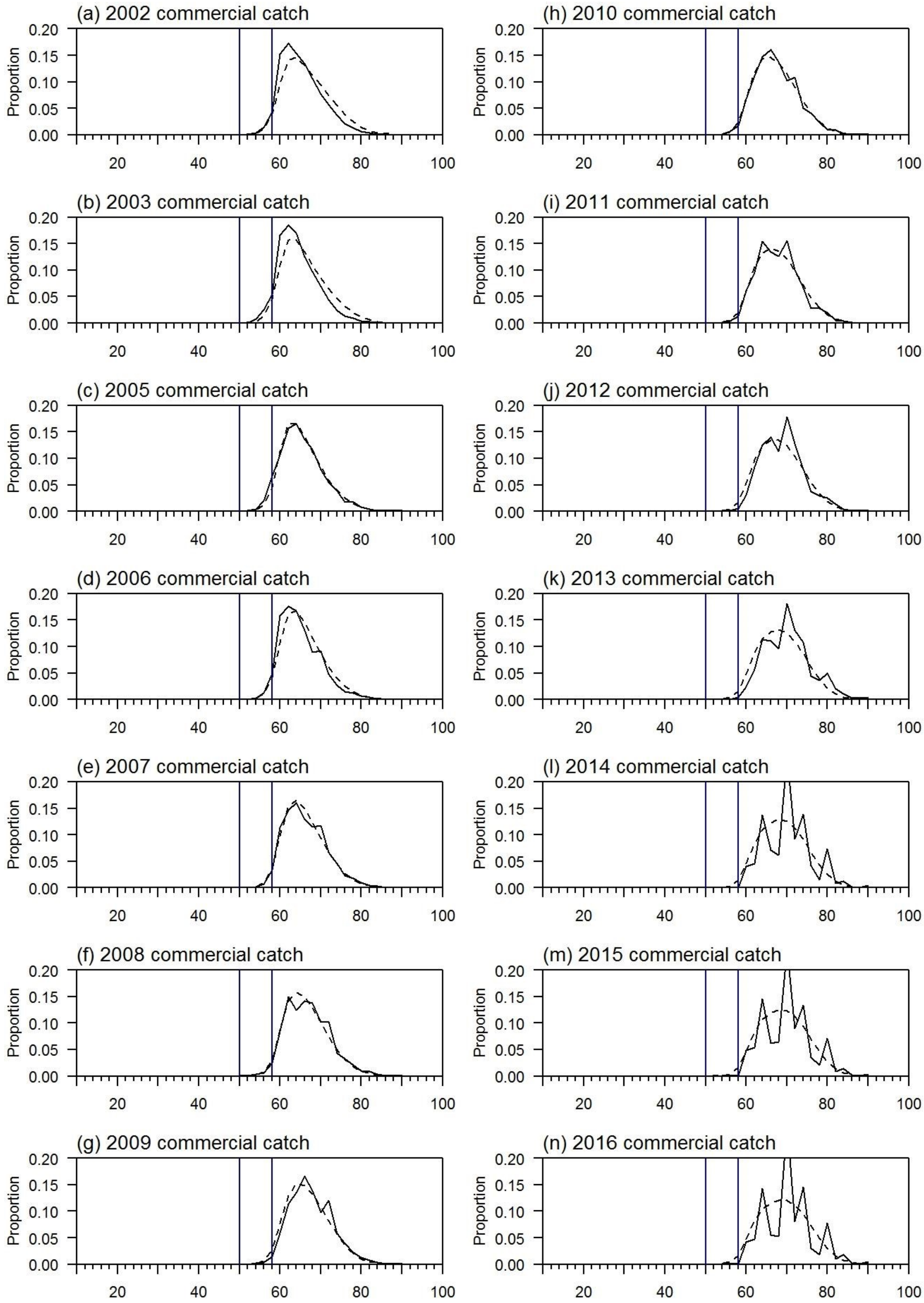

Figure 54: 2017 basic model MPD estimates of fits to the (a)-(g) 2002, 2003, 2005–2009 and (h)-(n) 2010–2016 commercial catch length frequency distributions. Vertical lines separate the small (<50 mm), pre-recruit (≥ 50 mm and <58 mm), and recruit (≥ 58 mm) size groups.

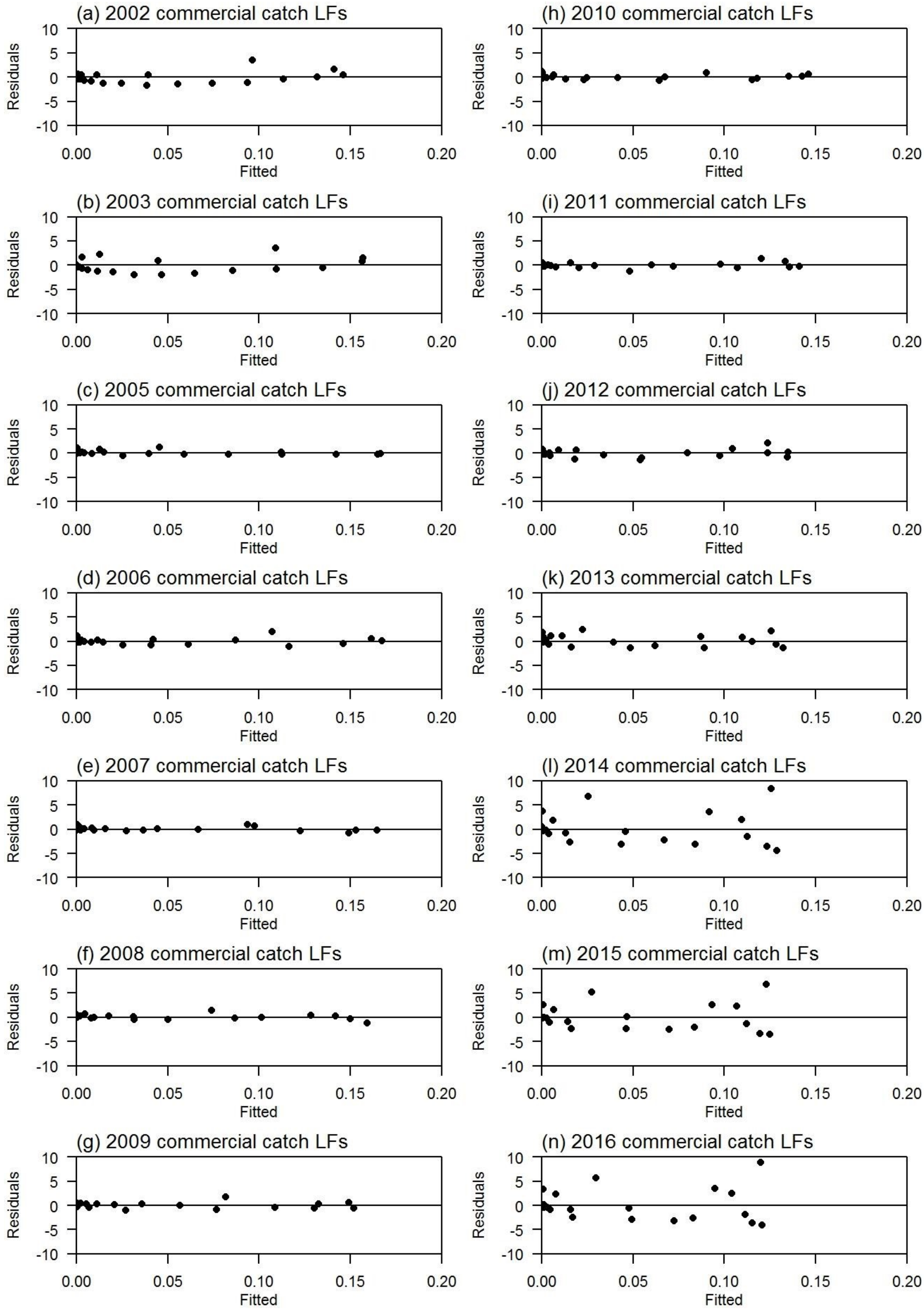

Figure 55: 2017 basic model MPD estimates of residuals versus fitted values for the (a)–(g) 2002, 2003, 2005–2009 and (h)–(n) 2010–2016 commercial catch data.

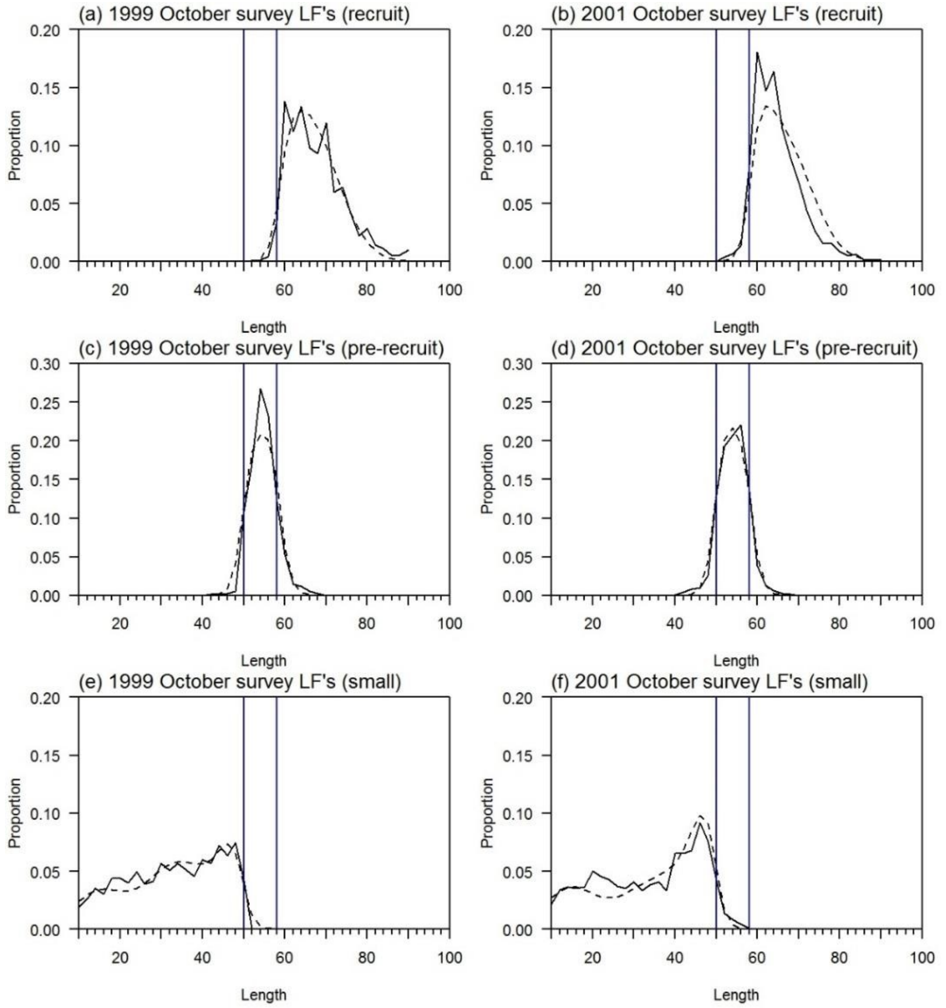

Figure 56: 2017 basic model MPD estimates of fits to the survey data length frequency distributions for (a–b) recruit-sized, (c–d) pre-recruit size, and (e–f) small oysters from the 1999 and 2001 abundance surveys respectively. Vertical lines separate the small (<50 mm), pre-recruit (≥ 50 mm and <58 mm), and recruit (≥ 58 mm) size groups.

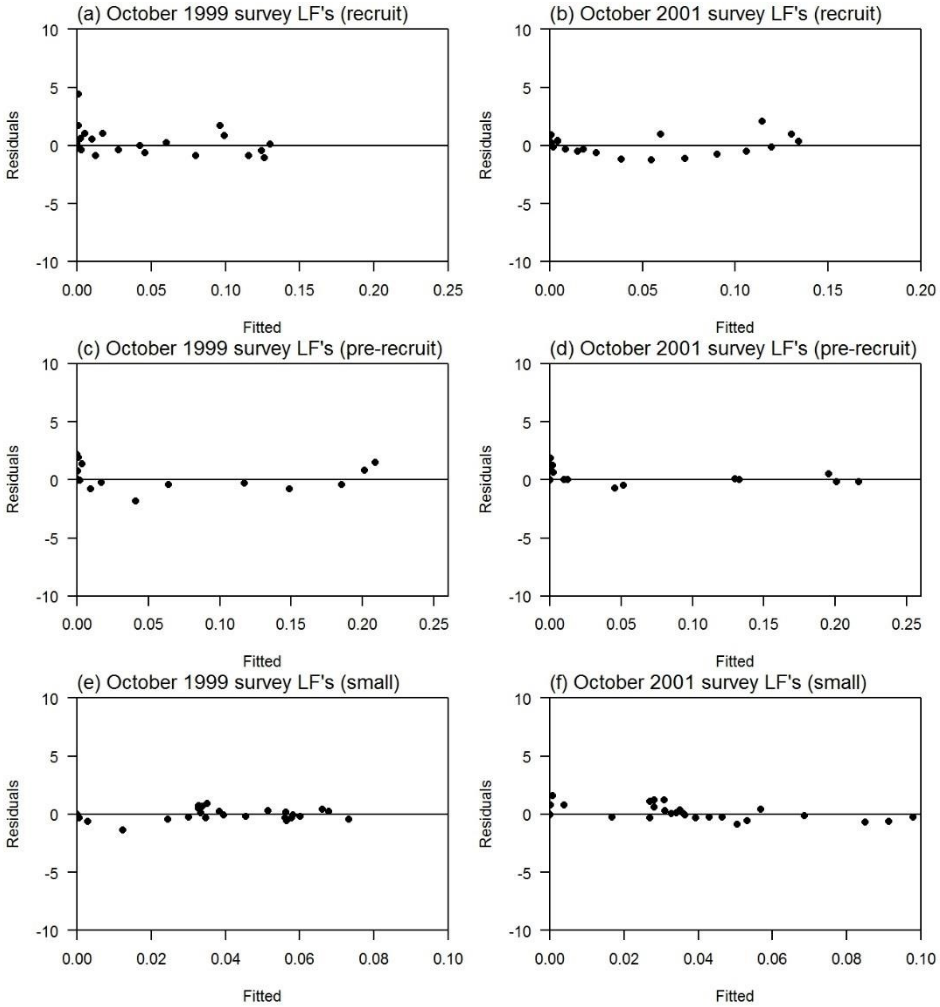

Figure 57: 2017 basic model MPD estimates of residuals versus fitted values for the (a–b) recruit size, (c–d) pre-recruit size, and (e–f) small oysters from the 1999 and 2001 abundance surveys respectively.

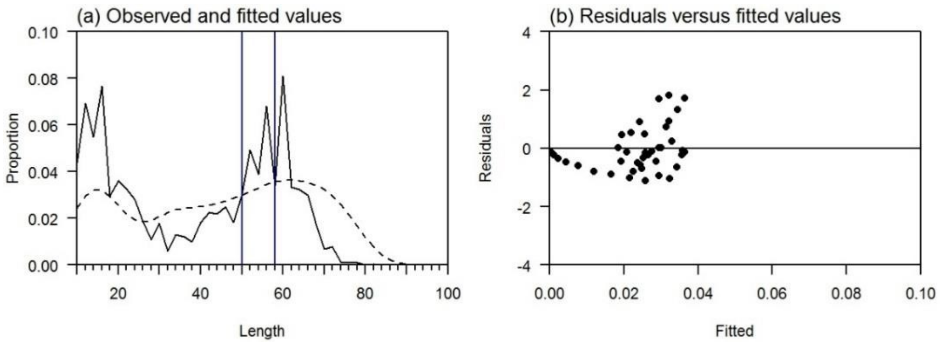

Figure 58: 2017 basic model MPD estimates for the 1990 dive survey length frequency distributions (a) observed (solid line) and MPD estimates of fits (dashed line), and (b) residuals versus fitted. Vertical lines separate the small (<50 mm), pre-recruit (≥ 50 mm and <58 mm), and recruit (≥ 58 mm) size groups.

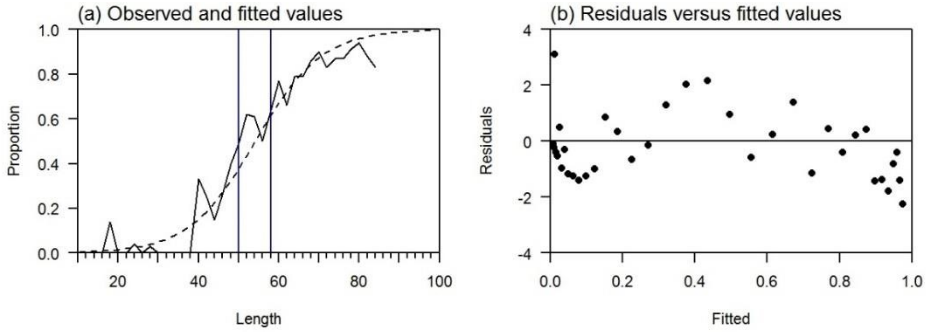

Figure 59: 2017 basic model MPD estimates for the Jeffs & Hickman (2000) maturity data (a) observed (solid line) and MPD estimates of fits (dashed line), and (b) residuals versus fitted values. Vertical lines separate the small (<50 mm), pre-recruit (≥ 50 mm and <58 mm), and recruit (≥ 58 mm) size groups.

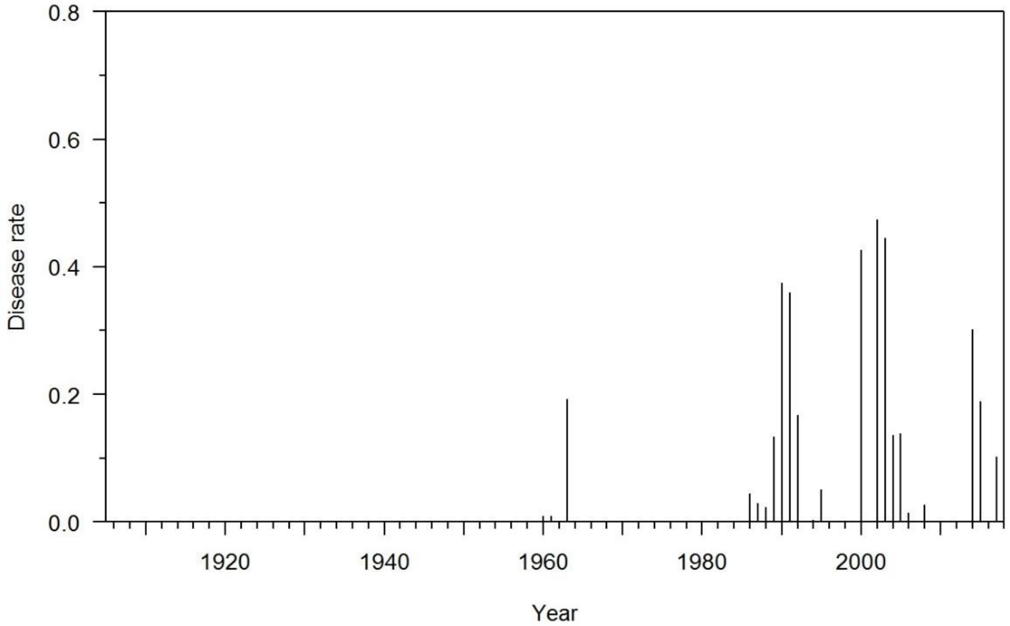

Figure 60: 2017 basic model MPD estimates of disease mortality rate.

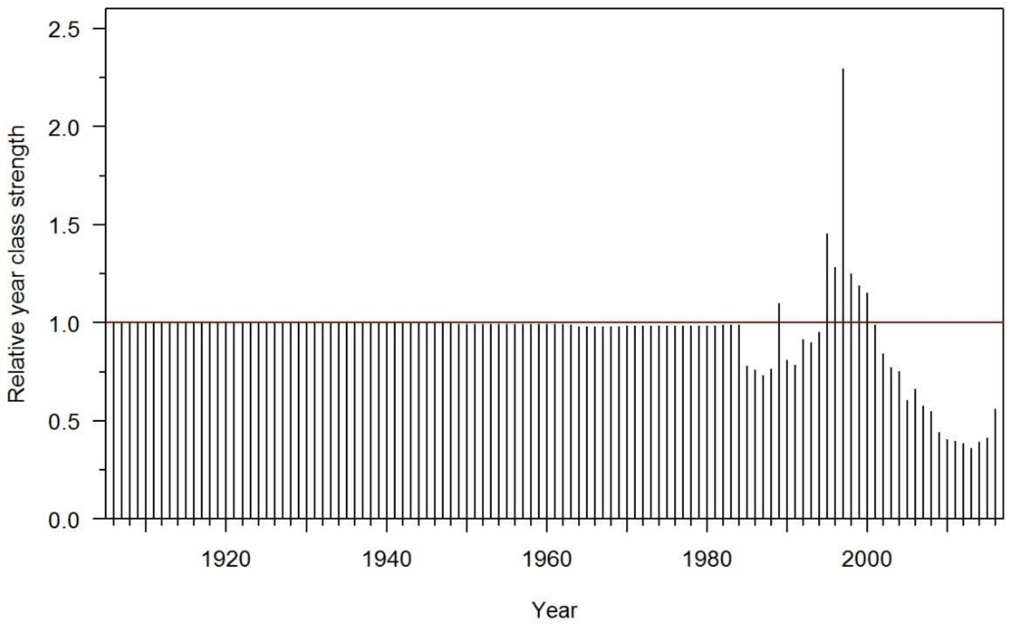

Figure 61: 2017 basic model MPD estimates of relative year class strength.

8.2 2017 Revised model

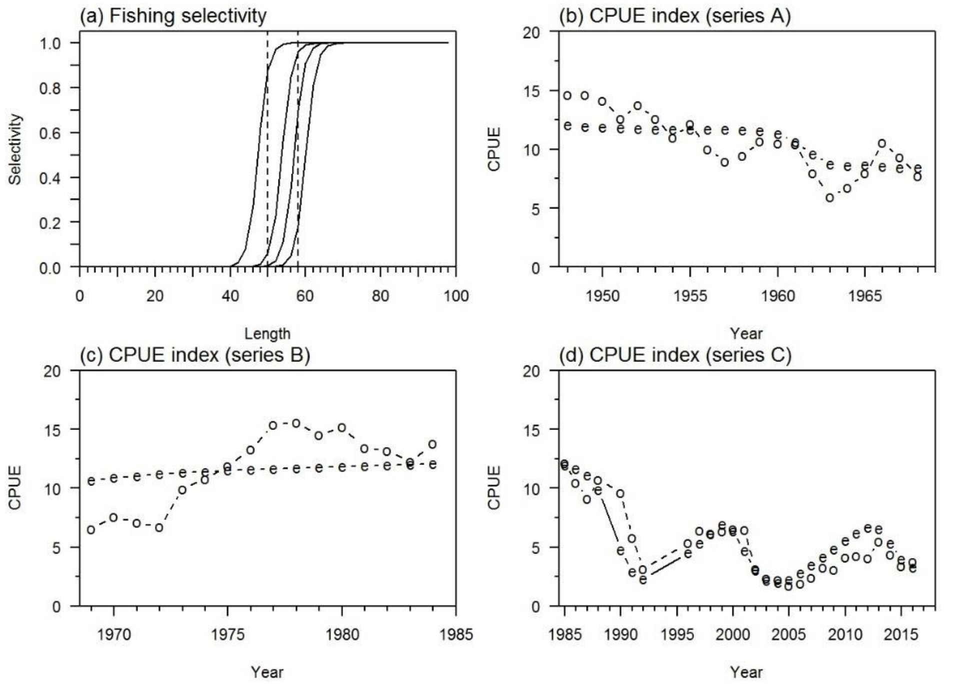

Figure 62: 2017 revised model MPD estimates of (a) fishing selectivity and model fits to (b) series A, (c) series B, and (d) series C CPUE indices ("e"=expected and "o"=observed). Dashed lines separate the small (<50 mm), pre-recruit (≥ 50 mm and <58 mm), and recruit (≥ 58 mm) size groups.

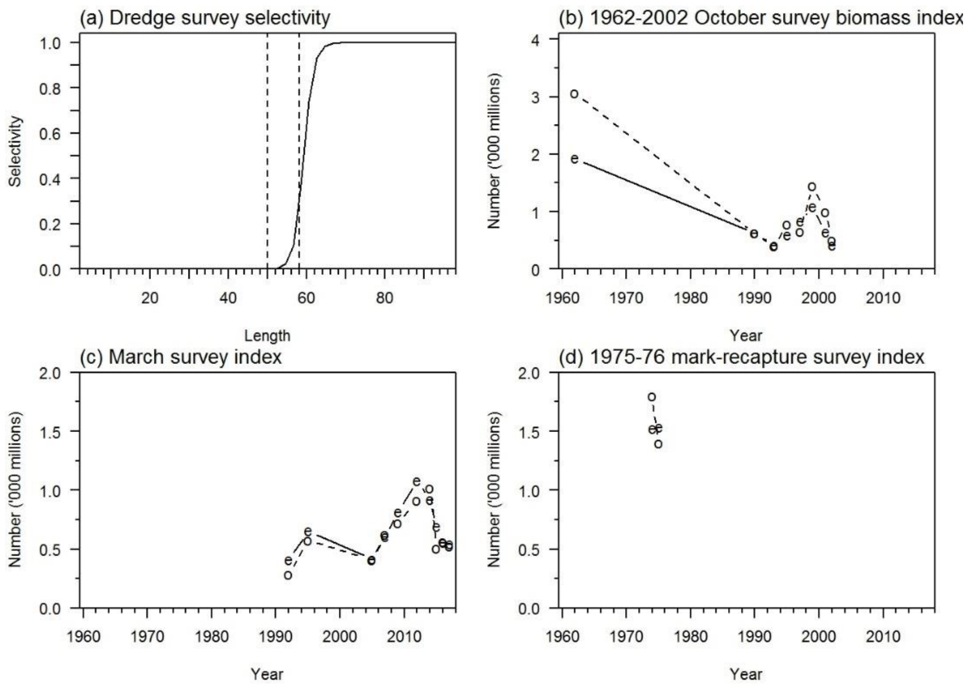

Figure 63: 2017 revised model MPD estimates of (a) recruit-sized oyster dredge survey selectivity and model fits to recruit-sized oyster abundance indices for the (b) October surveys 1964–2002, (c) March surveys 1992–2017, and (d) 1975–76 mark-recapture survey ("e"=expected and "o"=observed). Dashed lines separate the small (<50 mm), pre-recruit (≥ 50 mm and <58 mm), and recruit (≥ 58 mm) size groups.

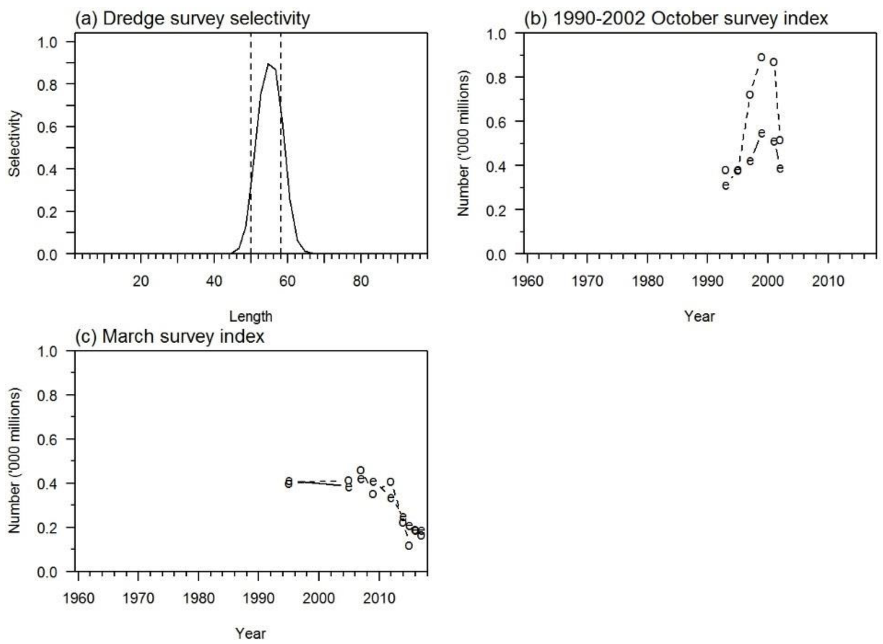

Figure 64: 2017 revised model MPD estimates of the (a) pre-recruit-sized oyster dredge survey selectivity and model fits to pre-recruit-sized oyster abundance indices for the (b) October surveys 1990–2002, and (c) March surveys 1995– 2017 ("e"=expected and "o"=observed). Dashed lines separate the small (<50 mm), pre-recruit (≥ 50 mm and <58 mm), and recruit (≥ 58 mm) size groups.

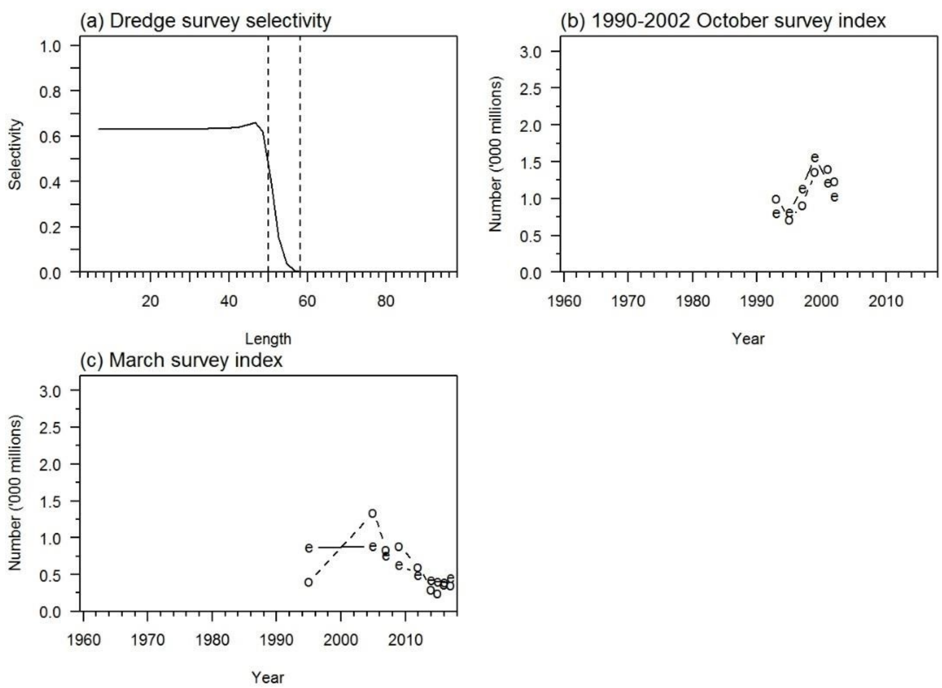

Figure 65: 2017 revised model MPD estimates of (a) small-sized oyster dredge survey selectivity and model fits to small-sized oyster abundance indices for the (b) October surveys 1990–2002, and (c) March surveys 1995–2017 ("e"=expected and "o"=observed). Dashed lines separate the small (<50 mm), pre-recruit (≥ 50 mm and <58 mm), and recruit (≥ 58 mm) size groups.

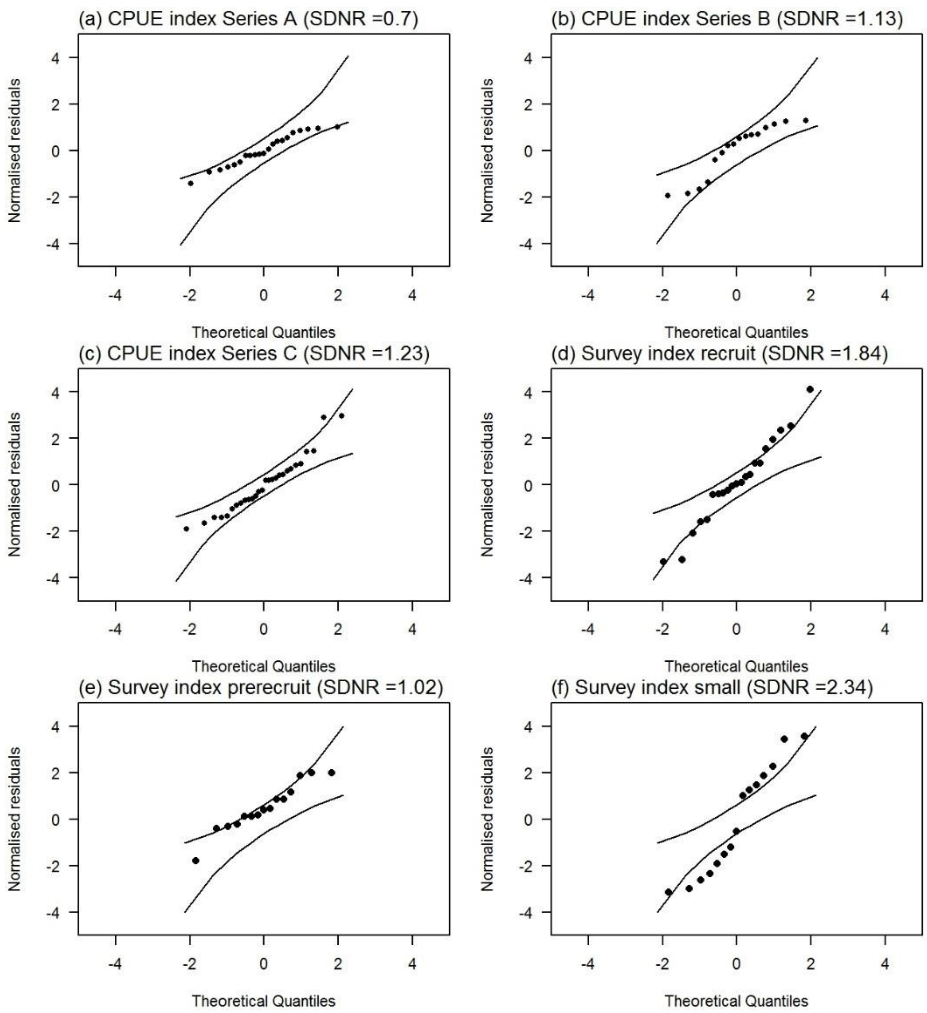

Figure 66: 2017 revised model MPD estimates of fits (normal quantile-quantile plots) to the (a) series A, (b) series B, (c) series C CPUE indices, and 1964–2017 survey indices combined for (d) recruits (≥ 58 mm), (e) pre-recruit (≥ 50 mm and <58 mm), (f) small (<50 mm) size groups.

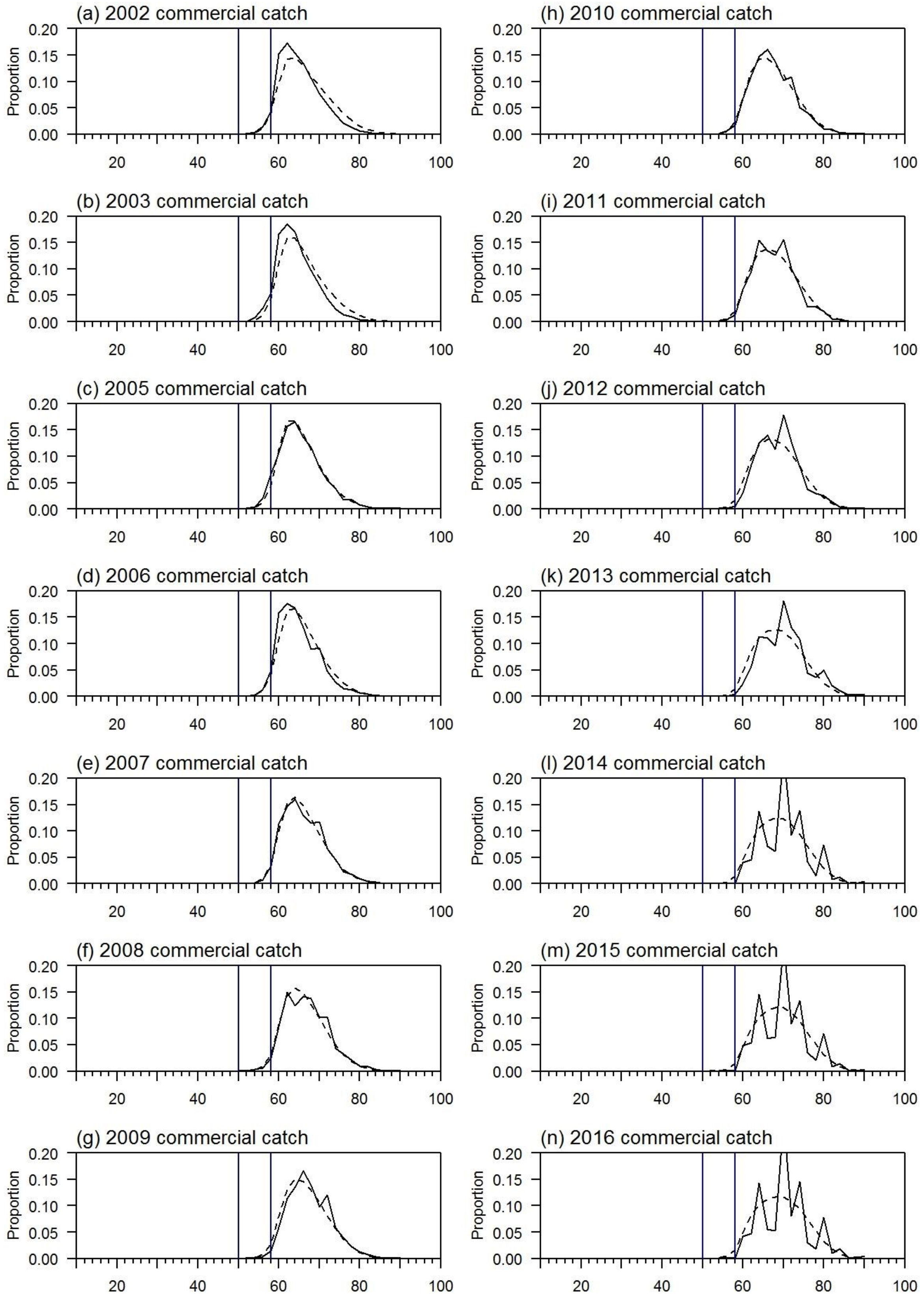

Figure 67: 2017 revised model MPD estimates of fits to the (a)–(g) 2002, 2003, 2005–2009 and (h)–(n) 2010–2016 commercial catch length frequency distributions. Vertical lines separate the small (<50 mm), pre-recruit (≥ 50 mm and <58 mm), and recruit (≥ 58 mm) size groups. X-axis shows length in millimetres.

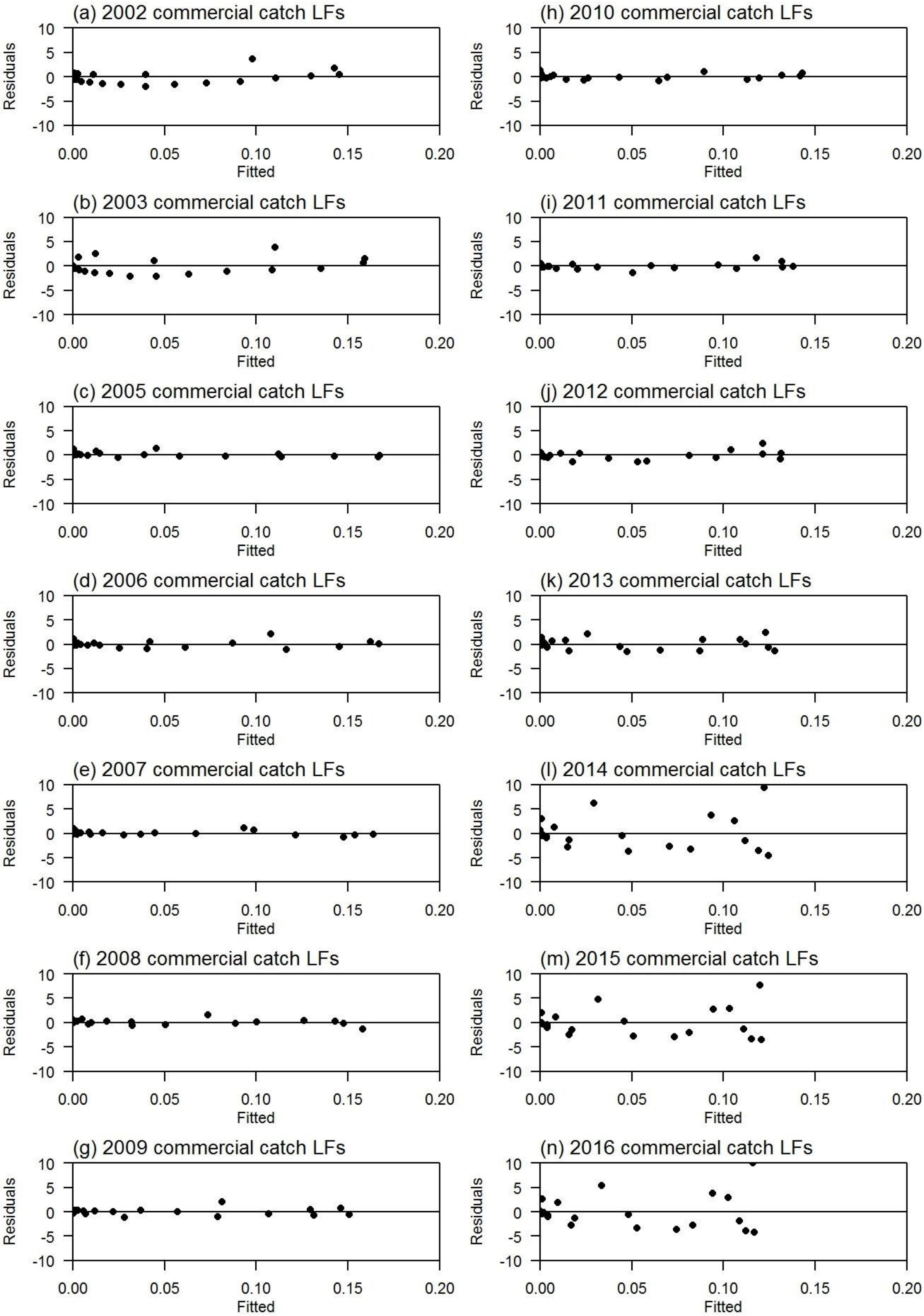

Figure 68: 2017 revised model MPD estimates of residuals versus fitted values for the (a)–(g) 2002, 2003, 2005–2009 and (h)–(n) 2010–2016 commercial catch data.

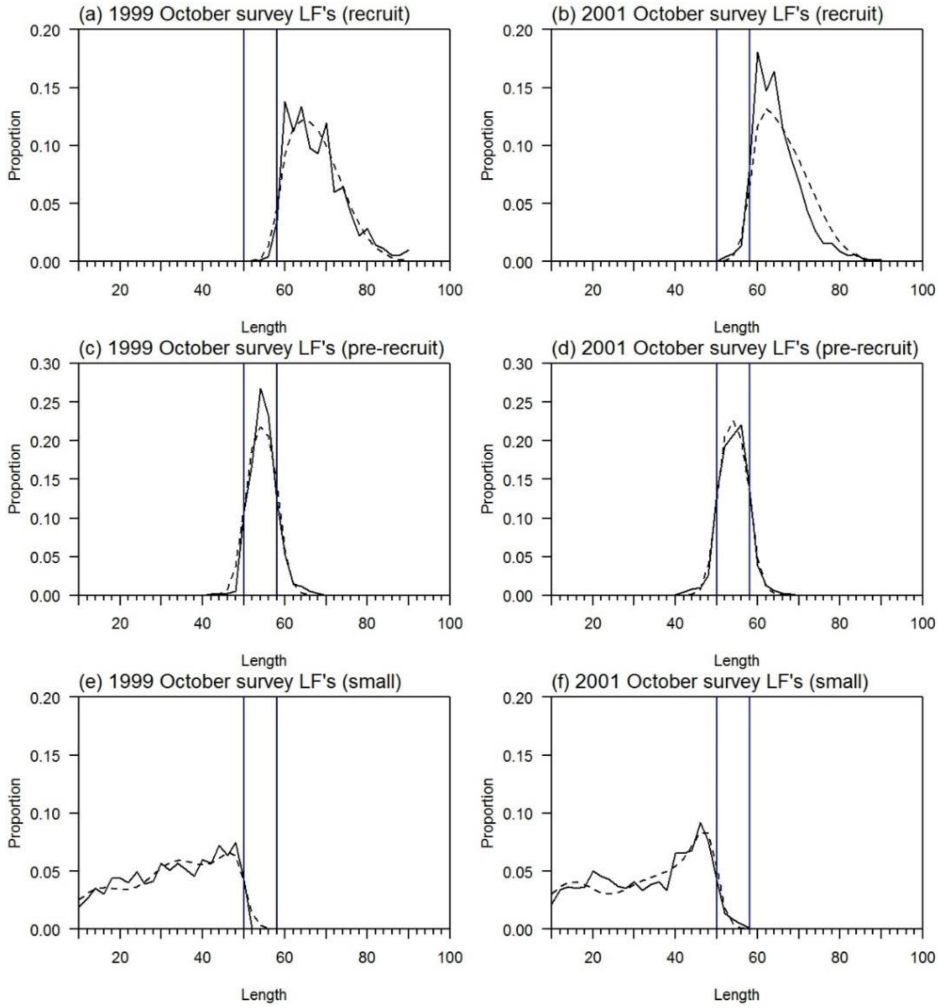

Figure 69: 2017 revised model MPD estimates of fits to the survey data length frequency distributions for (a–b) recruit-sized, (c–d) pre-recruit size, and (e–f) small oysters from the 1999 and 2001 abundance surveys respectively. Vertical lines separate the small (<50 mm), pre-recruit (≥ 50 mm and <58 mm), and recruit (≥ 58 mm) size groups.

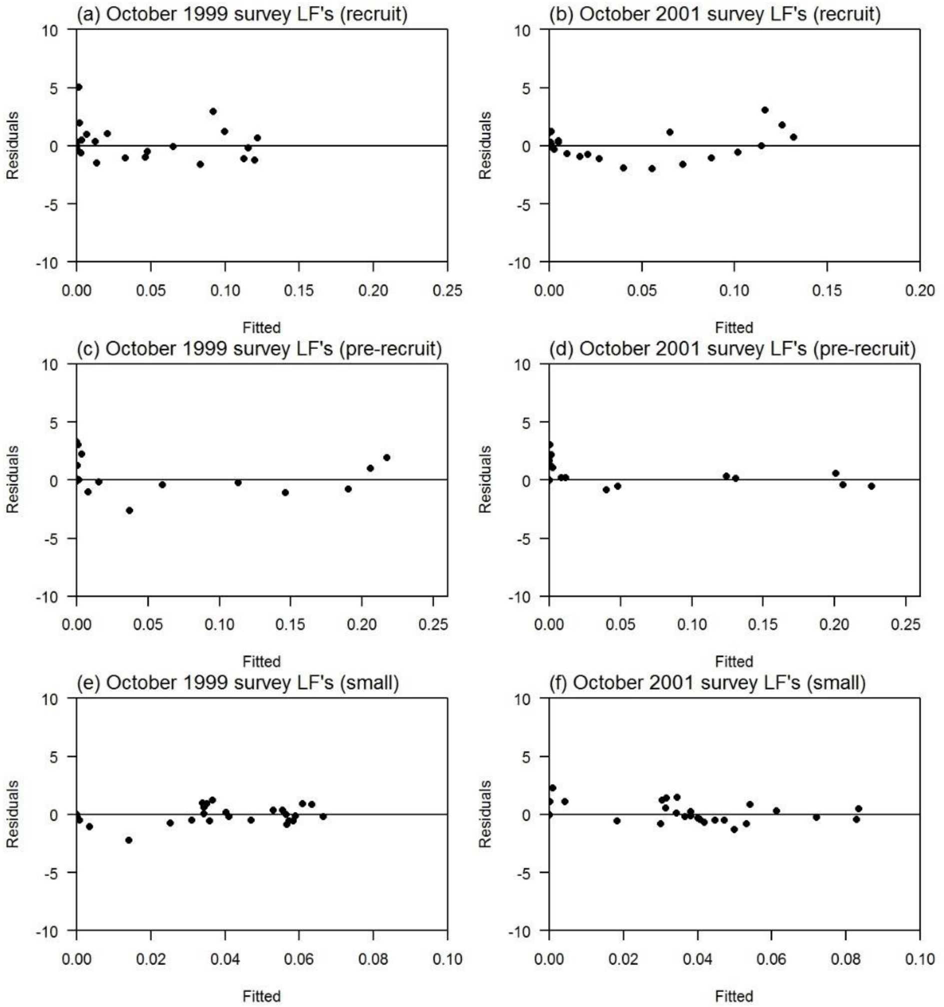

Figure 70: 2017 revised model MPD estimates of residuals versus fitted values for the (a–b) recruit size, (c–d) pre-recruit size, and (e–f) small oysters from the 1999 and 2001 abundance surveys respectively.

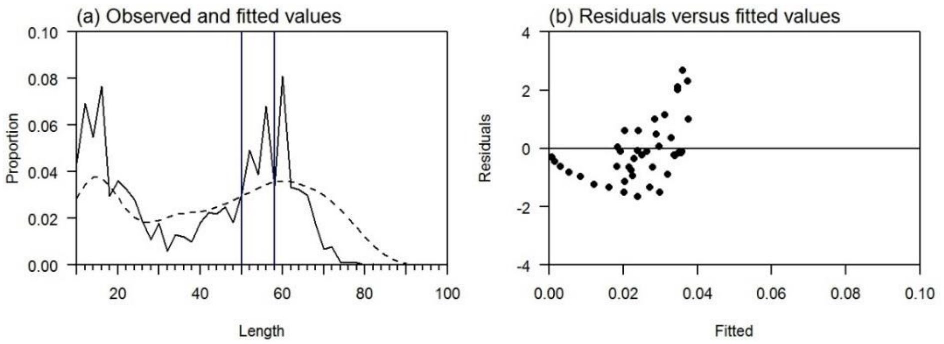

Figure 71: 2017 revised model MPD estimates for the 1990 dive survey length frequency distributions (a) observed (solid line) and MPD estimates of fits (dashed line), and (b) residuals versus fitted values (curved lines show 95% confidence intervals for the multinomial distribution). Vertical lines separate the small (<50 mm), pre-recruit (≥ 50 mm and <58 mm), and recruit (≥ 58 mm) size groups.

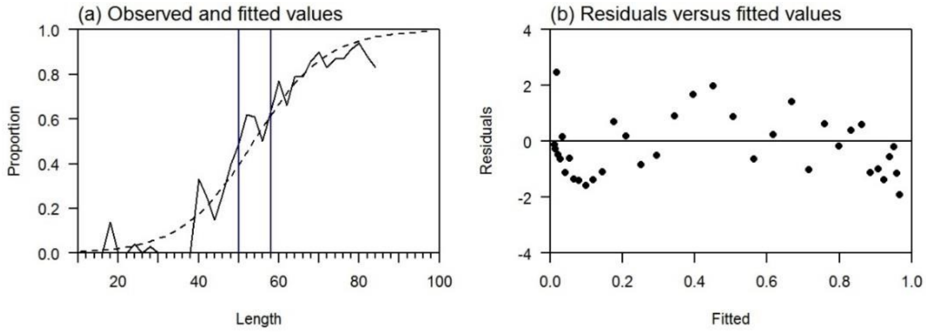

Figure 72: 2017 revised model MPD estimates for the Jeffs & Hickman (2000) maturity data (a) observed (solid line) and MPD estimates of fits (dashed line), and (b) residuals versus fitted values. Vertical lines separate the small (<50 mm), pre-recruit (≥ 50 mm and <58 mm), and recruit (≥ 58 mm) size groups.

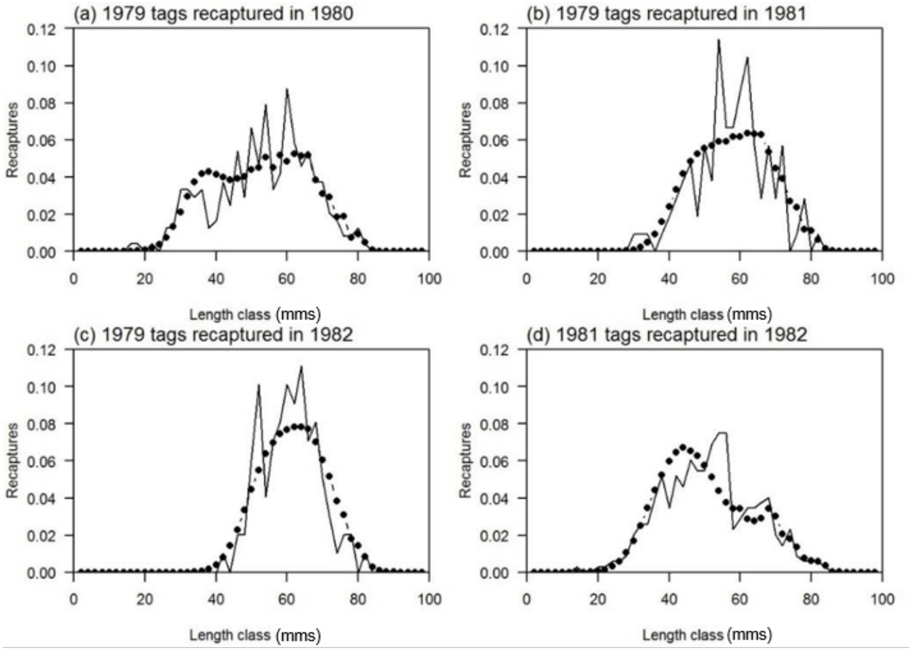

Figure 73: 2017 revised model MPD estimates of the observed and expected length frequency distributions of the mark recapture data for (a–c) 1979 marked fish recaptured in 1980–81, and (d) 1981 marked fish recaptured in 1981.

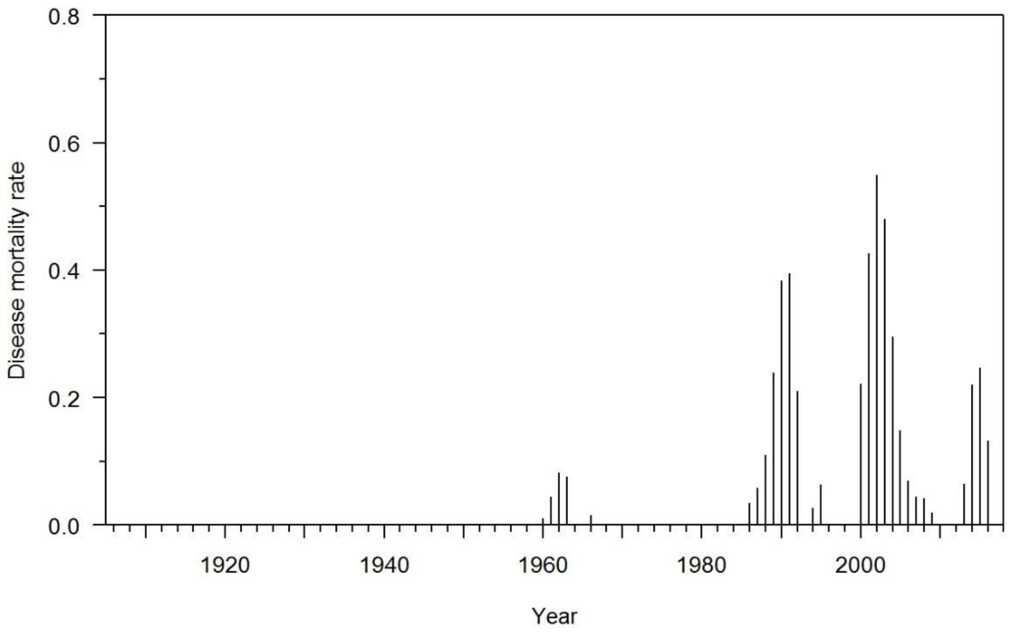

Figure 74: 2017 revised model MPD estimates of disease mortality rate.

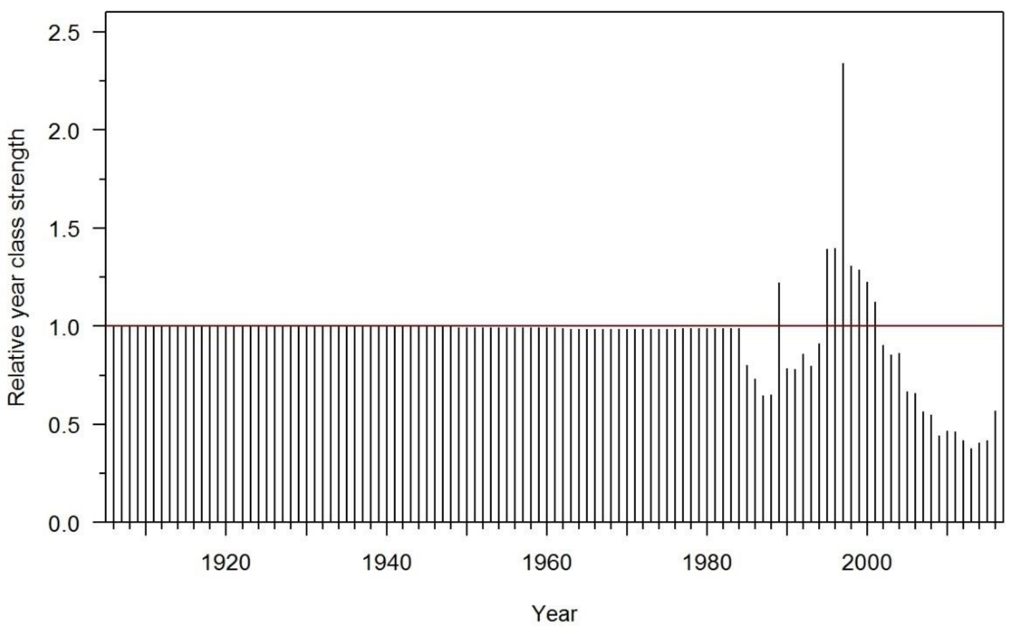

Figure 75: 2017 basic revised MPD estimated of relative year class strength.

8.3 2017 Basic 4cpue model

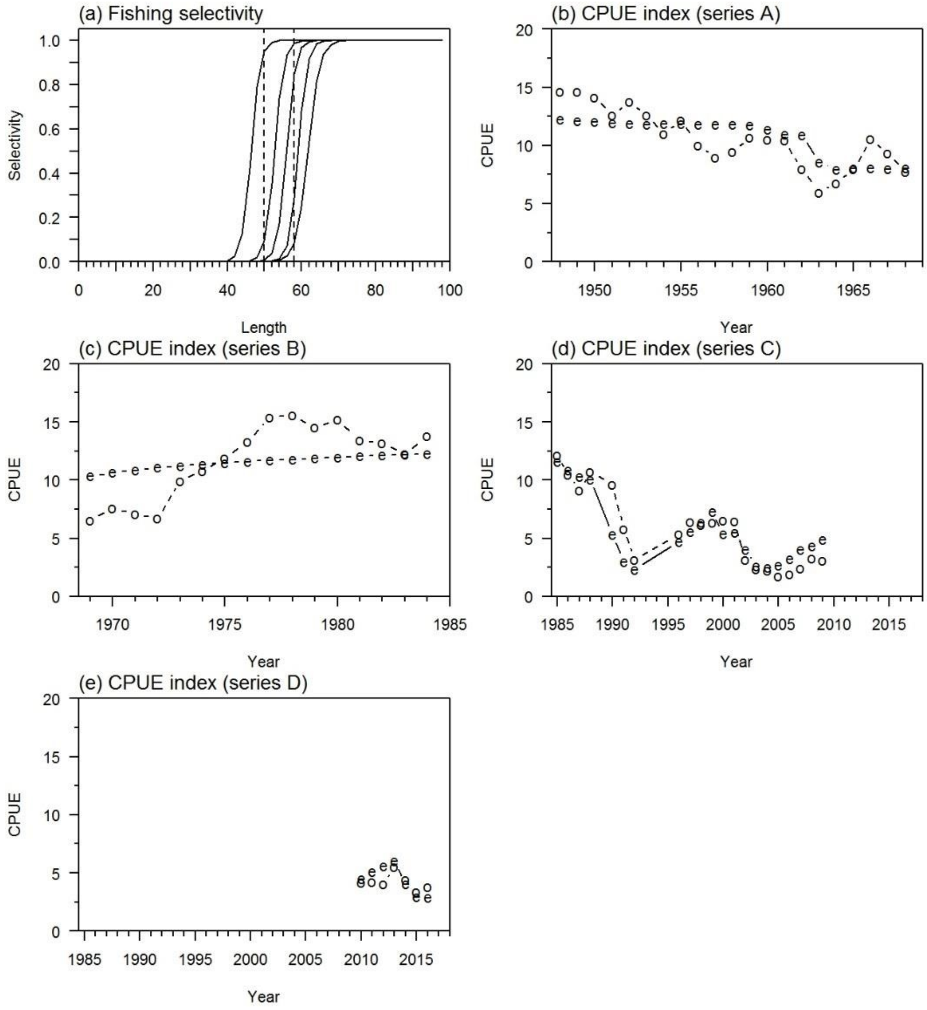

Figure 76: 2017 basic 4-cpue model MPD estimates of (a) fishing selectivity and model fits to (b) series A, (c) series B, (d) series C and (e) series D CPUE indices ("e"=expected and "o"=observed). Dashed lines separate the small (<50 mm), pre-recruit (≥ 50 mm and <58 mm), and recruit (≥ 58 mm) size groups.

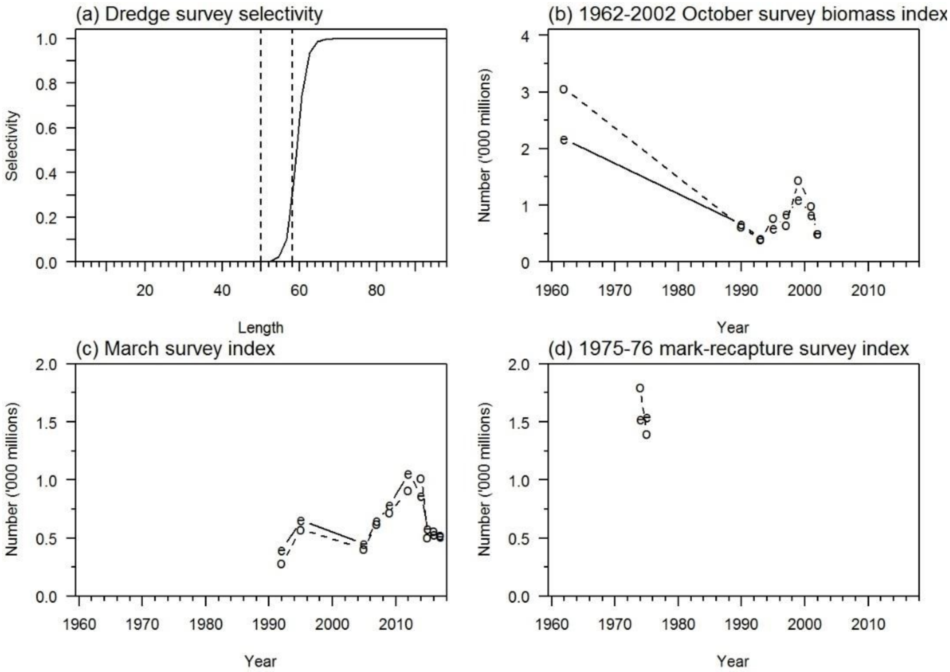

Figure 77: 2017 basic 4-cpue model MPD estimates of (a) recruit-sized dredge survey selectivity and model fits to recruit-sized abundance indices for the (b) October surveys 1964–2002, (c) March surveys 1992–2017, and (d) 1975–76 mark-recapture survey ("e"=expected and "o"=observed). Dashed lines separate the small (<50 mm), pre-recruit (≥ 50 mm and <58 mm), and recruit (≥ 58 mm) size groups.

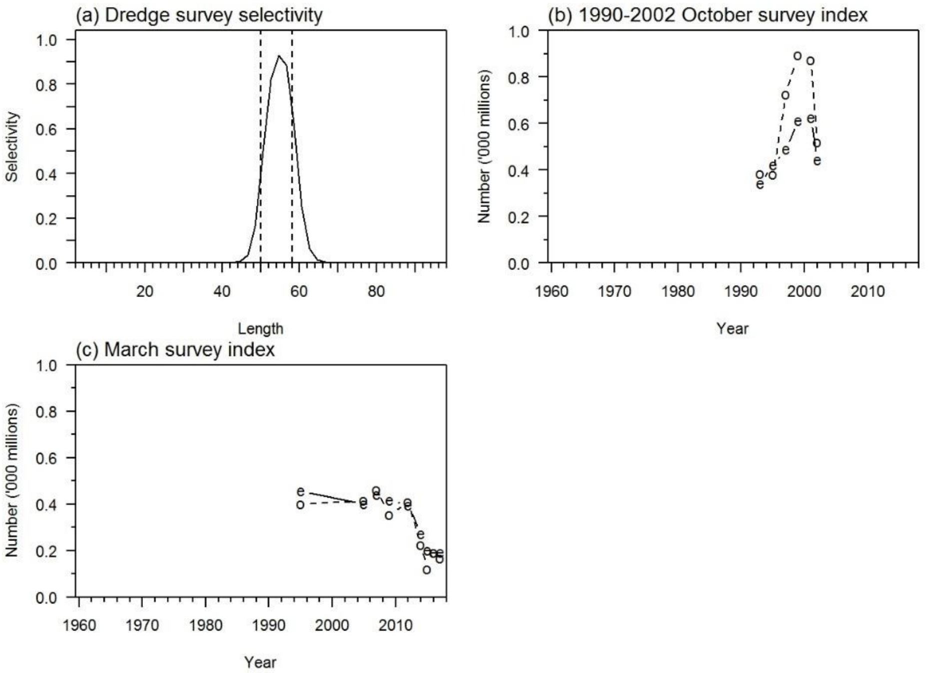

Figure 78: 2017 basic 4-cpue model MPD estimates of the (a) pre-recruit-sized dredge survey selectivity and model fits to pre-recruit-sized abundance indices for the (b) October surveys 1990–2002, and (c) March surveys 1995–2017 ("e"=expected and "o"=observed). Dashed lines separate the small (<50 mm), pre-recruit (≥ 50 mm and <58 mm), and recruit (≥ 58 mm) size groups.

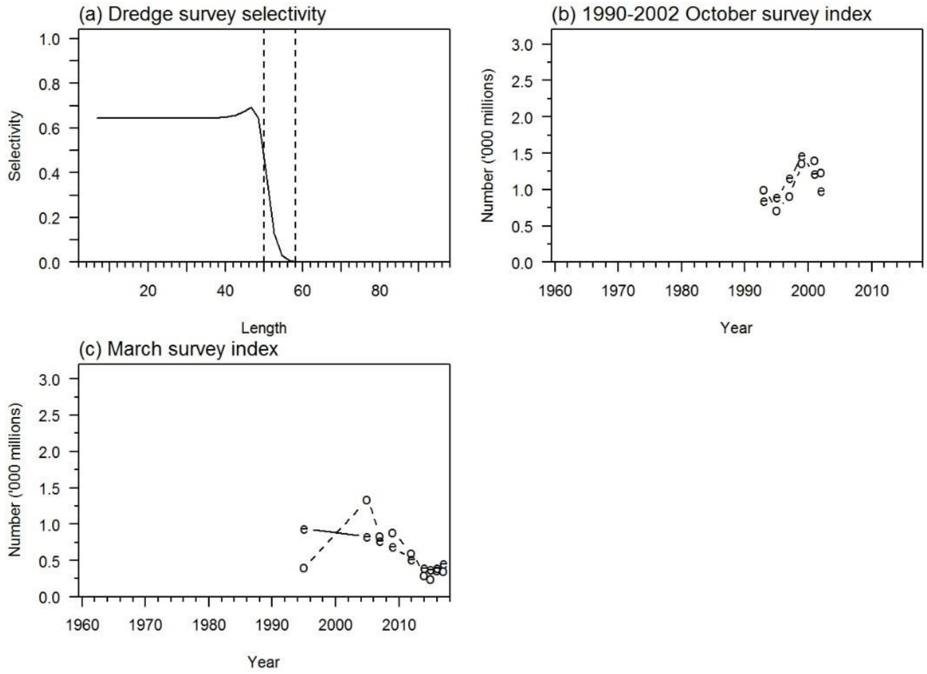

Figure 79: 2017 basic 4-cpue model MPD estimates of (a) small-sized oyster dredge survey selectivity and model fits to small-sized oyster abundance indices for the (b) October surveys 1990–2002, and (c) March surveys 1995–2017 ("e"=expected and "o"=observed). Dashed lines separate the small (<50 mm), pre-recruit (≥ 50 mm and <58 mm), and recruit (≥ 58 mm) size groups.

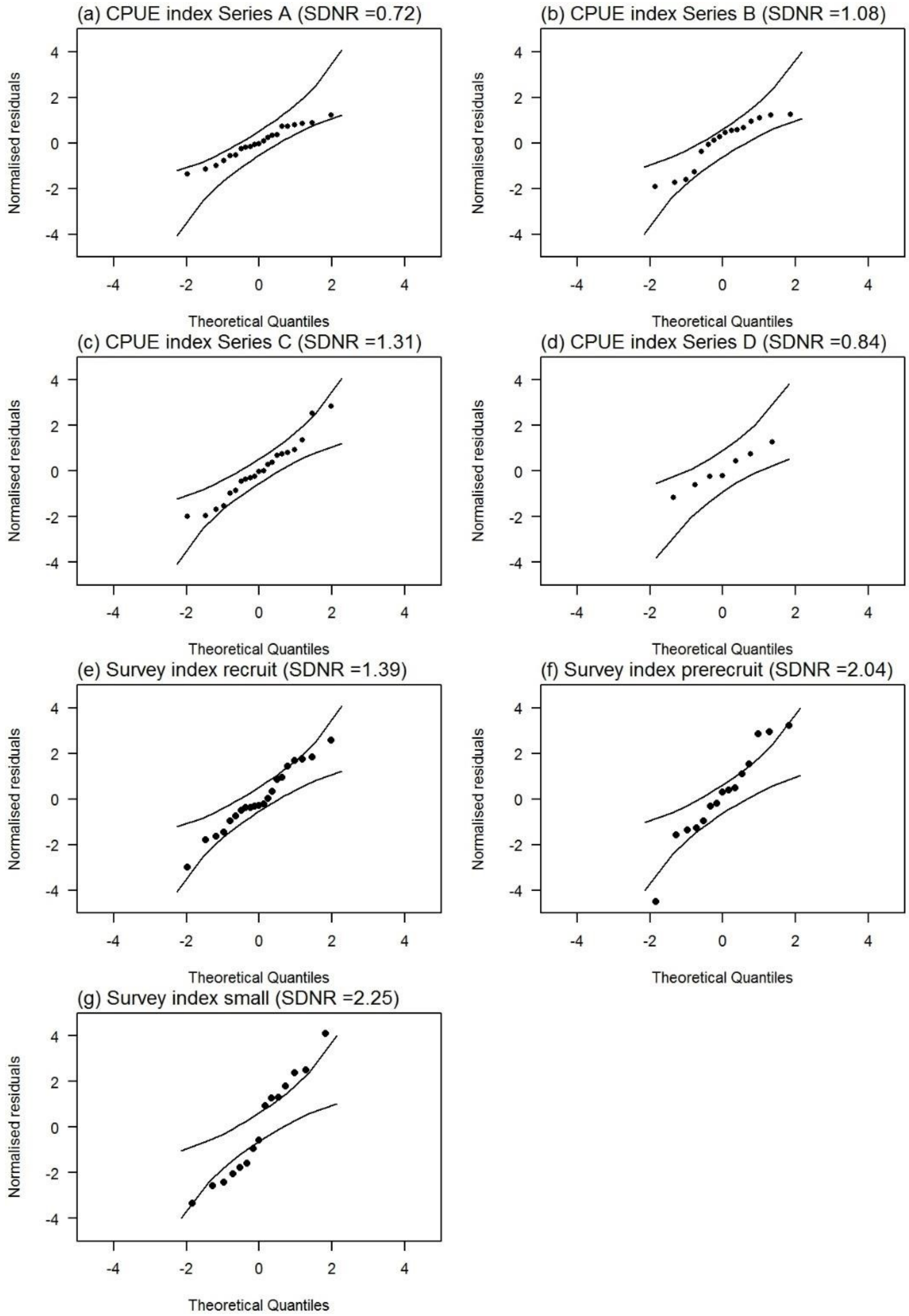

Figure 80: 2017 basic 4-cpue model MPD estimates of fits (normal quantile-quantile plots) to the (a) series A, (b) series B, (c) series C, (d) series D CPUE indices, and 1964–2017 survey indices combined for (e) recruits (≥ 58 mm), (f) pre-recruit (≥ 50 mm and <58 mm), (g) small (<50 mm) size groups.

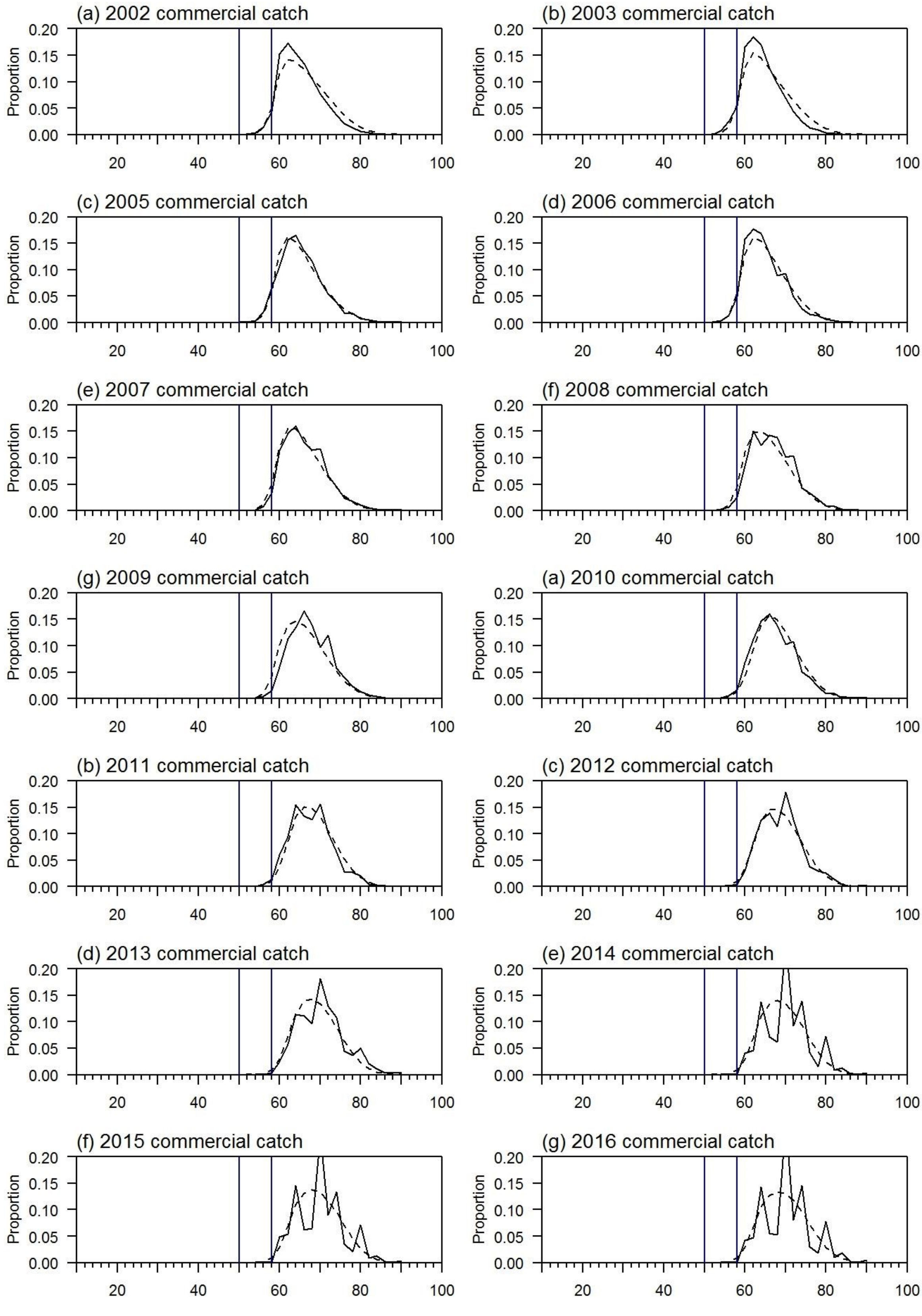

Figure 81: 2017 basic 4-cpue model MPD estimates of fits to the (a)-(g) 2002, 2003, 2005–2009 and (h)-(n) 2010–2016 commercial catch length frequency distributions. Vertical lines separate the small (<50 mm), pre-recruit (≥ 50 mm and <58 mm), and recruit (≥ 58 mm) size groups. X-axis gives length in millimetres.

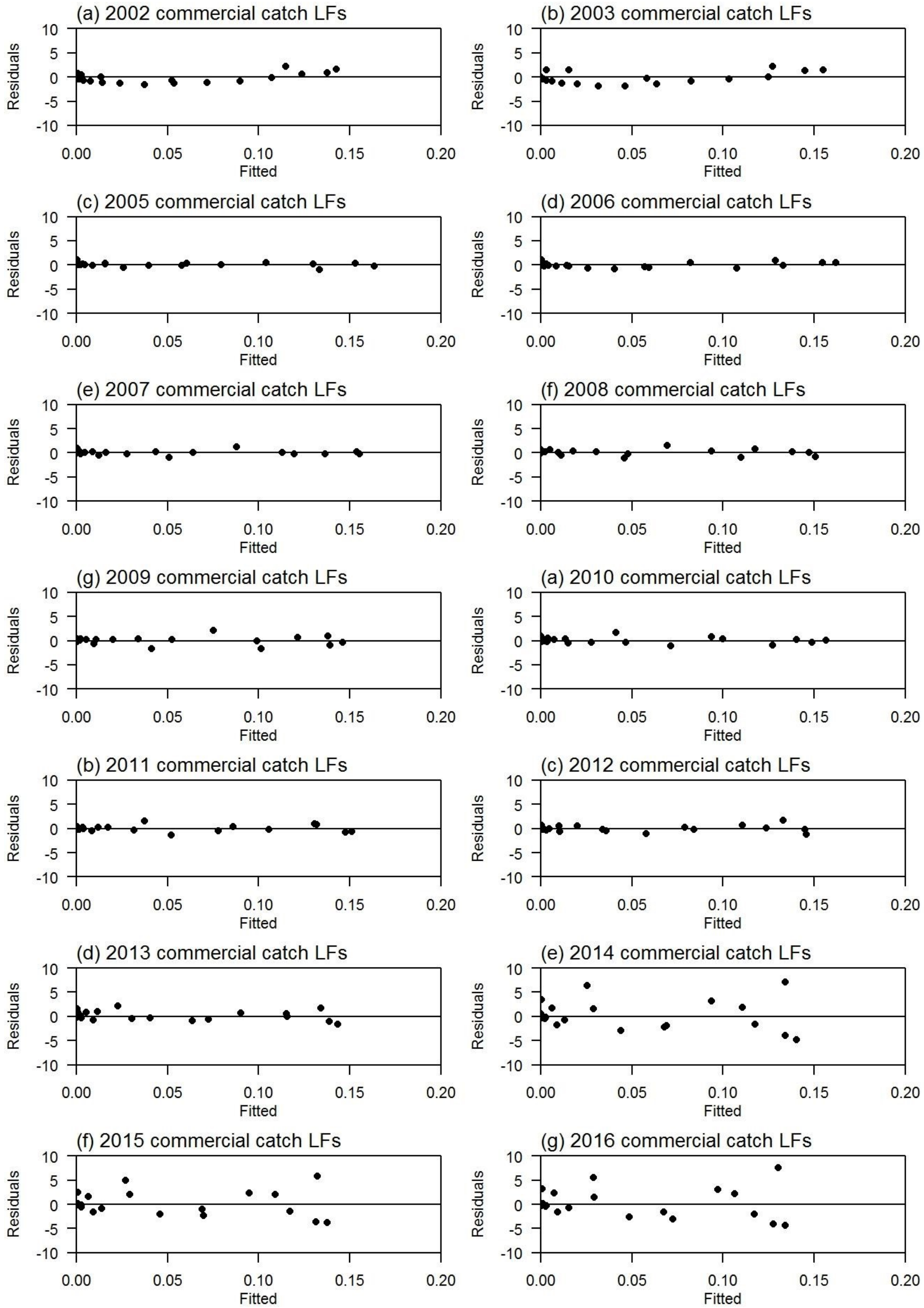

Figure 82: 2017 basic 4-cpue model MPD estimates of residuals versus fitted values for the (a)-(g) 2002, 2003, 2005–2009 and (h)-(n) 2010–2016 commercial catch data.

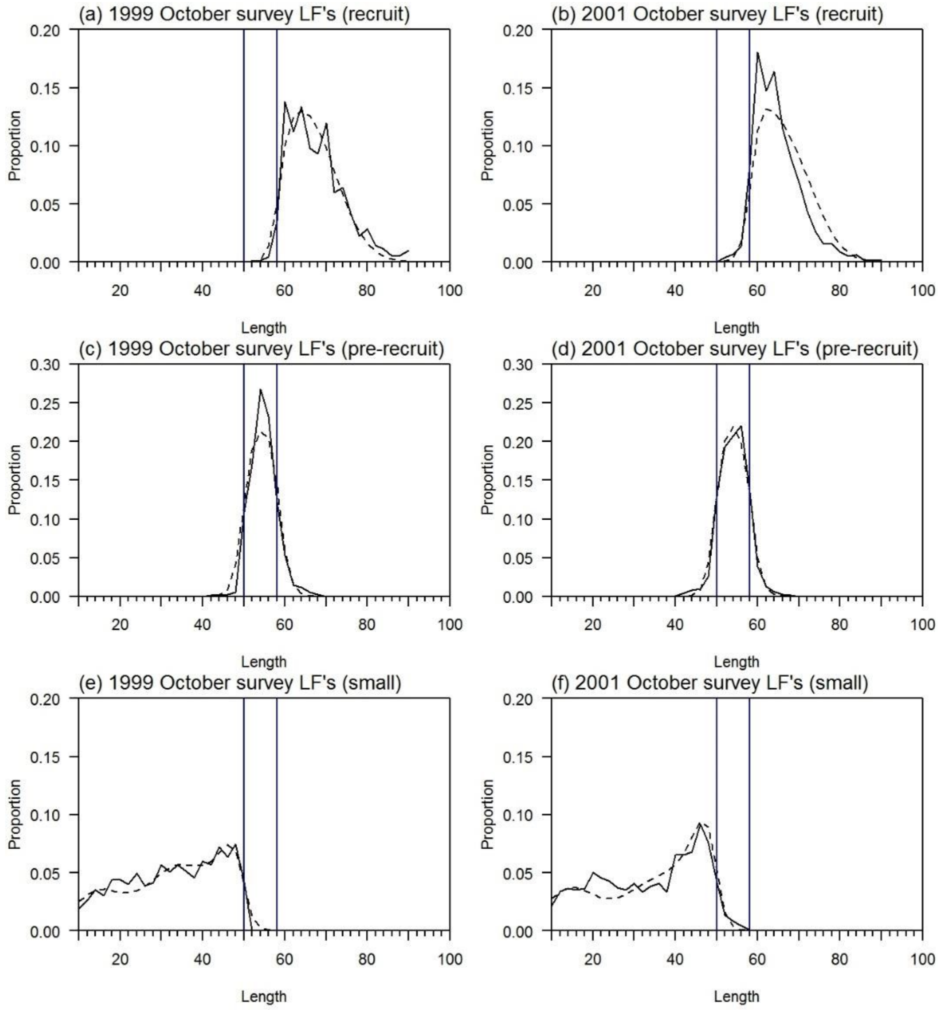

Figure 83: 2017 basic 4-cpue model MPD estimates of fits to the survey data length frequency distributions for (a–b) recruit-sized, (c–d) pre-recruit size, and (e–f) small oysters from the 1999 and 2001 abundance surveys respectively. Vertical lines separate the small (<50 mm), pre-recruit (≥ 50 mm and <58 mm), and recruit (≥ 58 mm) size groups.

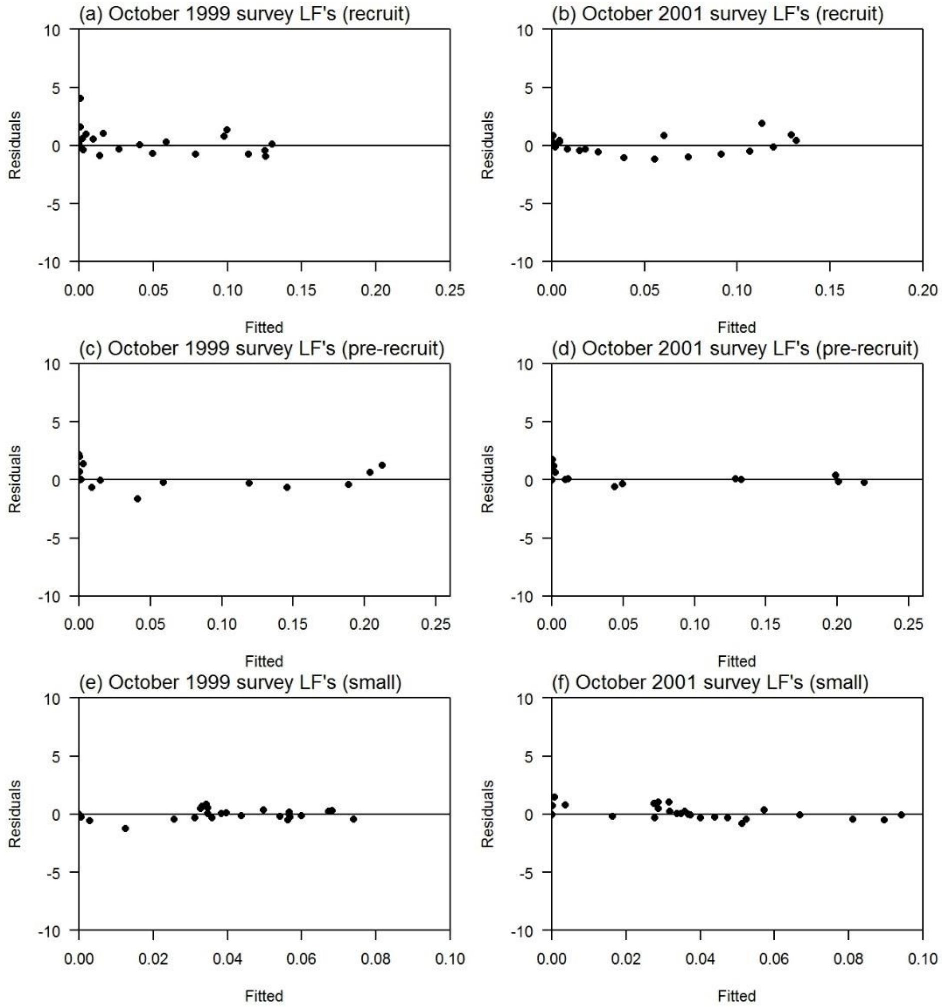

Figure 84: 2017 basic 4-cpue model MPD estimates of residuals versus fitted values for the (a–b) recruit size, (c–d) pre-recruit size, and (e–f) small oysters from the 1999 and 2001 abundance surveys respectively.

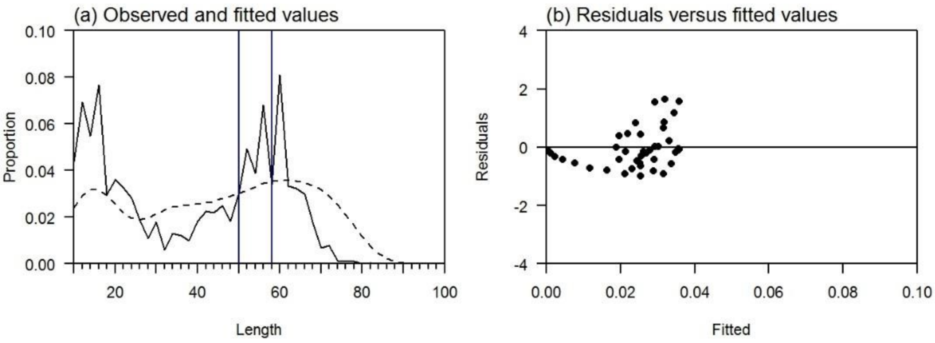

Figure 85: 2017 basic 4-cpue model MPD estimates for the 1990 dive survey length frequency distributions (a) observed (solid line) and MPD estimates of fits (dashed line), and (b) residuals versus fitted. Vertical lines separate the small (<50 mm), pre-recruit (≥ 50 mm and <58 mm), and recruit (≥ 58 mm) size groups.

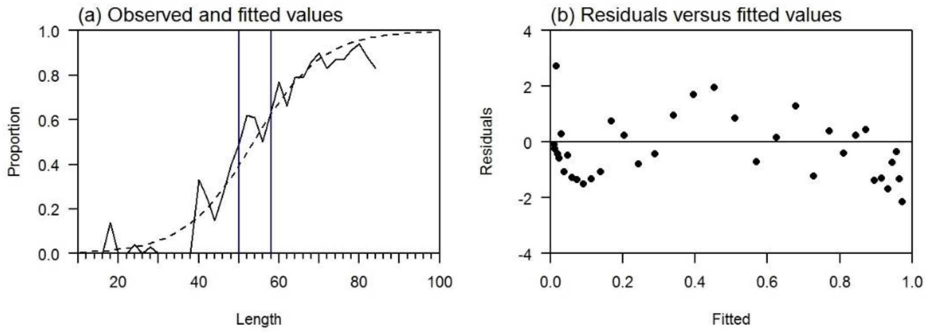

Figure 86: 2017 basic 4-cpue model MPD estimates for the Jeffs & Hickman (2000) maturity data (a) observed (solid line) and MPD estimates of fits (dashed line), and (b) residuals versus fitted values. Vertical lines separate the small (<50 mm), pre-recruit (≥ 50 mm and <58 mm), and recruit (≥ 58 mm) size groups.

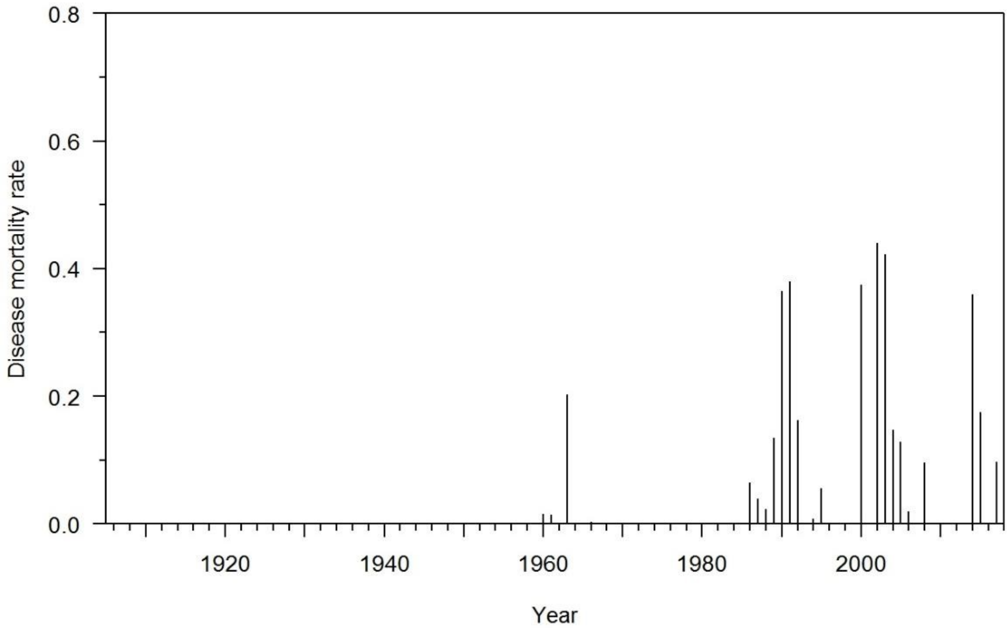

Figure 87: 2017 basic 4-cpue model MPD estimates of disease mortality rate.

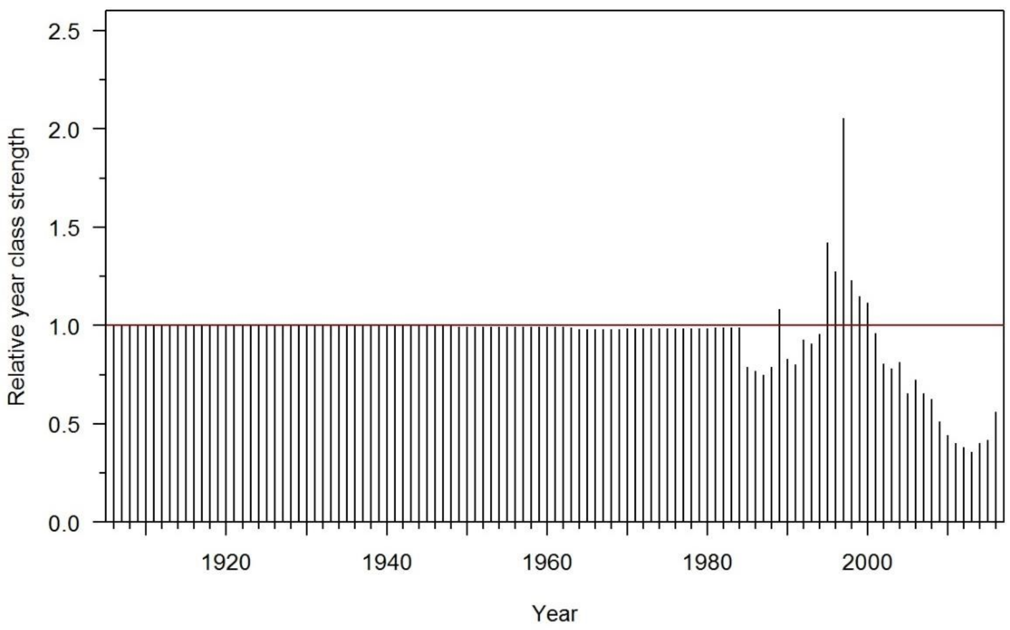

Figure 88: 2017 basic 4-cpue model MPD estimates of relative year class strength.

8.4 2017 Revised 4cpue model

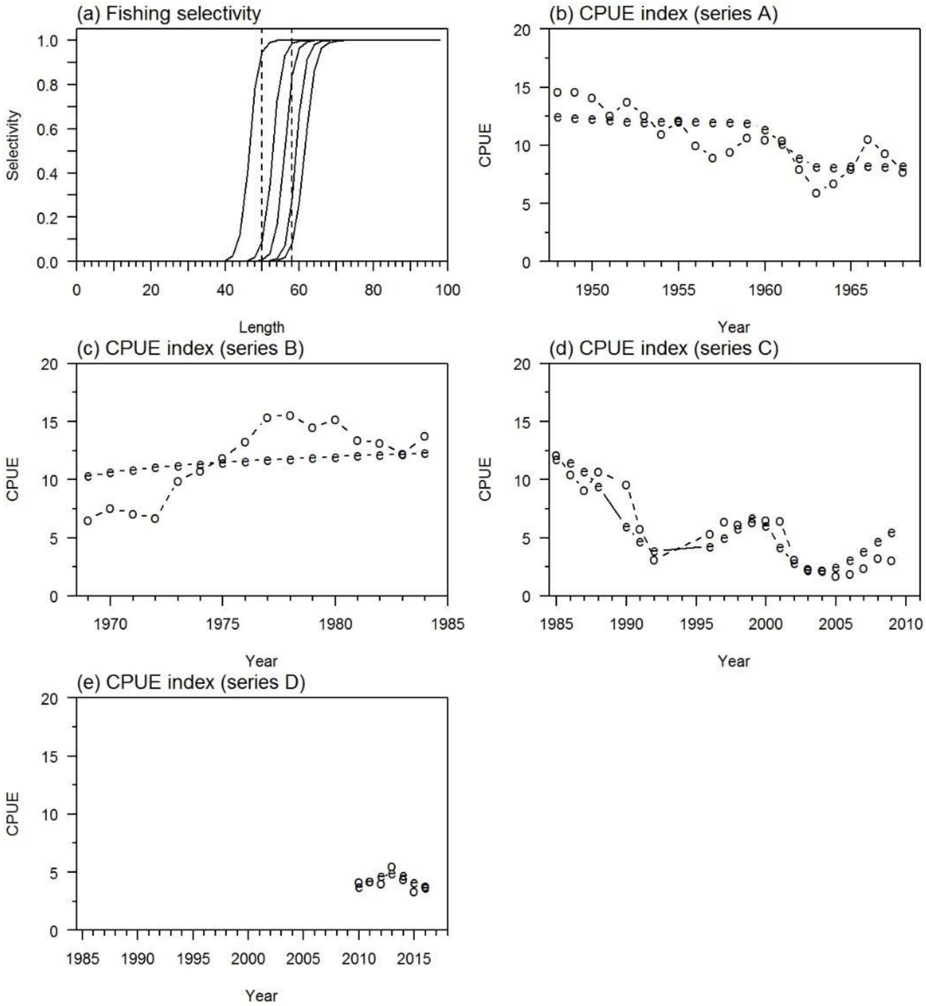

Figure 89: 2017 revised 4-cpue model MPD estimates of (a) fishing selectivity and model fits to (b) series A, (c) series B, (d) series C and (e) series D CPUE indices ("e"=expected and "o"=observed). Dashed lines separate the small (<50 mm), pre-recruit (≥ 50 mm and <58 mm), and recruit (≥ 58 mm) size groups.

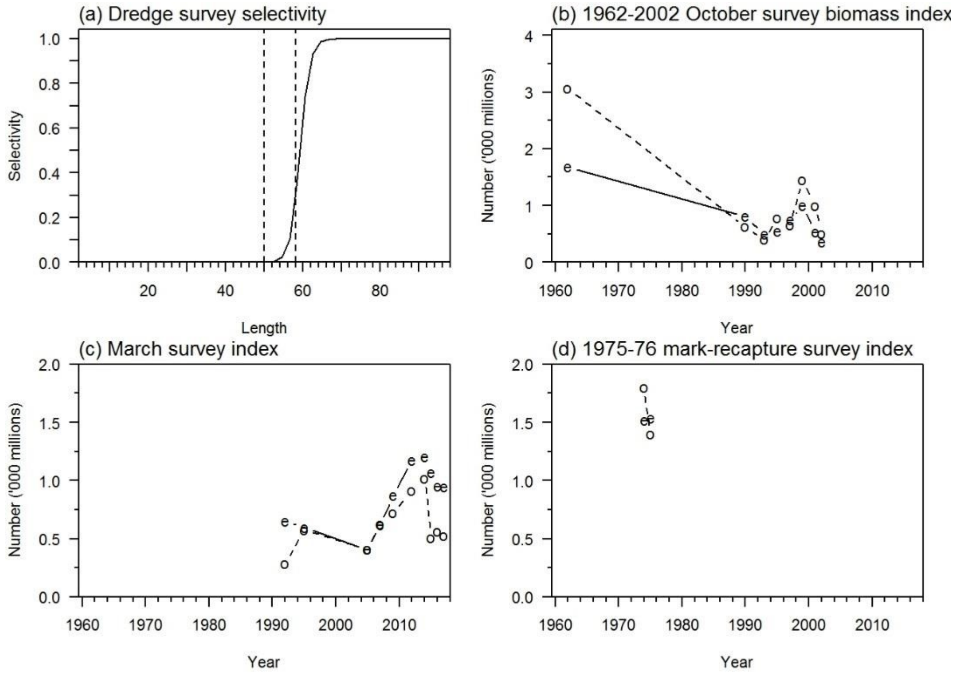

Figure 90: 2017 revised 4-cpue model MPD estimates of (a) recruit-sized dredge survey selectivity and model fits to recruit-sized abundance indices for the (b) October surveys 1964–2002, (c) March surveys 1992–2017, and (d) 1975–76 mark-recapture survey ("e"=expected and "o"=observed). Dashed lines separate the small (<50 mm), pre-recruit (≥ 50 mm and <58 mm), and recruit (≥ 58 mm) size groups.

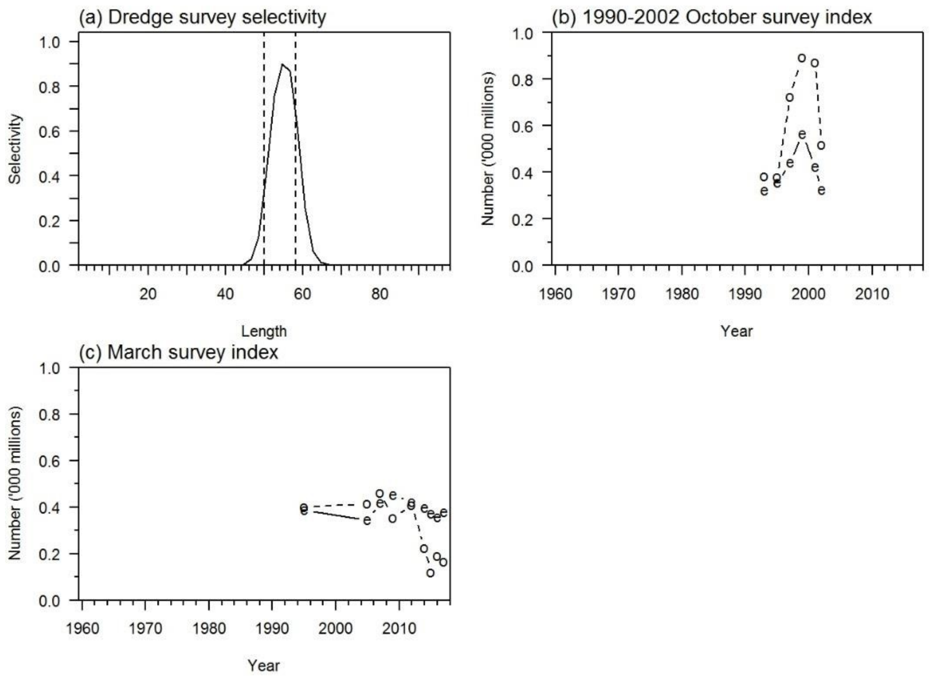

Figure 91: 2017 revised 4-cpue model MPD estimates of the (a) pre-recruit-sized dredge survey selectivity and model fits to pre-recruit-sized abundance indices for the (b) October surveys 1990–2002, and (c) March surveys 1995–2017 ("e"=expected and "o"=observed). Dashed lines separate the small (<50 mm), pre-recruit (≥ 50 mm and <58 mm), and recruit (≥ 58 mm) size groups.

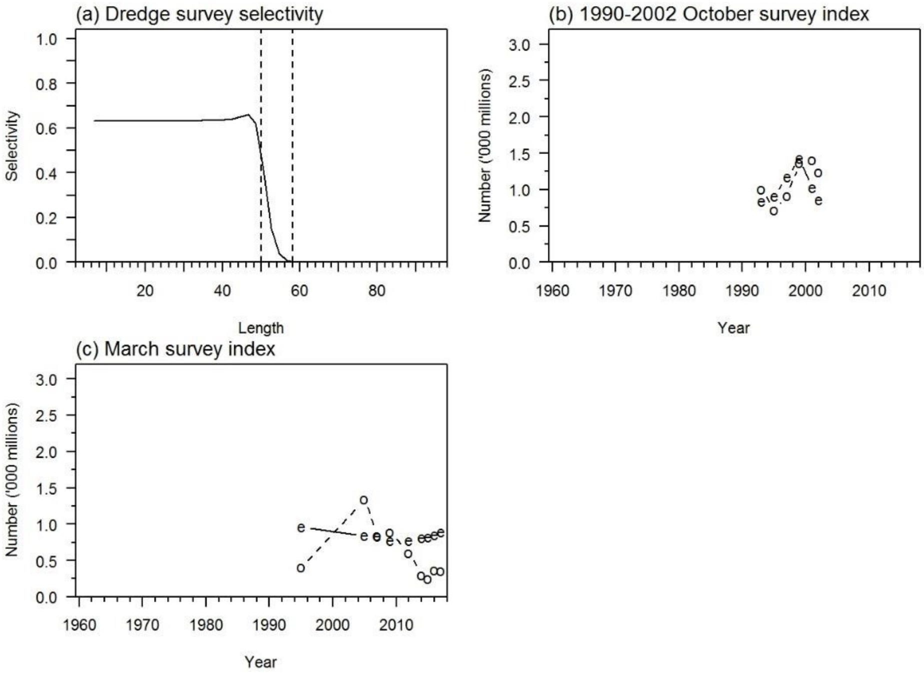

Figure 92: 2017 revised 4-cpue model MPD estimates of (a) small-sized oyster dredge survey selectivity and model fits to small-sized oyster abundance indices for the (b) October surveys 1990–2002, and (c) March surveys 1995–2017 ("e"=expected and "o"=observed). Dashed lines separate the small (<50 mm), pre-recruit (≥ 50 mm and <58 mm), and recruit (≥ 58 mm) size groups.

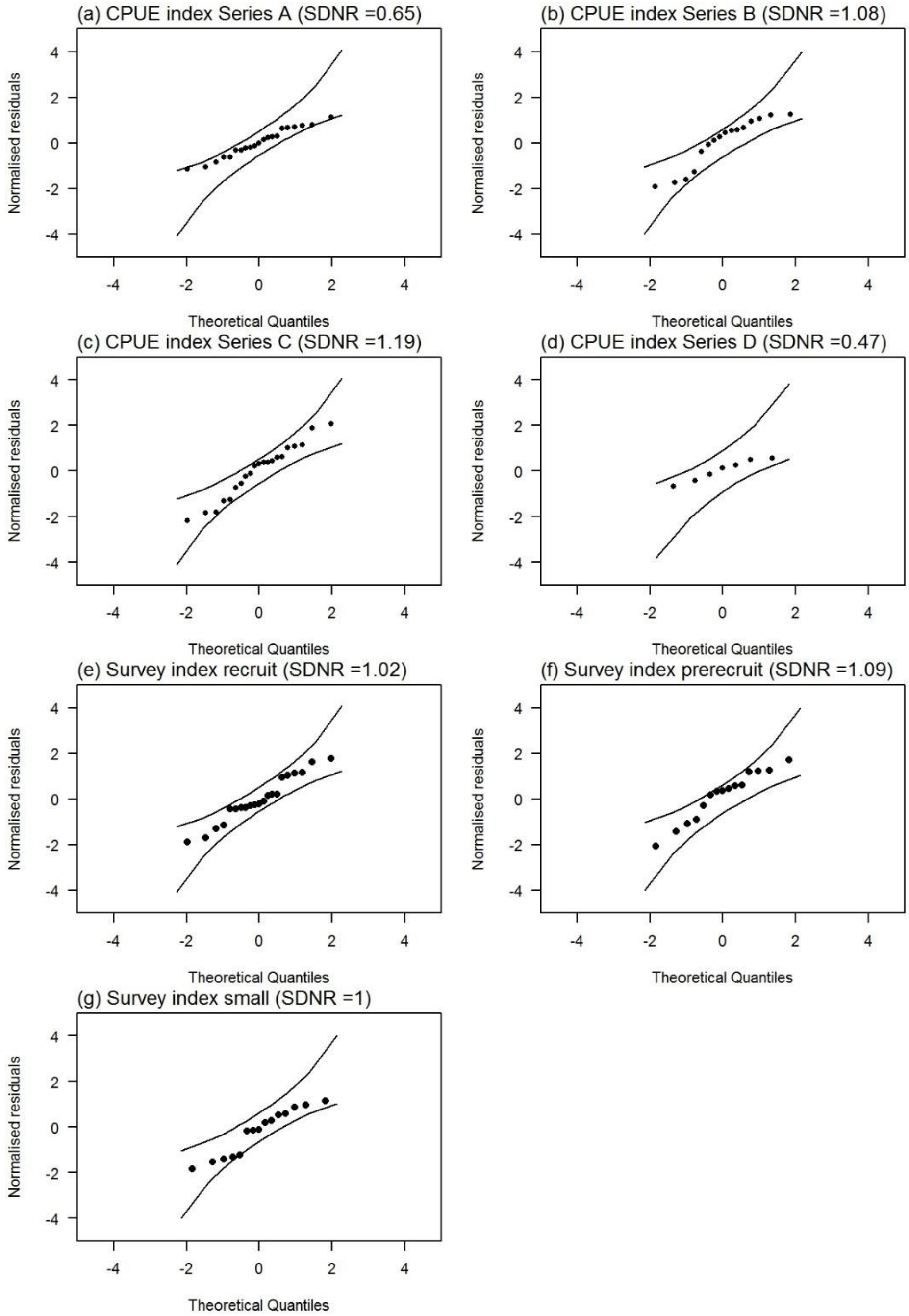

Figure 93: 2017 revised 4-cpue model MPD estimates of fits (normal quantile-quantile plots) to the (a) series A, (b) series B, (c) series C, (d) series D CPUE indices, and 1964–2017 survey indices combined for (e) recruits (≥ 58 mm), (f) pre-recruit (≥ 50 mm and <58 mm), (g) small (<50 mm) size groups.

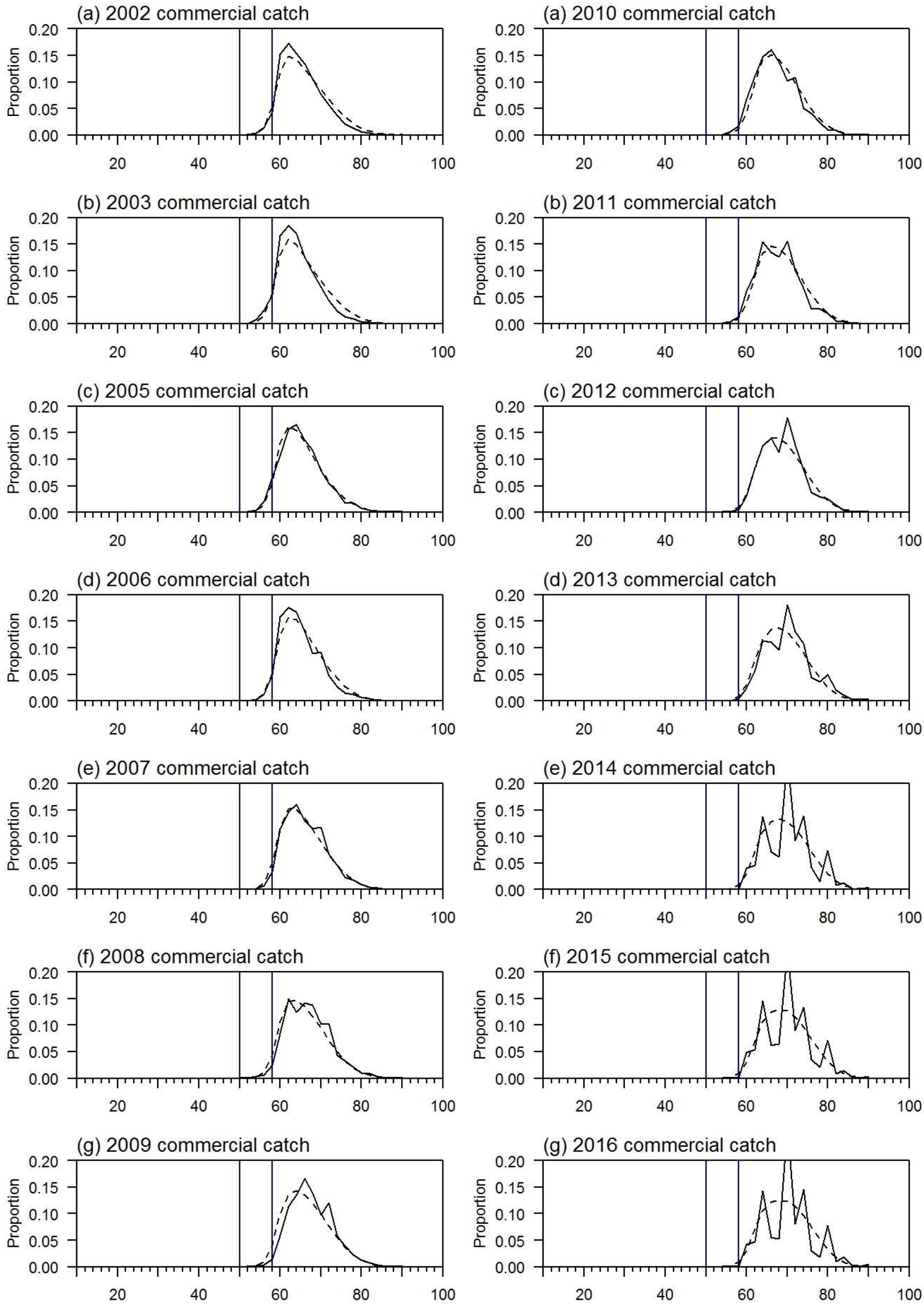

Figure 94: 2017 revised 4-cpue model MPD estimates of fits to the (a)-(g) 2002, 2003, 2005–2009 and (h)-(n) 2010–2016 commercial catch length frequency distributions. Vertical lines separate the small (<50 mm), pre-recruit (≥ 50 mm and <58 mm), and recruit (≥ 58 mm) size groups.

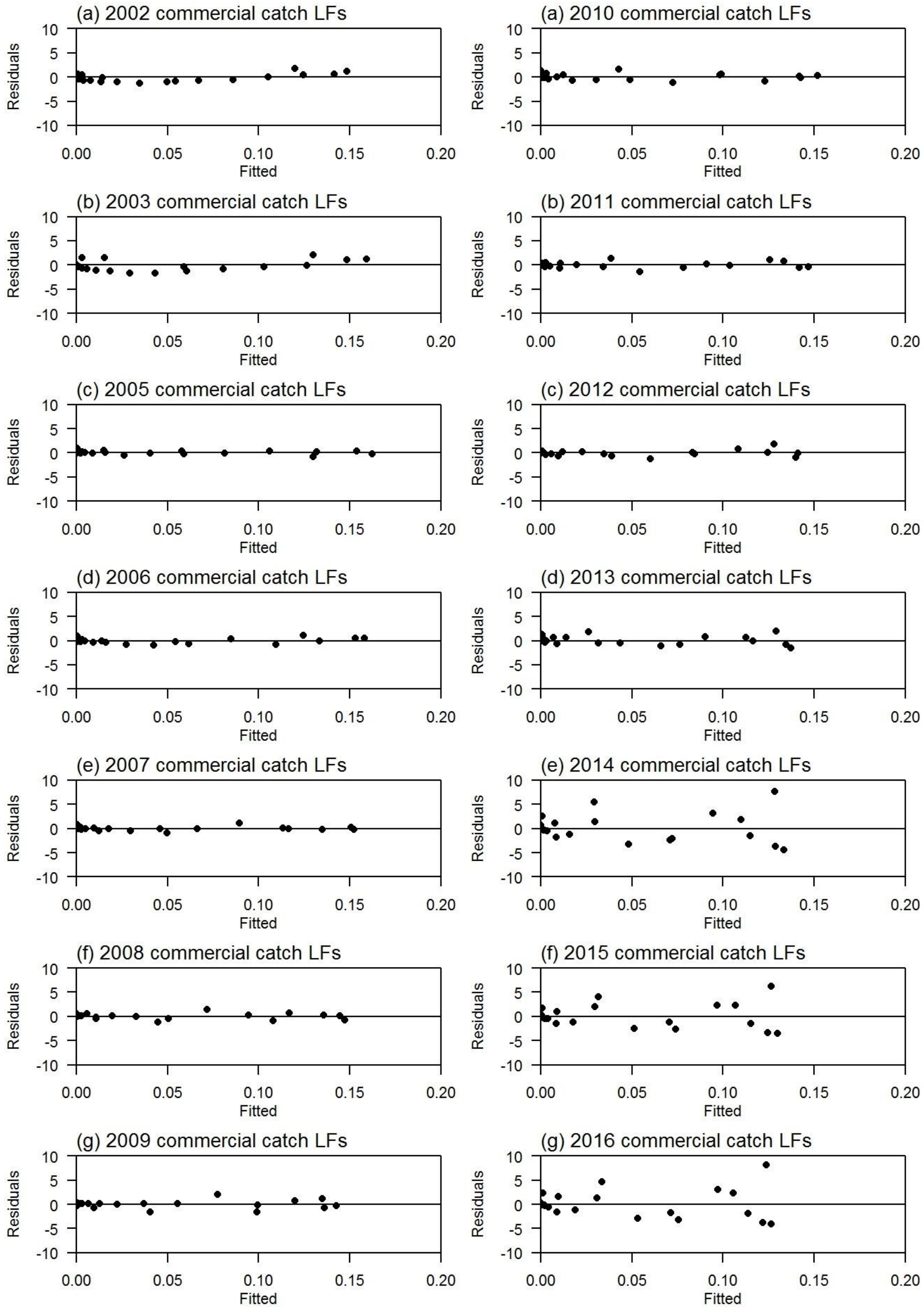

Figure 95: 2017 revised 4-cpue model MPD estimates of residuals versus fitted values for the (a)-(g) 2002, 2003, 2005–2009 and (h)-(n) 2010–2016 commercial catch data.

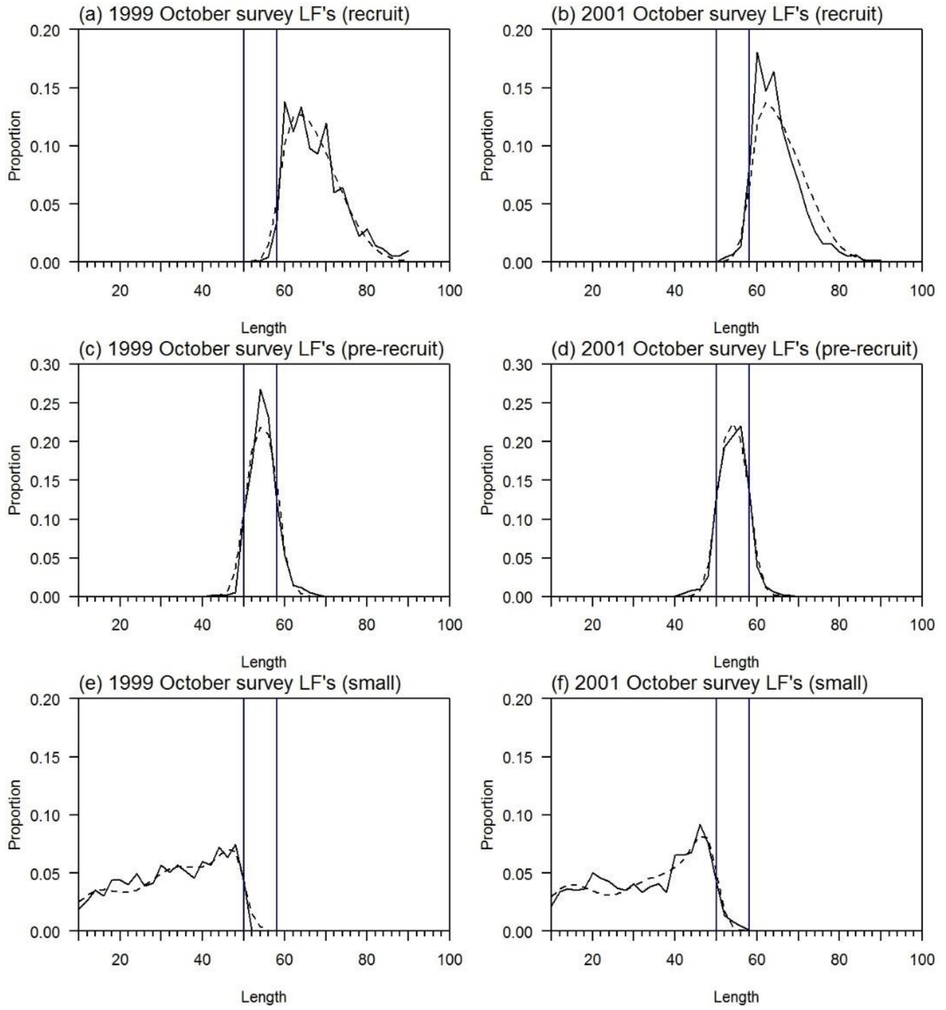

Figure 96: 2017 revised 4-cpue model MPD estimates of fits to the survey data length frequency distributions for (a–b) recruit-sized, (c–d) pre-recruit size, and (e–f) small oysters from the 1999 and 2001 abundance surveys respectively. Vertical lines separate the small (<50 mm), pre-recruit (≥ 50 mm and <58 mm), and recruit (≥ 58 mm) size groups.

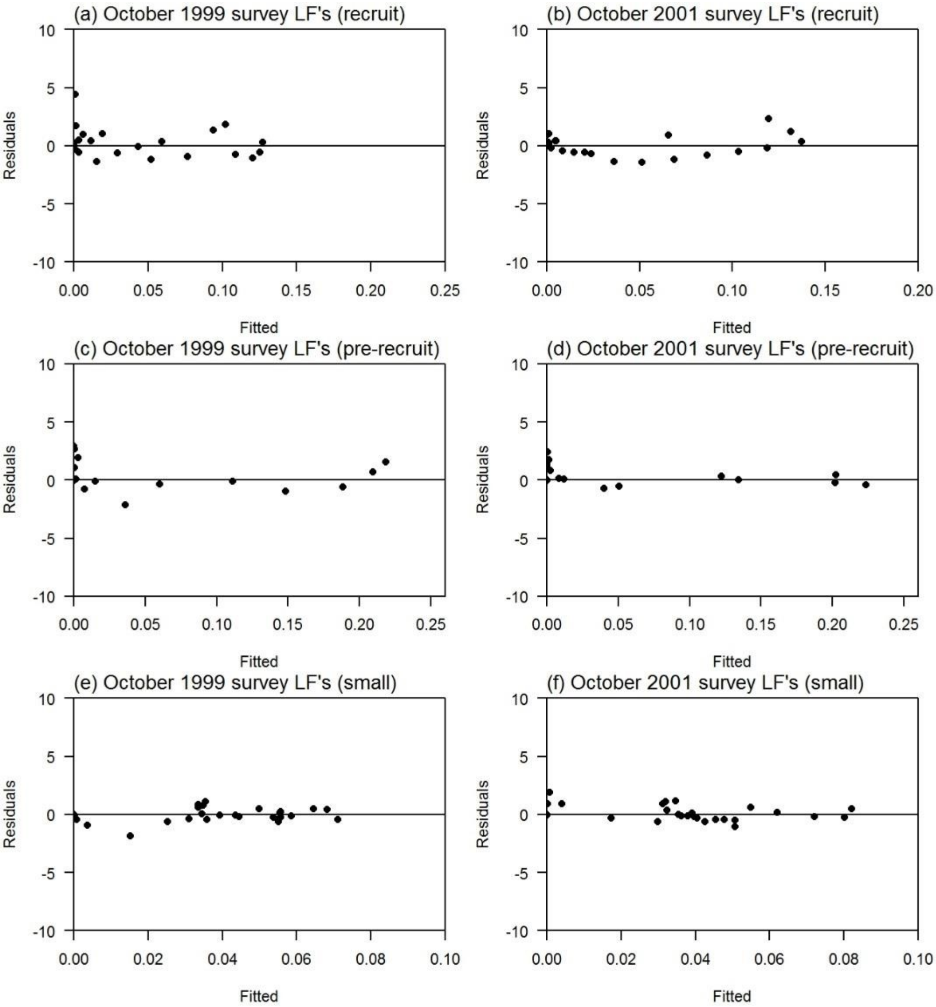

Figure 97: 2017 revised 4-cpue model MPD estimates of residuals versus fitted values for the (a–b) recruit size, (c–d) pre-recruit size, and (e–f) small oysters from the 1999 and 2001 abundance surveys respectively.

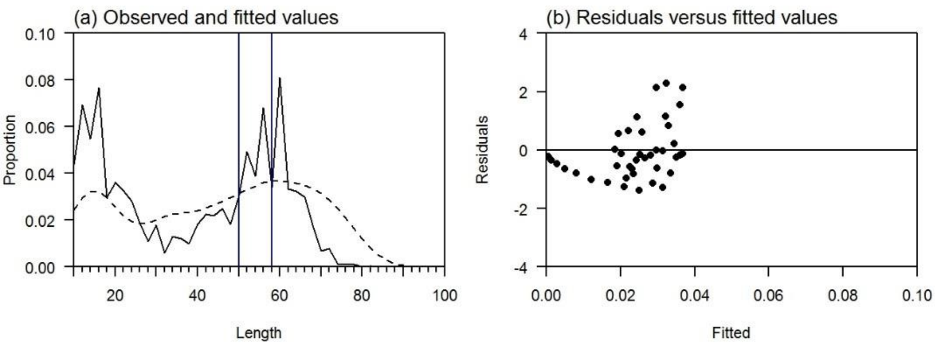

Figure 98: 2017 revised 4-cpue model MPD estimates for the 1990 dive survey length frequency distributions (a) observed (solid line) and MPD estimates of fits (dashed line), and (b) residuals versus fitted values (curved lines show 95% confidence intervals for the multinomial distribution). Vertical lines separate the small (<50 mm), pre-recruit (≥ 50 mm and <58 mm), and recruit (≥ 58 mm) size groups.

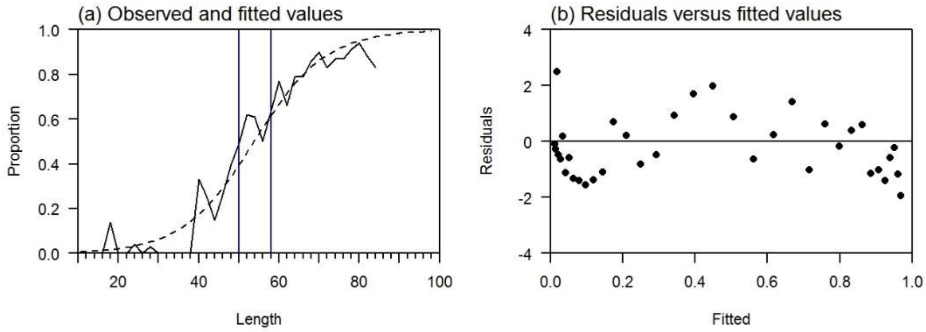

Figure 99: 2017 revised 4-cpue model MPD estimates for the Jeffs & Hickman (2000) maturity data (a) observed (solid line) and MPD estimates of fits (dashed line), and (b) residuals versus fitted values. Vertical lines separate the small (<50 mm), pre-recruit (≥ 50 mm and <58 mm), and recruit (≥ 58 mm) size groups.

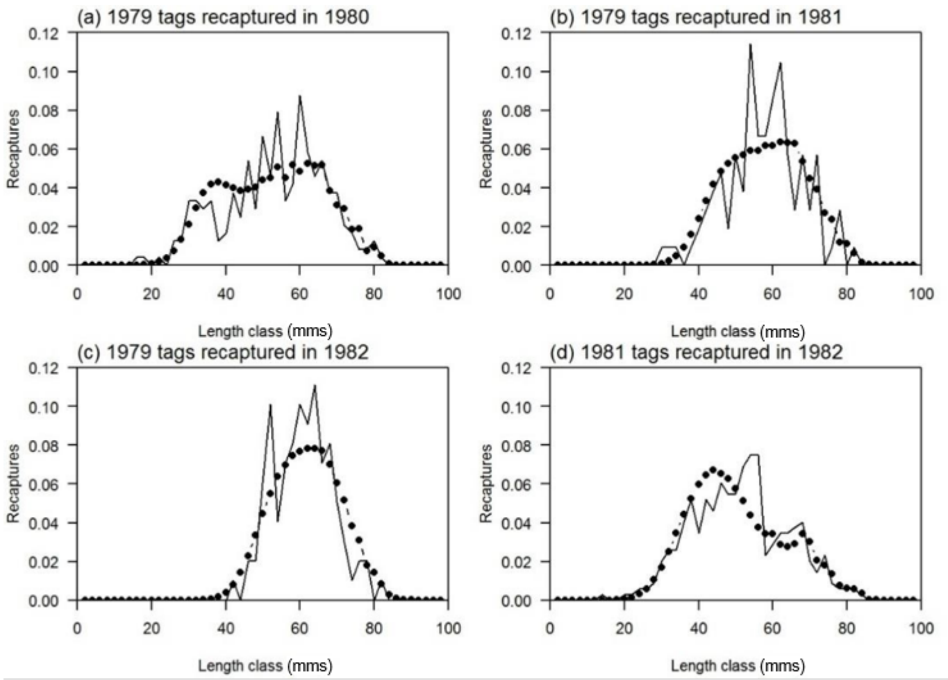

Figure 100: 2017 revised 4-cpue model MPD estimates of the observed and expected length frequency distributions of the mark-recapture data for (a–c) 1979 marked fish recaptured in 1980–81, and (d) 1981 marked fish recaptured in 1981.

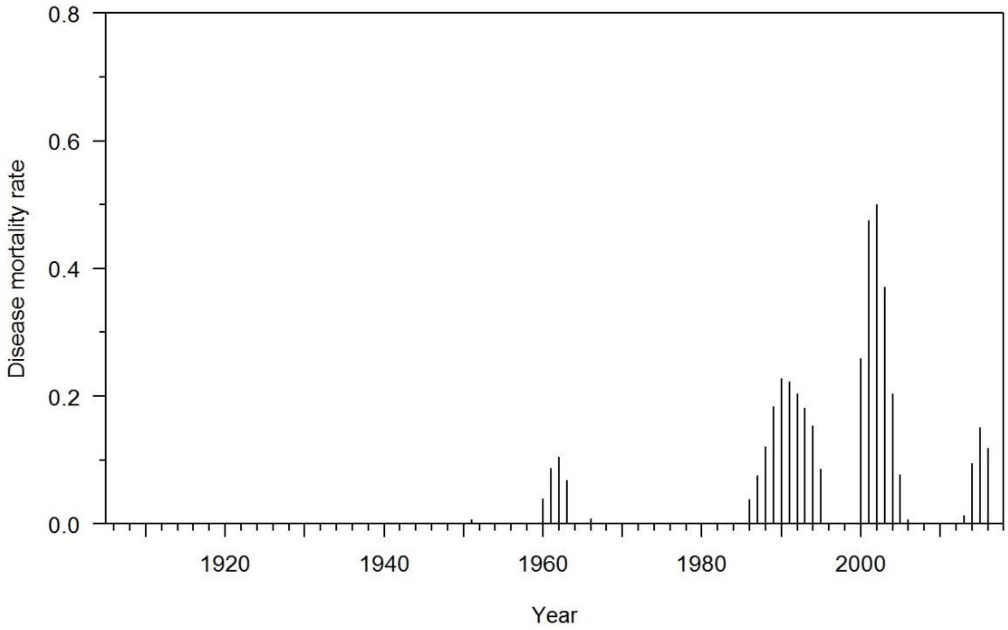

Figure 101: 2017 revised 4-cpue model MPD estimates of disease mortality rate.

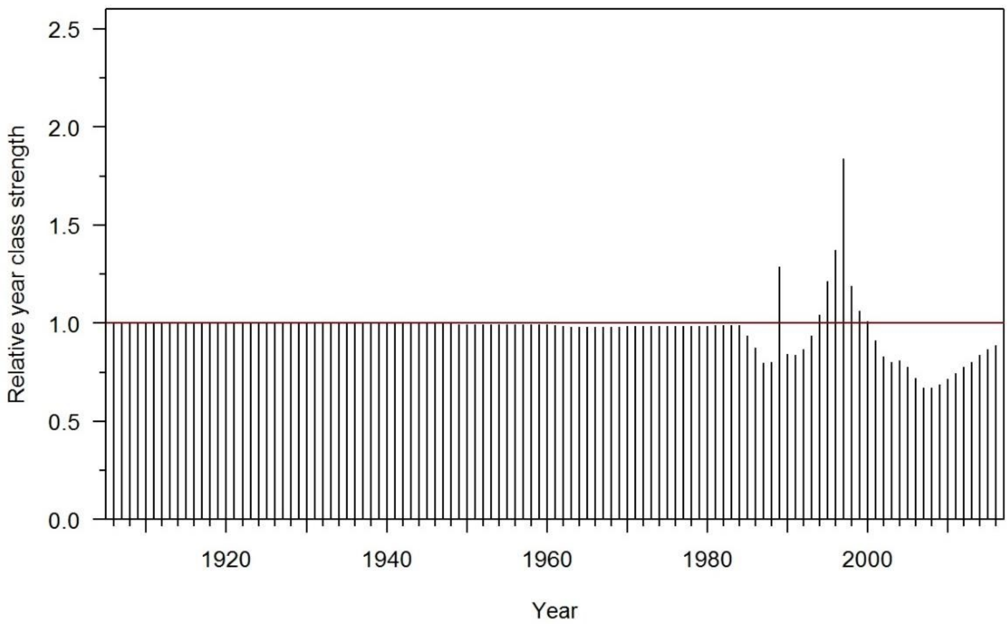

Figure 102: 2017 revised 4-cpue model MPD estimates of relative year class strength.

9. APPENDIX B: MCMC DIAGNOSTICS

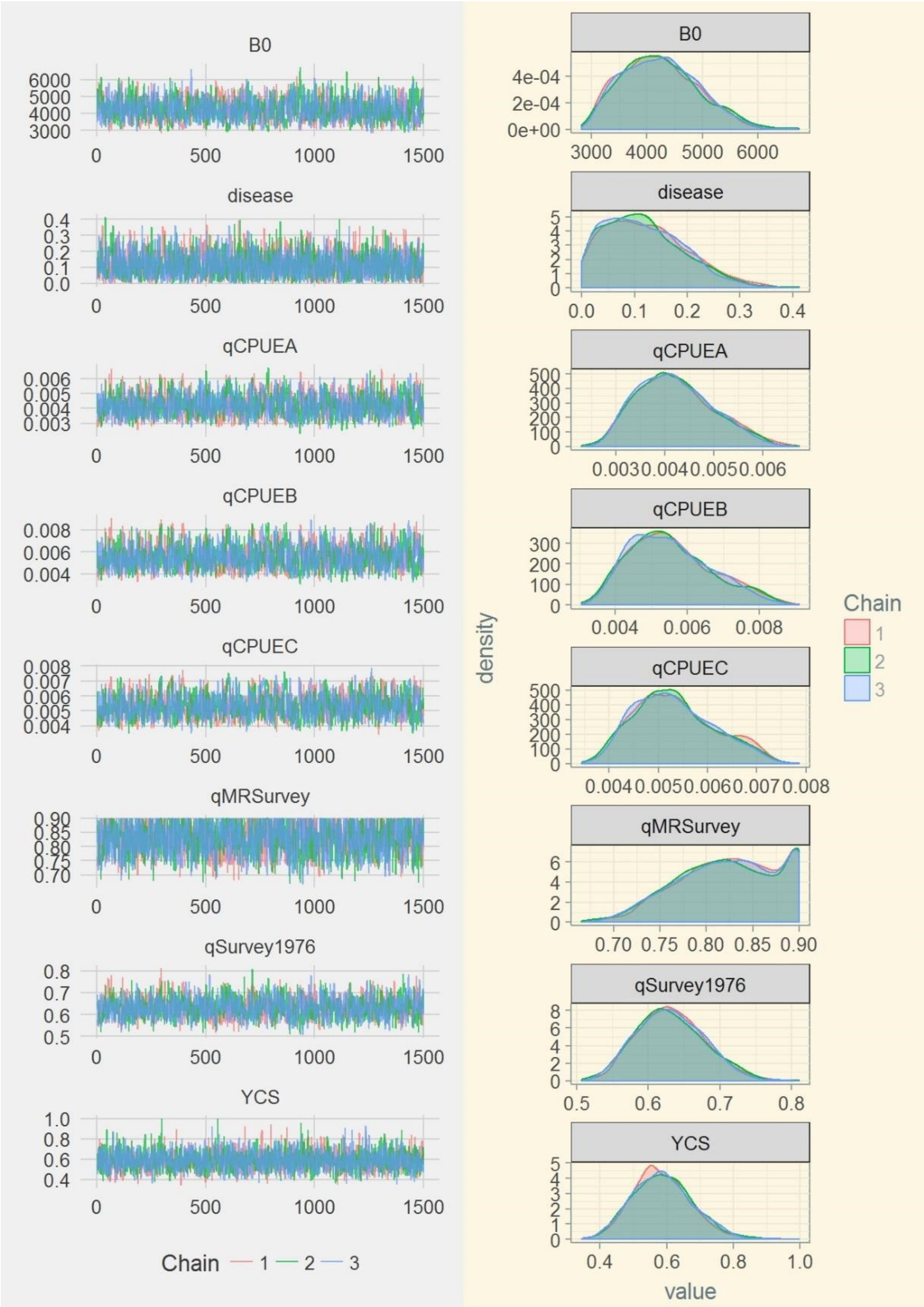

Figure 103: Trace plots (left) and density plots (right) for parameters from three MCMC chains run for the 2017 basic model. Fully overlapping chains and densities suggest chains have converged in a similar space (Fernandez-i-Marin, 2016).

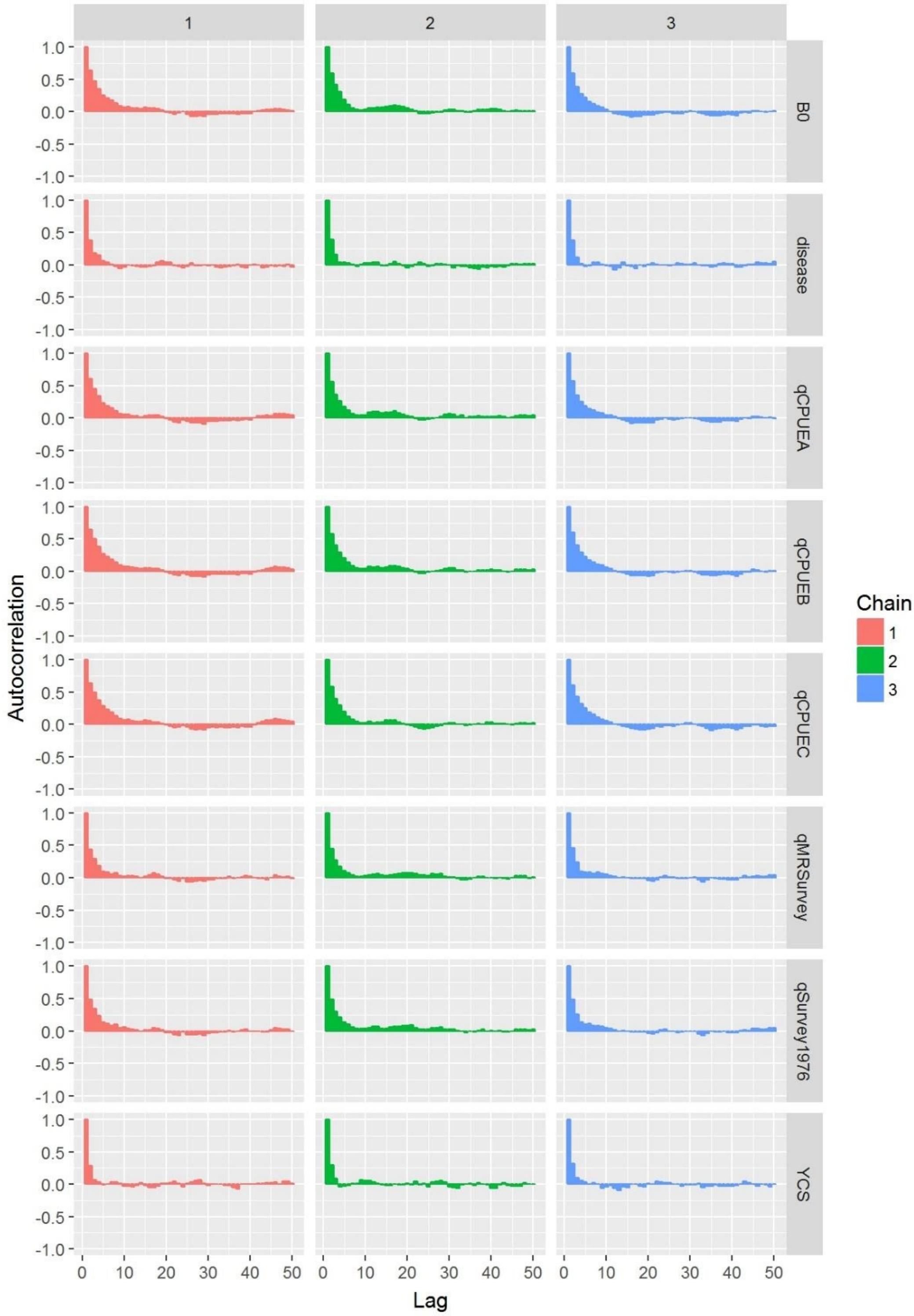

Figure 104: Autocorrelation plots for parameters from three MCMC chains run for the 2017 basic model. The autocorrelation plot expects a bar at one in the first lag, but no autocorrelation beyond it (Fernandez-i-Marin, 2016).

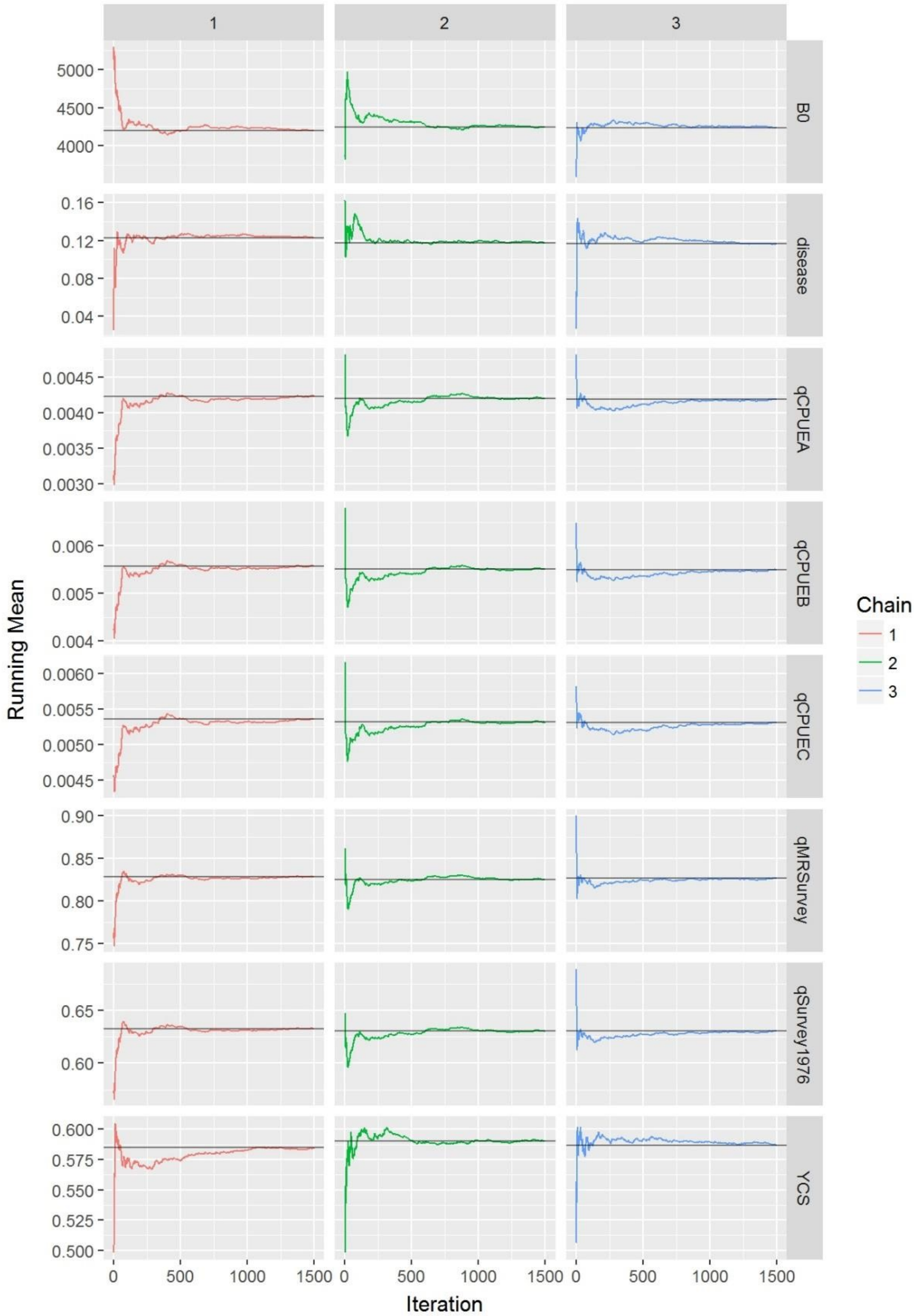

Figure 105: Running mean plots for parameters from three MCMC chains run for the 2017 basic model. A converged chain should quickly approach the overall chain, and all three chains should converge to the same mean (Fernandez-i-Marin 2016).

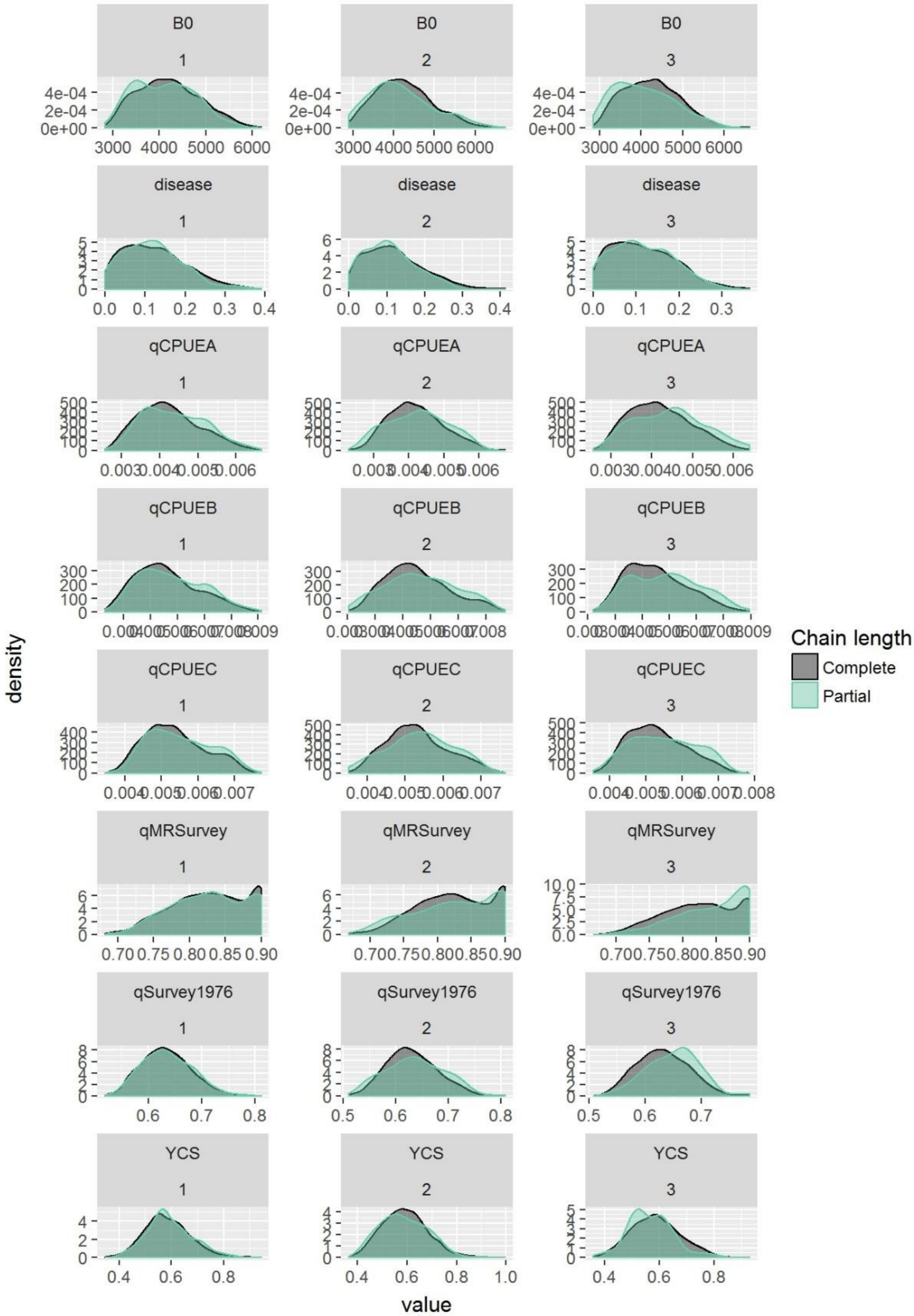

Figure 106: Density plots comparing the whole chain (black) with the latest part (last 10% of the values, in green) of the chain for parameters from three MCMC chains run for the 2017 basic model. For a converged chain the initial and final parts of the chain should be sampling the same target distribution, so the overlapping densities should be similar (Fernandez-i-Marin 2016).

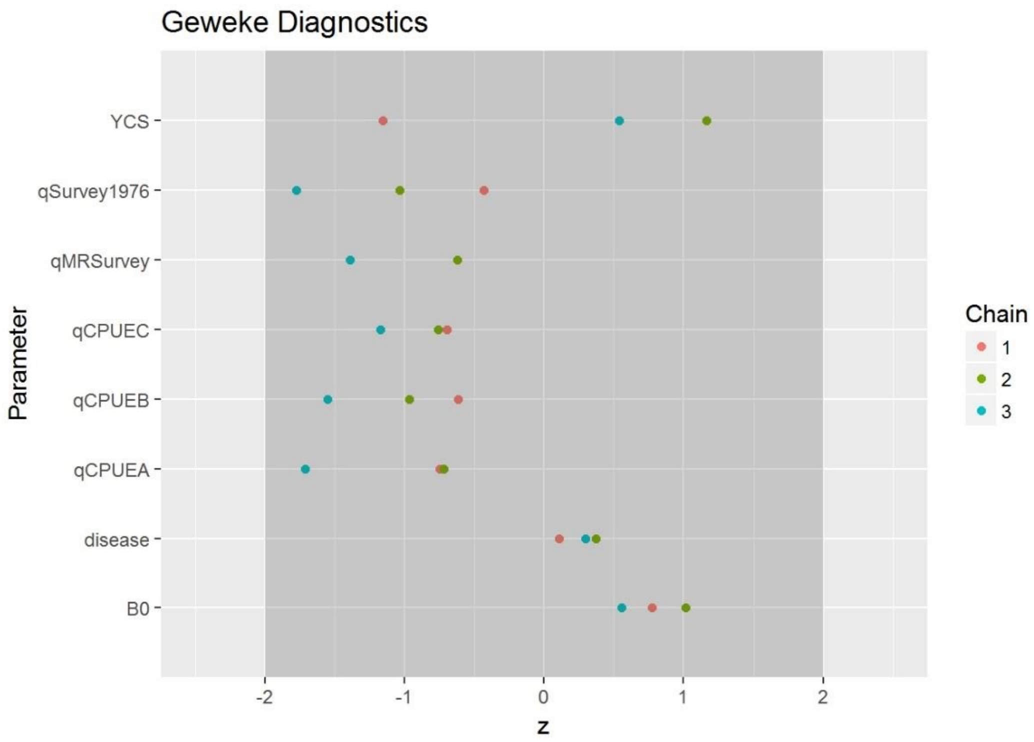

Figure 107: Geweke z-scores for parameters from three MCMC chains run for the 2017 basic model. The Geweke statistics compares the first part of the chain with the last part and for a converged chain, the expected outcome should have a 95% value between -2 and 2 (Fernandez-i-Marin 2016).

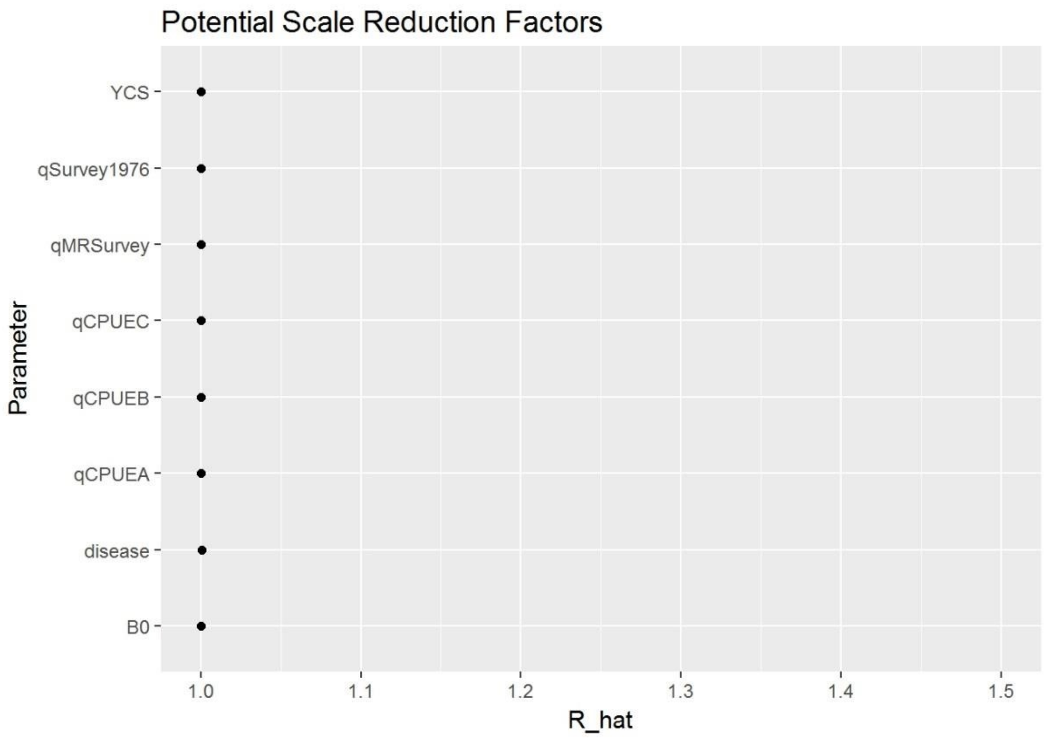

Figure 108: Potential Scale Reduction Factor values for parameters from three MCMC chains run for the 2017 basic model. The Potential Scale Reduction Factor statistics compares the between-chain variation with the within-chain variation and the outcome is expected to be close to 1 for convergence (Fernandez-i-Marin 2016).

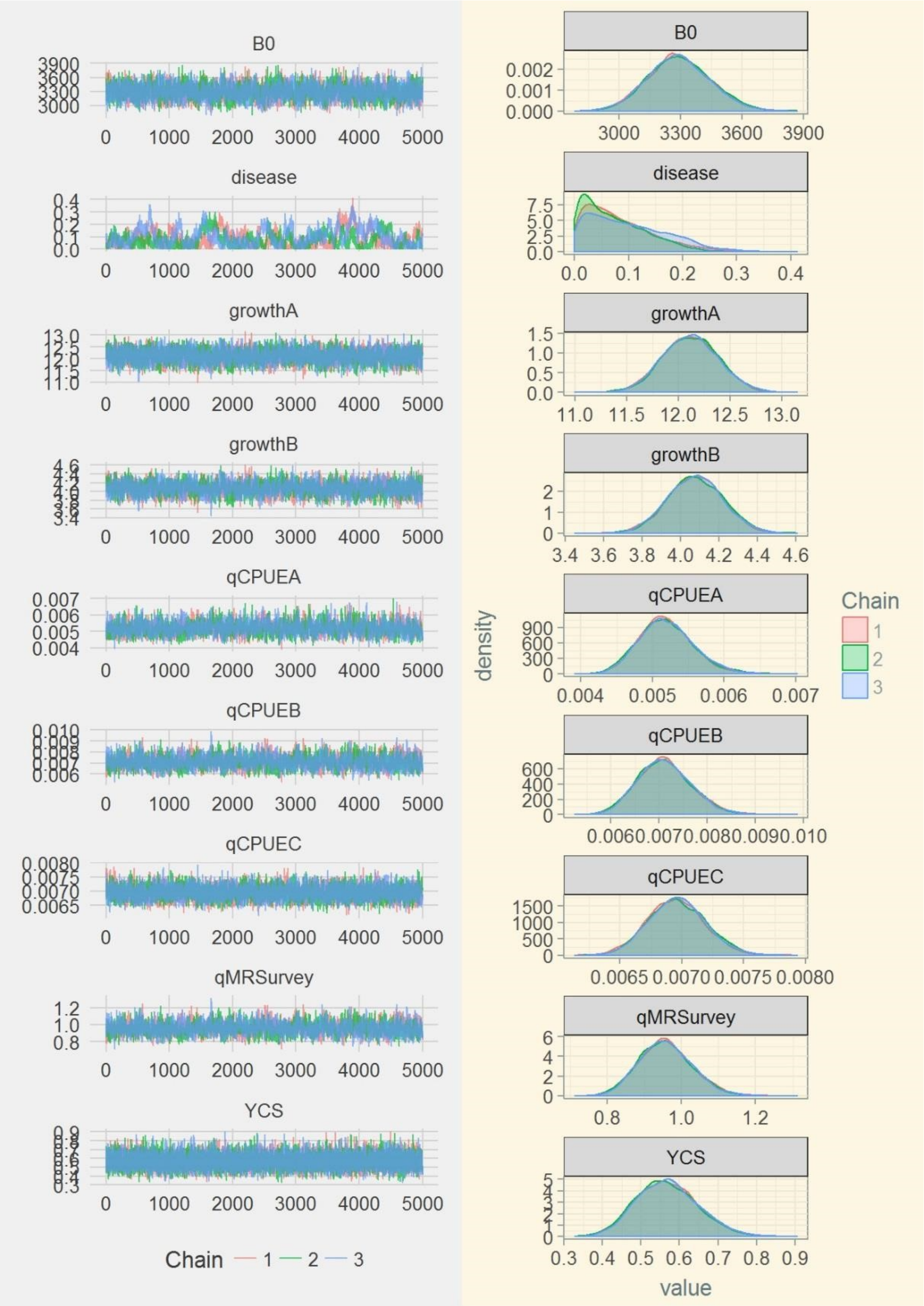

Figure 109: Trace plots (left) and density plots (right) for parameters from three MCMC chains run for the 2017 revised model. Fully overlapping chains and densities suggest chains have converged in a similar space (Fernandez-i-Marin 2016).

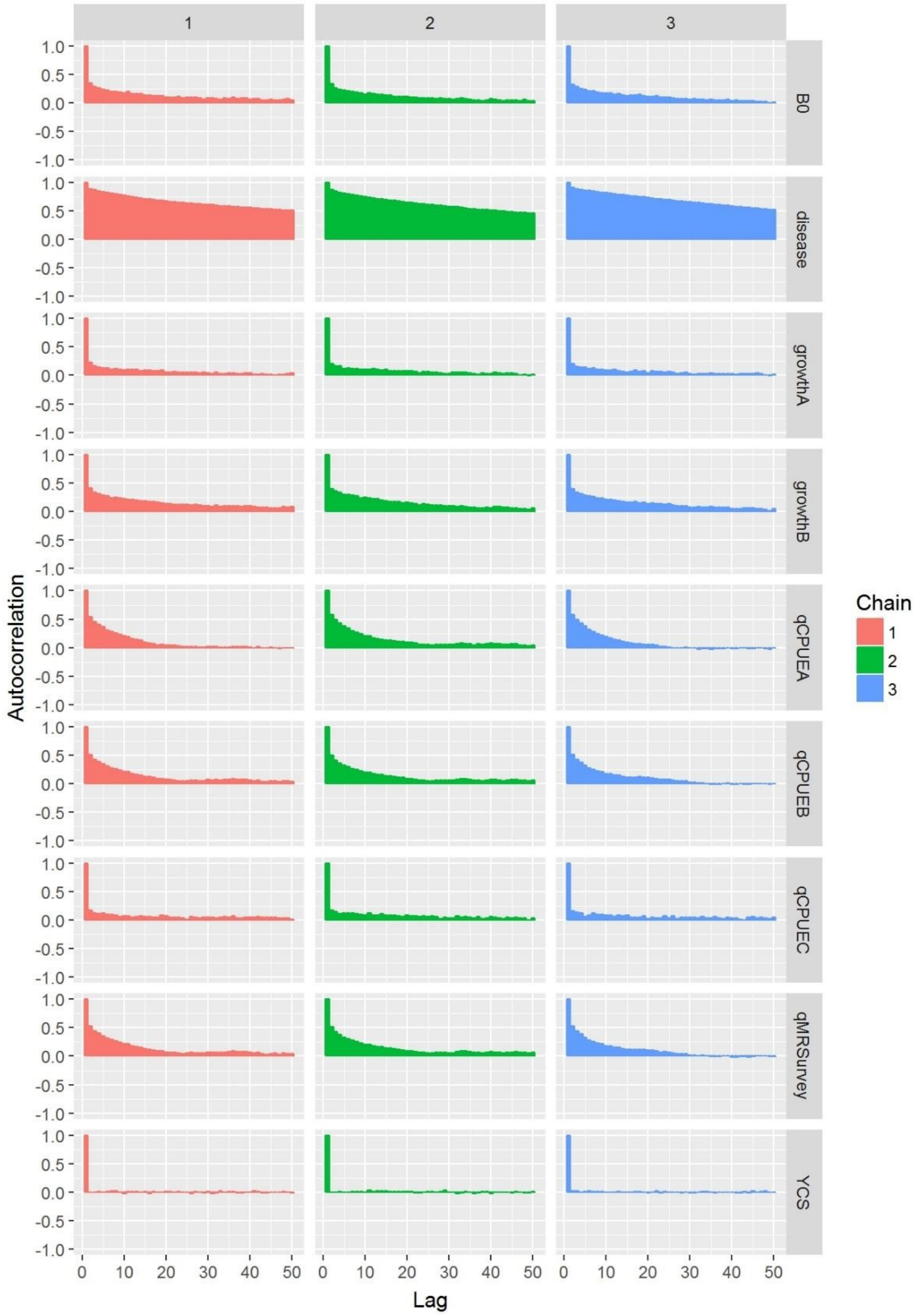

Figure 110: Autocorrelation plots for parameters from three MCMC chains run for the 2017 revised model. The autocorrelation plot expects a bar at one in the first lag, but no autocorrelation beyond it (Fernandez-i-Marin 2016).

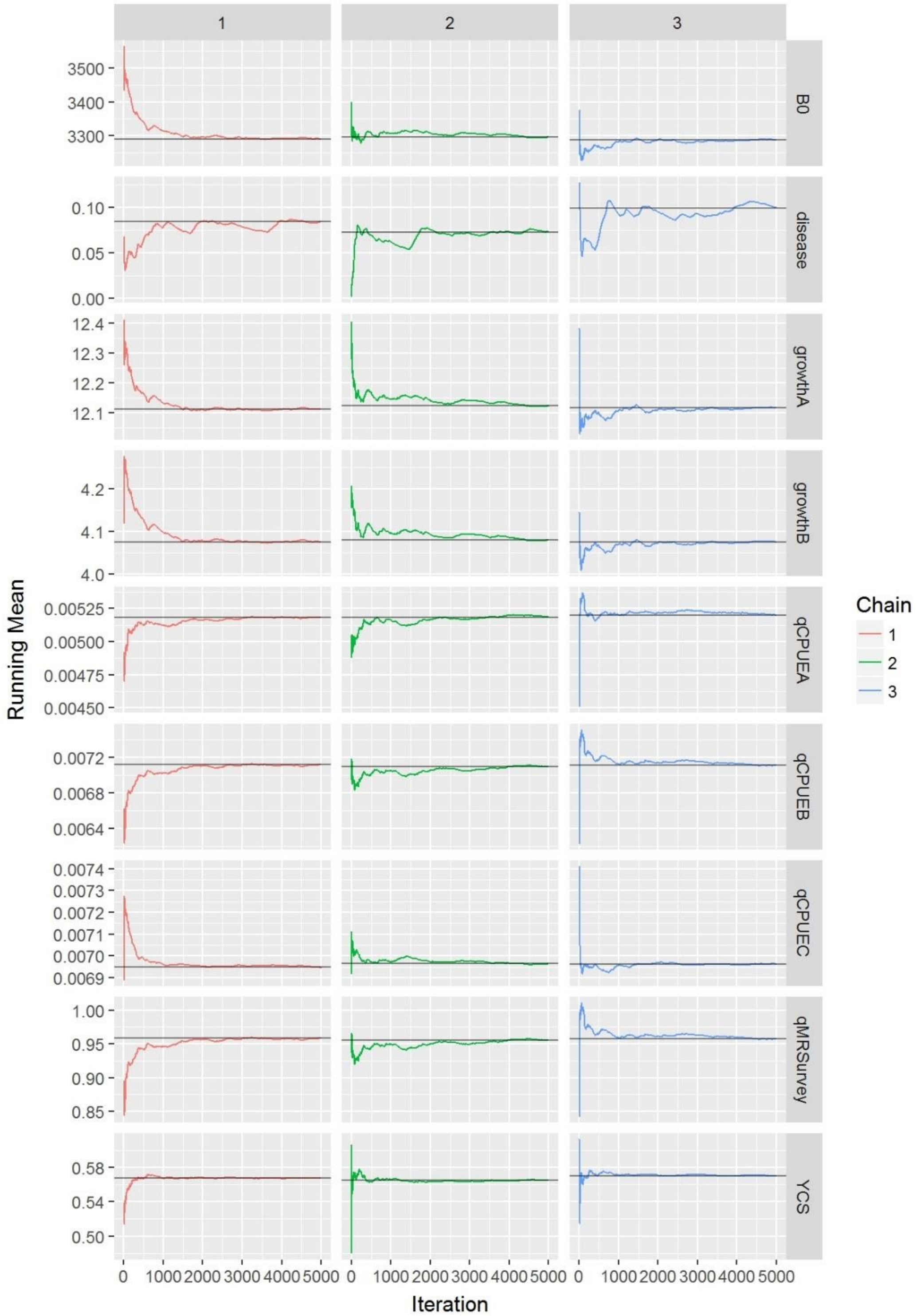

Figure 111: Running mean plots for parameters from three MCMC chains run for the 2017 revised model. A converged chain should quickly approach the overall chain, and all three chains should converge to the same mean (Fernandez-i-Marin 2016).

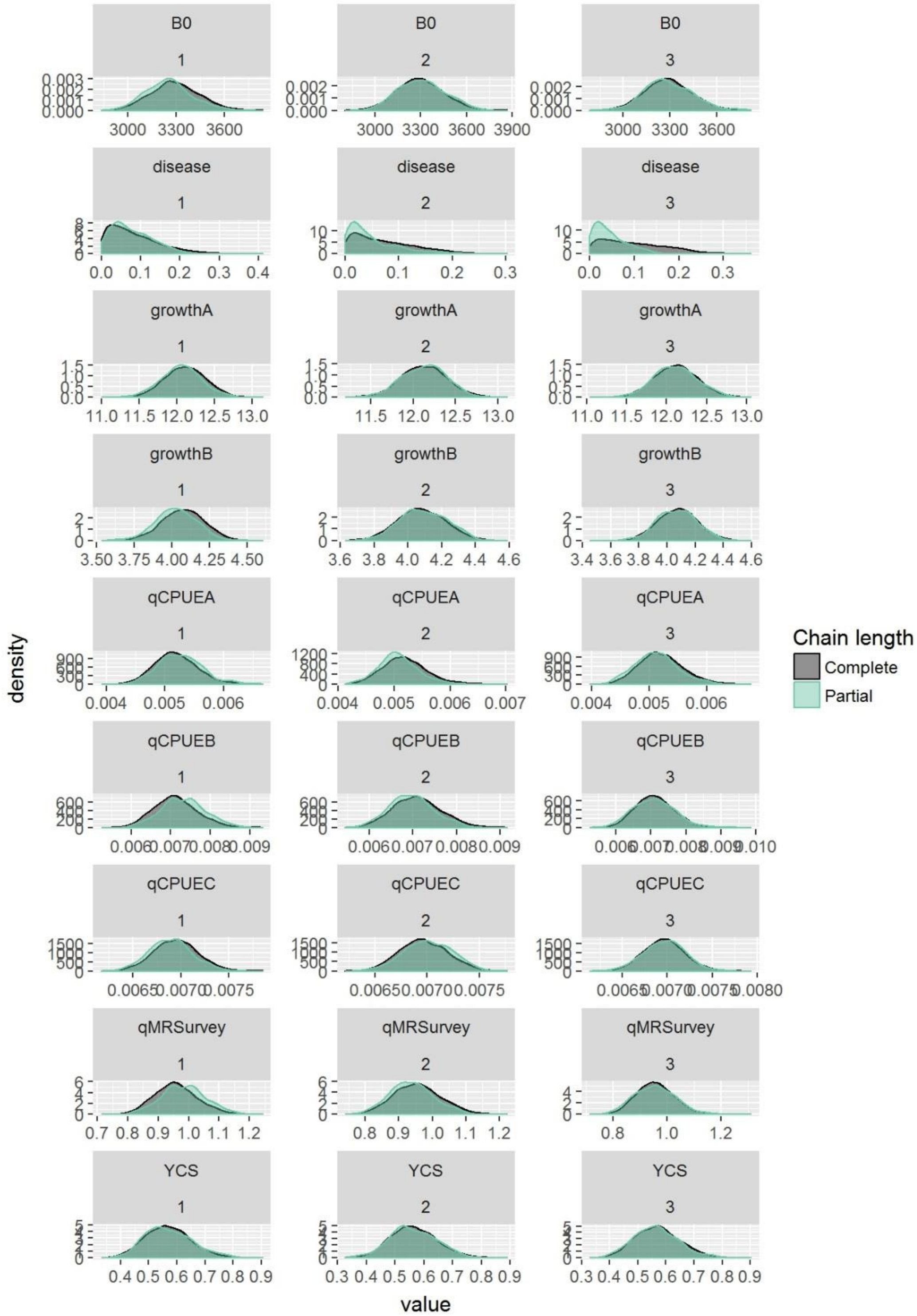

Figure 112: Density plots comparing the whole chain (black) with the latest part (last 10% of the values, in green) of the chain for parameters from three MCMC chains run for the 2017 basic model. For a converged chain the initial and final parts of the chain have to be sampling the same target distribution, so the overlapping densities should be similar (Fernandez-i-Marin 2016).

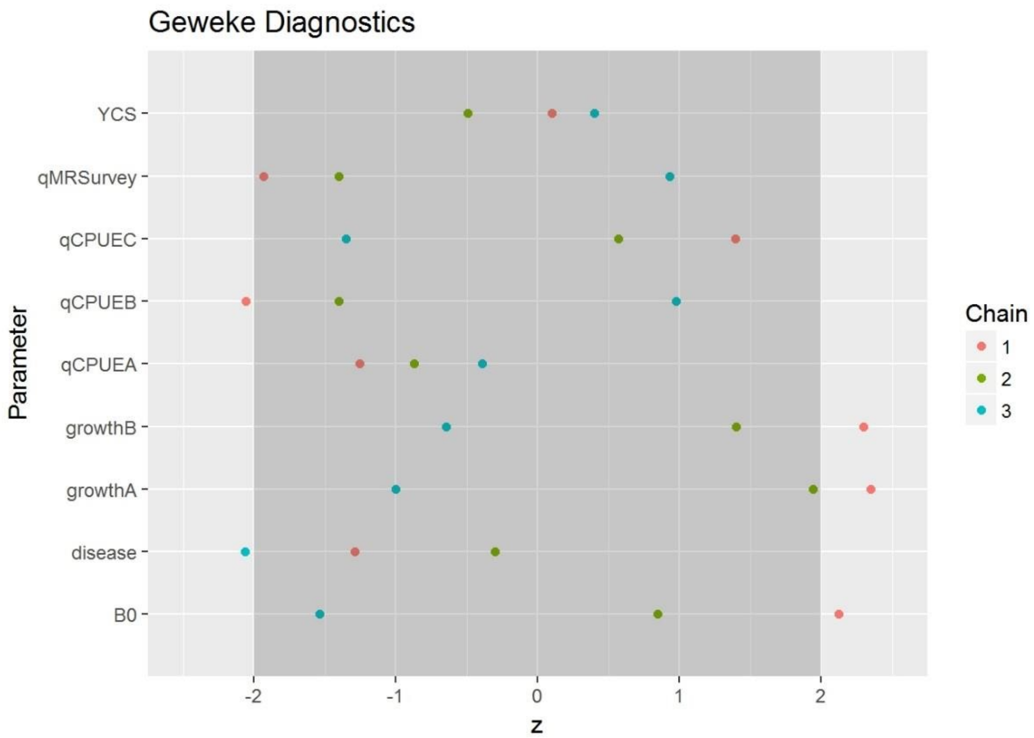

Figure 113: Geweke z-scores for parameters from three MCMC chains run for the 2017 revised model. The Geweke statistics compares the first part of the chain with the last part and for a converged chain, the expected outcome should have a 95% value between -2 and 2 (Fernandez-i-Marin 2016).

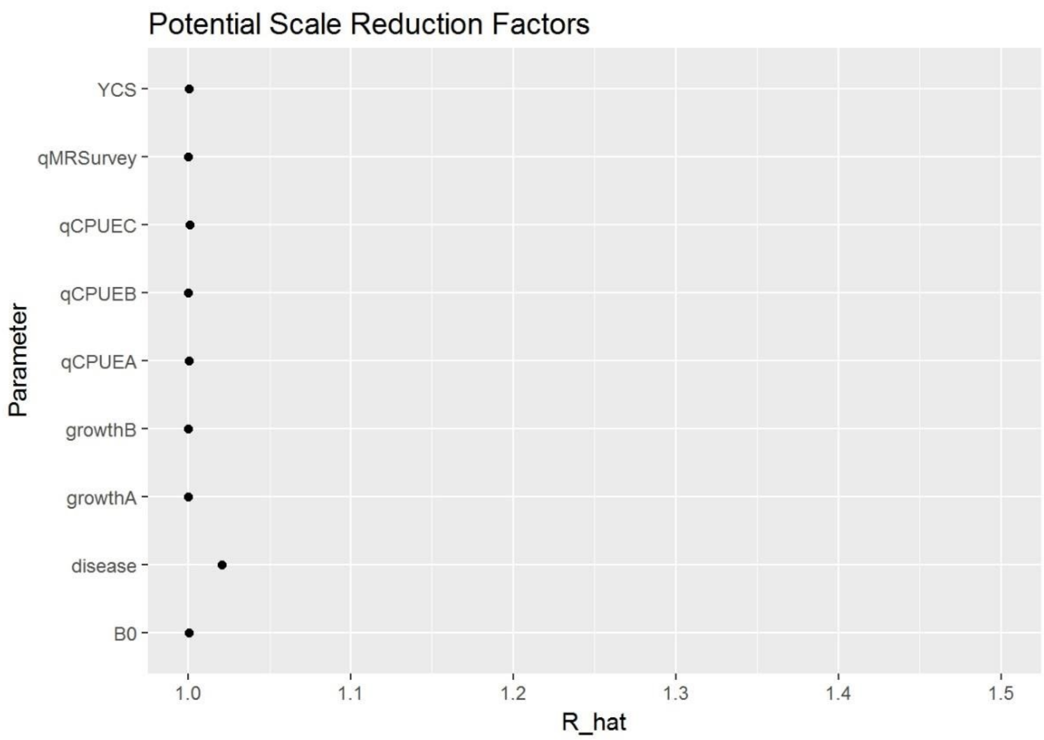

Figure 114: Potential Scale Reduction Factor values for parameters from three MCMC chains run for the 2017 revised model. The Potential Scale Reduction Factor statistics compares the between-chain variation with the within-chain variation and the outcome is expected to be close to 1 for convergence (Fernandez-i-Marin 2016).